UNIVERSITY OF SOUTHAMPTON

FACULTY OF PHYSICAL SCIENCES AND ENGINEERING

Electronics and Computer Science

Energy-Efficient Traffic-Aware Street Lighting Using Autonomous Networked Sensors

by

Sei Ping Lau

Thesis for the degree of Doctor of Philosophy

January 2016

UNIVERSITY OF SOUTHAMPTON

ABSTRACT

FACULTY OF PHYSICAL SCIENCES AND ENGINEERING
Electronics and Computer Science

Doctor of Philosophy

ENERGY-EFFICIENT TRAFFIC-AWARE STREET LIGHTING USING AUTONOMOUS NETWORKED SENSORS

by Sei Ping Lau

Street lighting is a ubiquitous utility. It does not only illuminate the streets during the night but also helps to prevent crime and traffic collisions. However, to sustain its operation is a heavy burden both financially and environmentally. Because of this, several initiatives have been proposed to reduce its energy consumption. However, most initiatives are mainly aimed at energy conservation and have given little consideration about the usefulness of street lighting.

A Streetlight Usefulness Model, an evaluation metric used to measure the usefulness of street lighting to road users, is proposed. Using StreetlightSim, a real-time co-simulation environment developed as part of this research, the energy efficiency and usefulness of six existing street lighting schemes have been evaluated. Their performances were used as baseline results which later justified the proposal of Traffic-aware Lighting Scheme Management Network (TALiSMaN). Simulation results show that TALiSMaN can achieve comparable or improved usefulness ($> 90\%$) to existing schemes, while consuming as little as $1 - 55\%$ of the energy required by existing schemes.

To consider the limitation of 'off-grid' streetlights – those powered locally by renewable energy, TALiSMaN has been enhanced with an energy demand predictor to ensure that a limited energy budget can be used fairly throughout the whole night. This enhanced scheme is known as TALiSMaN-Green. Combined with knowledge of the amount of energy stored, and predicting sunrise times, TALiSMaN-Green modulates the lighting levels requested by TALiSMaN if the energy stored is predicted to be insufficient for an entire night. The results show that this scheme extends the operational lifetime of solar-powered streetlights from 2 to 16 hours. Evaluated with real traffic flow and solar readings, TALiSMaN-Green can maintain streetlight usefulness at $60 - 80\%$ (mean $= 73\%$ with standard deviation of 9%). In comparison, the streetlight usefulness of TALiSMaN was reduced to below 30%.

Contents

List of Figures

List of Tables

Declaration of Authorship

I, Sei Ping Lau, declare that the thesis entitled *Energy-Efficient Traffic-Aware Street Lighting Using Autonomous Networked Sensors* and the work presented in the thesis are both my own, and have been generated by me as the result of my own original research. I confirm that:

- this work was done wholly or mainly while in candidature for a research degree at this University;
- where any part of this thesis has previously been submitted for a degree or any other qualification at this University or any other institution, this has been clearly stated;
- where I have consulted the published work of others, this is always clearly attributed;
- where I have quoted from the work of others, the source is always given. With the exception of such quotations, this thesis is entirely my own work;
- I have acknowledged all main sources of help;
- where the thesis is based on work done by myself jointly with others, I have made clear exactly what was done by others and what I have contributed myself;
- parts of this work have been published as listed in Section 1.4

Signed:.....

Date:.....

Acknowledgements

Undertaking this doctoral journey has been a life-changing experience and it would not have been achievable without the support that I have received from many people.

First and foremost, my sincere gratitude to my supervisory team, Geoff Merrett, Alex Weddell, and Prof Neil White for their supervision, encouragement and support. It was an honour to be able to work with them. I am especially grateful to Geoff and Alex for their constant feedback, having confidence in my work and inspiring me to achieve more than I could imagine.

I gratefully acknowledge the Ministry of Education, Malaysia and Universiti Malaysia Sarawak for granting me the opportunity to further my studies at the University of Southampton. Also, I am thankful for the research facilities provided by the School of Electronics and Computer Science, and for the use of the IRIDIS High Performance Computer Facility throughout my studies at Southampton.

My thanks also go to my friends in the ESS group, especially Teng Jiang and Huma Zia, who were always there for discussion and advice. Outside of my studies, I am especially lucky to have Chong Eng Tan, and my cousin Marlene Lee and her family for bringing joyful festival seasons to my family.

Finally, thanks to my parents for giving me strength and support over the past four years. Special acknowledgement must go to my wife, Mei Ching for being extremely patient and accommodating during my studies. Lastly, thanks to my two wonderful children, Denise and Ethan who are always putting a smile on my face.

With the oversight of my supervisory team, this thesis has been proofread and edited by Jane L. Watson of JLW Proofreading Services. However, no of intellectual content were made as a result from this service.

Abbreviations

AADF	Annual average daily traffic flow
AI	Artificial intelligence
AODV	Ad hoc on demand distance vector algorithm
ARIMA	Auto-regressive integrated moving average
CAP	Contention access period
CCT	Correlated colour temperature
CDF	Coordinated depth forwarding protocol
CEN	European Committee for Standardization
CFP	Contention free period
CIE	International Commission on Illumination
CRI	Colour rendering index (also known as R_a)
CSMA-CA	Carrier sense multiple accesses with collision avoidance
DfT	Department for Transport, UK
DoW	Day-of-Week data aggregation strategy
EWMA	Exponentially weighted moving average
FB	IEC 61499 Function block
FC	Fuel cell
FWMA	Fixed-weighted moving average
GGPSR	Geocast greedy perimeter stateless routing protocol
GPS	Global positioning system
GPRS	General packet radio service
GPSR	Greedy perimeter stateless routing
GTS	Guaranteed time slot
HPS	High pressure sodium
IQR	Interquartile range
JiST	Java in simulation time
LED	Light emitting diode
MAC	Media access control layer
MAE	Mean absolute error
MOVE	Mobility model generator for vehicular network
NED	Network description language
ns	Network simulator

OMNeT++	Objective modular network testbed
OTcl	Object tool command language
PHY	Physical layer
PIR	Passive infrared
PKU-STRAW-L	Peking University street random waypoint for Lamp
PLC	Power line communication
PDD	Previous-D-Days data aggregation strategy
RREQ	Route request message
RT	Routing table
SMA	Simple moving average
SMS	Short message service
STRAW	Street random waypoint mobility model
SUMO	Simulation of urban mobility
SWANS	Scalable wireless ad hoc network simulation
TALiSMaN	Traffic-aware lighting scheme management network
TIGER	Topologically Integrated Geographic Encoding and Referencing
TCP	Transmission control protocol
TraCI	Traffic control interface
TraNS	Traffic and network simulation environment
VANET	Vehicular ad hoc network
Veins	Vehicles in network simulation
WDE	Weekday-Weekend data aggregation strategy
WSNs	Wireless sensor networks

Nomenclature

α_{θ}	Weighting factor of road traffic volume by days of week
α_{ped}	Weighting factor of time spent by a pedestrian looking at the footpath
α_{cond}	Conditioning factor to the requested lighting level, φ
α_{exp}	Weighting factor of exponentially weighted moving average
α_{fix}	Weighting factor of fixed-weighted moving average
α_{sel}	Coefficient of predictor selection metric
α_{solar}	Random solar noise factor
γ	Ratio of streetlight lighting level at x metres from a road user to the minimum required lighting level designated for the road where the road user is travelling on
Γ	Total number of simulated road users per day
φ_{mot}	Lighting level of a streetlight for detected motorist (%)
φ_{ped}	Lighting level of a streetlight for detected pedestrian (%)
Δ_{ped}	Additional pedestrian traffic composition (%)
d_{aprox}	Approximate relative distance from a streetlight to the detected pedestrian (m)
d_{avg}	Average distance to the next adjacent streetlight
d_{det}	Euclidean distance to the nearest sensor node that detects the road user (m)
d_{rad}	Maximum detection range of a road-user sensor (m)
E_h	Lighting level on a horizontal plate (lx)
E_{cap}	Capacity of an energy storage device (Wh)
E_{cons}	Energy consumed by a streetlight (Wh)
E'_{demand}	Expected energy demand of a streetlight until sunrise (Wh)
$E_{harvested}$	Harvested solar energy (Wh)
E_{stored}	Energy stored in a battery (Wh)
I_{sel}	Predictor selection metric
P_{max}	Maximum power rating (W)
P_{solar}	Observed solar power (W/m^2)
$P_{efficiency}$	Solar power conversion efficiency (%)
P_{size}	Size ratio of a solar cell

R_a	Colour rendering index
R_{MAE}	Ratio of MAE to average daily energy demand of TALiSMaN at specific traffic volume
$R_{resources}$	Ratio of computing resources required by a predictor to available computing resources of a wireless sensor node
T_{BO}	Random number of back-off periods
T_{CCA}	Clear channel assessment period
t_{exp}	Expiration time of the state delay counter (s)
t_{rise}	Actual sunrise time
t'_{rise}	Estimated sunrise time
U_{mot}	Streetlight usefulness for motorist
U_{ped}	Streetlight usefulness for pedestrian
$U_{ped(avoid)}$	Streetlight usefulness for pedestrian in obstacle detection, navigation and facial recognition
$U_{ped(prospect)}$	Streetlight usefulness for pedestrian's perceived safety
V_{mot}	Annual average daily traffic flow for vehicular traffic (vehicles per hour)
V_{comb}	Annual average daily traffic flow with both vehicular and pedestrian traffic (road users per hour)
V_θ	Average daily, or average weekday and weekend traffic volumes
V_{avg}	Average weekly traffic volume
z	Ratio of the lighting level at location x metres from a road user at time t to the lighting level required at the illumination zone where location x is located
Z_{ped}	Illumination zone of streetlight according to the relative distance to detected pedestrian

Chapter 1

Introduction

Street lighting is a ubiquitous utility that can be found in most urban areas, and is used for a number of different purposes. As street lighting improves visibility during the hours of darkness, crime detection becomes easier and the presence of authority, such as the police, becomes more visible [1]. As a result, potential offenders are likely to desist from committing crimes. For example, crimes in Dover, Bristol, Birmingham, Dudley and Stoke-on-Trent, UK have been reduced by 38% by having adequate street lighting [2]. Fear of crime discourages many people from travelling at night; one of the causes of this is dark or poorly lit roads. As a result, improved street lighting encourages more socio-economic activities during the night [3, 4]. Consequently, this promotes greater road use after dark. Street lighting also has a prominent role in reducing the risk of accidents after dark by reducing traffic collisions by over 50% [5]. Compared to during daylight hours, the risk of an accident involving pedestrians on a lit road increases by 141%. For unlit roads, however, this figure rises by 360%.

Although the benefits of street lighting are clear, sustaining its operation has become a concerning issue to local governments, both financially and environmentally. Globally, there are over 90 million streetlights consuming approximately 114 TWh of energy annually [6]. This represented about 33% of the UK's annual electricity consumption in 2012 [7], equivalent to an emission of 52 million tonnes of CO_2 (based on the 2012 power conversion factor of 0.46 kg/kWh [8]). With rising energy prices and rapid urbanisation, the cost of street lighting is expected to grow as the number of streetlights is predicted to increase by over 300% by 2025 [9]. For example, in 2011, Nottinghamshire County Council in the UK spent more than £5m on the energy cost for street lighting, representing a 360% increment compared to 2005 [10].

Efforts to reduce the energy cost of street lighting, and hence reduce carbon emissions, have focussed on two aspects: replacement of each streetlight's luminaire, and its control mechanism. The replacement of end-of-life streetlights with newer and more energy-efficient luminaires has delivered significant energy savings. For example, in Thailand,

a 25 – 30% energy saving was achieved with a new High Pressure Sodium (HPS)-based luminaire [11]. Recent developments in Light-Emitting Diode (LED)-based luminaires have resulted in a further 25% power reduction, and have virtually no disadvantage/deterioration over being regularly switched, and deliver light instantly when switched on [12, 13].

Conventionally the control, or 'switching mechanism' of a streetlight, is realised by a clock with a predefined schedule or an integrated light sensor which indicates when the surrounding environment becomes dark. Once switched on, streetlights remain lit continually throughout the night. However, this conventional or 'always-on' lighting scheme can result in energy wastage, especially when roads are only intermittently used and lighting at full brightness is not necessary. Examples of this include the early hours of the morning, when very low traffic volumes are expected. Owing to this, 75% of local councils in the UK have selectively dimmed or completely turned off streetlights during late and early hours when low traffic volumes are expected [14]. Warwickshire County Council in the UK anticipates an annual saving of £0.5m and about a 25% reduction in CO_2 emissions caused by street lighting, if operating their streetlights on this basis [15].

In considering the energy and CO_2 emissions that can be saved via dimming, many have adopted communication and sensing technologies to improve the control of light levels. Remote-controlled street lighting offers significant prospects for saving energy as continual adjustment of light levels is possible [16–18]. With this approach, an operator at a remote control centre performs the necessary management and regulation of streetlight operation, such as dimming for energy conservation and health monitoring of the streetlights. In some cases, light levels are autonomously adjusted based on ambient information, such as weather and traffic conditions, collected by a local sensor array [19, 20]. Most of the proposed remote- and sensor-controlled street lighting approaches adopt wireless communication networks to establish a communication link between a remote control centre and an individual streetlight. Instead of sensing the traffic, Müllner and Riener [21] utilised Global Positioning System (GPS) and Internet-enabled smartphones to track the precise location of pedestrians, and hence only streetlights within a defined radius of them are turned on. Recently, the adoption of artificial intelligence (AI) techniques such as agent-based systems [18, 22], fuzzy logic [23] and artificial neural networks [24] in street lighting have also been reported. The main advantage of adopting AI is to enable the self-management of the streetlights with the ability to adapt with minimum human intervention.

The mains power grid is the typical energy source used for street lighting. Although energy demand for street lighting can be reduced via dimming, a significant amount of energy is still required. Access to the mains power grid and long-range communication network is limited in some areas. There has recently been increased interest in the use of renewable or green energy sources to provide their power [25]. These 'off-grid' streetlights, or streetlights which are powered locally from renewable energy, are most useful in remote

and isolated places such as rural villages and isolated islands. They offer an economical alternative as neither cabling nor connection to a mains power grid is required [26]. Several renewable energy sources have been considered for off-grid streetlights such as solar [27, 28], wind [29] and fuel cells [30]. To overcome the limitations of relying on a single source, a combination of multiple renewable energy sources such as solar-wind [29, 31] and solar-fuel cells [30, 32] have also been considered. Generally, these 'off-grid' streetlights appear to be autonomous and unconnected.

1.1 Research Justification

Numerous research efforts have considered the use of sensing and communication technologies to allow precise and adaptive control of light levels (dimming) to conserve energy [16–18]. Importantly, many of these focus solely on energy conservation rather than consider the resulting usefulness of the street lighting. Standards exist [33, 34] for the design of effective street lighting. These standards consider road function, traffic density and complexity and existence of facilities for traffic control to select suitable light levels. However, adaptive street lighting (where streetlights can dim or switch off) and individual road users' needs have been given little consideration in these standards. While a significant body of disparate research exists concerning the perception and use of street lighting from the perspective of both motorists and pedestrians [35–38], this has not yet been collated to assist the design and evaluation of street lighting schemes.

In general, remote- and sensor-controlled street lighting schemes require a centralised controller and a fixed infrastructure such as the mains power grid and long-range communication networks (e.g. cellular networks) [17, 18, 21]. However, they also exhibit a single point of failure [23] as their performance depends upon the reliability of these long-range communication networks [39, 40]. In many rural or undeveloped areas, the coverage and reliability of the cellular network is highly variable [41] and a wired infrastructure unavailable [28]. One opportunity to overcome this limitation would be in creating a decentralised system without relying on a fixed infrastructure.

While most dimming approaches have focused on improving the energy-efficiency of 'grid-powered' streetlights, their application to 'off-grid' streetlights is restricted. Studies show that solar-powered streetlights using a multi-sensor control system can reduce energy consumption by 40% [42]. Still, this approach overlooks the possibility that harvested energy could be insufficient for street lighting across an entire night. This means that the streetlights may, for example, operate normally until the middle of the night, but run out of energy and be completely inoperable after that. This is because energy harvested from solar or wind fundamentally varies due to weather conditions, whereas grid-powered streetlights have a reliable electricity supply to sustain their daily operation.

Additionally, off-grid streetlights also typically store energy in batteries that have a restricted capacity, which limits the maximum energy available.

1.2 Research Questions

This research investigates distributed approaches to on- and off-grid energy efficient and effective street lighting. Based on this, the research seeks to provide answers to the following research questions:

(a) How can the usefulness of street lighting be quantified from the perspective of different road users?

(b) How useful and energy-efficient are existing state-of-the-art street lighting schemes?

(c) How can the brightness of street lighting be autonomously and adaptively adjusted without a need for centralised control or existing infrastructure, while maintaining a similar usefulness to conventional 'always-on' street lighting?

(d) How can a street lighting network be powered from an intermittent and bounded harvested energy supply, while maximising its usefulness over a period of an entire night?

1.3 Research Contributions

Addressing the questions, the research presented in this thesis has led to a number of contributions:

- A **streetlight usefulness model** is proposed which provides an evaluation metric to evaluate the usefulness of street lighting from the perspective of both motorists and pedestrians. This model is based on literature on visual task requirements and perceived safety of these road users. This model has enabled the usefulness of existing street lighting schemes to be evaluated, providing baseline results used in this research. This addresses research question (a).

- **StreetlightSim**, a novel simulation environment that models both road traffic patterns and adaptive networked streetlights is developed. This is the primary tool used to evaluate the approaches proposed in this thesis and against existing state-of-the-art lighting schemes. It is open-source, and has been made available to the research community since 2014. To date, there have been over 150 downloads of the tool from around the world. Together with the proposed streetlight usefulness model, this tool provides a means to analyse both the 'how useful' and 'how efficient' parts of research question (b).

- **TALiSMaN** (**T**raffic **A**ware **Li**ghting **S**cheme **Ma**nagement **N**etwork), a distributed autonomous and adaptive street lighting scheme based on road traffic sensing, is proposed. This lighting control scheme allows adaptive lighting adjustment of 'grid-powered' streetlights to satisfy the individual road user's needs, cooperatively via wireless communication and sensing technologies. Simulation results show that the scheme is able to provide improved or comparable usefulness compared to existing street lighting schemes, but with a significant improvement in energy efficiency (requiring only 1 – 55% of the energy, depending on traffic volume). This addresses research question (c).
- **TALiSMaN-Green** investigates the use of an energy demand predictor to address the shortcoming of existing 'off-grid' streetlights. It ensures the fair use of the limited energy budget of solar-powered streetlights across a complete night. Simulation results show that TALiSMaN-Green is able to prolong the operation while maintaining the consistent usefulness of a network of solar-powered streetlights across a complete night, even with a highly constrained energy budget. This answers research question (d).

1.4 Published Papers

The following papers have been published as a result of the research presented in this thesis. A selection of these papers can be found in Appendix A.

Journal:

- **S. P. Lau**, G. V. Merrett, A. S. Weddell, and N. M. White, "A Traffic-Aware Street Lighting Scheme for Smart Cities using Autonomous Networked Sensors", Computers & Electrical Engineering, Special Issue on Green Engineering Towards Sustainable Smart Cities, 2015.

Conference papers:

- **S. P. Lau**, G. V. Merrett and N. M. White, "Energy-efficient street lighting through embedded adaptive intelligence", in Proceedings of International Conference on Advanced Logistics and Transport, Tunisia, 2013, pp. 53 – 58.
- **S. P. Lau**, G. V. Merrett, A. S. Weddell, and N. M. White, "StreetlightSim: A simulation environment to evaluate networked and adaptive street lighting", in Proceedings of IEEE Asia Pacific Conference on Wireless and Mobile, Bali, 2014, pp. 66 -71.

- **S. P. Lau**, A. S. Weddell, G. V. Merrett and N. M. White, "Energy-neutral solar-powered street lighting with predictive and adaptive behaviour", in Proceedings of 2nd International Workshop on Energy Neutral Sensing Systems, Memphis, 2014, pp. 13 – 18.
- **S. P. Lau**, A. S. Weddell, G. V. Merrett and N. M. White, "Solar-Powered Adaptive Street Lighting Evaluated with Real Traffic and Sunlight Data", poster presented to ACM Conference on Embedded Networked Sensor Systems (SenSys), Seoul, South Korea, 2015.

1.5 Structure of the Thesis

The remainder of this thesis is organised as follows:

Chapter 2 begins with an overview of the requirements of street lighting from both the motorist's and pedestrian's perspective. Then, a review of street lighting control for energy conservation is presented. This chapter continues with a detailed background on Wireless Sensor Network (WSN) adoption in networked street lighting. Lastly, a review of existing simulation tools for WSN and road traffic simulations is presented.

Chapter 3 proposes a streetlight usefulness model to quantify the usefulness or practicality of street lighting from different road users' perspectives. This chapter also establishes baseline results in terms of usefulness and energy efficiency of state-of-the-art street lighting schemes. To allow the holistic evaluation of these lighting schemes, this chapter also covers StreetlightSim, the simulation environment developed as part of this research. This includes assumptions, simulation models, and evaluation metrics used in this thesis.

Chapter 4 presents the concept of a new adaptive WSN-based lighting scheme, TALiSMaN, for 'grid-powered' streetlights. Simulation results are presented which demonstrate that TALiSMaN provides significant energy savings while providing comparable or improved streetlight usefulness compared to existing lighting schemes.

Although TALiSMaN outperforms the existing lighting schemes, it was unsuitable for addressing the characteristics of solar-powered ('off-grid') streetlights. In **Chapter 5**, TALiSMaN is extended to TALiSMaN-Green, which incorporates predictive behaviour to manage the limited energy budget synonymous with off-grid streetlights. This approach is evaluated through simulation, to illustrate the use of prediction algorithms to enable the operation and usefulness of a network of solar-powered streetlights across a complete night, even with a highly constrained energy budget.

Chapter 6 concludes the research, and outlines areas of future research activity.

Chapter 2

Effective and Efficient Street Lighting

As established in Chapter 1, the role of street lighting in society is indisputable. However, sustaining its operation provides a heavy burden both financially and environmentally. Owing to this, energy efficient initiatives to sustain streetlight operations have been proposed. Still, the principal objectives of having street lighting need to be attainable with these initiatives. To provide an overview of this, Section 2.1 explores the factors that constitute effective street lighting. Section 2.2 presents an overview of energy efficient initiatives in street lighting from three aspects: lamp technology, lighting level control, and renewable energy. Recently, the adaptation of communication networks has become increasingly proposed for street lighting control; a review on this is presented in Section 2.3. A review of existing simulation tools for networked street lighting is presented at the end of this chapter.

2.1 Effective Street Lighting

The requirement of effective lighting considers road users' perceptions that they can see more clearly, better, further, and have an appropriate degree of brightness for undertaking different activities [43, 44]. The British Standard for street lighting states [33]:

> *"Road lighting encompasses the lighting of all types of highways and public thoroughfares, assisting traffic safety and ease of passage for all users. It also has a wider social role, helping to reduce crime and the fear of crime, and can contribute to commercial and social use at night of town centres and tourist locations. Road lighting should reveal all the features of the road and traffic that are important to the different types of road user, including pedestrians and police."*

In some studies, the ergonomic comfort of lighting is also considered [45]. Literature has shown that street lighting significantly improves road user safety by reducing the frequency of accidents after dark [5, 46]. In this section, the factors that constitute effective street lighting are presented.

2.1.1 Recommendations and Standards

One of the most important documents for designing effective street lighting is the International Commission on Illumination's (CIE) Technical Report 115 "Recommendations for the lighting of roads for motor and pedestrian traffic" [47]. This document considers different lighting levels for roads according to factors, such as function of the road, traffic density, traffic complexity, traffic separation, and the existence of facilities for traffic control. These factors are subjectively evaluated, and the nations adopting CIE 115 are expected to extend these factors to suit their own specific requirements and situations. For example, Table 2.1 summaries some of the street lighting standards, and their photometric requirements. In a recent revision [48], CIE 115 introduces the concept of 'adaptive' lighting to minimise the energy demand for street lighting. Compared to 'conventional' or 'always-on' street lighting where the lighting level remains unchanged throughout the entire operational hours, 'adaptive' lighting allows for variable lighting levels at different times according to a weighting. For example, a lower lighting level can be used during better weather, when there is more ambient light, or when less traffic volumes are expected.

Table 2.1: Summary of street lighting standards used in various countries

Country	**Standard**	**Requirement**
United Kingdom	BS 5489.1:2013 Road lighting Part 1: Selection of lighting classes (explains how the CEN/TR standards may be applied to road and traffic categories defined in the UK) [49]	0.3 – 2.0 cd/m^2
Member countries of European Committee for Standardization (CEN)	CEN/TR 13201.1 Road lighting - Part 1: Selection of lighting classes [50]	0.3 – 2.0 cd/m^2
United States of America	ANSI / IESNA RP-8-14 Roadway lighting [51]	0.3 – 1.2 cd/m^2
Australia and New Zealand	AS/NZS 1158.1.1 Lighting for roads and public spaces: Vehicular traffic (Category V) lighting - Performance and design requirements [52]	0.35 – 1.5 cd/m^2
Japan	JIS Z 9110 Recommended levels of illumination [53]	0.5 – 1.0 cd/m^2

2.1.2 A Motorist's Perspective

Driving is a complex operation as it involves several visual tasks [54]. These include: (a) positional, (b) situational, and (c) navigational tasks. For safe and comfortable night-time driving, these tasks require different visual cues to be revealed in sufficient time. For the positional task, motorists needs to maintain their lateral position by constantly adjusting steering and speed. To do this, visual cues about road markings on roads, edge lines, and kerbs must be seen in sufficient time. The main objective of the situational task is to execute necessary manoeuvres to avoid hazards. This involves changes in speed, direction and position of a moving vehicle. To safely perform this task, motorists require visual cues about the surrounding environment, such as nearby vehicles, pedestrians, cyclists and other objects that potentially carry a risk to them. While executing navigational tasks, motorists select a route, and follow it until they arrival at their destination. For proper navigational, motorists need visual cues on landmarks, environment, intersections, guide signs, and other formal information sources to be perceived within a reasonable distance.

While driving, revealing essential visual cues (especially potential hazards which, have been acclaimed as a leading contributor to traffic accidents [55]) in sufficient time or distance is important. The definition of sufficient time or distance varies depending on factors such as travelling speed, motorist reaction delay, and deceleration of the vehicle. As travelling speed increases, the required time or distance for different driving tasks is also extended, allowing motorists to carry out necessary manoeuvres within a reasonable degree of comfort and safety. A comfortable and safe manoeuvre should involve a deceleration of less than 3 m/s^2 while travelling at a speed of above 30 km/h, and avoid the potential chance of injury to oneself or other traffic [56]. Table 2.2 summarises the distance for different manoeuvres required by a motorist at different speeds.

Table 2.2: Required preview distance for different manoeuvre when travelling at different traffic speeds (according to road classes)(adapted from [56]).

Manoeuvre	**Preview distance (m)**		
	Road classes		
	A	*B*	*C*
Maintaining the lateral position within the driving lane	45	75	105
Maintaining the route	150	375	700
Overtaking	450 – 750	600 – 1250	-
Stopping	60	175	350
Evasion	45	125	250
Emergency stop (assuming deceleration of 5 m/s^2)	55	140	270

Class A: Urban road with maximum traffic speed of 15 m/s (∼30 mph or 50 km/h)
Class B: Rural road with maximum traffic speed of 25 m/s (∼55 mph or 90 km/h)
Class C: Motorway with maximum traffic speed of 15 m/s (∼75 mph or 125 km/h)

A vehicle's headlamps can assist motorists to reveal some of the visual cues required when travelling after dark. However, as shown in Figure 2.1, the effectiveness of these light sources has a limited distance. In fact, they become ineffective as the surrounding environment becomes complex, such as in populated areas where the contrast of many visual cues presents little difference from the background [54]. Studies have also demonstrated that a driver can begin to recognise the presence of a pedestrian at an average distance of 0 to 52 m while using dipped headlamps [57]. This scenario is mitigated by having street lighting as it extends the visual range of motorists [58]. Therefore, an effective street lighting should provide required visual cues and reveal potential hazards at a greater distance, thus allowing safer travel after dark.

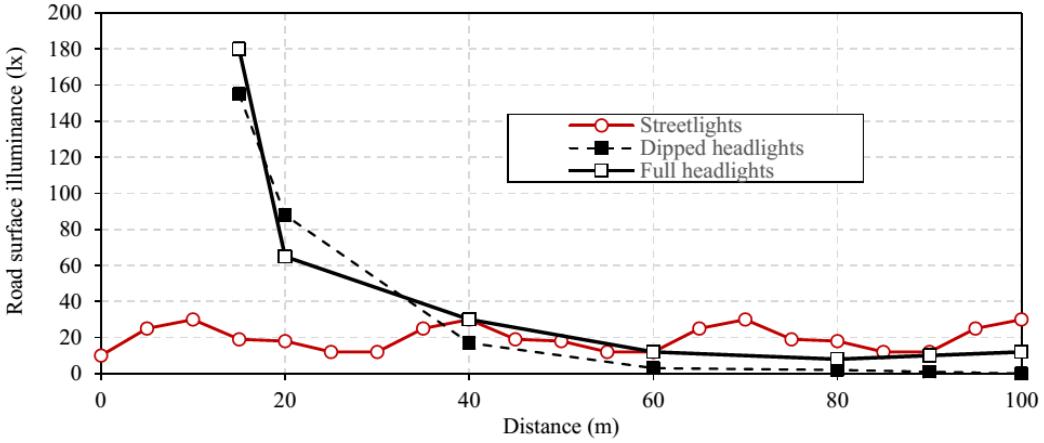

Figure 2.1: The performance of vehicle headlamps (adapted from [58]).

In general, effective street lighting considers average luminance, luminance pattern (also known as uniformity), threshold increment and surround ratio [35]. Among these factors, average luminance and uniformity affect motorists' ability to detect potential hazards. For example, studies show that traffic accidents at night reduce by 21% compared to those happening during the daytime with a one lux increment in illuminance [59]. The effect of various illuminances and uniformities to hazard detection has been extensively studied [60–63]. These studies have reported that reducing the lighting level can result in a longer hazard detection time, or reaction delay. Consequently, this increases the stopping distance where a motorist must be able to stop safely after a potential hazard is detected.

2.1.3 A Pedestrian's Perspective

From a pedestrian's perspective, an effective street lighting assists them in obstacle detection and navigation, identification of other pedestrians (face recognition), and fulfilling their psychological needs (perceived safety) [35–38, 64].

Obstacles can cause pedestrians to fall and may result in serious injuries (e.g. fractures, cuts, gashes or bruises [65]) if they are not detected in time. Thus, an effective street lighting should improve a pedestrian's ability to detect potential obstacles in their walking path. A pedestrian's ability to detect obstacles has been studied with different lamp types, illuminance, and subject ages [66]. The study suggested that the subjects have better obstacle detection as illuminance increases. However, there was a trivial improvement on this once illuminance reached a threshold value of 2 lx in a laboratory environment or about 5.7 lx at road surface illuminance [67]. Young subjects (less than 45 years old) performed better in obstacle detection under all lamp types compared to those of more than 60 years old. The study also reported that the performance of obstacle detection for both age groups can be improved with light sources with higher correlated colour temperature (CCT) and colour rendering index (R_a). Figure 2.2 shows the different apparent colours of objects under light sources with different CCT values. As shown in the figure, a light source with higher CCT value is able to reveal the natural colours of an object, and making objects easier to be recognised from each other and their background.

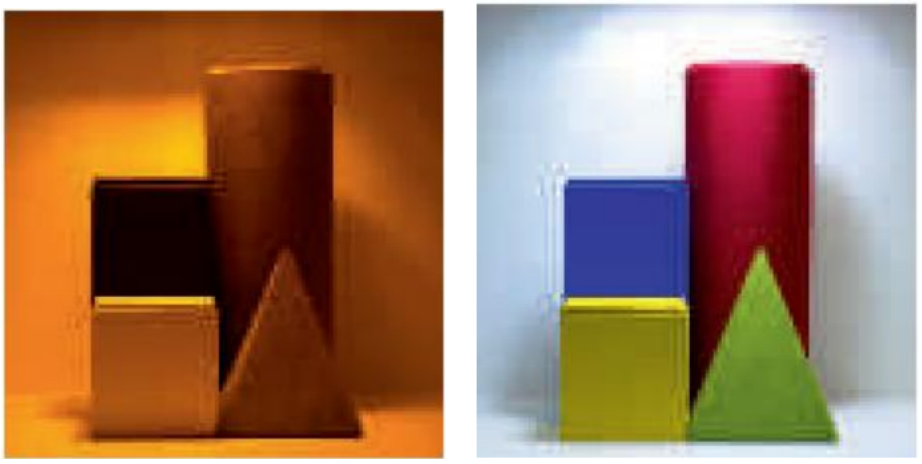

(a) (b)

Figure 2.2: The apparent colour of objects under a light source with (a) low, and (b) high CCT values (reproduced from [68]).

Although increased illuminance can improve the ability to detect obstacles, some studies have reported that pedestrians have a propensity to look two paces ahead when navigating to avoid an obstacle [69, 70]. For the elderly, this is about 1.2 m [71]. Therefore, the detection distance of an obstacle requires a greater distance than this. Fotios and Cheal [67] reported that, to detect a 25-mm height obstacle at a distance of 10 paces (6 m), requires a laboratory illuminance of 0.62 lx, or road surface illuminance of 1.8 lx.

Identification of other pedestrians requires considerably higher lighting requirements compared to obstacle detection [66, 72]. Based on proximity zones [73], effective street lighting should allow identification of other road users at a minimum distance of 4 m.

This can be achieved with a lighting level of 1 lux [35]. These figures were also supported by Raynham and Saksvikronning [74] who studied facial recognition under light sources with different CCT and R_a values. Their results suggested that white light with higher CRI values gives better performance in facial recognition compared to yellow light (low CCT value). Fujiyama *et al.* [72] investigated the effect of five lighting levels, ranging from 0.6 lx to 627 lx, on the distance required for facial recognition. Their results suggested that the distance required for facial recognition has a proportionate relationship with lighting level. Although higher lighting levels extend the facial recognition distance of an approaching pedestrian, further increase in the lighting level has a trivial effect once a plateau is reached. They also reported that the comfortable distance to avoid collisions with an approaching pedestrian is between 4 and 5 m, and these distances slightly decrease with higher lighting levels. However, under low lighting levels (less than 12 lx), these distances increase to between 8 and 9 m.

The effect of three lighting distributions, namely conventional, ascending, and descending brightness, on pedestrians' perceived safety has been investigated [38]. Figure 2.3 illustrates these lighting distributions. For conventional light distribution, all streetlights share the same lighting level. In an ascending light distribution, the streetlight in the pedestrian's immediate surroundings is dimmed, and gradually brightened for those that lie further away from them. A descending lighting distribution is the opposite scenario to the ascending condition. Based on field experiments, the test subjects expressed that they have a similar, and in some cases better sense of safety with the descending lighting distribution, compared to conventional lighting conditions. Among all the lighting distributions, the ascending was the least favoured by test subjects. These results were further validated by a recent study which includes four additional lighting distributions [64]. The study revealed that lighting levels at the proximity of the subjects carry more weight for the subjects' well-being compared to those at a distance. This result is consistent with the descending lighting distribution shown in the earlier study.

2.1.4 Discussion and Summary

Recommendations and standards exist to govern effective street lighting designs. These documents take various factors into account when considering the most suitable lighting levels for roads. However, to accommodate the different needs for street lighting, the resultant lighting levels may exceed or fall below the actual levels required by some road users. Subsequently, this leads to energy wastage. For example, pedestrians prefer higher lighting levels at proximity compared to those at a distance. For motorists, however, they require a fully lit road to assist them in revealing visual cues that guide them to safe travel after dark. In fact, the required lit road segment varies with their travelling speeds and intended driving tasks.

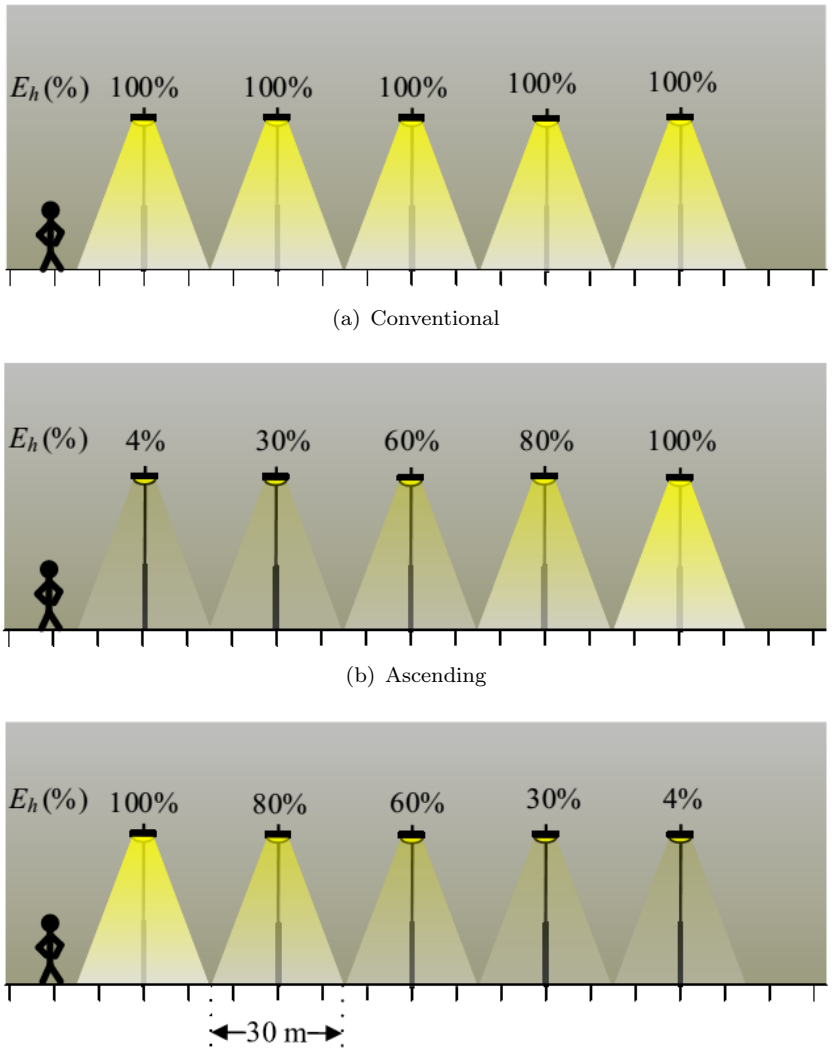

(a) Conventional

(b) Ascending

(c) Descending

Figure 2.3: Different street lighting distributions. E_h (%) is the percentage of the horizontal illuminance for a pedestrian road (adapted from [38]).

Variable lighting levels at different times of the day are suggested in recommendations and standards. This can reduce the energy demand of street lighting, and thus lower carbon emission. However, studies have shown that reduced lighting levels can impair the visual performance of motorists in detecting potential hazards in their travelling paths. For pedestrians, this no longer gives them a sense of safety during late night travel, as lighting becomes inadequate for facial recognition and does not provide a good overview of the surroundings. In short, this deviates from the initial purpose of having street lighting.

2.2 Energy Efficient Street Lighting

As presented in Chapter 1, the introduction of street lighting can reduce both crime and traffic collision, and encourage social-economic activities after dark. However, the financial and the environmental costs resulting from street lighting have become concerning issues for local government. In addition to rapid urbanisation that requires more streetlights, the rise in energy prices has also caused a substantial increment to local government budgets for street lighting [10]. Figure 2.4 shows electricity prices over a period of ten years (2004 – 2013). In this section, state-of-the-art energy efficient street lighting is presented.

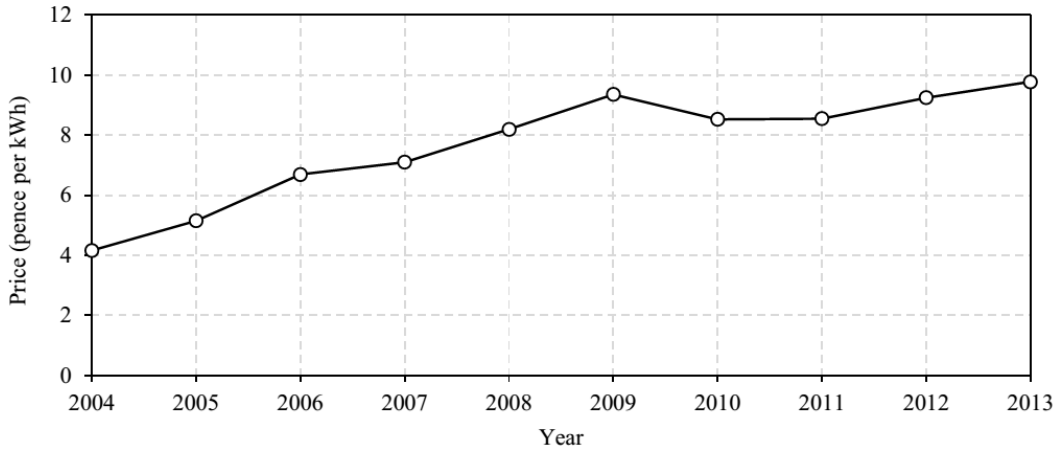

Figure 2.4: Prices of electricity for non-domestic use between 2004 – 2013 (adapted from [75]).

2.2.1 Light Sources

One of the easiest methods to have instant energy saving is retrofitting end-of-life streetlights with more energy efficient light sources (Table 2.3 gives the performance of some commonly used light sources). To date, sodium-based lamps are the most common lamp type for street lighting application. This is because such lamps provide better illumination for less energy. However, sodium-based lamps emit yellowish/warm light which is low in CCT (1800 K – 2000 K) and R_a values (0 – 25) [76]. By comparison, metal halide lamps, which have CCT values between 3000 and 4300 K, and R_a values at 85 [76], were found to be more suitable for street lighting [77, 78]. The use of new, more energy efficient light sources has also been demonstrated by local government in the UK. For example, in 2010, Hampshire County Council [79] and Surrey County Council [80] initiated a street lighting replacement and upgrading programme where most of the streetlights in residential areas were upgraded to white light rather than the older yellow lights. With this programme, Surrey County Council expected savings of 60 metric tonnes of carbon and 150 GWh of electricity over a 25-year operation.

Table 2.3: Lamp technology comparison according to luminous efficacy and their mean lamp service life.

Light Source	**Lumens/Watt**	**Mean Lamp Life (Hours)**
Mercury Vapour [81]	35 – 65	16 000 – 24 000
Fluorescent [82]	33 – 104	16 000 – 20 000
Metal Halide† [83, 84]	33 – 104	16 000 – 20 000
High-Pressure Sodium (HPS) [83, 84]	93 – 141	20 000 – 30 000
Low-Pressure Sodium Lamp (LPS)	80 – 180	18 000 – 24 000
Light-Emitting Diode (LED) [85–88]	58 – 249‡	100 000 – 150 000

† Includes ceramic metal halide
‡ 249 Lumens/Watt is achieved in a laboratory setting [88]

Recent advancements in light-emitting diode (LED) lighting have dramatically improved its luminous efficacy, making it one of the most promising solutions for street lighting application [88]. Various LED street lighting pilot projects have been initiated, primarily to investigate its performance against existing sodium-based street lighting [89–92]. It was reported that LED lamps can lead to 20% energy savings compared to sodium-based streetlights [93]. In general, LED lamps offer a relatively higher CCT (3200 K – 6400 K) and R_a values (80 – 90) compared to sodium-based light sources. Another advantage of LED lighting is that it provides instant lighting once switched on, compared to some 15-minute ignition time required by sodium-based lamps [76]. With LED lamps, not only immediate energy savings can be achieved but their extended lifespan also has been proven to be cost efficient in the long run.

2.2.2 Lighting Level Control

Most streetlights are switched on and remain lit throughout the night. The switching mechanism is either triggered by a clock with a predefined schedule or an integrated light sensor indicating when the surrounding environment becomes dark. However, such operations can result in energy wastage, especially when the lighting is not required or full brightness is no longer necessary. Examples of this are illustrated by Figure 3.2, where a very low volume of road traffic is expected during the middle of the night and early morning. In this section, state-of-the-art techniques in controlling lighting levels, or dimming for energy conservation are highlighted. A summary of these techniques and their performance is shown in Table 2.4.

2.2.2.1 Time-based

As indicated by its name, the time-based control adjusts the lighting level according to a predefined schedule. These schedules often consider reducing the lighting levels when lower traffic volume is expected, for example during midnight and early morning, and

return to full brightness during rush hours. This operation is coherent with the British Standard [33] which states that *"... in some limited situations a lighting installation may be completely extinguished during certain periods of the night when usage is very low."* According to Kostic and Djokic [94], there are two ways to achieve this: (a) two-lamp luminaires and (b) single-lamp luminaires. To conserve energy, the two-lamp luminaires switch off one of the lamps during low traffic. To the best of the author's knowledge, this method is less favoured compared to single-lamp luminaires. One of the causes of this is the housing of the current luminaires is designed to fit one lamp. Thus, retrofitting the current luminaires with two lamps requires a total replacement to the housing.

Single-lamp luminaires often use dimmable lamp types together with step-dimming ballasts. In some cases, the streetlights are networked to allow them to be remotely dimmed from a remote centralised site (Section 2.3 details on this). In the UK, a time-based lighting scheme known as Part-night lighting has been adopted by many local councils to conserve energy [15, 95–97]. This scheme, however, does not require dimmable lamps as the streetlights are completely switched off between midnight and early morning. For safety consideration, some of the streetlights, especially those at strategic locations, are excluded from the scheme. For example, Figure 2.5 illustrates the streetlights (green dots) that are excluded from operating Part-night lighting. According to Warwickshire County Council, UK, they were anticipating an annual saving of £500 000 and three thousand tonnes of carbon by operating their 39 000 streetlights with this scheme [15].

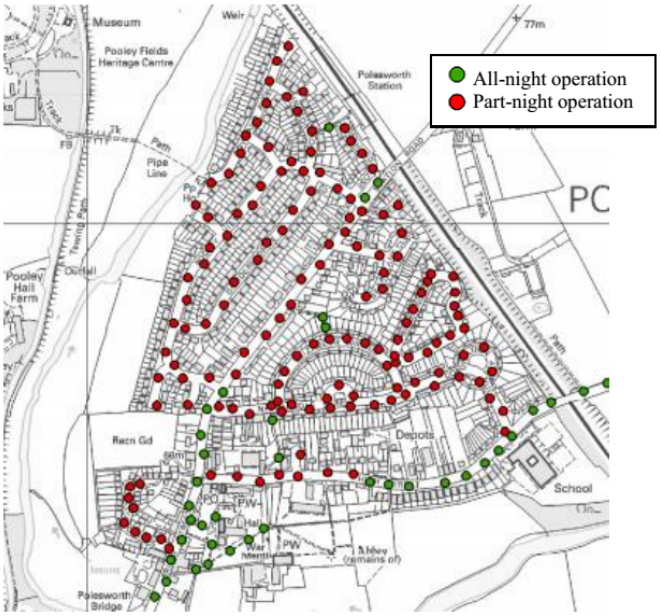

Figure 2.5: Part-night operation of some of the streetlights in Polesworth, Warwickshire (adapted from [15]).

Compared to completely switching off the streetlights in Part-night lighting, step-dimming ballasts are used to reduce the lighting levels according to a preconfigured schedule. For example, Philips Chronosense [98] allows a single-step dimming, and claims to have the

potential for 20% annual energy savings, depending on the adopted multi-wattage ballast and dimming schedule shown in Figure 2.6 (a). Philips Dynadimmer [98] allows streetlight operators to define five different lighting levels during streetlight operational hours. It was claimed that Dynadimmer can have 40% annual energy savings if the dimming schedule in Figure 2.6 (b) is adopted.

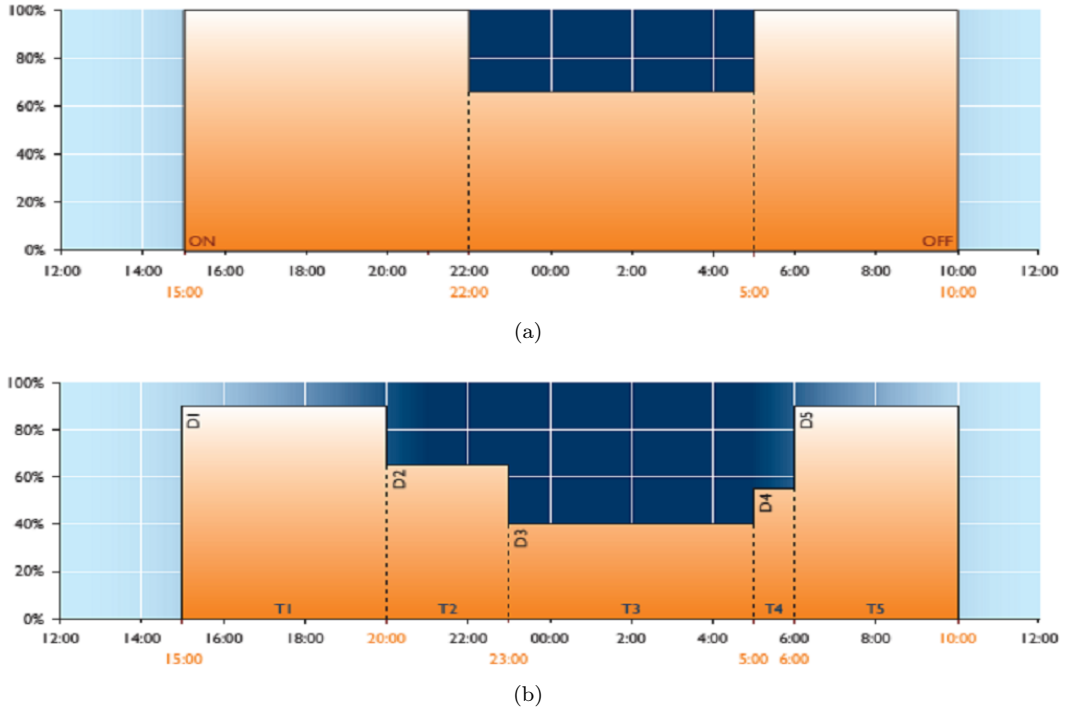

Figure 2.6: A typical lighting adjustment (% of maximum) during different operational hours of (a) Philips Chronosense and (b) Philips Dynadimmer. The main difference between Philips Chronosense and Dynadimmer is the number of dimming steps allowed. Chronosense allows a single-step dimming whereas Dynadimmer permits more dynamic dimming across the night (reproduced from [98]).

2.2.2.2 Sensor-based

Sensors can be used to switch on and off the streetlights. At places, especially where streetlight operational hours are affected by seasonal change, most streetlights are fitted with integrated light sensors, namely photo electric control units (PECUs), to turn lights on and off at preconfigured ambient lighting levels. Figure 2.7 shows a streetlight fitted with a PECU. Due to the ignition time required for certain lamp types, e.g. low pressure sodium-based lamps, to reach their maximum lumen output, these controllers have been configured to switch on when ambient lighting levels fall below 70 lux at dusk, and off as lighting levels increase to 35 lux at dawn [99]. These configurations, however, waste approximately an extra burning hour as ambient lighting at times is still sufficient. Now, with advanced electronic control gears, the streetlights can reach their maximum

lumen output in less time, and thus these initial configurations can be trimmed to, for example, 55 lux on and 28 lux off, to conserve energy [100]. With this initiative, an annual cost saving of £20 000 and a 55 metric tonnes carbon reduction was expected. Compared to binary operation (switching on/off the streetlights) by PECUs, there is increasing interest in continual adjustment to the lighting levels which coincides with local environment, such as weather and traffic conditions. This ambient information is collected by local sensors, which include light, audio, motion or presence, location, and seismic sensors. As the detection range of some sensors is limited [101], this information, in some cases, is shared amongst the streetlights to create a section of lit road segment, collaboratively.

(a) (b)

Figure 2.7: (a) A streetlight fitted with a photo electric control unit (PECU); (b) Typical PECUs (reproduced from [99]).

The lighting levels of streetlights can be adjusted continually to compensate for the available ambient lighting. For example, due to illumination from nearby buildings, the ambient lighting at places next to these buildings is brighter than those in open spaces [20]. This scenario can be recognised with a light sensor, and thus allow for streetlights at different places to have distinctive lighting levels according to their local conditions. This can avoid unnecessary higher lighting levels and thus reduce energy wastage. For places that experience snowy winters, such as Nordic countries, the reflected light from snow was taken into consideration while adjusting lighting levels [102]. With this consideration, the streetlights can reduce their power by 45%, leading to an estimated annual energy saving of 8 GWh from 85 000 streetlights.

Streetlights can maintain a lower lighting level, and increase to full brightness (100%) once a vehicle or pedestrian is detected by a presence sensor. This concept was adopted by TU Delft in their intelligent dynamic street lighting solution [103]. In their solution, the streetlights always operated at 20% power. By utilising a 360° presence detection module mounted on the streetlights, they were able to detect a passing road user, and used this information to increase the lighting levels of the surrounding streetlights to full brightness. Thus, road users were able to move under a fully lit road. It was claimed this solution could reduce energy consumption and carbon emission by up to 80%, compared

to that without any dimming mechanism. In other work, a set of proximity sensors was used to detect a road user entering a road section [16]. Once the road user is detected, all the streetlights within a road section increase their lighting level from 60% to 100% of the lamp's rated power for a duration of four minutes. It was reported that energy consumption of the streetlights was reduced by 37% compared to that without any dimming mechanism.

Similar lighting control was also proposed by Liu *et al.* [104]. The difference between Liu *et al.* with previous works is that vehicle sensing was used to detect entering and exiting vehicles at road intersection zones. The vehicle sensing was achieved by using magnetic loops buried under the roads. To gain more precise control of the streetlight operation, the travelling direction of vehicles is also determined by detecting the lane they are in. With this information, the on-route streetlights in an intersection zone increase their power to 100%, and dim to 60% after the vehicle exits the zone. According to Liu *et al.* [104], this control was able to reduce energy consumption by 24% during off-peak hours (00:00 – 05:00) compared to that without any dimming. However, this method presents a major flaw as the streetlights can continue to operate at the highest lighting level if dimming is not triggered by exiting vehicles. This could happen if the vehicles remain within the zones.

Nefedov *et al.* [19] assumed that a passing vehicle can be detected at a distance of 60 m. After considering the stopping distance (82 m) required for a vehicle travelling at 80 km/h (50 mph), the lighting levels, four streetlights before and one streetlight after a detected vehicle, are increased from 30% to full power. Consequently, a road segment of 240 m before and 60 m after the vehicle is lit. Based on their simulation results, energy savings of between 14 and 70% can be achieved, with savings increasing as traffic density decreases. However, it is not clear that a fully lit road segment of a distance three times larger than the required stopping distance was needed.

Sun *et al.* [42] proposed a multi-sensor system to prolong the operational lifetime of their solar-powered streetlight. The multi-sensor control module was built from audio and passive infrared (PIR) sensors to increase human body recognition, thus providing better opportunity to control the streetlights efficiently. A audio sensor was used to respond to a continuous or short interval audio signal. However, it was ineffective for lower decibel signals. Because of this, a PIR sensor was adopted to improve the accuracy of human body recognition. In their study, the streetlight consistently operated at 40% power, and increased to 70 and 100% once audio and PIR sensors were triggered respectively. According to them, an energy saving up to 40% was achieved with this control, therefore prolonging streetlight operational lifetime.

For the above work, the sensors were either buried under roads or mounted on the streetlights, waiting to be triggered by passing vehicles or pedestrians. Thus, the precise location of the road users is unknown. Lately, location sensors have been used to find

the exact whereabouts of a pedestrian or vehicle, and thus allow more precise control of the streetlights surrounding them. This, however, requires them to be instrumented with location sensors, and constantly broadcast their locations to nearby streetlights. For Müllner and Riener [21], Global Positioning System (GPS) and Internet-enabled smartphones were used in their pedestrian-aware street lighting system. Based on the received GPS signal, the streetlights within pedestrian-defined zones fade-in when pedestrians approach them and fade-out once they walk away. To determine and ensure the correct street lighting needed around pedestrian locations, two zoning concepts were introduced, namely radial safety zone and polygonal infrastructure zone. A radial safety zone defines which streetlights should be switched on or off, and its size is adjusted by pedestrians via a smartphone application which reflect individual fear level (scale of 0 to 100) while waking on the street, whereas a polygonal infrastructure zone prevents unnecessary streetlights, for example those opposite roads or rivers, from being activated by the radial safety zone. However, Müllner and Riener did not detail the relationship between radial safety zone with respect to the fear level, and the potential energy savings of their proposal.

Mohomed [105] relied on Vehicular Ad-hoc Networks (VANET) to relay vehicles' GPS location, speed, and direction to nearby streetlights. With this information, streetlights within a vehicle's travelling route were lit when vehicles came into their proximity. Two lighting controls were suggested: (a) coarse-grained, where streetlights are switched on / off based on the zone where the vehicle is located; (b) fine-grained, where streetlights before the vehicle are lit, and those after the vehicle switched off once the vehicle passes them. These lighting controls share many similarities as proposed by Zotos *et al.* [16] and Nefedov *et al.* [19]. It was reported that coarse-grained control can reduce streetlight energy consumption by 65% compared to 'always-on' lighting, whereas, fine-grained control can further reduce the energy required by coarse-grained controls by 50% [105].

The use of location sensing provides a potential mechanism for precise traffic-aware street lighting, but solutions are inherently limited to owners of such devices. This is illustrated by the fact that only 39% of people in the UK own smartphones, with a significant bias towards younger age groups (16 to 34 years old) [106]. Enabling GPS sensing and Internet connectivity in a smartphone has been shown to increase power consumption by 600 mW [107] and 650 mW [108] respectively. Considering a smartphone's limited battery capacity, such power consumption can deplete a typical battery in a few hours. Moreover, the issues surrounding location-privacy may also prove to be a major obstacle for such traffic-aware street lighting schemes.

2.2.2.3 Artificial Intelligence

To optimise streetlight management and its operation, some works have considered artificial intelligence (AI) in street lighting control. By adopting AI, the lighting control

becomes more adaptive to changes while minimising human intervention in the process. For example, AI based on fuzzy logic and knowledge-based systems was adopted by Volosencu *et al.* [109] in their city-wide street lighting control. In their work, a fuzzy logic controller was used to determine suitable lighting levels for an area based on aggregated information about local ambient lighting and traffic density. This controller was supervised by a real-time knowledge-based controller whose function was to recognise any out of the ordinary situations, such as festivals, traffic congestion, road works, and emergencies, which require a lighting adjustment to the local streetlights. However, this approach is a high level concept, and Volosencu *et al.* failed to discuss potential energy savings with their proposal. The fuzzy logic approach also adopted by Elejoste *et al.* [23] shares many similarities with Volosencu *et al.* [109]. The main difference between these approaches is that Elejoste *et al.* proposed that each streetlight be individually controlled by an intelligent mote, thus allowing autonomous lighting adjustment to each streetlight. These motes were driven by a set of fuzzy rules which were updated by a neuro-fuzzy inference system. Since the computational cost for the fuzzy rules is high, the neuro-fuzzy inference system is often located at a remote centralised site together with all the required information for training processes.

A multi-agent system is a collection of sophisticated programmes that interact autonomously amongst themselves to solve a common problem. In street lighting control, these programmes are embedded in sensor nodes whose function is to perceive the ambient environment collectively, and then adjust the lights to the most suitable levels for an area. This system has been adopted by Moghadam and Mozayan [22] in their street lighting control. Two distinctive agents were formed in their approach: (a) geographical agents that compute streetlight operating schedules for different geographical areas, after considering differences in seasons, weather conditions, locations and atmospheric brightness at those areas; and (b) learning agents that refine these schedules by adjusting lighting levels of the streetlights according to local knowledge, i.e. traffic conditions. The learning agents reduced the lighting levels to low (50% power) when low traffic volume was known. In contrast, lighting levels were increased to 100% when the road had high traffic volume. Based on simulation results, the multi-agent based lighting control reduced the energy consumption of the streetlights by 30% compared to without any dimming mechanism. Escolar *et al.* [18] also applied a similar multi-agent system in their lighting control. Instead of having a binary switching between low and full lighting as proposed by Moghadam and Mozayan, Escolar *et al.* refined the proposed lighting control into three steps, i.e. High (full power), Medium (50% of the lamp's rated power) and Low (25% of the lamp's rated power). The transition between these steps was controlled by an agent, the behaviour of which was defined by the presence of a road user when ambient lighting reached certain threshold values. It was reported that this approach can reduce energy consumption by at least 35% compared to that without any dimming.

An artificial neuron network (ANN) is a machine-learning technique that employs a number of interconnected processing elements (neurones), arranged in layers – input, hidden and output, and working together on a large amount of input (data) to solve specific problems. Pizzuti *et al.* [24] used this technique to learn, and then predict traffic flow to adjust the streetlights to a suitable lighting level. Compared to a statistical approach, an average weekly distribution of traffic flow sampled hourly, Pizzuti *et al.* demonstrated ANN can improve traffic flow prediction accuracy by nearly 50%, and thus ANN offers a better prospect for more efficient lighting control. When the predicted traffic flow reaches a maximum threshold value, full lighting is used, otherwise the lighting level is reduced to 50% if traffic flow is predicted to be below a minimum threshold value. For any traffic flow value that lies between the minimum and the maximum threshold values, the lighting levels scale proportionally with the predicted values. Based on the simulation results, this control reduced energy consumption by 43% on average, compared to 'always-on' lighting.

Zhong *et al.* [110] argued that self-controlled streetlights, for example those fitted with timers or PECUs, can lead to inconsistent lighting operations as they are vulnerable to seasonal change, weather conditions and dust. As a result, some streetlights may misbehave, for example switching on the lights during daytime due to a faulty reading by an individual sensor. To overcome this, they proposed a group-based lighting control inspired from group decision making of social animals and insects. Streetlights are put into groups, and each group is led by a group leader. Using a light sensor, each streetlight (the group members) measures the ambient light intensity periodically, and then forwards a 'turning-on' vote to its group leader once the ambient light reaches a threshold value. If 50% of the streetlights voted 'turning-on', a 'turning-on' command is issued to all the streetlights to switch on their lights. However, energy efficiency of this proposal was not evaluated, as their focus was on enabling group decision making in street lighting control.

2.2.3 Renewable Energy

Recently, renewable energy sources have also been considered as an alternative energy source for street lighting. This setup is often considered in many isolated places, such as rural villages or remote islands. However, due to increasing electricity costs, some were also considering using these energy sources to power the streetlights on motorways [111] as illustrated by Figure 2.8. This is because streetlights powered by these energies offer an economical alternative as neither cabling nor connection to the mains power grid is needed. Furthermore, these energies emit zero carbon whilst generating electricity.

The energy-harvesting streetlights are commonly powered by solar, or are hybrid with wind or fuel cell. The energy harvested from these sources is stored in batteries, to be used after dark. The system size of these streetlights considers the annual energy required for

Figure 2.8: Solar-powered streetlights (reproduced from [111]).

lighting, local weather conditions, as well as the efficiency of energy-harvesting related components, such as solar panel, wind turbine, charge controller, energy storage, in converting these energies into electricity [17]. As the amount of harvested energy varies according to weather conditions, it is also a common practice to size up the system with larger solar panel and battery capacity (depending on the energy demand of the system and local weather conditions) to harvest and store enough energy for a few days of continuous lighting operation [87].

In Thailand, solar-powered streetlights have been evaluated to determine the most suitable system-setting in a typical rural area of the country [26]. The system uses two 70 W solar panels and a battery that is capable of storing 1.2 kWh of energy. The system was evaluated with three different lamps: low pressure sodium (18 W), high pressure sodium (50 W) and fluorescent (36 W). The streetlights were switched on between 18:00 – 22:00 and 05:00 – 06:00. Although the operational lifetime of the fluorescent lamp is shorter than the two other lamps, it was the best lamp for the area. This is because this lamp was widely available at local stores, and it cost less (unit price) than other lamps.

In Brazil, the predominant energy source is hydroelectric. However, the power distribution for such energy is huge and expensive due to Brazil's continental dimension. To overcome this problem, solar-powered streetlights bundled with an LED lamp were proposed [27, 28]. These streetlights comprised a 180 W solar panel, 1.5 kWh battery storage, and 50 W LED lamp, after considering the energy required for one day operation (assuming 6 hours at 100% power and another 6 hours at 50% power) and the load is disconnected from the battery when its charge drops to 30% of its rated capacity. The literature argues that the proposed system is highly efficient (conversion efficiency at 80%) as all the power stages are in direct current, thus eliminating the potential power

loss during AC-DC power conversion. In addition, the average power consumption of LED lamps (50 W) is lower than sodium-based lamps (70 W) while producing the same effective lumens.

Because of variable weather conditions, energy-harvesting streetlights operating solely on one energy source are not an ideal solution. Thus, hybrid-powered streetlights were considered in some places [29,30,32]. To improve the operation of solar-powered streetlights, a hybrid power system based on a fuel cell (FC), solar cell and battery was proposed [32]. This initiative was driven by the fact that solar energy varies significantly in some regions and seasons. Therefore, to sustain the operation of solar-powered streetlights the number of solar cells needs to be increased as well as the energy storage. However, with a fuel cell generating electricity after the battery is depleted, the number of required solar cells can be kept to a minimum. Becherif *et al.* [30] conducted a study on a hybrid power control strategy and energy management after considering the solar cell and FC as the primary power sources for their hybrid-powered streetlights. Two strategies were considered in their work. If solar is selected as the principal energy source, then it is used to charge the battery for lighting during the night time. The FC will provide the necessary energy to guarantee a continuous operation whenever the battery is depleted, whereas if the FC is considered as the principal energy source for lighting, the battery is expected to provide energy during peak power loads and be the principal power source whenever the FC is depleted.

The ideal of having hybrid-powered streetlights was also presented by Georges and Slaoui [29] in their wind-solar-powered streetlight design. According to them, the wind-solar based hybrid power system was a sensible solution because the improvements on the wind turbine maximised its power efficiency. They argued that the system, which was bundled with LED lamps (112 W), was one of the most energy efficient street lighting solutions as it consumed less energy for the same luminary output emitted by a high pressure sodium lamp (250 W). The financial analysis also indicated that the initial system investment could be recovered in 12 years (based on the 2007 electricity tariff in Lebanon). However, the wind-solar hybrid system is only applicable if the deployment locations have sufficient wind.

Generally, energy-harvesting streetlights harvest and store the energy at local storage points. According to Panguloori *et al.* [112], the standalone or decentralised solar-based lighting could be more efficient if the surplus energy was accumulated into a centralised solar power distribution system.

2.2.4 Discussion and Summary

Many techniques have been proposed to conserve energy in street lighting. These include retrofitting end-of-life streetlights with more energy efficient lamps, adjusting lighting

Table 2.4: Street lighting control techniques and their performance.

Technique	**Energy Saving**
The streetlights are completely switched off according to a preconfigured schedule [15].	An annual saving of £500 000 was expected from 39 000 streetlights.
Use one-step dimming ballasts to reduce the lighting levels to a preconfigured level at specified streetlight operation hours [98].	A potential annual saving of 20% compared to conventional or 'always-on' street lighting, if the dimming schedule shown in Figure 2.6 (a) is adopted.
The lighting level is reduced to five different lighting levels during specified streetlight operational hours [98].	A potential annual saving of 40% compared to conventional street lighting, if the dimming schedule in Figure 2.6 (b) is adopted.
The lighting levels of streetlights are continually adjusted to compensate available ambient lighting [102].	A potential annual energy saving of 8 GWh from 85 000 streetlights.
Adjust the sensitivity levels of photo electric control unit to shorten the lamps' ignition time [100].	A potential annual saving of 20% compared to conventional or 'always-on' street lighting, if the dimming schedule shown in Figure 2.6 (a) is adopted.
Use a 360° presence detection module to detect a passing road user, and use this information to increase the lighting level of the surrounding streetlights from 20% to full brightness [103].	A potential annual saving up to 80% compared to without any dimming mechanism.
Use proximity sensors to detect a road user entering a road section, and use this information to increase the lighting level of the streetlights from 60% to full brightness, for a duration of four minutes [16].	The energy consumption was reduced by 37% compared to without any dimming mechanism.
Use magnetic loops to detect passing vehicles, and use this information to increase the lighting level of the on-route streetlights in an intersection zone to 100%, and dim to 60% after the vehicle exits the zone [104]	Able to reduce energy consumption by 24% during off-peak hours (00:00 – 05:00) compared to without any dimming mechanism.
A road segment of 240 m before and 60 m after a passing vehicle is lit [19].	Energy savings of between 14 and 70% can be achieved compared to without any dimming mechanism, with savings increasing as traffic density decreases.
The streetlights is consistently operated at 40% power and increased to 70% and 100% once audio and PIR sensors are triggered [42].	An energy saving up to 40% was achieved compared to without any dimming mechanism.
Use VANET to relay vehicles' location, speed, and direction to nearby streetlights, and use these information to control the lighting level of the streetlights [105].	The coarse-grained control can reduce energy consumption by 65% compared to conventional street lighting. The fine-grained control can further reduce the energy required by coarse-grained controls by 50%.
Use a multi-agent system to determine the two different operating lighting levels (low and full lighting) [22].	Energy consumption of the streetlights was reduced by 30% compared to without any dimming mechanism.
Use a multi-agent system to determine the transition of three different operating lighting levels, i.e. High (full power), Medium (50% of the lamp's rated power) and Low (25% of the lamp's rated power) [18].	Energy consumption was reduced by at least 35% compared to that without any dimming.
Use ANN to learn, and then predict traffic flow to adjust the streetlights to a suitable lighting level [24].	Energy consumption was reduced by 43% on average, compared to conventional street lighting.

levels (dimming), and using renewable energies to power the streetlights. To give greater energy savings, these techniques are often integrated [20, 102]. A summary of these techniques and their performance is given by Table 2.4. Amongst these techniques, dimming has been widely explored. With sensing and AI integrations, dimming becomes more adaptive to environmental changes with minimum human intervention. However, many have failed to discuss the derived lighting levels during dimming. For example, lighting levels were dimmed between 20 and 60% power, and increased to 100% once a road user was nearby [16, 19, 42, 103, 104], but the British Standard [33] allows lights to be completely extinguished when the usage is very low. Moreover, in some works [16, 19, 105], streetlights were dimmed in groups or zones, but still the basis for group and zone forming is not reflecting the needs for street lighting established in Section 2.1. This could be because there is no technical mechanism exists to facilitate the analysis of the impact of dimmed street lighting on road users.

Energy-harvesting streetlights are favoured in remote places, such as rural villages or isolated islands, for two reasons: ease of installation as long haul cabling is not required; and use of renewable energy which emits zero carbon while generating electricity. When these streetlights were suggested for urban application [113], some argued that they, especially the ones powered by solar, were not cost effective and were visually intrusive [79, 111]. One of the causes of this is that these 'off-grid' streetlights require large solar panels and energy storages in order to provide a reliable source of light throughout the night, especially during the seasons when daylight is relatively shorter. This leads to an oversized and thus overpriced system. As mentioned in Section 2.2.3, one of the factors determining the system size of these streetlights is the amount of energy needed to provide light during the night. Thus, a smaller system can be adopted if the required energy is reduced. Based on the reviewed literature, the use of energy efficient lamps, sensing and AI can significantly reduce the energy required by 'grid-powered' streetlights. However, their application to solar-powered street lighting is restricted as they have yet to consider that the energy harvested from solar varies due to weather conditions. As a result, these streetlights may, for example, operate normally until the middle of the night, but run out of energy and be completely inoperable in the early morning. Because of this, a different lighting control is required for these streetlights. This lighting control needs to minimise energy consumption, so that the solar panels and energy storage devises (batteries) can be as small and cheap as possible. Moreover, this lighting control should also consider the limited energy budget of these streetlights without compromising the lighting needs for road users.

2.3 Introduction to Networked Steeet Lighting

From recent literature and commercially available products, e.g. Mayflower [114], street lighting can be categorised into either standalone or centralised control. The standalone

control is commonly used on streetlights fitted with timers or PECUs, allowing them to operate autonomously without requiring any networking capability. This control is also used in most of the energy-harvesting streetlights discussed in Section 2.2.3. Due to the lack of networking capability, the retrieval of the operation status from these streetlights is also absent. Subsequently, streetlight operators rely on patrols to scout for, or the public to report on a faulty streetlight. Figure 2.9 shows some of the tools that can be used by the public for this.

A centralised control uses various well-established long- and short-range communication technologies to form a link between a remote centralised site and streetlights. Table 2.5 summarises the adopted communication technologies in networked streetlights. With these communication technologies, streetlight operators can monitor, issue operation commands, such as switch on/off, dim, and receive alarms for abnormal operation conditions, such as faulty lamps, to/from the networked streetlights, at a centralised control site. Commonly, the centralised control spreads over several tiers. These tiers comprise a centralised control site, local branches, and light controllers and sensors installed at each streetlight. The commands are initiated by the centralised site, and then propagated to every streetlight via local branches as their gateways. The centralised site includes a complex software management system that comprises GIS and database systems to store streetlight management data which can be accessed via an interactive system interface [115–117]. The local branches act as a gateway translating and forwarding commands, and collecting streetlight operation status, and then relaying them back to a centralised site.

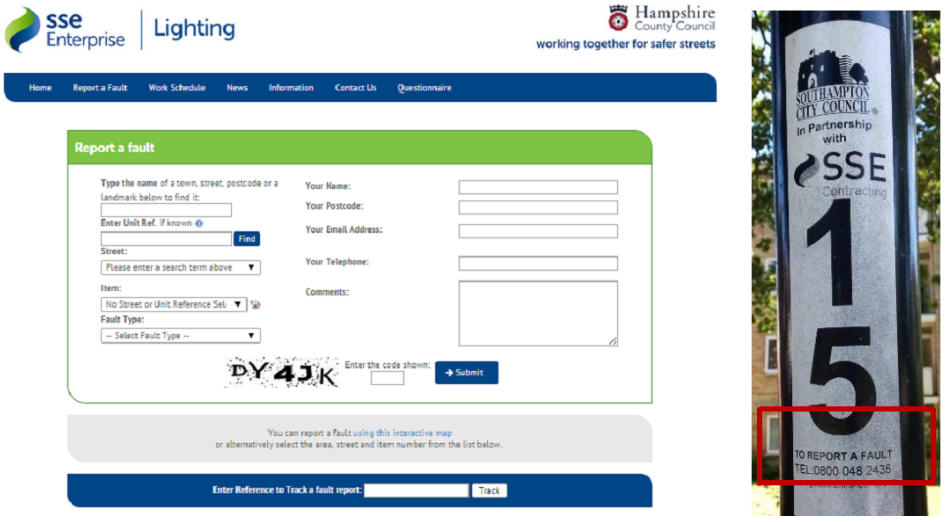

(a) (b)

Figure 2.9: Tools for reporting a faulty streetlight: (a) web form [118], and (b) a note for the public to report a faulty streetlight.

Table 2.5: Communication technologies in networked street lighting systems.

Year	**Communication Technology**		**Remark**
	Remote centre to Local branches	*Local branch to Streetlights*	
2005	• Internet (telephone network [119])	• PLC [119]	
2006	• Text message services from mobile telephone network [115] • Internet (Mobile telephone network) [116, 120]	• PLC [115, 120] • ZigBee [116]	
2007	• Internet (Mobile telephone network) [121]	• WSN [121]	• Using MICA2 to form WSN
2008	• Internet (Mobile telephone network, [122]) • TCP / IP compatible network [123]	• PLC [122, 123]	
2009	• Wireless transceiver (nRF401 chip) operating on 433 MHz of ISM frequency band [124] • Internet (Mobile telephone network) [125, 126]	• PLC [124] • ZigBee [125–127]	• [126] focused on enabling ZigBee in streetlight monitoring and suggested using Ethernet or Mobile telephone network • [127] focused on ZigBee performance in streetlight system (also discussed the routing problem of)
2010	• Internet (Mobile telephone network [117, 128]) • TCP/IP compatible network [129]	• PLC [117, 128] • WSN [129]	• Explicit detail on WSN was not available in [129]
2011	• Text message services from mobile telephone network [130] • Internet (Mobile telephone network [131, 132]) • TCP/IP compatible network [21, 133]	• PLC [132, 133] • ZigBee [20, 21, 131], • IEEE 802.15.4 compatible devices [134]	• [130] focused on enabling SMS from streetlights to remote control • [134] focused on the routing problem in streetlight topology
2012	• Internet (Mobile telephone network [135]) • TCP/IP compatible network [96] • ZigBee Coordinator [136]	• ZigBee [96, 136, 137] • 6LoWPan	• [96] used Internet-ZigBee gateway to interconnect the ZigBee network with centralised control. • [136] used a ZigBee coordinator at centralised control • [137] focused on enabling WSN for inter-streetlight communication
2013	• ZigBee Coordinator [17]	• ZigBee [17]	• [17] used a ZigBee coordinator with extended communication range (about 1.5 km)
2014		• Mobile telephone network (Short Message Service) [138]	• [138] linked the energy-harvesting streetlights directly to centralised control

2.3.1 Long-Range Wireless Communication

In many networked streetlights, long-range communication technology uses general packet radio service (GPRS) to extend the communication range [117, 120, 121, 139] between a centralised site and the local branches. There have been some attempts to establish communication between a centralised site and streetlights directly without any local branches as gateways. For example, Siregar and Soegiarto [138] equipped each solar-powered streetlight with a cellular network modem to relay current and voltage status back to the monitoring centre. They argued that wireless technologies, such as ZigBee, have limited communication range. Thus, the effort to manage these wireless devices will be enormous, especially when streetlights are spread over a large area, compared to the cellular network which is already widely available, managed and maintained by telephone companies. However, the reliability of GPRS can be compromised, especially during peak hours where access to the service is limited [39].

Short Message Service (SMS), a text messaging service for fixed line or mobile phone devices was also explored for networked streetlights [115, 130, 138]. However, user friendliness is not the design priority in these works as users need to type in special commands to remotely switch the streetlights on or off. In addition, SMS is prone to typo errors, and users have to memorise different commands for their systems. The limited character allowance (160 characters) in each SMS also constrains its usability in streetlight application. Furthermore, SMS also suffers delays in delivery, or loss due to congestion in the cellular network [40].

2.3.2 Short-Range Wireless Communication

As shown in Table 2.5, there is growing interest in adopting system wide wireless communication in the networked street lighting system, although wired network, such as power line communication (PLC), is also to be found. Recent networked streetlights are keen to adopt WSNs, especially those based on IEEE 802.15.4 standard such as ZigBee, as a means to establish a link between local branches and the streetlights, and inter-streetlight communications. One of the causes that is driving this development is the advantage demonstrated by WSNs over PLC as summarised in Table 2.6.

2.3.2.1 IEEE 802.15.4 / ZigBee

IEEE 802.15.4 standard [140] is proposed for low rate wireless personal area network (LR-WPAN). It defines the characteristics of the physical (PHY) and media access control (MAC) layer. The network devices in IEEE 802.15.4 networks can either operate in beacon-enabled mode or non-beacon-enabled mode. In beacon-enabled mode, a superframe structure coordinates media access between all the associated nodes. A superframe

Table 2.6: Advantages and limitations of WSN and PLC in networked streetlight application [137].

WSN	PLC
• WSN devices cost less than PLC devices.	• High cost of devices compared to WSN devices.
• WSN is dependent on the environment that could affect changes in the communication path, and thus requires installation of repeater devices.	• No obstacles in the communication path.
• WSNs are affected by devices that function within the same band (Wi-Fi, Bluetooth).	• PLC is not affected by wireless interference.
• Integrate a high number of nodes (over 500) and have redundant communication paths.	• Incorporates a low number of nodes (under 70), and has limited communication distance (300 – 350m).
• Highly efficient for sink node applications and scalability that enables better control over the network and maintains high performance levels.	• A part of the network may remain isolated in case of a short circuit. Low resistance to interference/noise and impediments in transition of signal through transformers.

is sandwiched between two beacons which are periodically broadcast by the network coordinator. The period between these two beacons is comprised of two parts: (a) an active period; and (b) an optional inactive period as shown in Figure 2.10. The data exchange between the network devices commences during the active period, and then the devices will enter a low power (sleep) mode for energy conservation. For the non-beacon-enabled mode, a network device first waits for a random number of back-off periods, T_{BO}, before the media is assessed. If the channel is idle then data transmission is commenced; otherwise the device will wait for another T_{BO} until it reaches the maximum number of back-offs (default is 5). Once the maximum number of back-offs is reached, the packet will be discarded from transmission.

The beacon-enabled mode has better performance in terms of prolonging the network's lifetime. In a multi-hop network scenario, however, it experiences performance degradation compared to the non-beacon-enabled mode due to beacon collision [141]. In beacon-enabled mode, beacons are periodically broadcast by the network coordinator. Nodes associated with the network coordinator should receive these beacons persistently and synchronously. However, forwarding these beacons in a multi-hop scenario increases

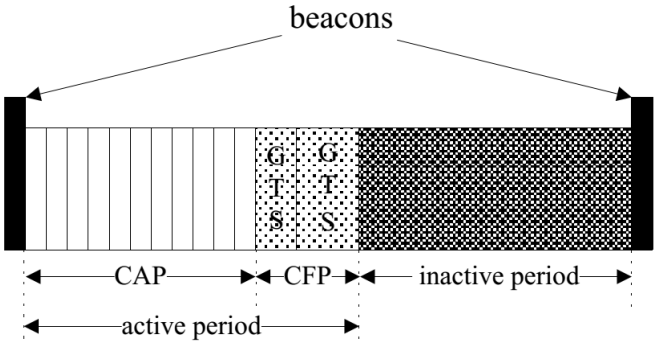

Figure 2.10: IEEE 802.15.4 superframe structure (based on [140]). The active period consists of two groups of time slots: contention access period (CAP) and contention free period (CFP). All the associated nodes will compete for their channel access during the CAP using carrier sense multiple accesses with collision avoidance (CSMA-CA) protocol. For guaranteed quality of service, an optional CFP is maintained by the network coordinators where network devices are given some guaranteed time slots (GTS) to use the channel.

the probability of beacon collision with other beacons, data frames, or control frames. Compared to the data frame or control frame collisions which can be resolved by retransmission, a beacon collision will result in the total collapse of the superframe structure. Thus, all the associated nodes will cease from transmission. Furthermore, the inactive period in beacon-enabled mode, as shown in Figure 2.10, also introduces a mandatory data transmission latency as nodes are seized from transmitting data during this time.

The ZigBee standard [142] is built upon IEEE 802.15.4 by defining the network and application layer. Compared to IEEE 802.15.4, three different network devices are defined in the ZigBee standard. They are: (a) ZigBee end-device which is analogous to an end-device in IEEE 802.15.4; (b) ZigBee coordinator which corresponds to IEEE 802.15.4 network coordinator; and (c) ZigBee router, an IEEE 802.15.4 full-function device equivalent to that responsible for ZigBee routing protocols. The ZigBee standard maintains star topology as supported by IEEE 802.15.4, but peer-to-peer topology has been extended to tree and mesh topologies. For networked streetlights, ZigBee coordinators are usually located at local branches and work as a gateway between the centralised site and the streetlights. Depending on the adopted network topology, ZigBee end-device or ZigBee router is equipped with sensors and/or lighting controller.

2.3.2.2 Routing Protocol

Routing is the ability to send data from one network device to another, which sometimes can be over several hops. As shown in Table 2.5, many of the proposed streetlight systems use ZigBee to establish inter-streetlight communication. One of the reasons for this is that ZigBee has "tree-based" and Ad-hoc On Demand Distance Vector (AODV) routing protocols ready to be used for its tree and mesh network topology respectively

[142]. There are numerous works to improve the routing performance in IEEE 802.15.4. A survey of these routing protocols can be found in Al-Karaki and Kamal [143], and Boranti *et al.*'s [144] studies. However, few have considered their use in a networked streetlight application.

To forward data in the tree topology, ZigBee routers need to maintain address information about their associated parent and child nodes. The parent-child association is established when a network device joins the network. Upon receiving a routing request, a ZigBee router determines whether the data is forwarded to one of its associated router children or end-device children. If the data is intended for one of its associated child nodes, then it is forwarded to the appropriate child node, otherwise it is forwarded to its parent node. The same routing process is repeated at the parent node until it reaches its destination. This routing protocol is simple, and thus allows routers to operate in beacon-enabled mode as specified in IEEE 802.15.4 standard.

In mesh topology, a routing table (RT) is needed to determine appropriate forwarding paths to destinations. Upon receiving a routing request, ZigBee routers consult their RT for the next hop to the destination. If such a hop is unavailable, a route discovery process to the destination is initiated based on AODV [145] protocol. During the route discovery, the network devices broadcast a route request message (RREQ) which eventually travels through the entire network. As the RREQ travels, it accumulates forwarding cost (hop count or other link quality estimations) in one of its message fields which will later be used in route selection. Once the RREQ reaches the destination device, the RREQ is replaced with a route reply message which will travel back to the RREQ's originator using the path previously discovered by the RREQ.

Flooding protocol is one of the classical data dissemination techniques which offers simplicity and aggressive data propagation. Whenever a node receives data, the node will broadcast it to all its neighbours if the data has never been forwarded before. However, the flooding protocol is rarely used for information propagation in WSNs as it suffers from implosion, resource blindness and broadcast storm problems [146, 147]. Instead, it is normally used for route discovery and network initialisation phase as demonstrated in AODV. Several improvements have been proposed to address the limitation of this classical protocol by introducing randomness and threshold in data forwarding decisions. Gossiping [148], Flossiping [149] and directed flooding with self-Pruning [150] are some of the examples that use randomness in their data forwarding decisions, whereas threshold-based flooding can be found in Graded Back-off Flooding [151], single gossiping with directional flooding [152], and Flash Flooding [153].

Jing *et al.* [154] designed a single-hop broadcast routing protocol by considering the hierarchical addressing used in their networked streetlights. According to their hierarchical addressing, the nearest streetlight controller to the local branch is assigned with the smallest running number. Likewise, the furthest streetlight from the local branch

is assigned with the largest running number. Once the data arrives at intermediate streetlights, the source and destination addresses are compared. If the source address is greater than the destination address and smaller than the intermediate node address, then the data is in the correct forwarding direction and it is broadcast to its one-hop neighbours. Otherwise, the data is discarded. To avoid multiple transmissions of the same data flooding the network, every streetlight is assigned with a random waiting time before the packet is broadcast.

Denardin *et al.* [134] argued that existing geographic routing protocols are insufficient to handle voids in the streetlight network. This is because these protocols were based on unrealistic assumptions. They combined two protocols to solve the void problems in the streetlight network. They used Coordinated Depth Forwarding (CDF) as a recovery mode for Greedy Perimeter Stateless Routing (GPSR) protocol when a void was encountered. Figure 2.11 shows the operation of the proposed protocol. When a void is encountered, the proposed protocol compares the forwarding orientation angle from the node w to the destination node v with an angle to any known base stations j. The base station with smallest absolute angle different from $(\overline{wv})$ and lower than $\pi/4$ is chosen as the candidate for depth forwarding away from the void. Based on their simulation results, the CDF has improved GPSR performance by around 28% based on the number of hops ratio.

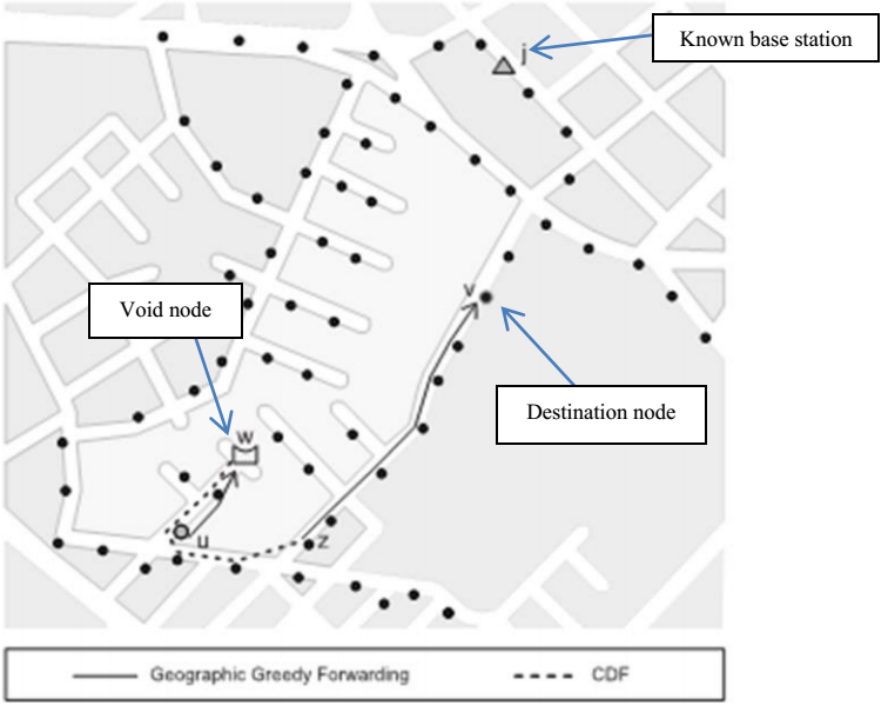

Figure 2.11: The operation of coordinated depth forwarding at node w before switching to perimeter stateless routing at node z (adapted from [134]).

Pantoni and Brandão [155] proposed two routing algorithms based on the Greedy Perimeter Stateless Routing protocol (GPSR), namely Geocast GPSR (GGPSR) and GGPSR II. The idea behind these algorithms was to forward the message to the destination's

central point based on a modified GPSR, without using a specific coordinated location. According to them, this feature is important as it is necessary to control and monitor a specific group of streetlights in certain areas. Once the message has arrived at the central point, the first receiving node broadcasts the message to all the nodes in the area. The difference between GGPSR and GGPSR II is the trigger conditions of the '*hello*' message. The '*hello*' message in GGPSR is triggered according to a pre-determined period, whereas the '*hello*' message in GGPSR II is triggered to inform data delivery failure. In their recent work to improve a successful packet delivery rate, they implemented a point-to-point confirmation message to their GGPSR [156]. If the confirmation message is not received within a specific time frame, the improved protocol will attempt to re-transmit the packet to the same node. If the problem persists, the next closest neighbour node to the destination node is selected for future forwarding. Based on the simulation results, the delivery rate based on the confirmation message is improved compared to its predecessor.

2.3.3 Discussion and Summary

Both long- and short-range wireless communications enable the remote monitoring and control of streetlights from a centralised control site. For the reviewed literature, the majority of long-range wireless communications rely on the cellular network-based Internet. However, a centralised system is subjected to single point failure [23] as its performance depends upon the reliability of the long-range communication network. Moreover, such a solution is unsuitable for places with limited access to a cellular network. This establishes the need for a distributed and autonomous lighting control.

As shown in Table 2.5, IEEE 802.15.4 based standards have been widely adopted for inter-streetlight communication. Their usage is mainly for disseminating management commands, and forwarding the streetlight operation status back to the centralised site. These operations are more tolerant to delay compared to relaying information on detected road users. As presented in Section 2.2.2.2, this information is used to control the streetlights in close proximity to detected road users [16, 21, 105], and claims to have up to an 80% energy saving [103]. However, if this information is delayed, the streetlights will respond more slowly than the road users' movements. As a result, streetlights will fail to operate as intended. Although IEEE 802.15.4 based WSNs were proposed for relaying this information, as per the author's best knowledge, the technical details and performance of IEEE 802.15.4 for relaying traffic information for real-time street lighting control is still unclear. One of the causes of this is the abstraction of the WSN operations in street lighting control, and the assumption that the network can perform as required.

2.4 Modelling and Simulating the Networked Street Lighting System

A model is a close representation of a physical system under study. During the modelling process, the relevant components of a system are identified, and the operation and interaction between the components are conceptualised. Simulation is the process of executing a modelled system. The output of the simulation is used to evaluate the operation strategies of the system, or to estimate the behaviour of the system that is subject to variability. Thus, simulation is used before an existing system is altered or a new system is developed [157].

Some of the proposed lighting controls have been tested via scaled-down hardware implementation or in an on-road study [23, 42, 115, 130]. Nevertheless, they were limited to a relatively small network (up to nine streetlights). This is perhaps because they were expensive to run, or to ease experimental control during the studies. Simulation allows for rapid evaluation and fine-tuning of networked streetlight systems, and thus it is widely used in many lighting control systems as presented in Section 2.2. To allow a holistic analysis of networked street lighting systems, tools are required that can model and simulate: (a) communication network; (b) streetlight operation; and (c) road traffic. This section gives an overview of simulation tools that have been/can be used for these purposes.

2.4.1 Simulating Communication Network

Network simulator version 2 (ns-2) [158] which was developed by UC Berkeley has received a lot of attention in communication network-related research as it supports a large number of routing protocols, network traffic models and network types. It is a discrete event simulator written in C++ and Object Tool command language (OTcl) as its simulation interface. Initially, ns-2 was used for simulating local and wide area networks. In recent years, ns-2 also extended its support to wireless networks, mobile ad-hoc networks and sensor networks, making it one of the more popular tools for communication network-related simulations. However, there is no clear boundary between the simulation kernel and the models; thus performing a repeatable and meaningful simulation with ns-2 requires advanced skills and a clear understanding of existing models. The first time user might have a longer learning curve for ns-2 as there are only a few manuals that are user-friendly. Additionally, the scalability of ns-2 is limited in terms of its memory usage and simulation run-time. These limitations appear to be a problem especially in the study of very large computer networks, such as WSNs, or peer-to-peer networks, which potentially comprise hundreds of thousands of nodes.

Network simulator version 3 (ns-3) was first released to the community in 2008 and unlike ns-2, ns-3 abandons the use of OTcl, and the new simulator is implemented purely for C++. Still, some parts of the simulation can be implemented using Python. ns-3 adopts architectural concepts from GTNetS [159], a simulator with good scalability characteristics, to improve its scalability compared to its predecessor [160]. Although, ns-3 is considered as a replacement for ns-2, it is not an extension of its predecessor and is not backward compatible. For this reason, the models previously implemented in ns-2 need to be manually ported to ns-3 [161].

Similar to ns, the Objective Modular Network Testbed (OMNeT++) [162] is another open source, discrete event simulator based on C++. However, NEtwork Description (NED) language is used to describe its network topology compared to OTcl used in ns-2. OMNeT++ models are independent from their simulation kernel; thus the modules never patch the kernel during the update. OMNeT++ component based architecture allows more complex and larger composite components to be assembled from reusable simple modules. The modules communicate by exchanging messages through gates, the input and output interface of the modules. The major drawback of OMNeT++ is a lack of many network protocol models compared to ns.

In recent years, several Java based simulators have been developed as an alternative to highly popular simulators like ns and OMNeT++. Java based simulators are usually platform independent but slower in simulation run-time. However, some literature shows that Java based simulators can excel in certain simulation scenarios [160]. J-Sim [163] (formerly known as JavaSim) is an open source, component based network simulation tool. J-Sim shares similarities with ns-2 and OMNeT++ as it also uses a secondary scripting language, i.e. Tcl/Java as its simulation interface. The components in J-Sim communicate with one another by sending and receiving data via their ports, instead of gates in OMNeT++, but the concept is similar.

Java in Simulation Time (JiST) is another Java based simulation tool proposed by Barr *et al.* [164]. It focuses on efficiency and transparency by utilising one programming language and runtime (ns-2, OMNeT++ and J-Sim are dual-language simulators). It is usually used together with Scalable Wireless Ad Hoc Network Simulation (SWANS), a simulator that is built on top of it. However, the official development of JiST has stalled.

2.4.2 Simulating the Road Users

Road traffic simulation is essential for enabling intelligent transportation system development. There are a few road traffic simulators either commercially available or in open-source format. An in-depth overview of these tools was reported by Boxill and Yu [165]. Nevertheless, not all the road traffic simulators are designed for both traffic and communication network related research. Recently, the concept of co-simulation, which

integrates two simulation environments, was explored in order to gain advantages from simulators in different domains. This section gives an overview of recent works that enables coupling between road traffic and communication network simulators.

Simulation of Urban MObility (SUMO) [166] is an open-source traffic simulation package developed by the German Aerospace Centre. Due to its microscopic feature, each vehicle is modelled and simulated individually, which means to say that it is a suitable tool for various vehicular-related research. Figure 2.12 shows the graphical user interface of SUMO while simulating vehicular traffic at two cross roads. Vehicular communication is one of SUMO's most popular applications in Vehicular Ad Hoc Network (VANET) research as its Traffic Control Interface (TraCI) provides for opportunities to couple with other external network simulators. For example, Traffic and Network Simulation Environment (TraNS) [167] is a tool used to couple SUMO with ns-2 to generate realistic online or offline mobility traces for VANET related simulations. The mobility traces generated by TraNS can also be used by JiST/SWANS [168]. A similar attempt is also performed with OMNeT++ where Vehicles in Network Simulation (Veins) [169] was developed. In order to improve the performance of network simulators, offline mobility traces have also been considered in some research work. Tools like the Mobility Model generator for Vehicular network (MOVE) [170] used SUMO for offline mobility traces generation. However, offline mobility traces are only able to investigate the influence of road traffic on network communication but not otherwise.

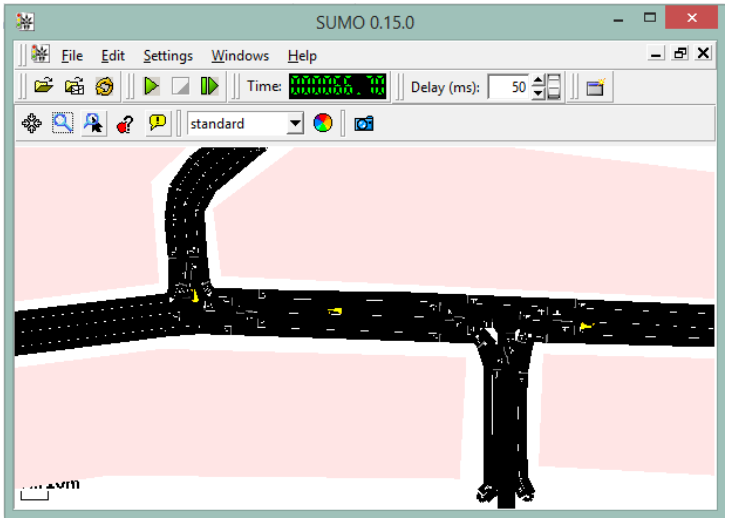

Figure 2.12: A screenshot of SUMO's graphical user interface, simulating vehicular traffic at two cross roads.

CARISMA [171] is a proprietary, time- and position-discrete based road traffic simulator, but it is a simple simulator as it only supports a relatively small scenario, i.e. two lanes per road, and all the roads have the same traffic capacity and priority. Despite this weakness, it is able to compute vehicle routes during runtime, and has become the simulator of choice for dynamic vehicle routing-related research. To allow coupling with other network simulators, CARISMA has been updated to support transmission control

protocol (TCP) connection and enabled coupling with ns-2 [172]. However, CARISMA is no longer supported.

VISSIM [173] is a microscopic, behaviour-based discrete road traffic simulation software package. As compared to SUMO, it is not available in an open-source format, and as a commercial product it requires a licence to operate. Since access to the source code is restricted, its functionalities can only be customised by adjusting certain parameters, and through its programmable software interfaces, i.e. Component Object Model interface and customisable dynamic link library, VISSIM can couple with other simulators, such as ns-2, MATLAB, and QualNet [174–176].

2.4.3 Simulating Streetlight Operation

PeKing University STreet RAndom Waypoint for Lamp (PKU-STRAW-L) is a streetlight simulation platform designed to investigate the use of a vehicular ad-hoc network (VANET) in streetlight control [177, 178]. This tool adopted JiST as its discrete event simulation engine. The motivation to adopt JiST is that it provides an integrated, configurable and flexible environment to evaluate VANET related research problems. Figure 2.13 shows the architecture of the simulator. The Street Lamp App-Engine layer is responsible for streetlight related settings, such as the location, power, and control scheme. The Street Random Waypoint (STRAW) mobility model is used to generate realistic vehicular traffic. However, STRAW requires the road network to be presented in the Topologically Integrated Geographic Encoding and Referencing system (TIGER), which is produced by the US Census Bureau. Because of this, the road network in the TIGER dataset is limited to cities in the US, so Yang *et al.* [178] designed their own road network in Peking University during their evaluations.

Popa and Marcu [179] used OMNeT++ to evaluate the energy savings of a pedestrian-aware street lighting control. To enable their evaluations, two OMNeT++ modules were created: (a) *human*, a simple module that represents a moving pedestrian; and (b) *device*, a compound module that represents a control device on the streetlights. Due to the simplistic evaluation criteria, a linear topology of ten streetlights, as illustrated by Figure 2.14, was considered in their evaluations. In a real scenario, however, the streetlight topology can be complicated, for example at road junctions or roundabouts. Similarly, a simple pedestrian mobility model was assumed in the human module. This module assumed that a pedestrian's walking speed is limited to 1 m/s, and has their positions updated every 14 seconds. The device module simulates the operation of a microcontroller that controls the street lighting based on the sensory data collected by a light sensor and a pedestrian sensor. Although these modules were developed to evaluate the performance of a pedestrian-aware lighting control, they are meant for a simple, small-scale scenario. Additionally, the developed modules only accounted for pedestrian

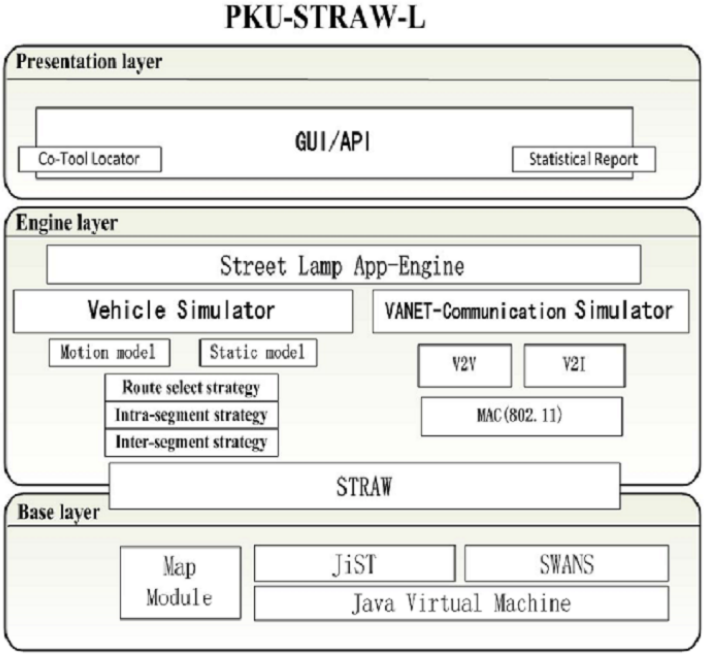

Figure 2.13: Architecture of PKU-STRAW-L (reproduced from [178]). JiST/SWANs is the core simulation engine of the tool. For streetlight related settings, a dedicated engine layer was developed, namely Street Lamp App-Engine. This engine is responsible for streetlight related settings, such as streetlight topology, and control policy.

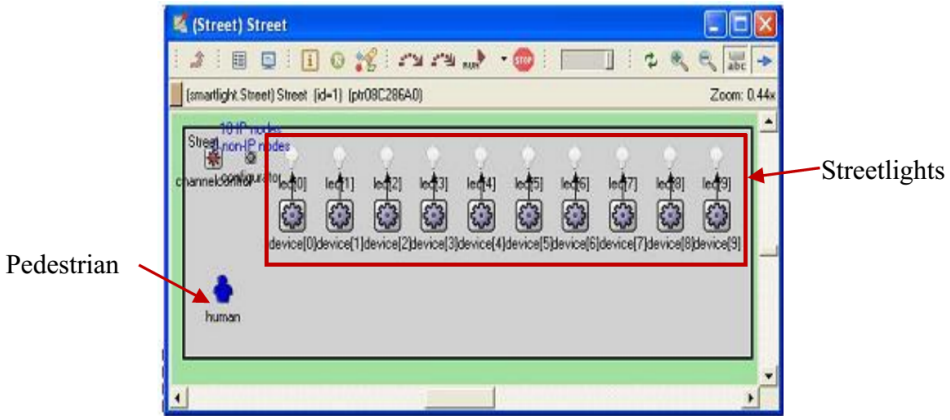

Figure 2.14: A linear topology consists of ten streetlights considered in [179].

traffic. In a real scenario, a residential road can consist of both pedestrian and motorised traffic. Thus, a thorough evaluation might not be viable by using this tool.

Nefedov *et al.* [19] integrated MATLAB/Simulink with IEC 61499 Function Block (FB), an open standard for distributed control and automation, to evaluate the performance of a motorist-based lighting control. MATLAB/Simulink is responsible for cellular automata based traffic modelling, and vehicle sensing. At each simulation timestep, MATLAB/Simulink relays the sensory data to the lighting control scheme implemented in the IEC 61499 FB. The data exchange between these simulators is achieved by a user

datagram protocol (UDP). They argued that the use of IEC 61499 FB can reduce deployment cost as the same implementation from FB can be deployed in hardware-in-the-loop testing. Thus, this can avoid potential programming errors during model translation. The proposed co-simulator is still in its infancy as the authors acknowledged that their work needed to be extended to different road layouts and realistic traffic data for more meaningful results. Moreover, the proposed co-simulator also lacks wireless communication modelling, which has become the trend for networked streetlight control (Section 2.3 details on this).

Pantoni and Brandão [156] used ns-2 to evaluate their confirmation-based Geocast routing algorithm which is intended for streetlight application. By using geodesic coordinates, the streetlight locations were populated into their simulation scenarios, and used to evaluate the performance of the proposed algorithm. As compared to other proposed simulators [19, 177, 180], optimising streetlight energy consumption is not their research focus. Thus, road traffic modelling was excluded in their simulations.

2.4.4 Discussion and Summary

There are an extensive range of simulation tools either in open-source format or commercially available. However, there is neither a single nor all-purpose simulator tool that fits all scenarios. Many simulators are rather proprietary for certain research interest and they are built on top of other simulators, such as, ns-2 and OMNeT++. Compared to commercial simulators, such as QualNet [181] and Opnet [182], open-source based simulators are widely adopted in research communities as they allow a high degree of customisation and rapid evaluation of the research ideas. However, some researchers prefer to use in-house simulation tools due to specific requirements and assumptions of their work [183].

Currently, to the best of the author's knowledge, there are three simulators, namely, PKU-STRAW-L [178], MATLAB/Simulink [19] and OMNeT++ [179], have been developed/extended specifically for simulating streetlight operations. Although these simulators have been used to evaluate the energy efficiency of traffic-aware lighting controls, the scalability of these simulators is limited to their intended simulation scenarios. Their road traffic models are simple, and thus do not reflect actual traffic scenarios. This leads to inconclusive results. Moreover, there is no mechanism to evaluate the impact of dimmed lighting from the road user's perspective. This establishes a need for a simulator that allows a holistic analysis of a networked street lighting system.

2.5 Research Gaps

Based on the literature reviewed in this chapter, there are many possibilities and potentials to use dimming or decreasing the lighting levels of street lighting to conserve energy. However, there are several limitations have been identified from the literature. The following outlines some of the identified research gaps.

There is currently no street lighting scheme which operates autonomously and adaptively, without sophisticated centralised solution whilst preserving road users' need for street lighting as demonstrated by conventional street lighting. Most of the energy-efficient lighting schemes focus on energy conservation rather than the usefulness of the street lighting. There is a large amount of disparate research about the perception and use of street lighting, from the perspective of both the motorists and the pedestrians, but this has not yet been brought together to assist the design and evaluation of street lighting schemes.

Most of the existing street lighting schemes require centralised control and relied on developed infrastructure such as mains power grid and cellular network. In many rural or undeveloped areas, the coverage and the reliability of the cellular network is highly variable and wired infrastructure for street lighting is not installed. Owing to these, there is a need for a decentralised system that can achieve the same functionality as existing street lighting schemes, without relying on fixed infrastructure.

Solar-powered streetlights have been considered for many rural or undeveloped areas. However, to provide a reliable light source after dark, especially during the winter seasons, larger solar panels and energy storage devices are needed. This has led to an oversized, and thus an overpriced system. Although the existing lighting schemes have shown significant energy savings on 'grid-powered' streetlights, the application of these schemes is restricted as they have yet to consider that the energy harvested from solar varies due to weather conditions.

In short, these research gaps lead to the research questions in Section 1.2.

Chapter 3

StreetlightSim: A Tool for Evaluating Street Lighting schemes

In Chapter 2, state-of-the-art lighting controls were reported to improve the sustainability of street lighting. This could be achieved by dimming or decreasing the lighting levels. The lighting levels of streetlights were dimmed between 20 and 60%, and increased to 100% either in groups or zones, once predefined events were triggered. However, the impact of such schemes from the perspective of road users has seldom been investigated. Therefore, this chapter proposes the streetlight usefulness model, an evaluation metric to assess the usefulness or practicality of street lighting from the perspective of motorists and pedestrians.

In Section 2.4, simulation tools have been used to evaluate lighting control schemes in terms of their energy savings [18, 19, 178] or network routing performance in streetlight topologies [156]. This is because these tools permit rapid evaluation and fine-tuning of the control schemes. However, to investigate the usefulness of lighting control schemes, a simulation tool should allow the schemes to be assessed from the road users' perspective. To permit this investigation, StreetlightSim, a novel simulation environment developed as part of this research is also being covered in this chapter. This is presented in Section 3.2. Together with the proposed streetlight usefulness model, the performance of existing state-of-the-art lighting schemes is subsequently evaluated with StreetlightSim, and is presented in Section 3.3.

3.1 Quantifying the Usefulness of Street Lighting

To minimise the energy consumption of streetlights, the most straightforward option is to turn them off altogether. However, this is against the purpose of having street lighting. Ideally, streetlights would only be turned on when they are useful. This section

considers what constitutes useful street lighting, from both a motorist's and a pedestrian's perspective. These stakeholders are considered to be the major beneficiaries of street lighting. Subsequently, a model is proposed to quantify the usefulness of street lighting, and is referred to as a streetlight usefulness model.

3.1.1 A Motorist's Perspective

As discussed in Section 2.1.2, street lighting helps to extend and broaden motorists' visual range beyond that offered by vehicle headlamps. This allows them to detect potential hazards in their direction of travel. Hazard detection is normally associated with the proximity of the hazard to the vehicle in either time or in distance, in which appropriate manoeuvres can be carried out to avoid a collision, and thus reduce the probability of injury to oneself or other road users. This distance is reflected as the stopping distance where a motorist must be able to stop their vehicle safely after a potential hazard is detected [184].

Based on the literature discussed in Section 2.1.2, following axiom is derived:

Axiom 3.1. *Motorists require a segment of the road in their travelling path to be illuminated for hazard detection. The lighting level within this segment is equally important for this task.*

Thus, streetlight usefulness for a motorist, U_{mot}, at time t is modelled by:

$$U_{mot}(t) = 100^{-1} \int_0^{100} \gamma(x,t)dx \tag{3.1}$$

where $\gamma(x,t)$ is the ratio of lighting level at x metres ahead of a motorist at time t to the minimum required lighting level for the road (Section 2.1 details some of the lighting levels used in various countries) which the motorist is travelling on.

This model assumes that:

(a) The length of the required lit road segment is 100 m [184], hence allowing motorists to detect harzard and then bring their vehicle to a stop within the distance. This distance is based on the fact that it covers most of the stopping distance required in a residential road, as summarised in Table 2.2. In the UK, residential roads typically have a speed limit of 30 mph (approximately 15 m/s or 50 km/h).

(b) The lighting level within this road segment is equally important for detecting hazard [185] and bring the vehicle to a stop. The lighting level is at the recommended level as specified by the adopted standards or guidelines (Table 2.1 summarises some of the standards or guidelines adopted by different countries).

3.1.2 A Pedestrian's Perspective

From the literature discussed in Section 2.1.3, effective street lighting should assist pedestrians in obstacle avoidance and navigation, identification of other pedestrians (facial recognition), and make them feel safer [35, 36]. As intuition would suggest, obstacle detection is improved as lighting levels increase [66, 67]. However, pedestrians begin to avoid obstacles at a distance of between 6 to 7 m [72]. To allow pedestrians to have a sense of security, streetlights should allow recognition of other road users at a distance of 4 m [35]. Nevertheless, studies show that they prefer to avoid collision with other road users at a distance of around 8 to 9 m [72].

Based on the above observations, following axiom is derived:

Axiom 3.2. *Pedestrians require a segment of the road in their walking direction to be illuminated for obstacles avoidance, navigation and identification of other pedestrians. The lighting level within this road segment is equally important for these tasks.*

Thus, the streetlight usefulness for pedestrian obstacle detection, navigation and facial recognition, $U_{ped(avoid)}$, is given by:

$$U_{ped(avoid)} = 10^{-1} \int_0^{10} \gamma(x,t)dx \tag{3.2}$$

where $\gamma(x,t)$ is the ratio of lighting level at x metres ahead of a pedestrian at time t to the minimum required lighting level for the road the pedestrian is travelling on.

This model assumes that:

(a) A pedestrian begins to detect obstacle, navigate and recognise other pedestrians at a distance of 10 m [72].

(b) The lighting level within this 10 m segment of road is equally important for these tasks [72], and is at the recommended levels as specified by the standards or recommendations (Table 2.1 summarises some of the standards or guidelines adopted by different countries).

In Section 2.1.3, studies have shown that subjects have a similar, and in some cases, better sense of safety when the street lighting has a descending lighting distribution as compared to conventional's [38, 64]. In the descending distribution, streetlights at the immediate surroundings of pedestrian is fully lit according to the adopted standards and guidelines, and gradually dimmed for those that lie further away from them. For conventional lighting distribution, all streetlights are lit at same lighting level as specified by the adopted standards or recommendations.

Based on the above observations, following axiom is derived:

Axiom 3.3. *To allow pedestrians to have a good overview of their surrounding and feel safe, they require a segment of road in front of and behind them to be illuminated. The lighting level at the proximity of pedestrians carries more weight compared to those at a distance.*

Thus, the streetlight usefulness for pedestrian's perceived safety, $U_{ped(prospect)}$, is modelled as below:

$$U_{ped(prospect)}(t) = 300^{-1} \int_{-150}^{150} z(x,t)dx \tag{3.3}$$

$$z(x,t) = \begin{cases} \varepsilon(x,t), & \varepsilon(x,t) \leq 1 \\ 1, & \varepsilon(x,t) > 1 \end{cases} \tag{3.4}$$

$$\varepsilon(x,t) = \frac{\gamma(x,t)}{1 - 0.2 \left\lfloor \frac{|x|}{30} \right\rfloor}, \quad -150 < x < 150 \tag{3.5}$$

where x is the distance in metres from a pedestrian at time t, $z(x,t)$ is the ratio of lighting level at location x metres from a pedestrian at time t to the lighting level required at the illumination zone where location x is located.

This model assumes that :

(a) Pedestrians feel safe when a 150 m road segment in front and behind them is lit [38, 64].

(b) These road segments are subdivided into five illumination zones, and each zone covers a 30 m length of road [38, 64]. A pedestrian prefers the nearest zone to them to be lit at 100% of the recommended lighting levels specified by the standards or recommendation, and gradually decreased by 20%, with respect to lighting level as outlined by the adopted standards or guidelines, for each zone further away from them [38] .

Over a period of time, a pedestrian will perform both obstacle detection and navigation/awareness. Hence, the overall streetlight usefulness for pedestrian, U_{ped}, is given by:

$$U_{ped}(t) = \alpha_{ped} U_{ped(avoid)}(t) + (1 - \alpha_{ped}) U_{ped(prospect)}(t) \tag{3.6}$$

where α_{ped} is the weighting of the time spent by the pedestrian looking at the footpath. In this thesis, $\alpha_{ped} = 0.45$ is adopted. This is based on the findings of Davoudian and Raynham [36], who found that pedestrians spend 40 – 50% of their time looking at the footpath.

To investigate the energy efficiency and the usefulness of a lighting control scheme, a tool that enables modelling and simulation of realistic traffic for both motorists and pedestrians, and streetlight operations is required. Importantly, this tool needs to facilitate

the capturing of the lighting levels used by the streetlights within the simulated traffic's travelling path. Then, these lighting levels are evaluated by the proposed evaluation metrics to quantify their usefulness from the perspective of different road users.

3.2 StreetlightSim: A Simulation Environment to evaluate Networked and Adaptive Street Lighting

As presented in Section 2.4, there have been many proprietary simulation tools developed to evaluate various aspects of lighting control schemes. For example, Yang *et al.* [178] developed PKU-STRAW-L to investigate VANET controlled streetlight operation, while Nefedov *et al.* [19] used a co-simulator, which comprised MATLAB and IEC 61499 FB, to evaluate a distributed lighting control based on vehicle sensing. These tools were intended to investigate the energy efficiency of lighting control schemes while operating under different traffic flows. However, their traffic models were simple, and they acknowledged that the models needed to be extended to different road layouts and realistic traffic data for more meaningful results [19]. In fact, evaluating the control schemes in terms of their usefulness is not their research focus.

This section reports on StreetlightSim, a novel co-simulator environment that integrates street lighting control with the simulation of realistic traffic.

3.2.1 Overview of StreetlightSim

As illustrated in Figure 3.1, the main components of StreetlightSim are built within OMNeT++ modules and Simulation of Urban MObility (SUMO 0.13.1), a road traffic simulator that acts as a real-time mobility trace generator, obeying specified road traffic patterns. StreetlightSim is adapted from the Vehicle in Network Simulation (Veins 2.0 RC2) framework [169], which provides a solid foundation for bidirectional coupling between OMNeT++ and SUMO. Veins also facilitates the modelling and simulation of individual vehicles, which offers a feasible platform to evaluate streetlight usefulness from the perspective of each individual road user. In addition, OMNeT++ allows the simulation of data processing and control algorithms, and communication networks – supporting frameworks and models including MiXiM, INET and INETMANET [186].

The following subsections explain the operation of StreetlightSim's components in Figure 3.1.

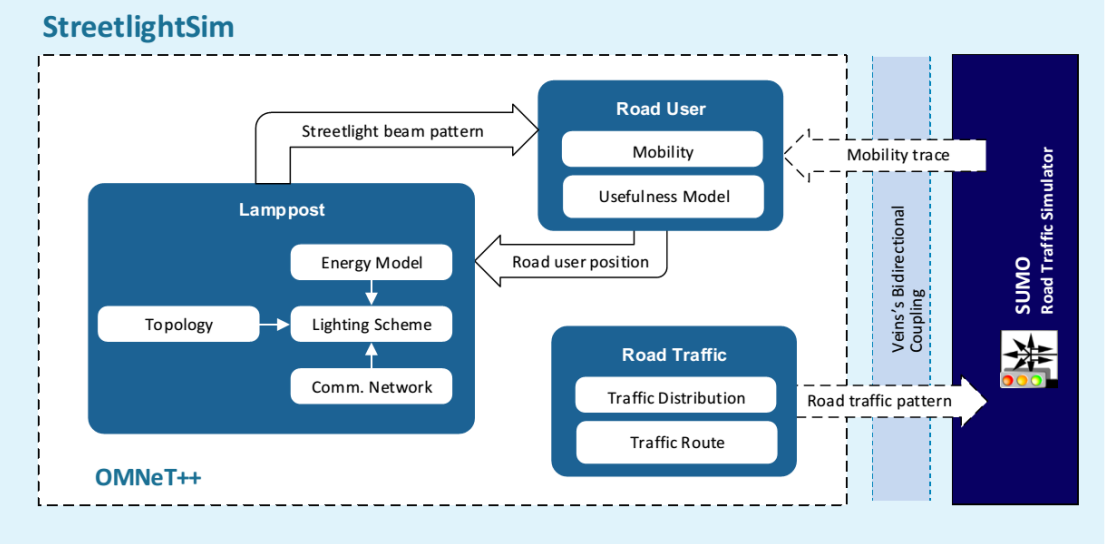

Figure 3.1: Block diagram of StreetlightSim. SUMO generates realistic mobility traces based on specified road traffic patterns. Then, OMNeT++ uses these traces as input to the lighting control algorithms. The created lighting condition is evaluated in terms of energy efficiency (energy model in Lamppost module) and usefulness (proposed streetlight usefulness model in Road User module).

3.2.1.1 Bidirectional Coupling

As presented in Section 2.4.2, SUMO provides TraCI developed to enable coupling with other simulators. TraCI is a client/server architecture-based interface providing an opportunity for real-time retrieval and manipulation of simulated objects, such as road users, traffic lights and streetlights, via a Transmission Control Protocol (TCP) connection. An OMNeT++ module from Veins [169] is adopted in StreetlightSim to establish a proxy TCP connection with TraCI. During simulation, TraCI forwards a series of commands via the established TCP connection, at regular time intervals. Upon arrival at SUMO, these commands are processed, and associated values are returned to the module at the next simulation timestep. Although TraCI specifies many standard commands, the most frequently used is to retrieve the real-time mobility trace generated by SUMO. The StreetlightSim uses these mobility traces as a trigger to update the simulation scenario.

3.2.1.2 Road Traffic Profile

In the original Veins implementation, road traffic profile is not explicitly specified. Instead, it uses the standard SUMO configurations such as *flow* or *route* to define a specific road traffic distribution. In Veins, it is justifiable to use such an approach as it was intended to investigate the influences of inter-vehicle communication on traffic flow. However, in evaluating the usefulness of street lighting control schemes, StreetlightSim requires a realistic road traffic distribution during streetlight operational hours.

To introduce a reasonable approximation of a road traffic profile, StreetlightSim uses the time-dependent traffic distribution ratio based on the statistics provided by Department for Transport (DfT), UK [187]. For example, Figure 3.2 (a) shows the mean traffic distribution ratio according to the days of week, and (b) shows the aggregated average weekday and weekend traffic ratios. These distribution ratios are multiplied by the Annual Average Daily traffic Flow (AADF) and are used to inject simulated motorists randomly as the simulation runs. AADF represents the daily average number of vehicles passing a point in the road network, based on empirical data collected over a complete year. Although AADF only accounts for vehicular traffic, pedestrians also utilise streetlights – therefore, pedestrian traffic is also introduced into the simulation. AADF with additional pedestrian traffic, V_{comb} is given by Eq. 3.7, and is assumed to share the same distribution exhibited by the vehicular traffic.

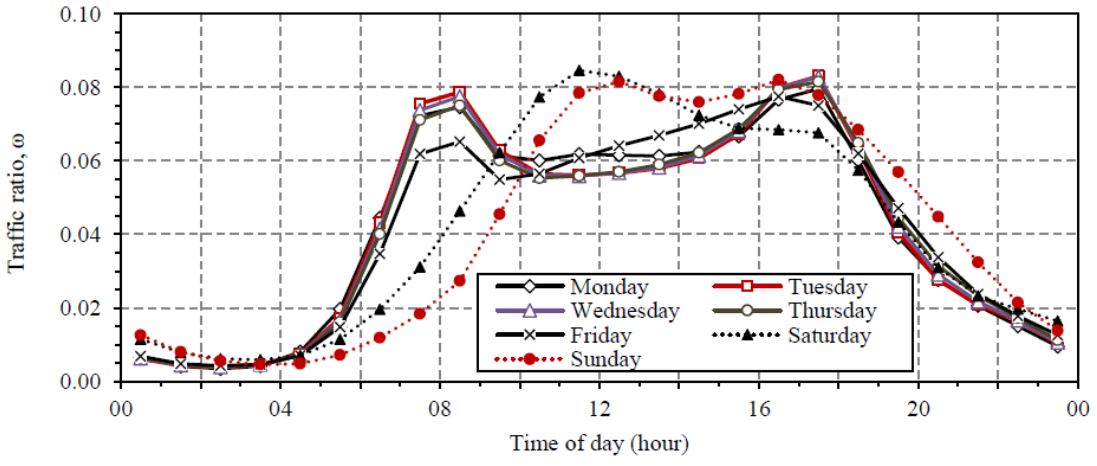

(a)

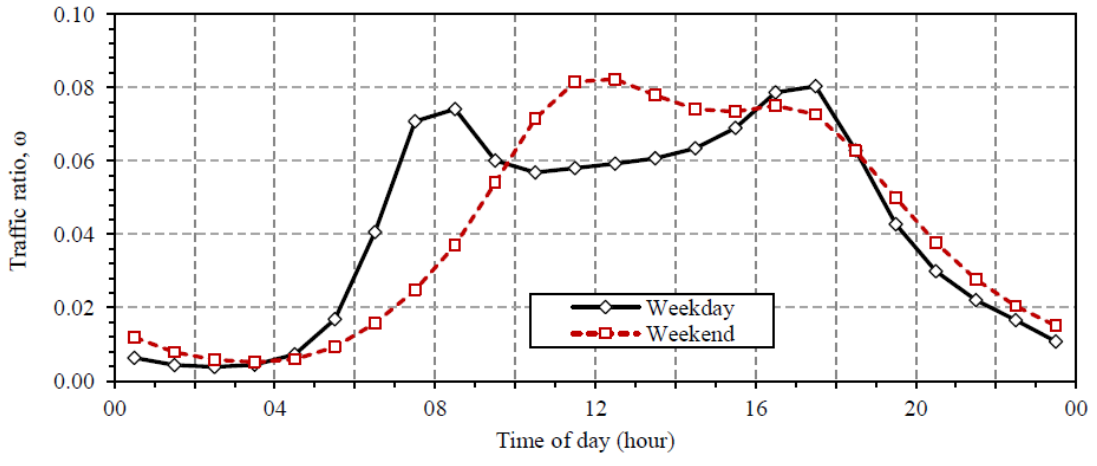

(b)

Figure 3.2: Vehicular traffic distribution ratio: (a) based on the days of week, and (b) aggregated by weekend and weekday (adapted from [187]).

$$V_{comb} = \frac{V_{mot}}{1 - \Delta_{ped}}, \quad 0 \leq \Delta_{ped} < 1 \tag{3.7}$$

where V_{mot} is the AADF for vehicular traffic (vehicles per day); and Δ_{ped} is the pedestrian traffic composition according to the city of interest (%).

Although both V_{mot} and V_{comb} represent an average daily traffic flow, total traffic flow is different according to the days of week [187]. To model this, the total number of road users introduced during the simulation according to the days of week is given by:

$$\Gamma(\theta) = \alpha_\theta V_{comb} \tag{3.8}$$

where θ represents either daily, weekday, or weekend traffic, and α_θ is the traffic weighting factor of these days as summarised in Table 3.1.

Table 3.1: Traffic weighting factors according to different days of the week (adapted from [187]).

Day of week, θ	**Traffic weighting,** α_θ
Monday	1.026
Tuesday	1.042
Wednesday	1.065
Thursday	1.091
Friday	1.134
Saturday	0.839
Sunday	0.803
Weekend	0.868
Weekday	1.132

Depending on the granularity of the traffic simulation, α_θ can also be aggregated into either weekday or weekend, as shown shaded in Table 3.1. In this thesis, α_θ is based on the ratio of average daily, or average weekday and weekend traffic volumes, V_θ, to average weekly traffic volume, V_{avg}, as given by Eq. 3.9. In this thesis, both V_θ and V_{avg} are derived based on traffic data provided by Department for Transport, UK [187].

$$\alpha_\theta = \frac{V_\theta}{V_{avg}} \tag{3.9}$$

The total number of road users introduced during the simulated hour h for a day θ is given by:

$$\Gamma(h, \theta) = \omega_{h,\theta} \Gamma(\theta) \tag{3.10}$$

where ω is the ratio of average traffic volume at hour h of day θ to V_θ, as given by Figure 3.2.

The specified number of road users during a simulated hour h is injected into SUMO randomly. To inject a simulated pedestrian or motorist into SUMO through TraCI, each of these road users needs to be associated with a correct path that specifies the route it travels as the simulation runs. SUMO provides tools to generate these random paths, e.g. *randomTrip.py* and *duaItera.py*. However, these paths are numerically identified and are not explicitly for either pedestrians or motorists. Therefore, they are not 'StreetlightSim-ready'. In order to convert these random paths into a usable format, StreetlightSim includes a tool to categorise these random paths either for pedestrians or motorists. The step-by-step guide for this is available at StreetlightSim's official website [188].

3.2.1.3 Lamppost

StreetlightSim is based on the MiXiM framework, making it possible to analyse the usefulness of street lighting schemes together with different wireless communication networks. As the performance of these communication networks is spatially-sensitive, their evaluation requires knowledge of real streetlight topologies. In StreetlightSim, the topology is derived using OpenStreetMap (www.openstreetmap.org) and JOSM (josm. openstreetmap.de). OpenStreetMap is a community-driven free, editable map of the world, and JOSM is a map editor for OpenStreetMap. The data from OpenStreetMap is used by StreetlightSim as the source map for the road network and random path generation. While it provides comprehensive data on the road network, it does not include the locations of streetlights. In order to use the OpenStreetMap in StreetlightSim, the minimum enhancement to the data is to identify the relative locations of streetlights within the topology. Depending on the simulation scenario, additional pedestrian footpaths could be added to the data to simulate pedestrian traffic as distinct from vehicular traffic. These enhancements can be accomplished using JOSM.

In the recent LED streetlight manual [87], the streetlight beam pattern is presented in a rectangular form or, more precisely, a bat-wing form. For StreetlightSim, however, the streetlight beam pattern is assumed to be in a circular form. This is to avoid any unnecessary bearing adjustment of a beam pattern at a bend or winding road during the simulations, thus reducing the complexity of the simulation models. Figure 3.3 shows the bearing adjustment of a rectangular beam pattern at a bend road compared to a circular beam pattern. The distance between streetlights depend on various factors, such as local regulations, population, traffic density, function of the road, and thus the size of the circular beam pattern depends on the actual streetlight topology studied. Based on the author's observation using aerial photography, an inter-lamp post distance of about 20 to 30 m is quite common on residential roads.

In an actual environment, the streetlights are always planted on the pavement or road edge, and use a tilted light arm, reflectors and refractors to project the necessary light onto the road surfaces [189]. However, to reduce the complexity of the simulation models,

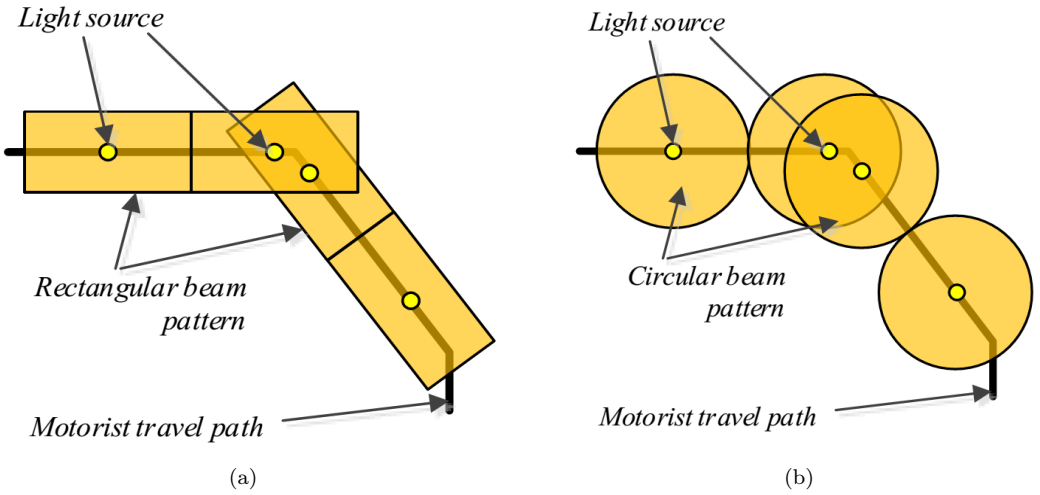

Figure 3.3: The beam patterns in (a) rectangular and (b) circular form at a bend road. The rectangular beam patterns need to be aligned with the road, but circular beam patterns are not required to do this.

the streetlights are positioned in the middle of a residential road but in their actual geographical location. Figure 3.4 shows a snapshot of the actual geographical location of a streetlight from an aerial photograph and its relative location during the simulations.

To evaluate the energy efficiency of street lighting schemes, the energy model shown in Eq. 3.11 is assumed. This model assumes that the streetlight energy consumption is directly proportional to its lighting level. For example, when the streetlight lighting level is set to 80%, the streetlight energy consumption is also reduced to 80% based on its maximum power rating, P_{max}.

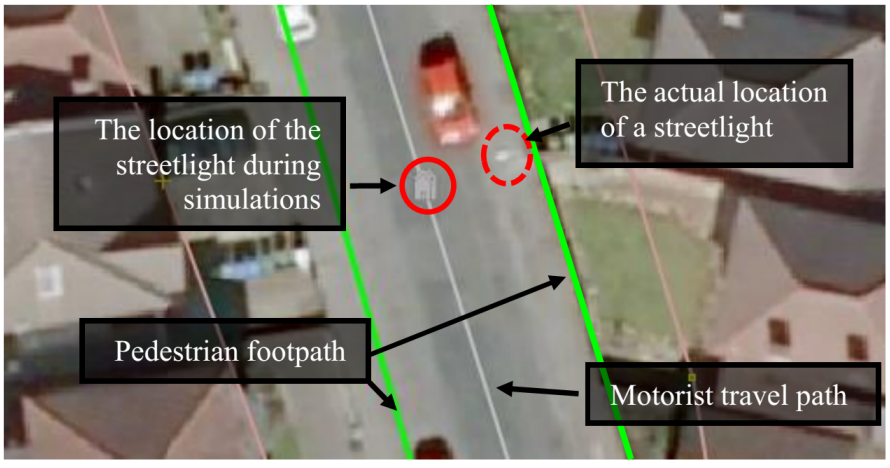

Figure 3.4: A snapshot of Java OpenStreetMap Editor (JOSM) showing the actual geographical location (dashed red circle) of a streetlight and its relative location during the simulations (solid red circle). The travelling paths for both the simulated motorist and pedestrian traffic are presented by the white and green solid lines respectively.

$$E_{cons}(n) = \sum_{t=(n-1)T}^{nT} P_{max}\varphi_t \tag{3.11}$$

where $E_{cons}(n)$ is the energy consumed by a streetlight after n discrete timesteps; φ_t is the lighting level of the streetlight at timestep t (%); P_{max} is the maximum power rating of the light source (W); and T is the duration of a single timestep n.

3.2.1.4 Road User

In StreetlightSim, this module has two functions: (a) represents the simulated road users in OMNeT++ which is characterised by the mobility traces generated by SUMO; and (b) evaluates the usefulness or practicality of the street lighting schemes according to the latest positions of the simulated road users. Depending on the granularity of the simulation timestep, real-time mobility traces of the simulated road users are continuously returned by SUMO during simulation runs. OMNeT++ receives these mobility traces and uses them to update the simulation scenario by adding new road users, updating the existing road users to their latest position, or removing them from the simulation scenario once they have reached the end of their route. At each simulation update, the usefulness or practicality of the street lighting is measured using the proposed evaluation metrics, as modelled by Eq. 3.1 and 3.6.

3.2.2 Model Validation

In order to verify that the described operations of StreetlightSim are accurately translated into OMNeT++, a series of validations are performed. The following subsections describe the validation results of the models described in Section 3.2.1.

3.2.2.1 Road Traffic Profile

To validate the traffic model in StreetlightSim, five different V_{comb} values are used: 180, 438, 1347, 3508 and 6554 road users per day. These values represent the minimum, 1st quartile, median, 3rd quartile and maximum V_{mot} values respectively of residential roads in Southampton, UK. To model realistic traffic in Southampton, UK, 14% of the traffic is assumed to be pedestrian during validations [188]. Figure 3.5 shows the sample results of the mean traffic distribution generated by StreetlightSim after 20 runs, according to a weekday and weekend traffic distribution ratio shown in Figure 3.2 (b). As shown, the generated traffic distributions match the trends shown in Figure 3.2 (b).

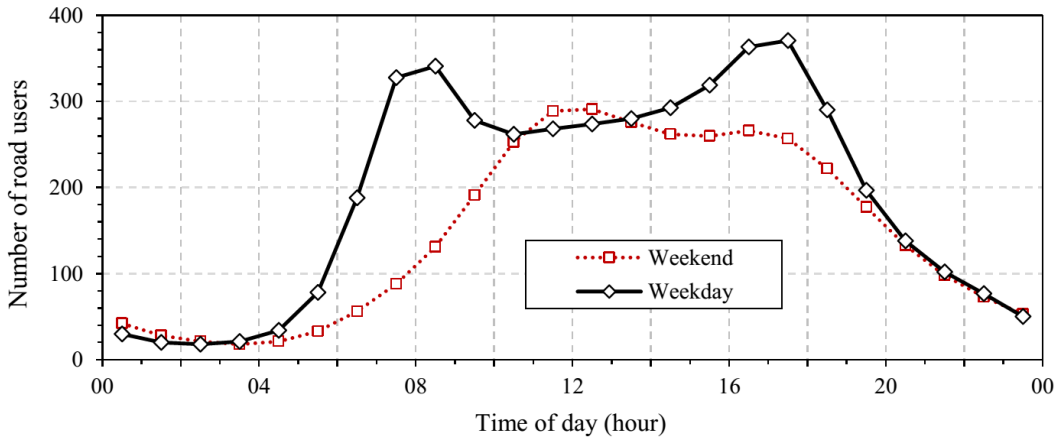

Figure 3.5: Simulation results showing the weekday and weekend traffic distribution generated by StreetlightSim at $V_{comb} = 3508$ road users per day.

Figure 3.6 (a) shows that there are obvious discrepancies between generated traffic against the data from DfT when $V_{comb} = 180$ road users per day is evaluated. These discrepancies have added three additional road users (an additional 2% more to $V_{comb} = 180$ road users per day) during the simulations. However, these discrepancies become trivial when other V_{comb} values are evaluated. These V_{comb} values result in an additional 1% road users during validations compared to specified V_{comb} values. For example, V_{comb} = 1347 road users per day as shown in Figure 3.6 (b). One of the causes of this trend is that a round number from Eq. 3.8 and 3.10 was adopted in StreetlightSim. This is because it is more practical to represent a simulated road user as an integer rather than a fraction during validations. Consequently, this has caused the discrepancies as shown in Figure 3.6 (a), when lower V_{comb} is validated. However, the use of the round number has trivial effect on the composition of the simulated traffic. Figure 3.7 shows the mean traffic composition of the simulated pedestrian traffic with different V_{comb} values after 20 simulation runs. Based on the simulation results, the mean composition of the pedestrian traffic is about 14% as intended, with standard deviation of less than 1%.

3.2.2.2 Energy Model

The energy model is validated using 112 streetlights operating according to three arbitrary lighting schemes as summarised in Table 3.2. When streetlights are operating according to lighting schemes 1, all the streetlights are always switched on with full brightness, whereas the lighting level of scheme 2 is gradually reduced to zero percent. The lighting scheme 3 is exactly the opposite of scheme 2 where its lighting level is gradually increased from zero to 100%. During the validations, all the streetlights are assumed to be equipped with a 25 W LED light lamp.

According to the results generated by StreetlightSim, the total energy consumption of lighting schemes 1, 2 and 3 after a 16-hour lighting operation are 44.80 kWh, 20.44

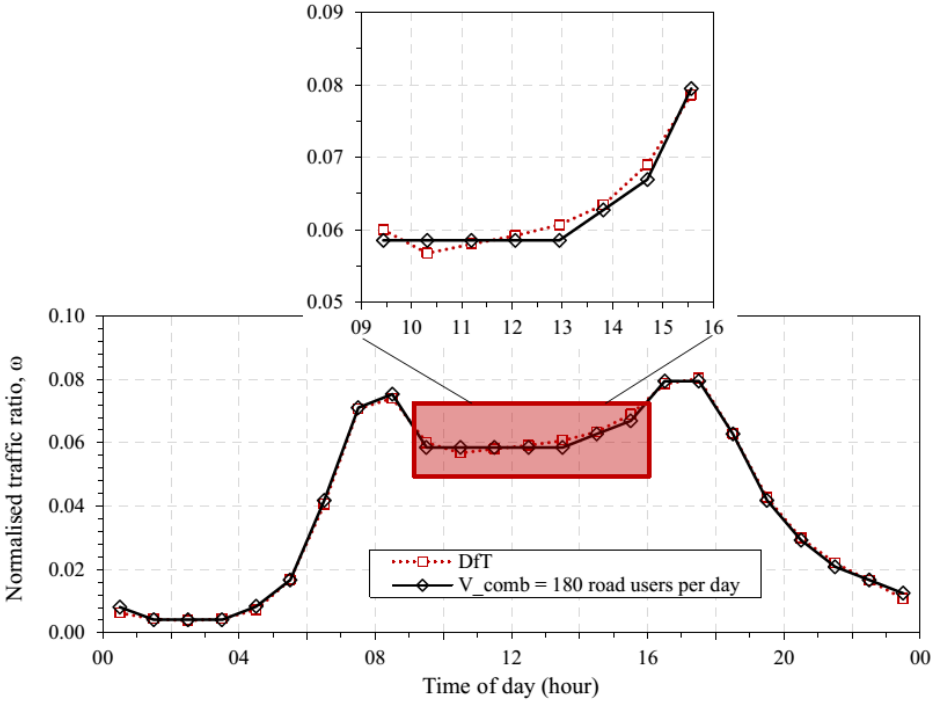

(a)

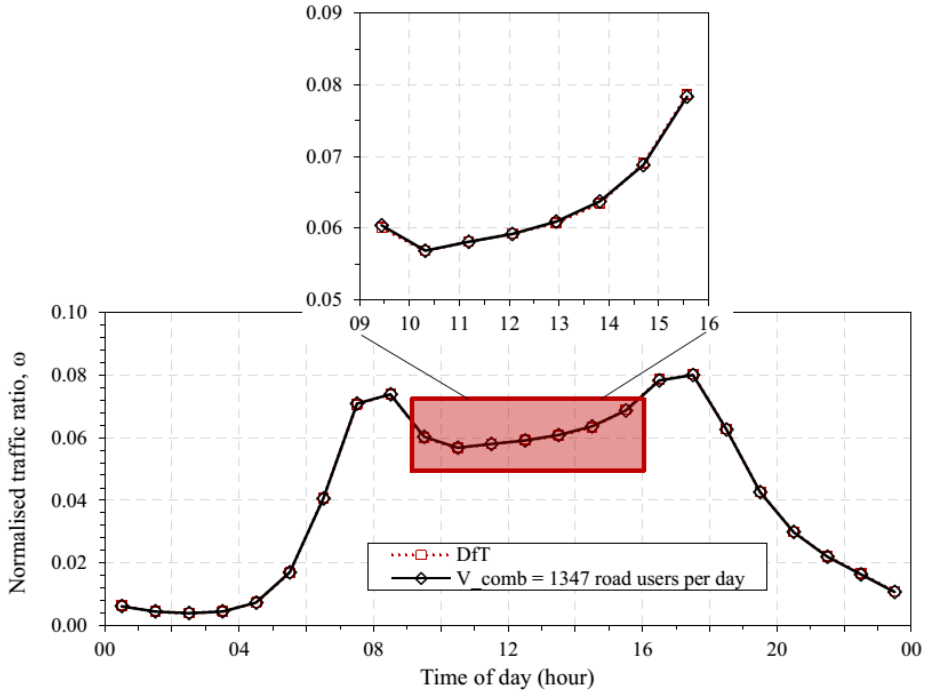

(b)

Figure 3.6: Traffic distribution ratio of simulated traffic against the data from DfT, according to weekday traffic distribution shown in Figure 3.2 (b). There are some discrepancies while generating the simulated traffic which result in an additional 2% of road users during the simulations.

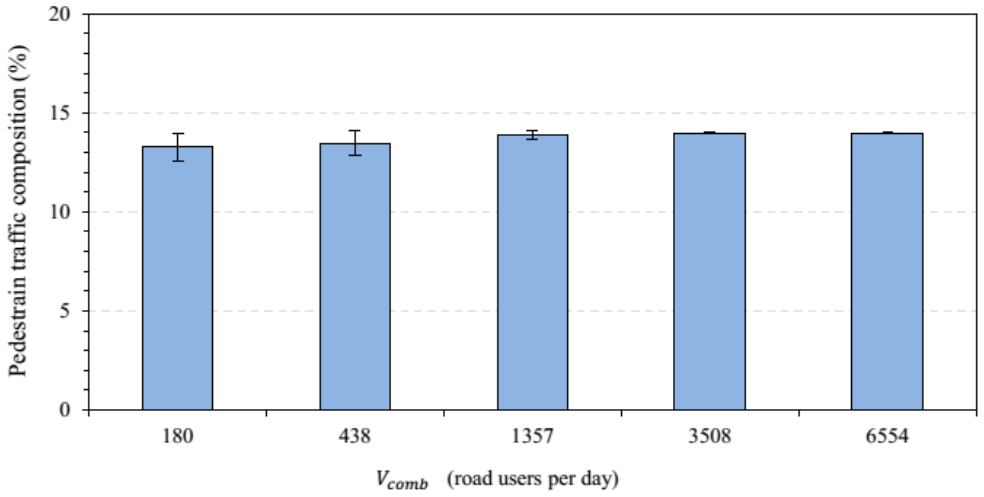

Figure 3.7: Simulation results show the mean of the pedestrian traffic composition is about 14%, while the road traffic model is validated with different traffic volumes. The error bars represent the standard deviations after 20 simulation runs.

Table 3.2: Streetlight operations for energy model validation.

	Lighting level of the streetlight, φ (%)		
Duration (hour)	*Lighting scheme 1*	*Lighting scheme 2*	*Lighting scheme 3*
3	100	100	0
2	100	90	10
2	100	60	20
1	100	50	40
1	100	40	50
1	100	20	60
2	100	10	90
4	100	0	100

kWh and 20.44 kWh respectively. These results are consistent with those numerically computed using Eq. 3.11. Figure 3.8 shows the cumulative energy consumed by all the streetlights while operating these schemes. The energy consumption of lighting scheme 1 is proportional to simulated hours, and reaches the maximum after 16 hours of operation. The energy consumption of lighting scheme 2 remains unchanged after operating for 12 hours as the streetlights were switched off during the remaining operational hours. As lighting scheme 2 is exactly the opposite of lighting scheme 3, the trends demonstrated by both schemes are mirror of each other.

3.2.2.3 Streetlight Usefulness Model

Based on the streetlight usefulness model proposed in Section 3.1, a constantly lit road of 100 m and 150 m is required to achieve the perfect (100%) streetlight usefulness for both U_{mot} and U_{ped}. In the real environment, these constantly lit road distances are

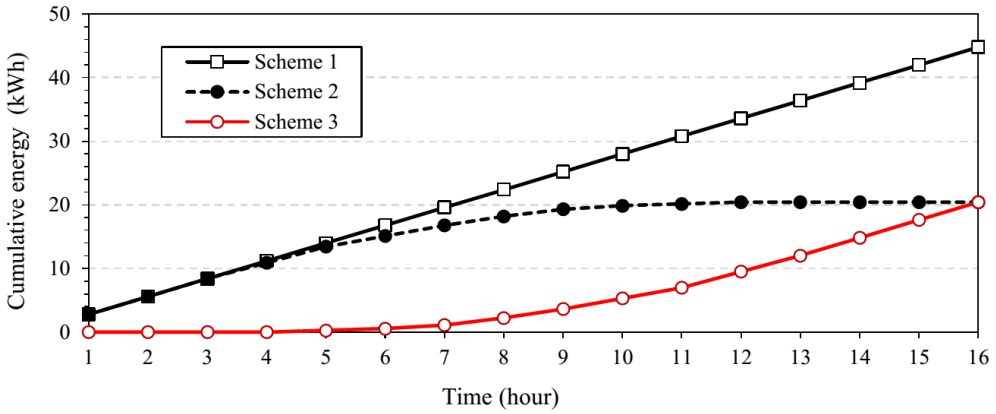

Figure 3.8: Simulation results showing cumulative energy consumed by 112 streetlights while operating lighting schemes summarised in Table 3.2. Total energy consumption of lighting schemes 1, 2, and 3 after a 16-hour lighting operation is 44.80 kWh, 20.44 kWh and 20.44 kWh respectively.

occasionally unavailable because of different road geometries and streetlight topologies. To address these scenarios, StreetlightSim uses two virtual polygons to determine the streetlights which their beam patterns are considered in a usefulness evaluation. In Figure 3.9, these polygons are aligned to the travel direction of simulated road users which representing their front and rear field of views (FoVs). Figure 3.9 shows the scenario where a pedestrian (presented by the red dot) is walking towards a bearing of north-northwest with four streetlights (s_1 to s_4) within the front FoV and one streetlight (s_5) within the rear FoV, assuming the distance from the pedestrian to s_1 and s_5 is 150 m and 40 m respectively. In this scenario, the evaluation distance of $U_{ped(prospect)}$ at the rear of the pedestrian is trimmed to the distance between the pedestrian and the beam pattern of s_5. This is applied to any scenario when the beam pattern of the furthest streetlight is less than the lengths required by the proposed usefulness model. If a FoV covers no streetlight, the area covered by the FoV is omitted from the usefulness evaluation. In the event of an intersection of beam patterns, for example between s_3 and s_4, the beam pattern with the higher lighting level is always used in the evaluation. If the lighting of these streetlights are at the levels as modelled by Eq. 3.1 and 3.6, and their beam patterns are covering the entire road surface, then the pedestrian is assumed to have experienced perfect (100%) usefulness at the current location.

Figure 3.10 shows the lighting scenario used to validate the proposed usefulness models. There are eight streetlights operating at full illuminance while the rest are switched off. A pedestrian and a motorist are initially positioned at $x = 0$, and usefulness of the streetlights is evaluated as they travel from left to right. The streetlight usefulness experienced by the road users is shown in Figure 3.11. Both the pedestrian and motorist experience 100% usefulness as they travel. However, usefulness is gradually reduced to zero as they approach the unlit segment of road on the right. This trend is consistent with the lighting scenario illustrated in Figure 3.10.

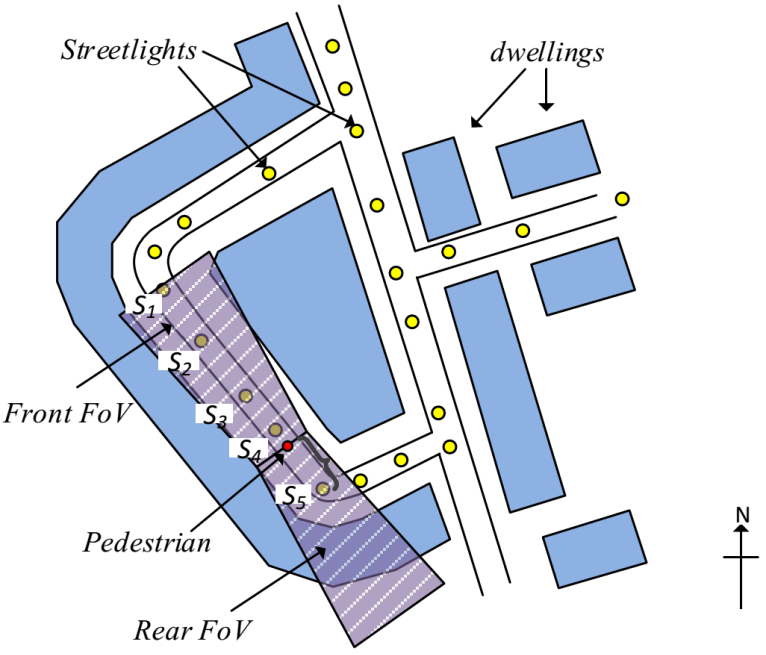

Figure 3.9: The distance between the beam patterns of streetlights s_1 and s_5 are considered for usefulness evaluation. In this scenario, the pedestrian (represented by the red dot) is assumed to have experienced the perfect (100%) streetlight usefulness if lighting levels of s_1 to s_5 are adjusted according to the pedestrian needs.

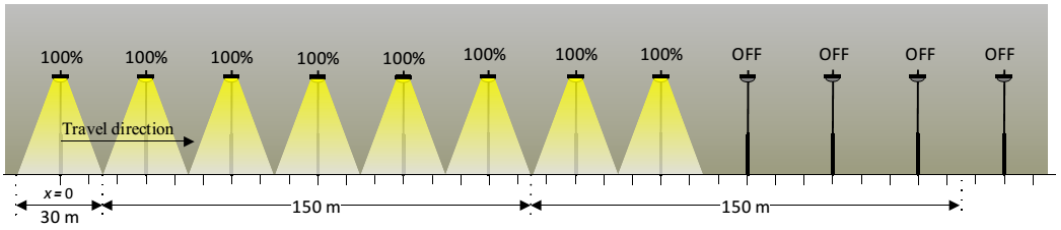

Figure 3.10: Lighting scenario used to validate the streetlight usefulness model.

3.3 Evaluating State-of-the-art Street Lighting Schemes

In this section, the state-of-the-art lighting schemes are evaluated in terms of their energy efficiency and streetlight usefulness experienced by road users. The results presented in this section serve as baseline results to the lighting scheme proposed in Chapter 4.

A streetlight network from a residential area located in Southampton, UK is adopted in this evaluation. This network consists of 112 streetlights which are scattered along approximately 3.5 km of residential roads. Figure 3.12 summarises the process flow for using StreetlightSim in this evaluation, and step-by-step guides are included with the downloadable version of StreetlightSim (www.streetlightsim.ecs.soton.ac.uk).

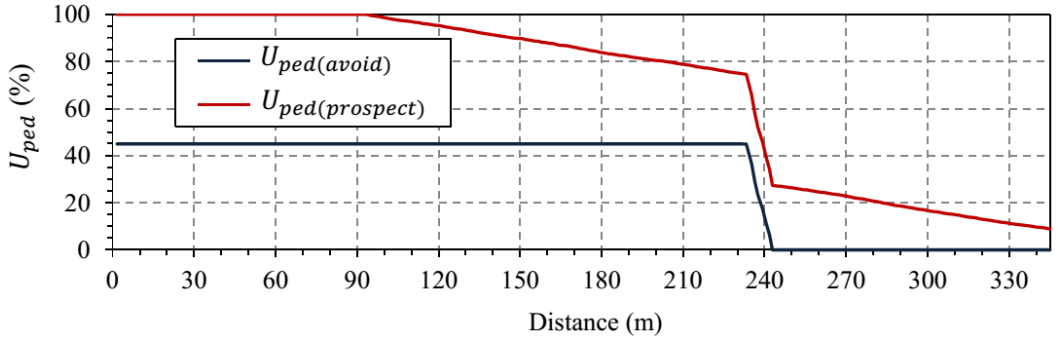

(a)

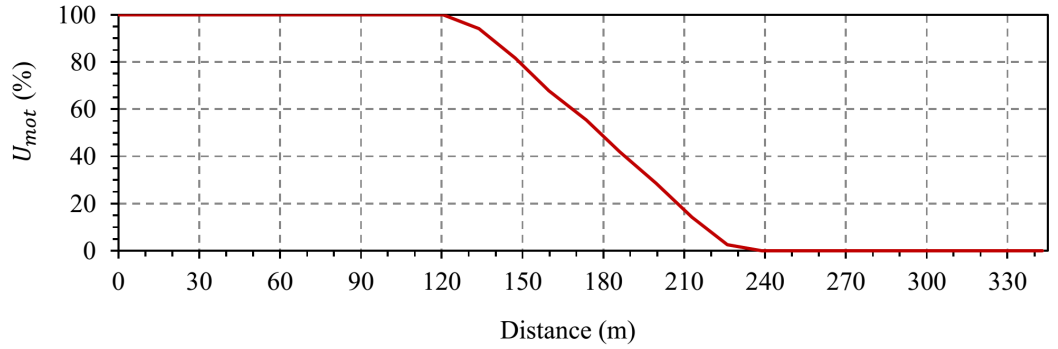

(b)

Figure 3.11: Simulation results showing the streetlight usefulness from (a) a pedestrian's perspective, and (b) a motorist's perspective while travelling right from $x = 0$ under the lighting scenario shown in Figure 3.10.

3.3.1 Simulation Setup

This section presents the simulation scenario and various parameters used for evaluating the state-of-the-art lighting schemes considered in this thesis.

3.3.1.1 Existing Lighting Schemes

A range of different approaches have been proposed to reduce the energy consumption of street lighting, as outlined in Section 2.2. However, this section only evaluates and compares the state-of-the-art schemes listed in Table 3.3. This is due to the fact that the explicit details of some of the schemes were not available when this thesis was prepared. The Conventional or 'always-on' lighting scheme is also included in this evaluation to serve as a benchmark for the proposed usefulness model.

3.3.1.2 Streetlights

An actual streetlight topology located in a residential area was modelled for this evaluation. The location of these streetlights was identified using an aerial photograph. Figure

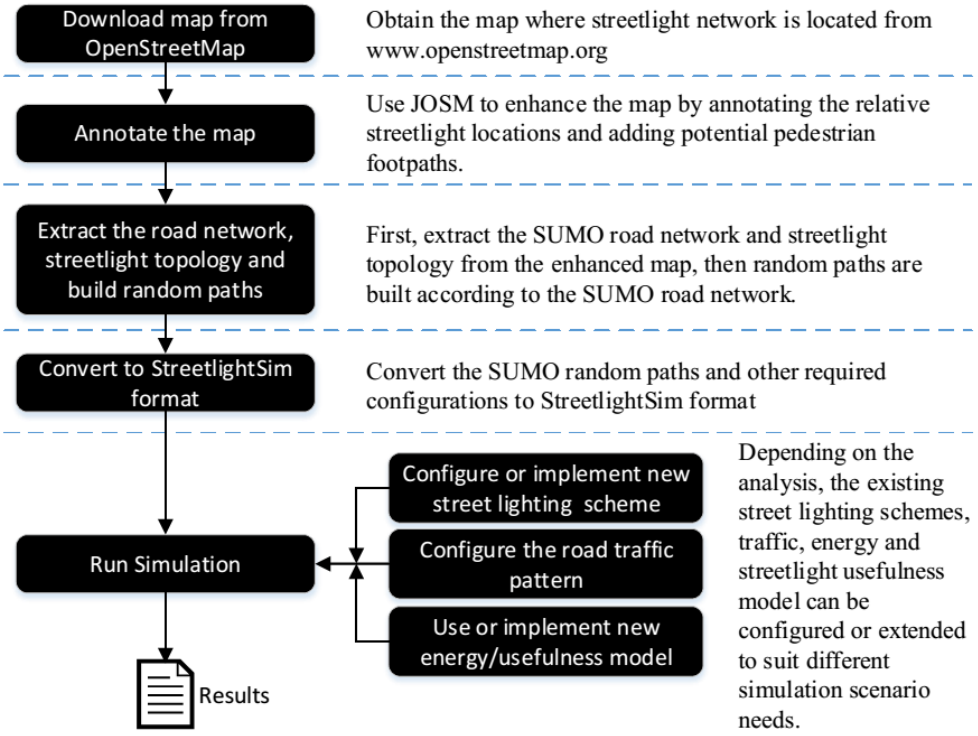

Figure 3.12: Process flow for using StreetlightSim to evaluate the state-of-the-art lighting schemes considered in this thesis.

3.13 shows the topology of the streetlights (represented by dots) in a residential area in Southampton, UK. For the purposes of evaluation, each streetlight is assumed to be equipped with a 25 W LED lamp, the beam pattern of which covers a 30 m road segment. The streetlights are assumed to start operating at sunset and finish at sunrise the next day. Based on the observations on the aerial photograph, the distance between streetlights varies, for example as a result of roundabouts and junctions. Thus, a near-perfect streetlight usefulness is achieved, as shown in Figure 3.14 (a).

The energy consumption of the different lighting schemes is influenced by the duration of their operation. This is dependent upon the geographical location, season, weather, and local environment. Therefore, for clarity of evaluation, the simulation scenario limits streetlight operational hours from 16:00 to 08:00 (16 hours). These operational hours represent one of the longest street lighting durations required during the winter months in the UK.

3.3.1.3 Road Traffic Profile

To approximate traffic flow on the residential roads shown in Figure 3.13, two traffic profiles are considered. They are weekday and weekend traffic profiles as shown in Figure 3.2 (b). During the simulation, V_{comb} values of 180, 438, 1347, 3508 and 6554 road users per day are considered, of which 14% of this value corresponds to pedestrian traffic. These

Table 3.3: Summary of evaluated street lighting schemes.

Lighting Scheme	**Operation**
Conventional/always-on	All the streetlights are switched on with 100% lighting level during the simulations.
Part-night [15]	All the streetlights are switched on at 100% except from 00:00 to 05:30 where the streetlights are switched off completely to conserve energy.
Philips Chronosense [98]	Similar to Conventional lighting scheme except from 22:00 until 05:00 when the lighting level of all the streetlights is reduced to 65%.
Philips Dynadimmer [98]	Streetlights operate at 40% between 23:00 and 05:00, 55% from 05:00 to 06:00 and 65% from 20:00 to 23:00. This scheme assumes that the lighting level of the streetlights is overrated, thus streetlights are switched on at 90% lighting level for the rest of the operational hours.
Multi-sensor [42, 101]	Each streetlight is equipped with a multi-sensor array that is capable of detecting road users who come into close proximity. The streetlights are always switched on at 40%, and increase to 70% and 100% if the distance between the streetlight and a detected road user is 20 m and 10 m respectively.
Zoning [21]	This lighting scheme assumes that the pedestrians are tracked via GPS- and Internet-enabled smartphones. The streetlights within the user-defined radius are switched on at 100% and those beyond the defined radius are switched off completely. For comparison purposes, the radius of 150 m is considered during the simulations. Motorists are not tracked by the scheme, but gain some consequential benefit from lighting intended for pedestrians.

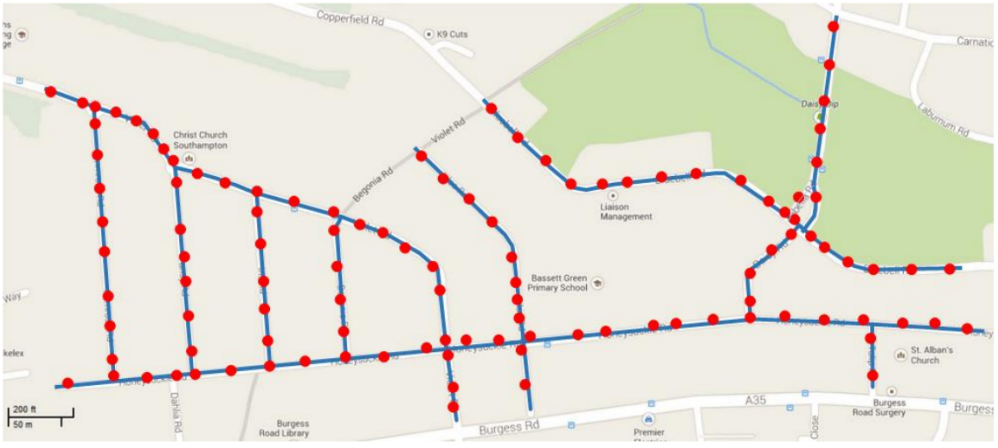

Figure 3.13: The locations of the streetlights (dots) and road network (shaded lines) considered during the simulation. This streetlight topology consists of 112 streetlights scattered within 3.4 km of residential roads (the base map was adapted from Google Maps).

V_{comb} values represent the minimum, 1st quartile, median, 3rd quartile and maximum AADF values for residential roads in Southampton, UK, respectively [190]. The mobility of a simulated road user is governed by a total of 100 random routes. The mobility speed of these road users varies according to on route traffic conditions, but is limited to a maximum 1.9 m/s for pedestrians [191] and 30 mph for motorists (the speed limit on residential roads in the UK).

3.3.2 Simulation Results

This section presents and discusses the performance of the considered lighting schemes after ten simulation runs.

3.3.2.1 Streetlight Usefulness Experienced by Road Users

Figure 3.14 (a) shows the interquartile ranges (IQRs) of mean streetlight usefulness experienced by each simulated road user, while streetlights are operating the Conventional lighting scheme. Although, this scheme always switches on the streetlights at 100% lighting level, a near-perfect streetlight usefulness ($> 90\%$) is demonstrated. This trend is also demonstrated by all the schemes evaluated in Figure 3.15 and 3.16. This result, however, is expected as some of the road segments between two adjacent streetlights are larger than the area streetlight beam pattern (30 m) can cover. Because of this there are small sections of unlit road that have prevented a perfect streetlight usefulness (100%) from being achieved. In general, the streetlight usefulness experienced by the simulated motorists is higher than that experienced by the simulated pedestrians. This is due to StreetlightSim's placement of streetlights at the centre of roads, and their circular beam pattern. Therefore, the simulated pedestrians encounter larger unlit road sections compared to the simulated motorists.

In Table 3.3, Part-night, Philips Chronosense and Dynadimmer adjust the lighting levels of the streetlights according to predefined timetables. Thus, they are considered as time-based lighting schemes, and, as a result of this, streetlight usefulness experienced by the simulated road users also fluctuates according to their predefined timetable. Figure 3.14 (b) shows the streetlight usefulness of Part-night lighting scheme. As shown in the figure, this scheme has a similar level of usefulness to Conventional lighting schemes, except between 00:00 and 05:30. However, this is expected as Part-night lighting scheme is scheduled to switch off the streetlights completely during these periods.

Figure 3.15 (a) shows the streetlight usefulness experienced by simulated road users while streetlights are operating Philip Chronosense. This scheme allows lighting levels to be reduced to a predefined value at a predefined time. In this thesis, the lighting level of the streetlights is reduced to 65% between 22:00 and 05:00 (a typical setting of Chronosense

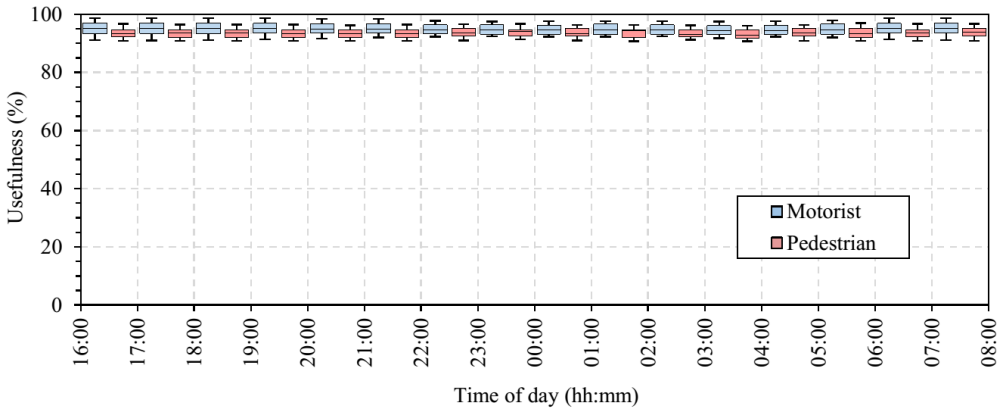

(a)

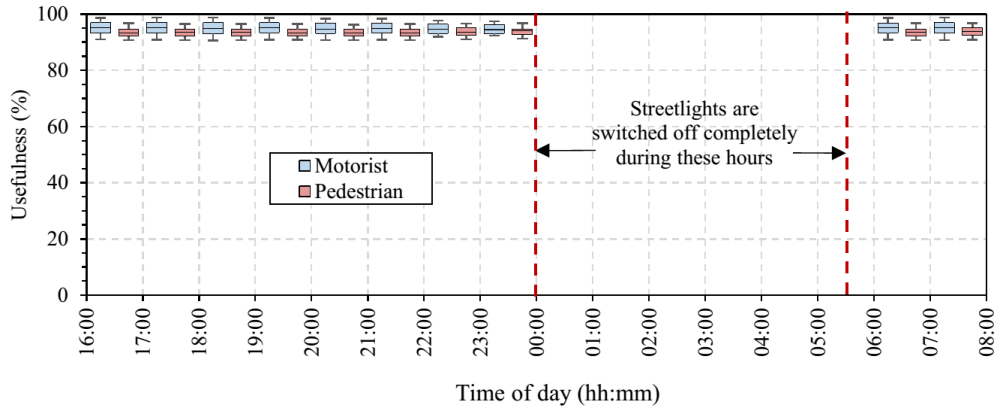

(b)

Figure 3.14: The IQRs of mean streetlight usefulness experienced by simulated road users, while streetlights are operating: (a) Conventional, and (b) Part-night lighting schemes. The error bars represent the minimum and the maximum mean usefulness experienced by road users. Due to placement of the streetlights at the centre of roads, and their circular beam pattern implemented in StreetlightSim, the usefulness experienced by the simulated motorists is higher than those experienced by the simulated pedestrians.

[98]). Correspondingly, streetlight usefulness during these hours is also reduced to 68 – 72% and 60 – 65% for the simulated motorists and pedestrians respectively. For the remaining hours, this scheme offers a similar level of usefulness to the Conventional lighting scheme. Compared to Chronosense, Dynadimmer allows multiple predefined lighting levels as summarised in Table 3.3. As shown in Figure 3.15 (b), the usefulness experienced by the simulated pedestrians and motorists varies according to five different operational periods. As the maximum lighting level of the scheme is at 90%, none of the simulated road users are able to experience streetlight usefulness above 90% as demonstrated by other evaluated schemes.

Figure 3.16 (a) shows the streetlight usefulness of Zoning lighting scheme. For pedestrian traffic, Zoning has a similar performance to that demonstrated by the Conventional lighting scheme. However, the streetlight usefulness experienced by motorists is severely

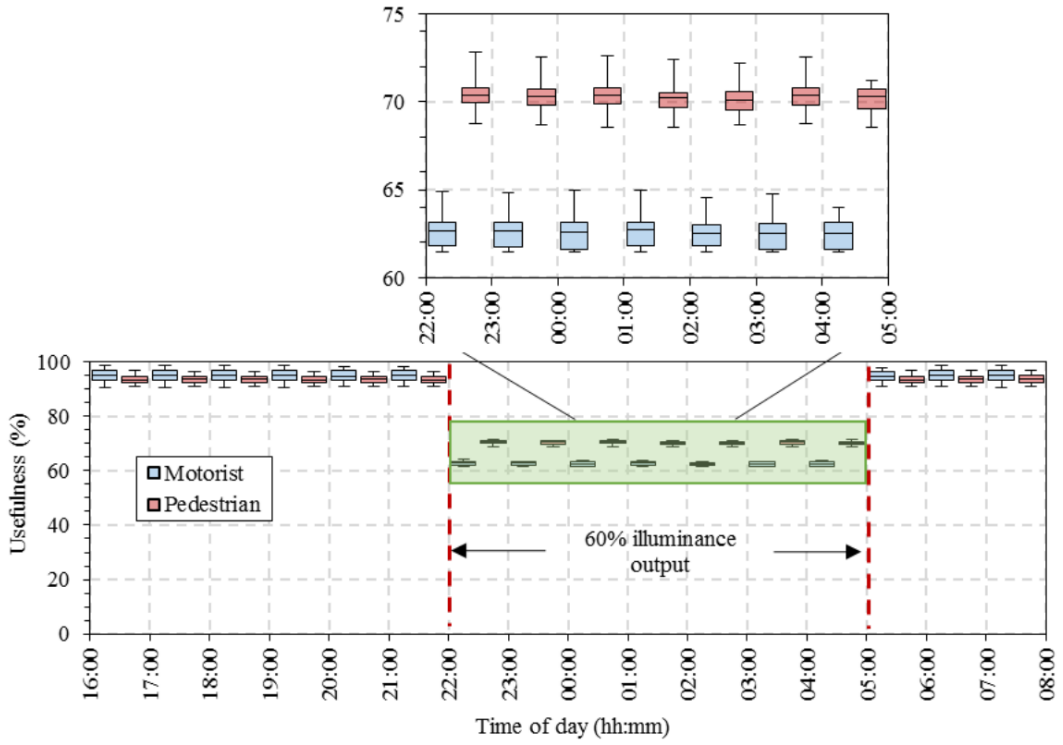

(a)

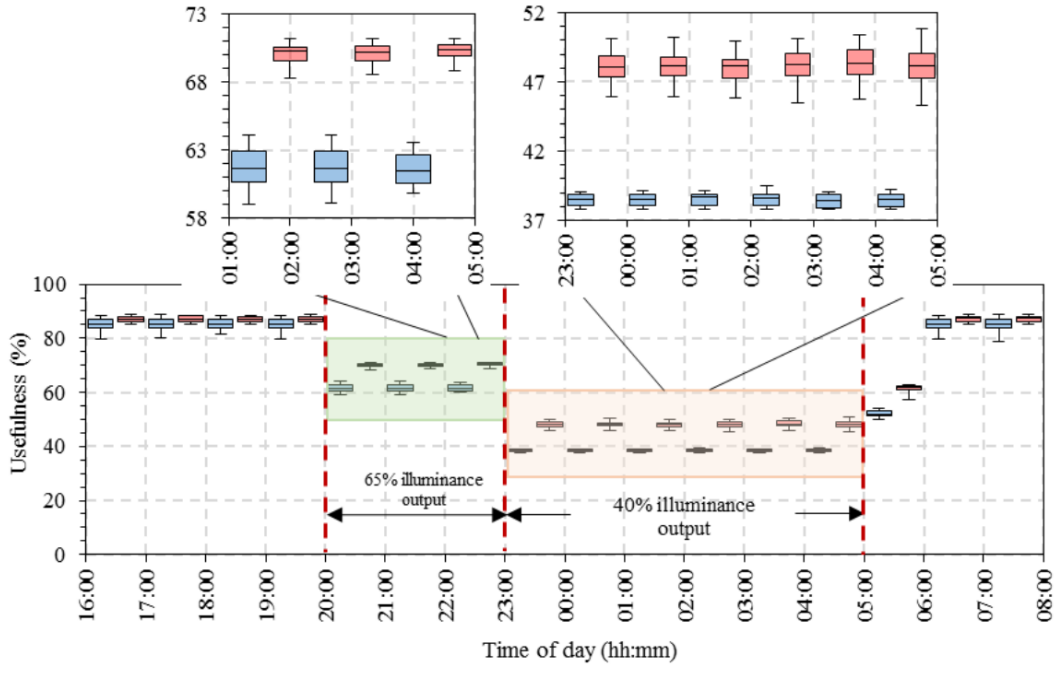

(b)

Figure 3.15: The IQRs of mean streetlight usefulness experienced by simulated road users while streetlights are operating: (a) Philips Chronosense, and (b) Philips Dynadimmer. The error bars represent the minimum and the maximum mean usefulness experienced by road users.

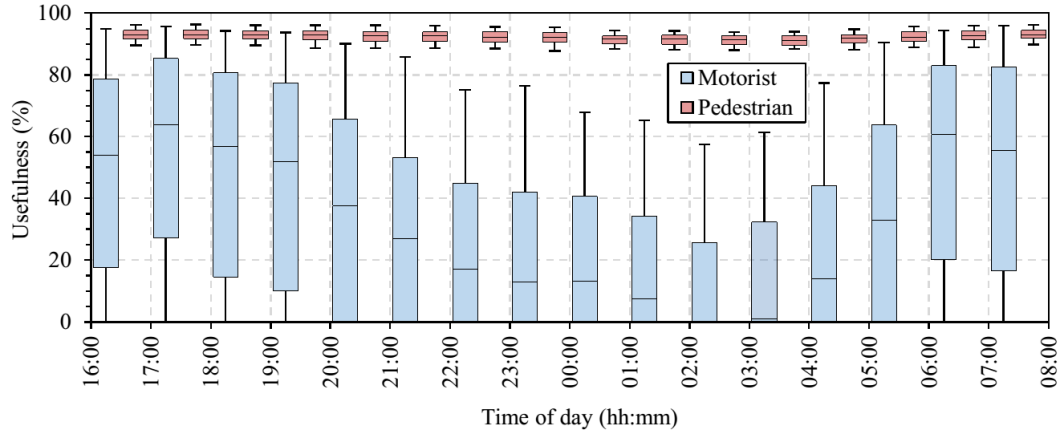

(a)

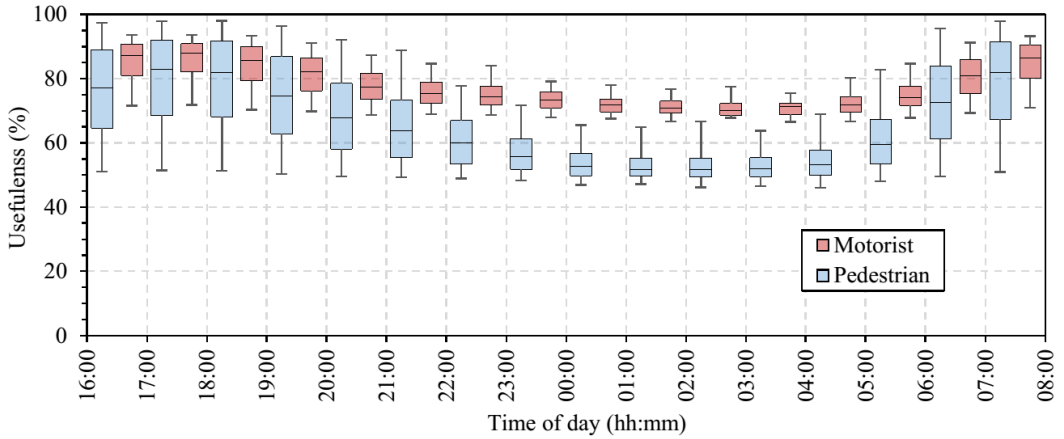

(b)

Figure 3.16: The IQRs of mean streetlight usefulness experienced by simulated road users, while streetlights are operating traffic-aware lighting schemes: (a) Multi-Sensor, and (b) Zoning. The error bars represent the minimum and the maximum mean usefulness experienced by road users.

impacted. This is expected as it is not designed for these users. Figure 3.16 (b) shows the usefulness of Multi-sensor lighting. For Multi-sensor, all streetlights are always at 40% lighting level, and this is increased to 70% and 100% when a road user is 20 m and 10 m away from the streetlight, respectively. Thus, this scheme is unable to create the lighting conditions that satisfy both the requirements of the pedestrian and the motorist, and has a reduced usefulness when it is compared to the Conventional lighting scheme. The increased traffic volumes between 16:00 – 20:00 and 06:00 – 08:00 cause the streetlights to constantly switch on at higher lighting levels, and hence higher usefulness can be observed at these times.

3.3.2.2 Energy Consumption

Figure 3.17 shows the mean total energy consumption of 112 streetlights in one week for different traffic volumes while operating the lighting schemes summarised in Table 3.3. Since time-based lighting schemes, i.e. Conventional, Chronosense, Part-night and Dynadimmer, are not dependent on traffic flow, their energy consumption remains constant when evaluated with different traffic flow. As expected, Conventional is the least energy efficient amongst the lighting schemes evaluated. This is expected, since the streetlights are always switched on at 100% lighting level. Chronosense, Part-night and Dynadimmer reduce lighting levels at specific hours, hence reducing energy consumption by 15%, 34% and 37% respectively, compared to Conventional.

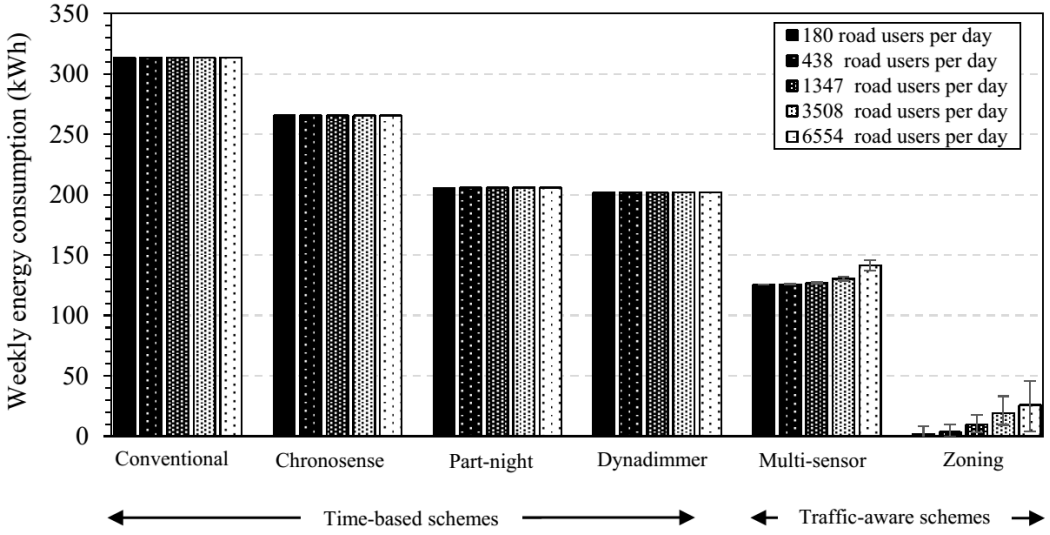

Figure 3.17: Mean weekly energy consumption of 112 streetlights while operating various street lighting schemes from 16:00 to 08:00 the next day. The error bars represent the maximum and the minimum energy consumption.

In general, the energy consumption of streetlights while operating traffic-aware lighting schemes, i.e. Multi-sensor and Zoning, increases with larger traffic volumes. This trend, however, is anticipated since these schemes are designed to save energy by switching off or dimming the lights when less traffic is presented. As a result of increasing traffic volumes, a near-continuous stream of traffic is developed within the detection range of each sensor. Hence, the time each streetlight spends active is also prolonged, and thus energy consumption is also increased. The effect of increasing traffic volumes on Multi-sensor lighting scheme, however, is less pronounced compared to Zoning. This is because the streetlights operating Multi-sensor are constantly switched on at 40% lighting level even when road users are not detected. Compared to the Conventional lighting scheme, Multi-sensor reduces energy consumption by 55 – 60%, where energy consumption increases with larger traffic volumes.

Amongst all the evaluated lighting schemes, Zoning consumes the least energy for all the scenarios considered. Compared to the Conventional lighting scheme, the energy consumption of Zoning is 1 – 8% of the energy required by Conventional, where energy consumption increases with larger traffic volumes. However, its energy is expended for only a small proportion of road users, i.e. pedestrians (14%). As shown in Figure 3.16 (a), streetlight usefulness experienced by motorists is lower and fluctuates significantly compared to pedestrians' with Zoning lighting scheme. This is because this scheme was originally designed to address the needs of pedestrians. Because of this, Zoning fails to provide comparable streetlight usefulness to the motorist as that demonstrated by other lighting schemes.

3.3.3 Limitation

There are several limitations that are worth noting when using StreetlightSim to evaluate the considered lighting schemes. As shown in Figure 3.2, the available traffic profiles are distributed by the hour; however, details on how traffic is distributed within an hour is unavailable. Because of this, StreetlightSim randomly injects simulated traffic as simulation runs. This, however, possibly reflects an actual traffic scenario. While the energy consumption of traffic-aware lighting schemes, i.e. Multi-sensor and Zoning, is traffic dependent, the reported results in Section 3.3.2 are limited to traffic profiles in the UK, although these evaluations are repeatable by replacing the traffic profiles with other places of interest.

3.4 Summary

This chapter proposed a streetlight usefulness model: an evaluation metric to measure the usefulness or practicality of street lighting from the perspective of a motorist and a pedestrian. This model was adopted and translated into StreetlightSim, a simulation environment developed as part of this research. This tool integrates the modelling and simulation of traffic, traffic sensing and streetlight operation. It has been used to evaluate the performance of lighting schemes summarised in Table 3.3. All the lighting schemes have been evaluated with 112 streetlights, which operate from 16:00 to 08:00 the next day, together with different traffic profiles and volumes. The performance of the Conventional or 'always-on' lighting scheme is also included in this chapter as the benchmark for the rest of the evaluated lighting schemes.

Based on the simulation results, Conventional lighting scheme consumes the most energy. In return, this scheme offers a near-perfect streetlight usefulness ($> 90\%$) to both simulated motorists and pedestrians during its operational hours. The energy consumption of time-based lighting schemes, i.e. Part-night, Philips Chronosense, and Philips

Dynadimmer, varies across their operational hours. The time-based lighting schemes reduce lighting levels of the streetlights between late evening and early morning to conserve energy when low traffic is expected during these hours. Consequently, this also reduces the usefulness of the lighting schemes during these hours. Traffic-aware lighting schemes have better energy efficiency compared to time-based lighting schemes as lighting levels of the streetlights are increased to 100% once a road user is detected in close proximity. Although traffic-aware lighting schemes outperformed time-based lighting schemes in terms of energy efficiency, their lighting control has yet to consider different lighting needs from the perspective of road users. An example of this is Zoning, a pedestrian-aware lighting scheme that has the lowest energy consumption amongst all the evaluated schemes. Although its energy consumption is the lowest, it has failed to provide equivalent streetlight usefulness demonstrated by the Conventional lighting scheme, especially for motorists. Similarly, due to lack of information sharing and collaboration between streetlights, Multi-sensor also is incapable of maintaining the same level of streetlight usefulness as demonstrated by the Conventional lighting scheme.

In the next chapter, the proposed streetlight usefulness model is considered in the design of a distributed traffic-aware lighting scheme, known as TALiSMaN. This scheme aims to preserve or improve the streetlight usefulness of existing lighting schemes while maintaining a reasonable energy use.

Chapter 4

TALiSMaN: A Traffic-Aware Lighting Scheme

From Chapter 2, many street lighting schemes have considered the use of information and communication technologies to allow the precise and adaptive control of street lighting to conserve energy. Importantly, many of these existing works were primarily aimed at reducing energy consumption, with very little consideration given to the associated impact of such schemes on the usefulness of the streetlights. In Chapter 3, the usefulness and the energy consumption of these schemes have been evaluated. Simulation results showed that some of the evaluated schemes have significantly reduced the energy use of street lighting. For example, the Part-night lighting scheme, which is widely used by local government in the UK [14] can reduce energy consumption by 34% compared to the Conventional or 'always-on' scheme. Nevertheless, the usefulness of the Part-night scheme drops to zero when it switches off the lights. Thus, to have an effective (fulfilling the need of road users) and efficient (low energy demand) street lighting scheme can be considered as an optimisation problem where the scheme needs to maximise the usefulness of having street lighting while minimising its energy consumption.

This chapter proposes TALiSMaN, a distributed **T**raffic-**A**ware **Li**ghting **S**cheme **Ma**nagement **N**etwork. The aim of this scheme is to fulfil the need of road users for street lighting by creating lighting conditions that achieve similar streetlight usefulness as offered by Conventional or 'always-on' lighting scheme. Although TALiSMaN aims to maintain similar level of streetlight usefulness as offered by Conventional lighting scheme, it is expected to have relatively lower energy demand compared to lighting schemes evaluated in Chapter 3. In Section 2.1, road users require a section of road to be lit and streetlights operate at variable lighting levels, thus TALiSMaN is expected to have reasonable energy demand as compared to lighting schemes evaluated in Chapter 3. This scheme presents a number of novel contributions over state-of-the-art lighting methods:

- TALiSMaN tailors its operation to different road users. This is based on the streetlight usefulness models presented in Section 3.1.
- Instead of requiring a centralised remote controller, TALiSMaN has been designed to operate autonomously over a short-range mesh network.

This chapter is structured as follows: Section 4.1 introduces the concept of TALiSMaN, and is followed by its operation and implementation over WSNs in Section 4.2. The proposed scheme is evaluated by simulating real streetlight topology from a residential area in Southampton, UK, and considers a range of different V_{comb} values. Section 4.3 presents the performance of the proposed lighting scheme in terms of streetlight usefulness achieved and energy consumed.

4.1 Concept of TALiSMaN

Based on the streetlight usefulness models proposed in Chapter 3, two observations can be reached: (1) the lengths of the required lit road segments are finite, i.e. 100 m and 150 m for motorists and pedestrians respectively; and (2) within these required lit road segments, pedestrians and motorists require different lighting conditions. TALiSMaN exploits these properties by progressively adjusting the lighting level of streetlights according to different road users' needs, and thus improves their energy efficiency by minimising their energy use. TALiSMaN detects road users and shares the information with nearby streetlights. Upon receiving the information, they cooperate to create optimum lighting conditions that meet the road users' needs, and avoid illuminating the road at higher levels as this simply wastes energy.

TALiSMaN considers the streetlight usefulness models proposed in Chapter 3, and the need for street lighting is translated into a relationship between a streetlight's proximity to the road user and the desired lighting level. This is summarised in Table 4.1. Instead of relying on a remote centralised control centre for managing streetlight operation, an autonomous WSN is adopted to implement TALiSMaN. Each streetlight incorporates a wireless sensor node with a short-range wireless communication module. This allows streetlights to form a multi-hop WSN with neighbouring streetlights to exchange information. The network is time-synchronised, and each streetlight is pre-programmed with its own location information and unique identification, which is shared with others during network setup.

The streetlights are equipped with a light controller and a road-user sensor [42,101]. The light controller modulates the lamp output to switch the streetlight on, off, or adjust its illuminance. To allow a near-instant response to continually changing illuminance requests, it is assumed that each streetlight uses a dimmable light-emitting diode (LED) lamp. The beam pattern of the lamp covers a limited area of a single road segment.

Table 4.1: The relationship between road users' distance and streetlight lighting levels.

Road User Type	**Distance from streetlight**, d	**Lighting level**
Pedestrian	$0 \leq d < 30$	100 %
	$30 \leq d < 60$	80%
	$60 \leq d < 90$	60%
	$90 \leq d < 120$	40%
	$120 \leq d \leq 150$	20%
	$d > 150$	0%
Motorist	$0 \leq d \leq 100$	100 %
	$d > 100$	0%

Although this sensor-based method provides less accuracy in detecting a road user's position than a GPS-based system [21], it does not require road users to be instrumented with dedicated smartphone apps or other hardware. Nevertheless, this method can provide substantial energy savings, as demonstrated in Section 4.3.2

In short, TALiSMaN is an alternative lighting scheme that creates adjusted lit road sections to satisfy different road users' needs for street lighting. This can be achieved by the collaboration of a group of networked streetlights. However, it is not the intention of this scheme to propose a new method of selecting appropriate lighting levels for streets as presented in existing standards or recommendations. Thus, it is assumed that lighting levels are predetermined according to adopted standards or recommendations, before this scheme is implemented.

4.2 Operation and Implementation of TALiSMaN using Autonomous Networked Sensors

As established in Chapter 2, there is an increasing interest in networking streetlights using a wireless communication network. Thus, this section presents the operation and the implementation of TALiSMaN from the perspective of WSNs.

4.2.1 System Operation

In order to enable the progressive control of streetlight lighting level, based on either presence detected by local sensors or information relayed by neighbouring streetlights, four different operational states are defined in TALiSMaN: 'Lamp on by sensor', 'Lamp on by neighbour', 'Lamp on by delay' and 'Lamp off'. Within these operation states, 'Lamp off' and 'Lamp on by sensor' are shared between neighbouring streetlights via an on-board wireless communication module. Figure 4.1 shows the state machine of these operation states during streetlight operational hours.

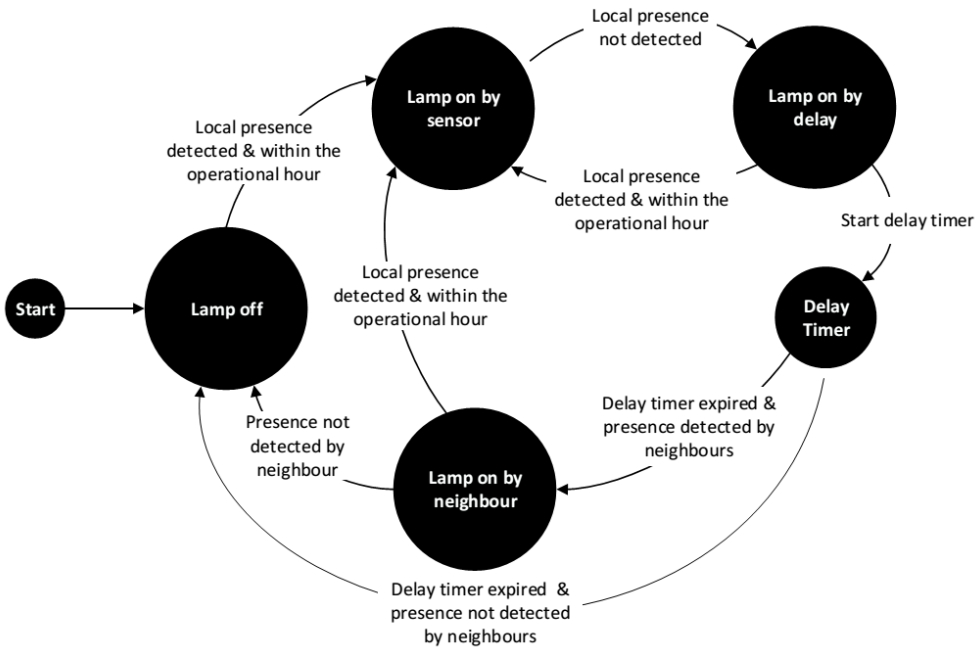

Figure 4.1: TALiSMaN operation state machine during streetlight operational hours.

When TALiSMaN shifts to 'Lamp on by delay', the state delay counter is reset and activated (Section 4.2.3 details on this). The operation state will remain here until the state delay counter expires or a road user is detected by a local road-user sensor. When the state delay counter expires, the received neighbours' operation states are evaluated, and the operation state shifts to 'Lamp on by neighbour' only if the neighbours are on. At this state, the streetlight remains switched on and its lighting level is adjusted to deliver the required lighting conditions (Section 4.2.2 details on this). The streetlight is switched off if none of the local or neighbouring road-user sensors have detected the presence of any road user. While the operation state is 'Lamp on by neighbour' or 'Lamp off', the operation states from neighbouring nodes are evaluated as each packet is received.

4.2.2 Adjusting the Lighting Level

For TALiSMaN, the lighting level of streetlights is adjusted for energy conservation while maintaining the optimum usefulness of having street lighting. However, creating a lit road segment that satisfies different road users' needs requires coordination between several streetlights. This is due to the assumption that a road-user sensor has a limited detection range and the coverage from the streetlight beam pattern is finite. The coordination between streetlights is facilitated by sharing road users' presence information with other streetlights within the required lit road segments. By sharing this information, the relative distance to the road user can be approximated using the Euclidean distance to the streetlight that detects the road user. When the precise location of a road user

is unknown, the receiving streetlights assume that the detected road users are at the 'best-case' distance from them. This approximate relative distance, d_aprox, assumes that the road user, from the perspective of the receiving streetlight, is always located at the nearest edge of the sensor range, as illustrated in Figure 4.2 and 4.3.

The following sections detail the modulation of the streetlight lighting level upon detection of a pedestrian and a motorist.

4.2.2.1 Modulation of Lighting Level Based On Detected Pedestrians

Figure 4.2 shows the development of the required lighting condition after a pedestrian is detected by a road-user sensor at streetlight s_2. After the presence of the pedestrian is shared amongst the streetlights s_1 to s_8, the lighting level of the respective streetlight, φ_{ped} is progressively modulated according to the following algorithm:

1: **if** operation state is 'Lamp off' **then**
2: $\varphi_{ped} = 0$
3: **end if**
4: **if** operation state is 'Lamp on by sensor' **or** 'by neighbour' **then**
5: $\varphi_{ped} = 1 - 0.2\ Z_{ped}(d_{aprox})$
6: **end if**
7: **if** if operation state is 'Lamp on by delay' **then**
8: current φ_{ped} remains
9: **end if**

where φ_{ped} is the required lighting level of the streetlight based on the approximate relative distance to the detected pedestrian, d_{aprox} (m); and Z_{ped} determines the illumination zone of the streetlight according to d_{aprox}.

In Section 3.1, five different illumination zones were considered for pedestrians, and the required lighting level of each zone sequentially reduced by 20%, with respect to the lighting level specified by the adopted standards and guidelines for the road. To allow streetlights in each zone to operate at these lighting levels, φ_{ped} is sequentially reduced by a factor of 0.2 per zone. Since each illumination zone is 30 m in length and a pedestrian prefers a lit road segment of 150 m before and after them, Z_{ped} has a maximum value of five. The illumination zone of a streetlight, Z_{ped} with respect to d_{aprox} is given by:

$$Z_{ped}(d_{aprox}) = \begin{cases} 0, & \left\lfloor \frac{d_{aprox}}{30} \right\rfloor = 0 \\ \left\lfloor \frac{d_{aprox}}{30} \right\rfloor - 1, & 0 < \left\lfloor \frac{d_{aprox}}{30} \right\rfloor \leq 5 \\ 5, & \left\lfloor \frac{d_{aprox}}{30} \right\rfloor > 5 \end{cases} \tag{4.1}$$

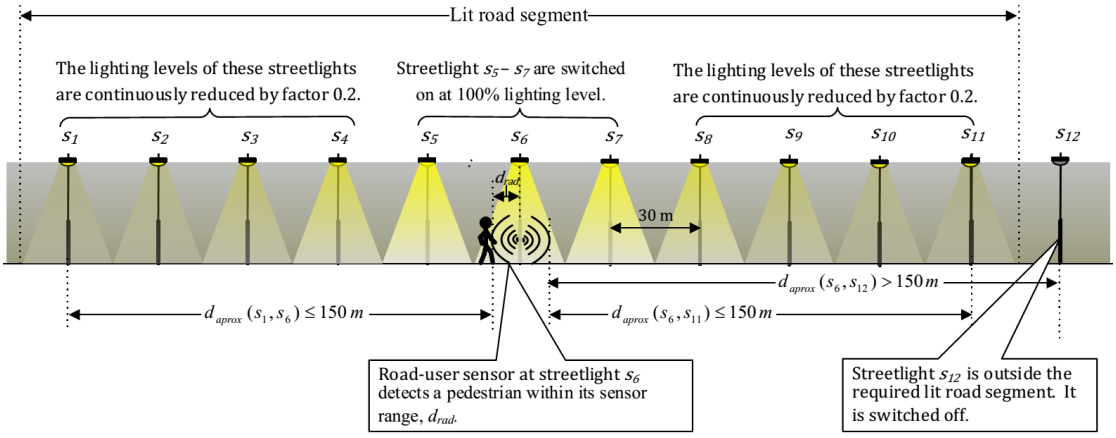

Figure 4.2: A lit road segment developed by streetlight s_1 to s_{12} based on the approximate relative distance, d_{aprox}, to the detected pedestrian. As $d_{aprox}(s_5, s_6)$ and $d_{aprox}(s_6, s_7)$ are less than 30 m, streetlights s_5, s_6 and s_7 are switched on at full brightness (100%). Assuming the streetlight beam pattern can cover a 30 m of road segment, these streetlights creates a 30 m and a 60 m of illumination zone behind and in front of the pedestrian respectively. For streetlights s_2 – s_4, and s_8 – s_{11}, their lighting levels are sequentially reduced by factor 0.2 with respect to the level of the streetlight that detects the pedestrian. Since $d_{aprox}(s_6, s_{12}) > 150$ m, streetlight s_{12} is completely switched off.

$$d_{aprox} = \begin{cases} 0, & d_{rad} \geq d_{det} \\ d_{det} - d_{rad}, & d_{rad} < d_{det} \end{cases} \tag{4.2}$$

where d_{det} is the Euclidean distance to the nearest streetlight that detects the pedestrian (m); and d_{rad} is the maximum detection range of the road-user sensor (m).

4.2.2.2 Modulation of Lighting Level Based On Detected Motorists

As the difficulty in detecting potential hazards increases with darker lighting conditions [185], the streetlight lighting level required by a motorist, φ_{mot} is always at 100% for a road segment 100 m ahead of them. Since road-user sensors are assumed to be unable to detect the direction that the detected motorist is travelling in, both road segments before and after the motorist are lit. Figure 4.3 illustrates the development of the required lighting condition upon detection of a motorist by a road-user sensor at streetlight s_1. After the presence of the motorist is shared between streetlights s_1 to s_5, their lighting level is modulated according to the following algorithm:

1: **if** operation state is 'Lamp off' **then**
2: $\varphi_{mot} = 0$
3: **end if**
4: **if** operation state is 'Lamp on by sensor' **or** 'by neighbour' **then**
5: $\varphi_{mot} = 1 - Z_{mot}(d_{aprox})$

6: **end if**
7: **if** if operation state is 'Lamp on by delay' **then**
8: current φ_{mot} remains
9: **end if**

where Z_{mot} is the function that determines whether a streetlight is within the required road segment that is needed to be lit. Z_{mot} is given by:

$$Z_{mot}(d_{aprox}) = \begin{cases} 0, & \left\lfloor \frac{d_{aprox}}{d_{avg}} \right\rfloor \leq \left\lfloor \frac{100}{d_{avg}} \right\rfloor \\ 1, & \left\lfloor \frac{d_{aprox}}{d_{avg}} \right\rfloor > \left\lfloor \frac{100}{d_{avg}} \right\rfloor \end{cases} \tag{4.3}$$

where d_{aprox} is the approximate relative distance to the detected motorist (m) as given by Eq. 4.2; and d_{avg} is the average distance to the next adjacent streetlight (assumed to be 30 m).

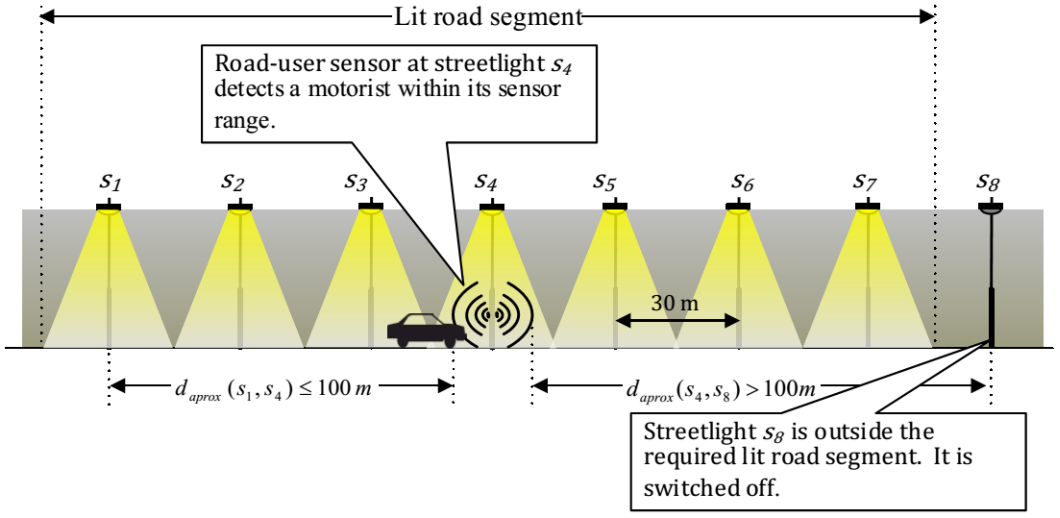

Figure 4.3: A lit road segment created by streetlight s_1 to s_8 while operating TALiSMaN. This lighting condition is created based on the approximate relative distance, d_{aprox}, to the detected motorist. For streetlights s_1 to s_7, their d_{aprox} to s_4 is less than 100 m, thus they are switched on at full brightness (100%); whereas $d_{aprox}(s_4, s_8)$ is more than 100 m, thus streetlight s_8 is completely switched off.

4.2.2.3 Combined Pedestrian-Motorist Light Level Modulation

Whenever pedestrians and motorists are detected simultaneously, the lighting level of the streetlight is set to $max(\varphi_{ped}, \varphi_{mot})$. This is to ensure that an optimum lit environment can be provided both to pedestrians and motorists.

4.2.3 Accommodating the Void Region

Void regions result from gaps in sensor coverage between streetlights. When road users travel into them, they can potentially cause unnecessary adjustment of the lighting levels. To reduce the impact of void regions, a state delay counter is adopted to prolong the TALiSMaN operation state at 'Lamp on by delay' until the road user is believed to have left the void region and has entered the sensing range of the next streetlight. This feature also mitigates the latency of the communication network, which is particularly relevant when neighbouring sensor nodes detect the presence of road users simultaneously and compete for the communication channel to disseminate the information.

In this thesis, the expiration time of the state delay counter, t_{exp}, is given by:

$$t_{exp} = \frac{d_{adj} - 2d_{rad}}{v}, \quad d_{adj} \geq d_{rad} \tag{4.4}$$

where d_{adj} is the distance to the furthest adjacent streetlight (m); d_{rad} is the detection range of the sensor node (m), and it is assumed to be 13 m [101]; and v is the expected slowest travelling speed of a particular road user (m/s).

Considering that only the presence of road users is known, the road user's slowest travelling speed is used to compute t_{exp}. The slowest travelling speed of a motorist on residential roads is assumed to be 4.5 m/s (10 mph). For pedestrians, 0.73 m/s is assumed to be the slowest walking speed after considering the 5th percentile of pedestrian walking speed distribution (mean walking speed is 1.34 m/s and standard deviation is 0.37 m/s) [191]. If both motorists and pedestrians are detected at any one moment, the pedestrian's slowest walking speed is always used to compute t_{exp}.

4.3 Evaluating the Performance of TALiSMaN

This section evaluates the performance of TALiSMaN from two metrics: (a) streetlight usefulness experienced by road users, as previously presented in Section 3.1; and (b) energy consumed by the streetlights while operating this scheme; the energy model previously presented in Eq. 3.11 is used for this.

4.3.1 Simulation Setup

To evaluate the performance of TALiSMaN, the scheme is translated and implemented into StreetlightSim. For clarity of the simulation, the simulation scenario and parameters previously used in Section 3.3.1 are also adopted in this chapter. Since TALiSMaN uses WSNs to relay and exchange information, a detailed setup of WSN is presented here.

4.3.1.1 Wireless Sensor Node

As presented in Section 4.2, the lighting level of streetlights is individually controlled by a wireless sensor node, based on the presence of road users. To enable the effective detection of road users, these nodes are assumed to be equipped with a multi-sensor array. Details of the sensor array, however, are outside the scope of this research. The sensing range and sample rate vary considerably between technologies [101]. For the purposes of evaluation, Table 4.2 summarises the parameters that are adopted in this evaluation.

Table 4.2: Sensor parameters and values.

Parameter	**Value**
Sensing range	13 m [101]
Sensor sampling rate	20 Hz

Information on detected road users is time-sensitive, so it has to be relayed to neighbouring sensor nodes with minimal delay. If this information is relayed too late, the performance of TALiSMaN will be reduced, because streetlights will respond less quickly to road users' movements, reducing streetlight usefulness and/or increasing energy consumption. To address this need, all the sensor nodes are assumed to operate using an IEEE 802.15.4 non-beacon enabled mode and adopt carrier sense multiple access with collision avoidance (CSMA-CA) as their media access control layer protocol [140]. While operating in this mode, sensor nodes are always active and ready to relay any information as required. Table 4.3 summarises the communication parameters adopted during the simulations. Since the focus of this work is on the energy efficiency of street lighting schemes and their respective streetlight usefulness, the simple path loss radio propagation model from the MiXiM framework was used in this work. To account for random variation in the channel, log-normal shadowing is also applied.

Table 4.3: IEEE 802.15.4 parameters and their values.

Parameter	**Value**
Bit rate	250 kbps
Radio propagation model[1]	Simple path loss model with log-normal shadowing effect
Minimum bit error rate	$1x10^{-8}$
Radio transmission power[2]	-3 dBm

1. An alpha value of 2.5, and a standard deviation of 6 with mean attenuation of 0 are used for the simple path loss and log-normal models respectively [192].
2. Based on the IEEE 802.15.4 model provided by the MiXiM framework [192], a transmission power of -3 dBm allows all the streetlights to communicate with their adjacent neighbours with a 99.9% successful packet delivery rate.

4.3.1.2 Routing Protocol

During simulations, the necessary information for TALiSMaN's operation is communicated using a 19–byte packet: 4 bytes for the packet source and destination address, 1 byte for the message type coding, message versioning, command coding, command data length and data, 4 bytes for the packet timestamp, and 2 bytes for the packet checksum. Given that the travel direction of the detected road users is not available to TALiSMaN, and to allow sensor nodes to create the lighting conditions that offer optimum streetlight usefulness collaboratively, information on detected road users is relayed to any sensor node within a 150 m radius of the source node. However, this requires a routing protocol to govern real-time end-to-end information propagation to all the streetlights within 150 m radius. As discussed in Section 4.3.1.1, the information on the detected road users is delay-sensitive and will be of limited use if the information is delay. Thus, retransmission or guaranteed delivery of this information is not the focus of this protocol, but it should allow propagation of the information to all the sensor nodes within the confined distance with minimum delay.

As discussed in Section 2.3.2.2, there is a number of routing protocols that could be adopted for disseminating necessary information for TALiSMaN's operation within the networked streetlights. However, the performance evaluation of these protocols for TALiSMaN operation is not the focus of this thesis. Therefore, packet flooding is adopted in our simulations due to its simplicity. Nevertheless, uncontrolled flooding can lead to unnecessary network congestion and increased delays, which would consequently affect the performance of TALiSMaN. Therefore, the packet flooding is refined by discarding packets once they have reached a distance of 150 m from the source node. During simulations, propagation errors and packet collision are introduced which cause packets to be dropped (see Köpke *et al.* [193] for details about radio propagation errors and packet collision).

To administrate end-to-end network packet propagation, the refined packet flooding protocol decides if a received packet is further forwarded to other streetlights depending solely on three forwarding conditions given by:

1: receive a packet from a node
2: **if** (C_1 and C_2 and C_3) = true **then**
3: insert the packet in to forwarded list, and then forward the packet
4: **else**
5: discard the packet
6: **end if**

where

Condition C_1 is true for a received packet if distance to source node is less than 150 m, which is half of the lit road segment (150 m before and after) required by pedestrians;

Condition C_2 is true for a received packet if it is not found in the forwarded list; and

Condition C_3 is true if a packet's lifetime is less than 2 s. This duration was chosen based on the assumption that the permitted maximum travelling speed of a vehicle on residential roads is 30 mph (∼13 m/s) and the streetlights are 30 m apart.

To prevent the WSN from generating and forwarding redundant information, streetlights only propagate their operational state when a road user is detected. After detection, nodes continually report their operational state to neighbouring streetlights at a rate of 2 Hz, while the road user continues to be within its sensing range. 2 Hz was chosen based on the simulation scenario considered, i.e. a 30 m average distance between two adjacent streetlights and a residential road with a speed limit of 30 mph, therefore allowing each passing road user to be detected at least twice.

Due to the routing protocol adopted and the high network congestion that results (packet loss of between 23 – 29% was experienced during simulations, see Appendix B), nodes are programmed to continue to generate packets for an additional period of time at a rate of 2 Hz, if a streetlight is entering 'Lamp off' state. This extra mechanism increases the probability of streetlights receiving the latest operational state from other streetlights, which consequently switch off their light if no road user is detected.

To determine the most appropriate of this additional packet generation time, the same streetlight topology as shown in Figure 3.13 is evaluated with additional packet generation time of 1 s, 5 s, 10 s, 15 s, 20 s, 30 s, 40 s, 50 s, and 60 s. As the traffic during 17:00 – 18:00 is the busiest during the streetlight operational hours considered in this thesis, the additional generation time that allows streetlights to consume the less energy within this hour is adopted. Figure 4.4 shows the mean energy consumption of 112 streetlights after ten simulation runs when evaluated with 1000 road users (14% of them pedestrians) over an hour of lighting operation (17:00 - 18:00). The results show that generating and forwarding the 'Lamp off' state for an extra 15 s yields the lowest energy consumption compared to other durations considered. Thus, in this thesis, the nodes are programmed to continue to generate packet of an additional 15 s at a rate of 2 Hz.

4.3.2 Simulation Results

In this section, the performance of TALiSMaN is presented in terms of the streetlight usefulness experienced by simulated pedestrians and motorists, and the total energy consumed by 112 streetlights over a week (5 days for weekday traffic and 2 days for weekend traffic).

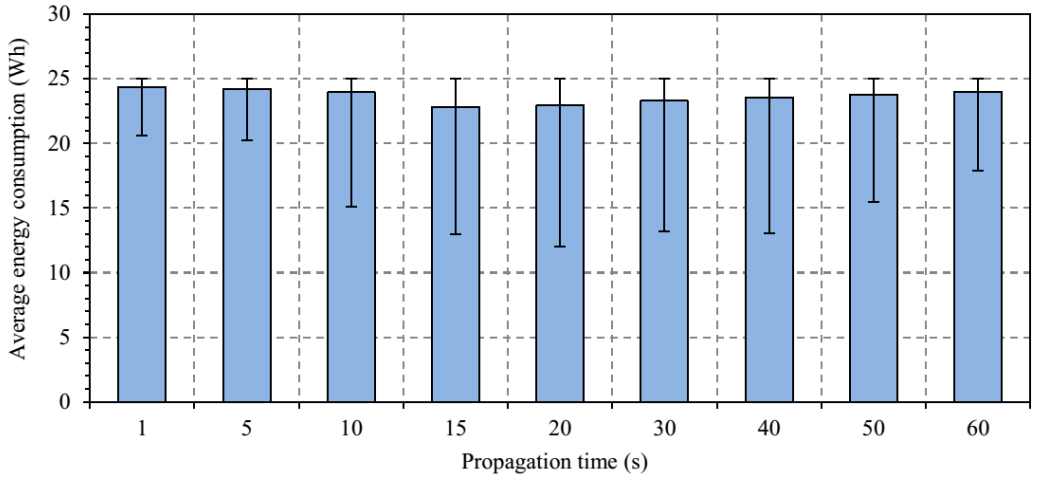

Figure 4.4: Effect of different additional packet generation times of 'Lamp Off' state on the energy consumption of 112 streetlights. The error bars represent the maximum and the minimum mean energy consumption of the streetlights.

4.3.2.1 Streetlight Usefulness Experienced by Road Users

To illustrate the behaviour of TALiSMaN, Figure 4.5 shows the lighting conditions of a road segment at different times as a result of a simulated pedestrian travelling towards streetlight s_{12}. At $t = 2$, the presence of the pedestrian is detected by streetlight s_8 and this information is shared between neighbouring streetlights, i.e. s_3 to s_{12}. Upon receiving the information, the lighting levels of these streetlights are adjusted to create the lighting conditions needed by the pedestrian. As the pedestrian travels towards streetlight s_{12}, these optimum lighting conditions are shifted to the right along with the presence detected by streetlight s_9 to s_{12}. Under such lighting conditions, TALiSMaN offers near-perfect streetlight usefulness to the pedestrian.

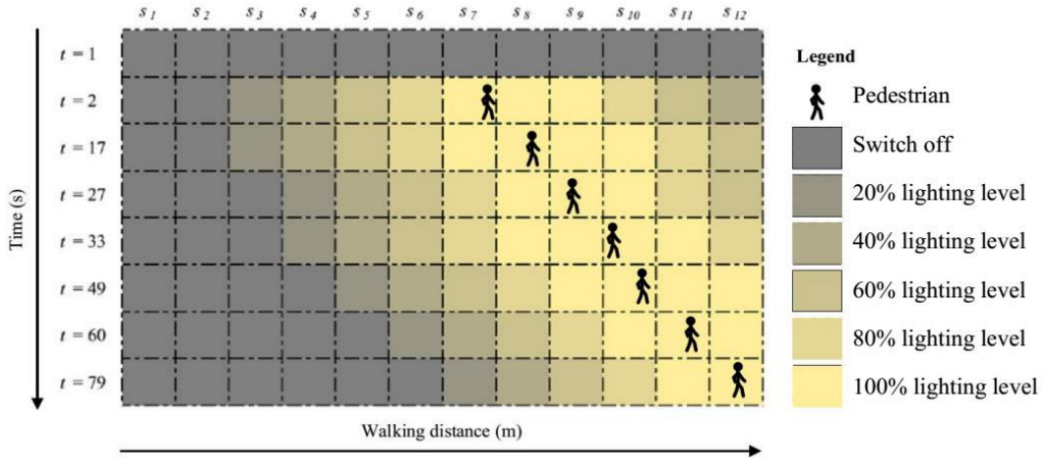

Figure 4.5: The dynamics of lit road segments (from top view) when a pedestrian is travelling from left to right.

Figure 4.6 shows the power output of a streetlight while operating TALiSMaN. During early operational hours, the power output of the streetlight is consistently 25 W. This trend is due to the near-continuous stream of road traffic during these 'rush hours' preventing streetlights from switching off. The same trend can be observed as it approaches the morning rush hour. The streetlight is mostly switched off between midnight and early morning as road traffic is lower compared to other operational hours. Although the streetlight is mostly switched off during these hours, TALiSMaN still retains the near-perfect usefulness of lighting to its users, as shown in Figure 4.7.

Figure 4.7 (a) shows the distribution of mean streetlight usefulness experienced by each simulated road user from 16:00 to 08:00 the next day, when streetlights are operating the TALiSMaN lighting scheme. For comparison, the distribution of average streetlight usefulness while streetlights operating conventional, which serves as the benchmark result for streetlight usefulness, and Zoning, which consumes the least energy to operate

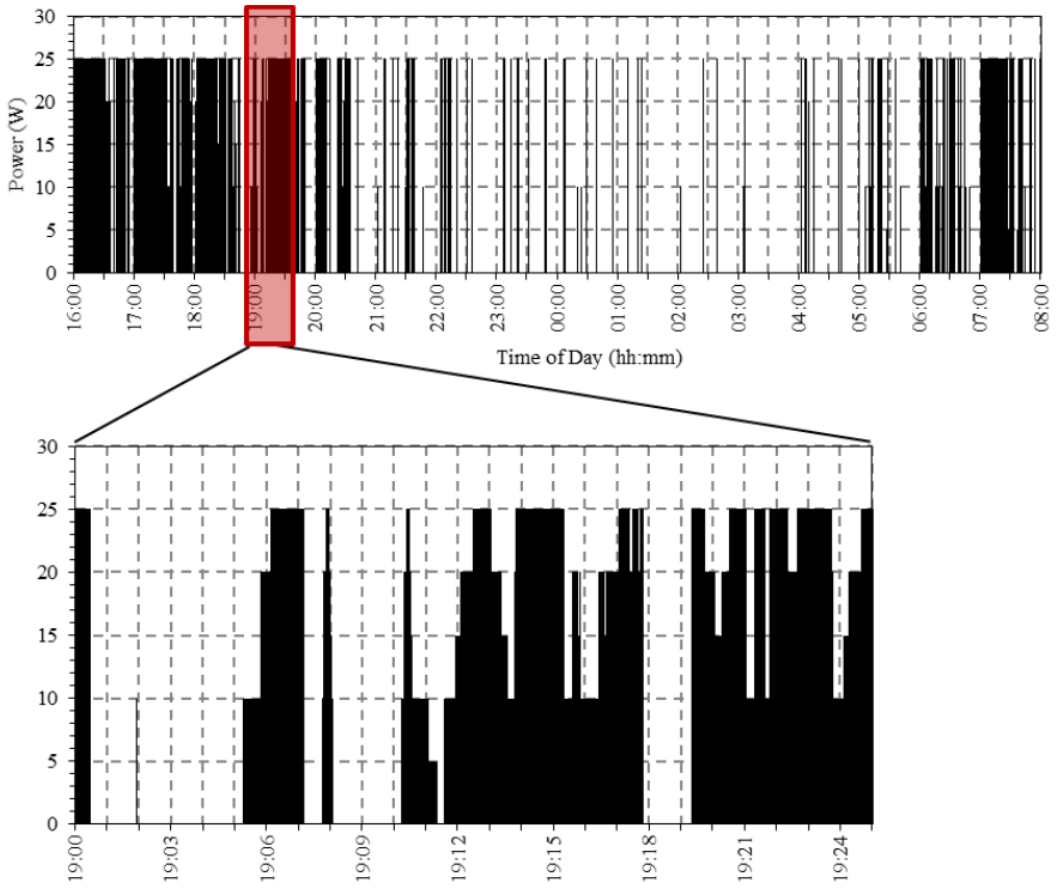

Figure 4.6: Power output modulation of a streetlight (25W) during operational hours from 16:00 until 08:00 the next day when TALiSMaN is evaluated with V_{comb} = 3508 road users per day.

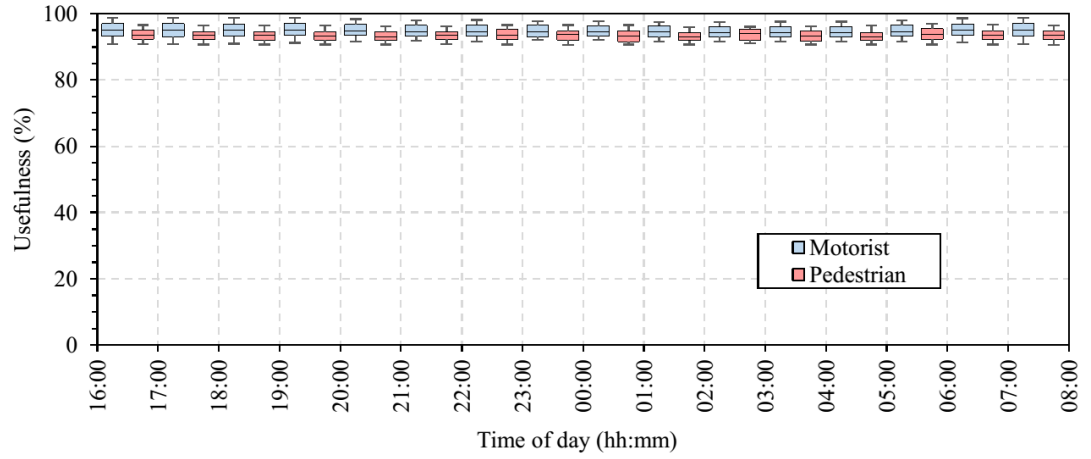

(a) TALiSMaN

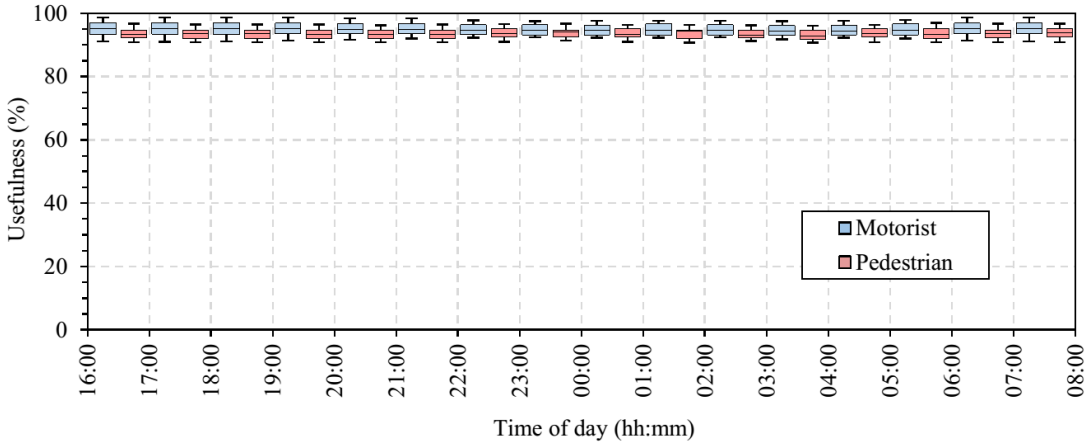

(b) Conventional

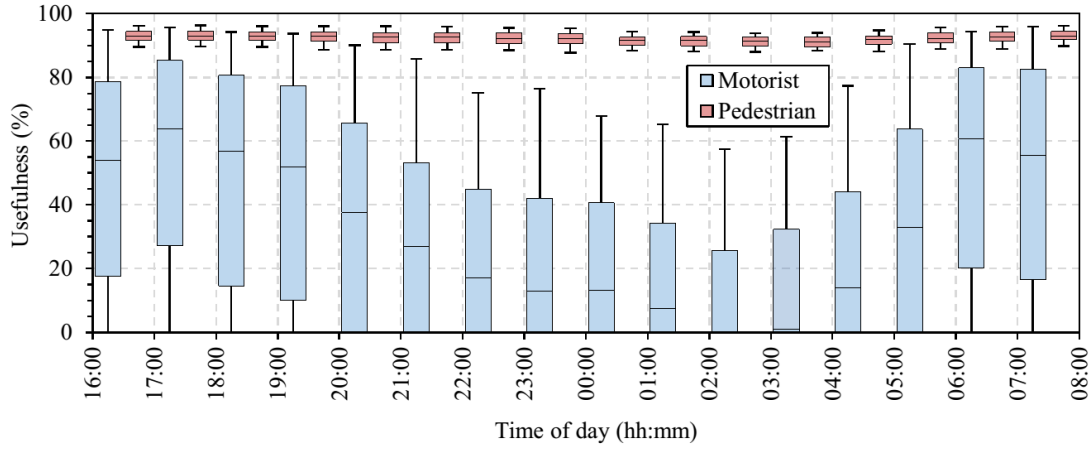

(c) Zoning

Figure 4.7: The IQRs of mean streetlight usefulness experienced by simulated road users, while streetlights are operating (a) TALiSMaN, (b) Conventional and (c) Zoning schemes during different operational hours.

amongst the lighting schemes evaluated in Chapter 3, are also included here. With TALiSMaN, it can be seen that all simulated road users experience at least 90% streetlight usefulness during these hours. This result is consistent whilst streetlights are operating the Conventional (or 'always-on') lighting scheme, as shown in Figure 4.7 (b). As discussed in Section 3.3.2.1, this near-perfect streetlight usefulness ($> 90\%$) is due to streetlight topology, streetlight beam pattern and placement of streetlights implemented in StreetlightSim. Compared to the performance of the other two traffic-aware schemes, i.e. Multi-sensor and Zoning, as shown in Figure 3.16, both schemes have failed to deliver comparable streetlight usefulness as demonstrated by the Conventional scheme. In fact, the experienced streetlight usefulness widely fluctuates at times due to their design considerations. This is also demonstrated by time-based lighting schemes where the usefulness is reduced at certain operational hours, because of reduced streetlight lighting levels. In short, TALiSMaN is capable of improving streetlight usefulness of existing schemes, and maintaining it at a similar level as demonstrated by the Conventional scheme.

4.3.2.2 Energy Consumption

To evaluate the energy demand of various street lighting schemes, the energy model shown in Eq. 3.11 is used. This model assumes that streetlight energy consumption is directly proportional to its lighting levels, e.g. when the streetlight lighting level is reduced to 80%, streetlight energy consumption is also reduced to 80% based on its maximum power rating.

With Shapiro-Wilk normality test, some of the simulation results appear to be not normally distributed (Appendix C details the normality test to some of the simulation data generated). Thus, instead of using t-test which requires data to be normally distributed, Mann-Whitney U-test is used in this section to evaluate the statistical significant of traffic volume, pedestrian-motorist ratio, and motorist's travelling speed to energy consumption of the traffic-aware lighting schemes, i.e. Multi-sensor, Zoning and TALiSMaN.

A) Effect of Different Traffic Volumes

Figure 4.8 shows the total energy consumption of 112 streetlights in a week according to different V_{comb} values (14% of the traffic is pedestrian) while operating TALiSMaN lighting schemes. For comparison, the energy consumption of Conventional, which serves as a benchmark for streetlight usefulness, and two traffic-aware schemes, i.e. Multi-Sensor and Zoning which were previously presented in Chapter 3, are also included.

Table 4.4 shows the U-test results on different traffic volume pairs to Multi-sensor, Zoning and TALiSMaN lighting schemes. The U-test results indicate that the increasing traffic

volume has statistically significant effect ($p < 0.05$) to energy consumption of traffic-aware lighting schemes. However, the magnitude of such effect to Multi-sensor is less as compared to TALiSMaN and Zoning. As shown in Figure 4.8, Multi-sensor lighting scheme consumes ∼14% more energy as traffic volume increases from 180 to 6554 road users per day, while energy consumption of Zoning and TALiSMaN increase more than 13 and 10 times respectively, under same traffic volume increment.

Table 4.4: Significance (2-tailed) p-value of U-test on different traffic volume pairs for Multi-sensor, Zoning and TALiSMaN lighting schemes.

Lighting scheme	**Tested pair (road users per day)**	***p*-value**
Multi-sensor	180 vs. 438	<0.05
	438 vs. 1347	<0.05
	1347 vs. 3508	<0.05
	3508 vs 6554	<0.05
Zoning	180 vs. 438	<0.05
	438 vs. 1347	<0.05
	1347 vs. 3508	<0.05
	3508 vs 6554	<0.05
TALiSMaN	180 vs. 438	<0.05
	438 vs. 1347	<0.05
	1347 vs. 3508	<0.05
	3508 vs 6554	<0.05

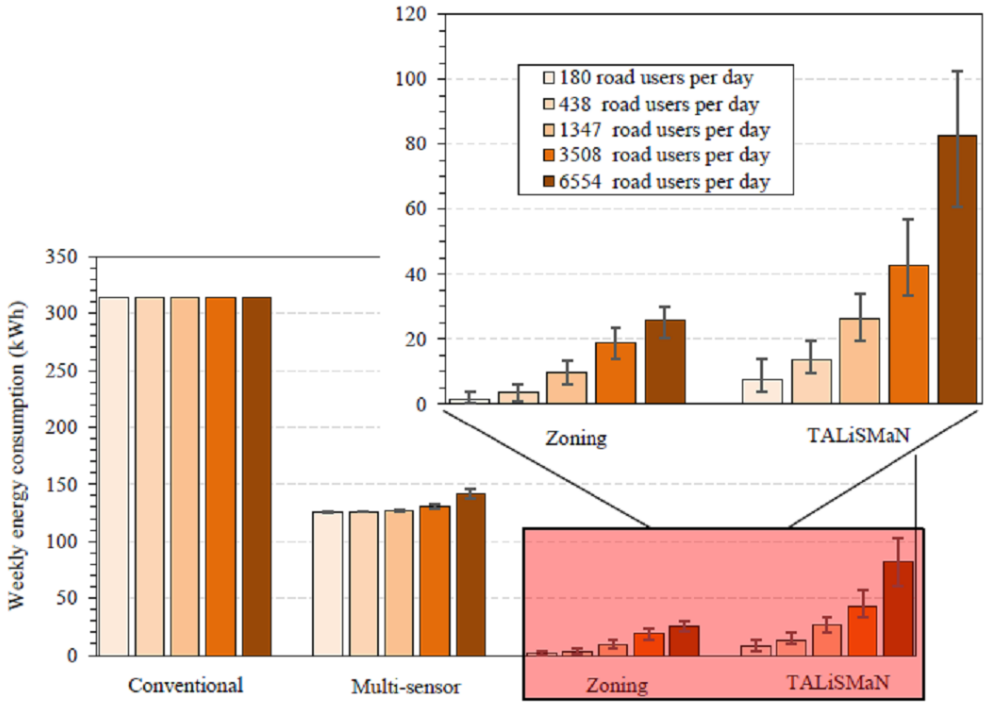

Figure 4.8: Mean weekly energy consumption of 112 streetlights while operating various street lighting schemes from 16:00 to 08:00 the next day. The error bars represent the maximum and the minimum energy consumption over ten repeated simulations.

TALiSMaN requires almost three times more energy on average compared to Zoning. This result is justifiable because TALiSMaN aims to provide the lighting conditions that fulfil different road users' needs for street lighting. In fact, as shown in Figure 3.16 (b), only pedestrians (14% of the total simulated traffic) experienced near-perfect streetlight usefulness from the energy consumed by Zoning, whereas motorists gained little benefit from the lighting intended for pedestrians. While Zoning may have application to areas with pedestrian-only traffic, for example some commercial areas and parks, it is clearly not applicable to those that have a mix of pedestrians and motorists. Furthermore, while Zoning requires pedestrians to carry GPS-enabled smartphones, TALiSMaN provides reasonable energy savings without any such demands. Therefore, the adoption of TALiSMaN in residential areas is more viable when compared to Zoning because traffic in such places normally comprises both pedestrians and motorists. Therefore, disregarding Zoning, TALiSMaN can be seen to consume between 2 – 55% (depending on V_{comb} value) of the energy required by Multi-Sensor, the best-performing state-of-the-art technique. Furthermore, compared to the Conventional lighting scheme, TALiSMaN only consumes 1 – 2% of the energy.

TALiSMaN exchanges information between streetlights via a wireless communication network, thus it requires additional infrastructure, i.e. wireless sensor motes, compared to Conventional or 'always-on' lighting scheme. With a TelosB wireless sensor mote which costs $\sim$ £65 [194], this additional infrastructure investment can be absorbed within five years with the energy saved by operating TALiSMaN. This is based on TALiSMaN consumes 1 – 2 % of the energy required by Conventional lighting scheme, and the 2013 electricity price for non-domestic in the UK (10 pences per KWh) [75]. However, in near future, this initial investment is expected to be less significant due to the advance in single-board computing hardware, such as Raspberry Pi Zero which costs USD 5 [195], has driven down the cost of computing hardware.

To evaluate the worst-case energy overhead of using wireless sensor mote, each streetlight has an IEEE 802.15.4 transceiver which is active for up to 16 hours per day, and consumes 100 mW for both data transmission and reception [196]. This represents an overhead of 1.25 kWh per week for 112 streetlights (or 1.6 Wh per day per streetlight) while operating these schemes. However, this overhead is 2 – 3% of the 40 – 65 kWh per week of energy saved by TALiSMaN compared with the Multi-sensor lighting scheme.

B) Effect of Different Pedestrian-Motorist Ratios

To investigate the effect of pedestrian-motorist ratios on traffic-aware lighting schemes, i.e. Multi-sensor, Zoning and TALiSMaN, Δ_{ped} values of 0%, 30%, 50% and 70% are considered in this evaluation. The Δ_{ped} value of 14% is also included as it represents the pedestrian-motorist ratio of Southampton, UK, and is the default value used in this

thesis. With a desktop computer equipped with Intel Core i7-2600, 16 GB of main memory, and 64-bit Windows 8, StreetlightSim requires approximately 140 to 180 minutes to simulate an hour streetlight operations (17:00 – 18:00) while validating TALiSMaN with $V_{comb} = 6554$ road users per day and considered Δ_{ped} values. Due to the extensive simulation time required, traffic between 17:00 – 18:00 and 02:00 – 03:00 of a weekday traffic profile are presented here. As shown in Figure 3.2, these hours represent the highest and the lowest traffic ratio in the UK. Although the simulations are limited to these hours, the results can be extrapolated to demonstrate the upper bound of the energy required by these schemes. Each of the scenarios is evaluated 30 times, and the results are shown in Figure 4.9 and 4.10, respectively.

Table 4.5 and 4.6 show the U-test results on the different pedestrian-motorist ratio pairs to Multi-sensor, Zoning and TALiSMaN lighting schemes during 17:00 – 18:00 and 02:00 – 03:00, respectively. These results suggest that an increasing pedestrian-motorist ratio has statistically significant effect ($p < 0.05$) to energy consumption of traffic-aware lighting schemes. This applies to all the pedestrian-motorist ratios, traffic volumes and streetlight operational hours considered, excepts for Multi-sensor and TALiSMaN when traffic volume is at 180 and 438 road users per day, and traffic is less busy, i.e. between 02:00 and 03:00. This is consistent with the energy consumption trend shown in Figure 4.9 and 4.10 as an increasing pedestrian-motorist ratio causes more energy use to all the traffic-aware lighting schemes considered. As a result of increasing pedestrian-motorist ratio and traffic volume, more pedestrian traffic is introduced during the simulations. As the pedestrian's walking speed is relatively slower (maximum speed at 1.9 m/s [191]) compared to a motorist's travelling speed (limited to 30 mph), the time each streetlight spends active is also prolonged, and thus energy consumption is also increased. However, the effect of an increasing pedestrian-motorist ratio on Multi-sensor is less pronounced, compared to the Zoning and TALiSMaN lighting schemes. This is due to the fact that streetlights operating Multi-sensor are only switched on to 100% when a pedestrian is within 10 m from the streetlights, whereas Zoning and TALiSMaN require streetlights within a 150 m radius from a detected pedestrian to be lit. Owing to this, Zoning and TALiSMaN require more streetlights to be switched on at higher lighting levels compared to Multi-sensor. In fact, as shown in Figure 4.9 (e), both schemes consume more energy compared to Multi-sensor, and approach the Conventional's (2.8 kWh) when larger Δ_{ped} and V_{comb} values are evaluated. This trend suggests that Zoning and TALiSMaN can cause streetlights to be consistently switched on at times or places dominated by high Δ_{ped} and V_{comb} values.

Another trend worth noting is that, for TALiSMaN, the effect of Δ_{ped} values to energy consumption is directly proportional when evaluated with lower V_{comb} values, i.e. 180 and 438 road users per day. This effect, however, soon becomes saturated at Δ_{ped} value of 50%, and this is more noticeable when V_{comb} values of 3508 and 6554 road users per day are evaluated. One of the causes of this trend is that the majority of streetlights

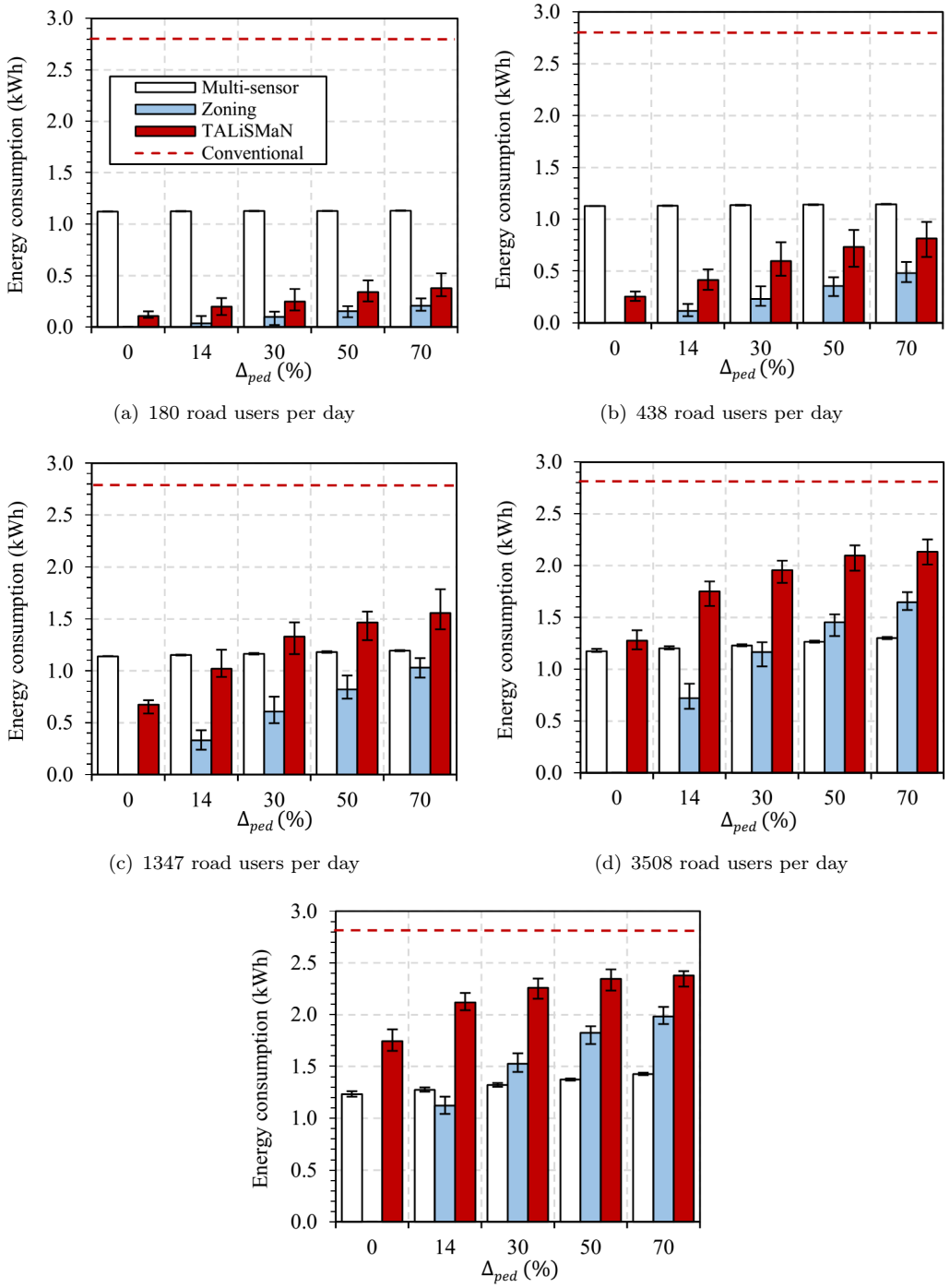

(a) 180 road users per day

(b) 438 road users per day

(c) 1347 road users per day

(d) 3508 road users per day

(e) 6554 road users per day

Figure 4.9: Energy consumed by 112 streetlights with different pedestrian-motorist ratios between 17:00 and 18:00 while operating different traffic-aware lighting schemes. The error bars represent the maximum and the minimum energy consumed by the schemes after 30 simulation runs. The dashed line represents the energy consumption of the Conventional (or 'always-on') lighting scheme.

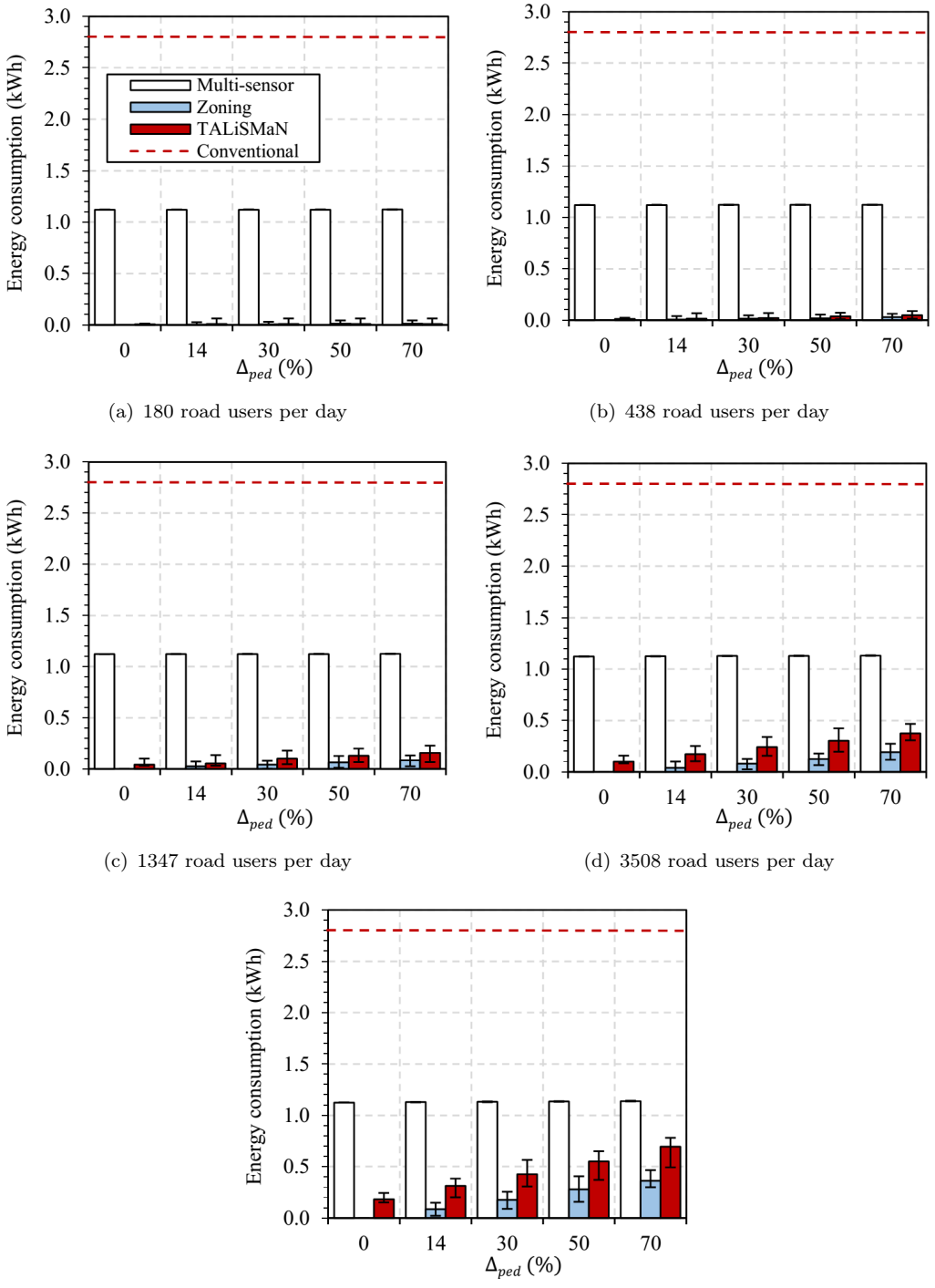

(a) 180 road users per day

(b) 438 road users per day

(c) 1347 road users per day

(d) 3508 road users per day

(e) 6554 road users per day

Figure 4.10: Energy consumed by 112 streetlights with different pedestrian-motorist ratios between 02:00 and 03:00 while operating different traffic-aware lighting schemes. The error bars represent the maximum and the minimum energy consumed by the schemes after 30 simulation runs. The dashed line represents the energy consumption of the Conventional (or 'always-on') lighting scheme.

Table 4.5: Significance (2-tailed) p-value of U-test on different pedestrian-motorist ratio pairs during streetlight operational hour between 17:00 – 18:00.

		Traffic volume (road users per day)				
Lighting scheme	**Tested pair**	*180*	*438*	*1347*	*3508*	*6554*
Multi-sensor	0% vs. 14%	<0.05	<0.05	<0.05	<0.05	<0.05
	14% vs. 30%	<0.05	<0.05	<0.05	<0.05	<0.05
	30% vs. 50%	<0.05	<0.05	<0.05	<0.05	<0.05
	50% vs. 70%	<0.05	<0.05	<0.05	<0.05	<0.05
Zoning	0% vs. 14%	<0.05	<0.05	<0.05	<0.05	<0.05
	14% vs. 30%	<0.05	<0.05	<0.05	<0.05	<0.05
	30% vs. 50%	<0.05	<0.05	<0.05	<0.05	<0.05
	50% vs. 70%	<0.05	<0.05	<0.05	<0.05	<0.05
TALiSMaN	0% vs. 14%	<0.05	<0.05	<0.05	<0.05	<0.05
	14% vs. 30%	<0.05	<0.05	<0.05	<0.05	<0.05
	30% vs. 50%	<0.05	<0.05	<0.05	<0.05	<0.05
	50% vs. 70%	<0.05	<0.05	<0.05	<0.05	0.32

Table 4.6: Significance (2-tailed) p-value of U-test on different pedestrian-motorist ratio pairs during streetlight operational hour between 02:00 – 03:00.

		Traffic volume (road users per day)				
Lighting scheme	**Tested pair**	*180*	*438*	*1347*	*3508*	*6554*
Multi-sensor	0% vs. 14%	0.30	<0.05	<0.05	<0.05	<0.05
	14% vs. 30%	0.55	0.34	<0.05	<0.05	<0.05
	30% vs. 50%	0.22	<0.05	<0.05	<0.05	<0.05
	50% vs. 70%	0.62	0.53	<0.05	<0.05	<0.05
Zoning	0% vs. 14%	<0.05	<0.05	<0.05	<0.05	<0.05
	14% vs. 30%	0.18	<0.05	<0.05	<0.05	<0.05
	30% vs. 50%	0.09	0.46	<0.05	<0.05	<0.05
	50% vs. 70%	0.72	0.06	<0.05	<0.05	<0.05
TALiSMaN	0% vs. 14%	0.30	0.12	<0.05	<0.05	<0.05
	14% vs. 30%	0.74	0.16	<0.05	<0.05	<0.05
	30% vs. 50%	0.82	0.11	0.07	<0.05	<0.05
	50% vs. 70%	0.72	0.11	0.06	<0.05	<0.05

have already been switched on for motorists, and thus an increasing Δ_{ped} value has little effect on TALiSMaN's energy consumption, especially with higher V_{comb} values. Since Zoning operates according to detected pedestrian traffic, there is no obvious saturation point for the evaluated Δ_{ped} and V_{comb} values, as demonstrated by TALiSMaN.

Although, in some scenarios, TALiSMaN and Zoning consume more energy than the Multi-Sensor lighting scheme, as shown in Figure 4.9 (c) – (e), the overall energy consumption of Zoning and TALiSMaN is expected to be relatively lower compared to Multi-sensor. This is because during non-rush hours, for example between 02:00 and 03:00 as shown in Figure 4.10, streetlights are mostly inactive while operating Zoning or TALiSMaN lighting schemes. Based on a survey, up to 30% of a road user's journey is accomplished by walking [197]. However, this data is based on the journeys which

constitute the major/longest part of the whole journey which is likely to happen during the daytime – out of streetlight operational hours.

C) Effect of Different Motorist Travelling Speeds

In this section, the effect of various motorist speeds on the energy consumption of Multi-sensor and TALiSMaN is investigated. Since the Zoning lighting scheme only considers pedestrian traffic, it is not included in this evaluation. During the simulations, the simulated traffic is comprised of 14% pedestrians, and the rest is motorist traffic which travels at speeds of 10 mph (∼5 m/s), 20 mph (∼9 m/s), 30 mph (∼13 m/s) and 40 mph (∼18 m/s).

Based on U-test result, as shown in Table 4.7 and 4.8, an increasing motorist travelling speed has statistically significant effect ($p < 0.05$) to energy consumption of all the traffic-aware lighting scheme considered. This applies to all the travelling speeds and streetlight operational hours considered. However, there are some exceptions, especially at lower traffic volumes when motorists travel at and above 20 mph, and traffic is less busy. This results are expected as the duration of the streetlights to stay active is relatively shorter when the road is clear and motorists travel in high speed. Although U-test shows that an increasing travelling speed has statistically significant effect in reducing energy consumption to Multi-sensor, the magnitude of the effect is less compared to TALiSMaN. Whilst this scheme is evaluated, its energy consumption is virtually unchanged with all the travelling speeds and V_{comb} values considered. This is shown in Figure 4.11 and 4.12. This result is expected as the streetlights are always switched on with 40% lighting level, and only increased to 100% lighting level once motorists are in proximity (10 m from the streetlight). However, this happens within a relatively short distance compared to 100 m in TALiSMaN.

Travelling speeds have an observable effect on TALiSMaN's energy consumption. Based on the simulation results, energy consumption is decreased by a rate of between 44 and 148 kWh per hour with every speed increment of 10 mph. This trend is expected

Table 4.7: Significance (2-tailed) p-value of U-test on different motorist speed pairs during streetlight operational hour between 17:00 – 18:00.

		Traffic volume (road users per day)				
Lighting scheme	**Tested pair**	*180*	*438*	*1347*	*3508*	*6554*
Multi-sensor	10 mph vs. 20 mph	<0.05	<0.05	<0.05	<0.05	<0.05
	20 mph vs. 30 mph	<0.05	<0.05	<0.05	<0.05	<0.05
	30 mph vs. 40 mph	0.13	<0.05	<0.05	<0.05	<0.05
TALiSMaN	10 mph vs. 20 mph	<0.05	<0.05	<0.05	<0.05	<0.05
	20 mph vs. 30 mph	0.07	<0.05	<0.05	<0.05	<0.05
	30 mph vs. 40 mph	0.12	<0.05	<0.05	0.11	0.13

Table 4.8: Significance (2-tailed) p-value of U-test on different motorist speed pairs during streetlight operational hour between 02:00 – 03:00.

		Traffic volume (road users per day)				
Lighting scheme	**Tested pair**	*180*	*438*	*1347*	*3508*	*6554*
Multi-sensor	10 mph vs. 20 mph	<0.05	<0.05	<0.05	<0.05	<0.05
	20 mph vs. 30 mph	0.05	0.05	0.05	<0.05	<0.05
	30 mph vs. 40 mph	0.26	0.15	0.39	0.13	<0.05
TALiSMaN	10 mph vs. 20 mph	<0.05	<0.05	<0.05	<0.05	<0.05
	20 mph vs. 30 mph	<0.05	0.30	0.58	<0.05	<0.05
	30 mph vs. 40 mph	0.82	0.31	0.06	<0.05	0.87

as the time streetlights remain lit is shortened when motorists increase their travelling speed. However, the reduction rates vary according to streetlight operational hours. For example, between 02:00 and 03:00 as shown in Figure 4.12, the energy reduction rates decline to between 3 and 70 kWh per hour.

D) Effect of Different Operational Durations

Figure 4.13 shows the weekly energy consumption of various lighting schemes according to seasonal change in different months of the year when evaluated with $V_{comb} = 6554$ road users per day. The operational hours of the streetlights are based on average sunset and sunrise times in Southampton, UK [198]. As the energy consumption of the streetlights is partially influenced by the duration of streetlight operational hours, all the lighting schemes exhibit a trend with the summer months having the lowest energy consumption over a year, reaching their peak during winter months. The length of daytime (i.e. when the streetlights are not switched on) is typically longer in summer months than winter months, hence shortening the required operational hours of the streetlights. In addition, as shown in Figure 3.2, road traffic during these hours is also expected to be lower. Because of this, energy consumption during these months is significantly lower compared to other months. Although energy consumption is reduced during the summer months, traffic-aware lighting schemes still outperform time-based lighting schemes.

4.4 Summary

This chapter proposed a distributed Traffic-Aware Lighting Scheme Management Network (TALiSMaN) to create lighting conditions that maximise the usefulness of street lighting, and improve the energy efficiency of streetlights by minimising their energy use. TALiSMaN uses a short range mesh network to relay and exchange information about detected road users. Based on this information, several networked streetlights collaborate to create lighting conditions that meet different road users' needs for street lighting. TALiSMaN has been evaluated with 112 streetlights together with different traffic profiles,

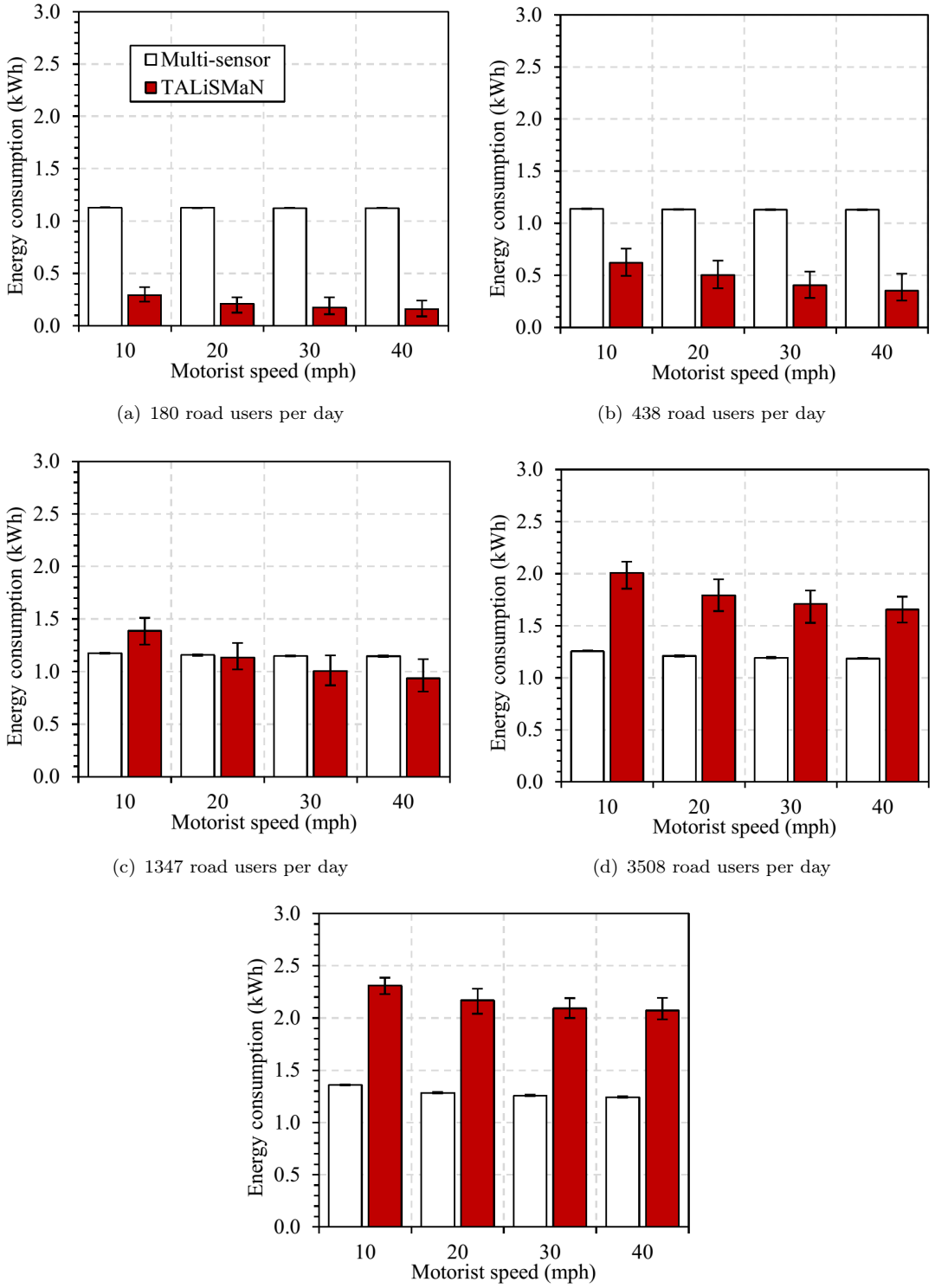

(a) 180 road users per day

(b) 438 road users per day

(c) 1347 road users per day

(d) 3508 road users per day

(e) 6554 road users per day

Figure 4.11: Energy consumed by 112 streetlights with different motorist speeds between 17:00 and 18:00 while operating Multi-sensor and TALiSMaN lighting schemes. The error bars represent the maximum and the minimum energy consumed by the schemes after 30 simulation runs.

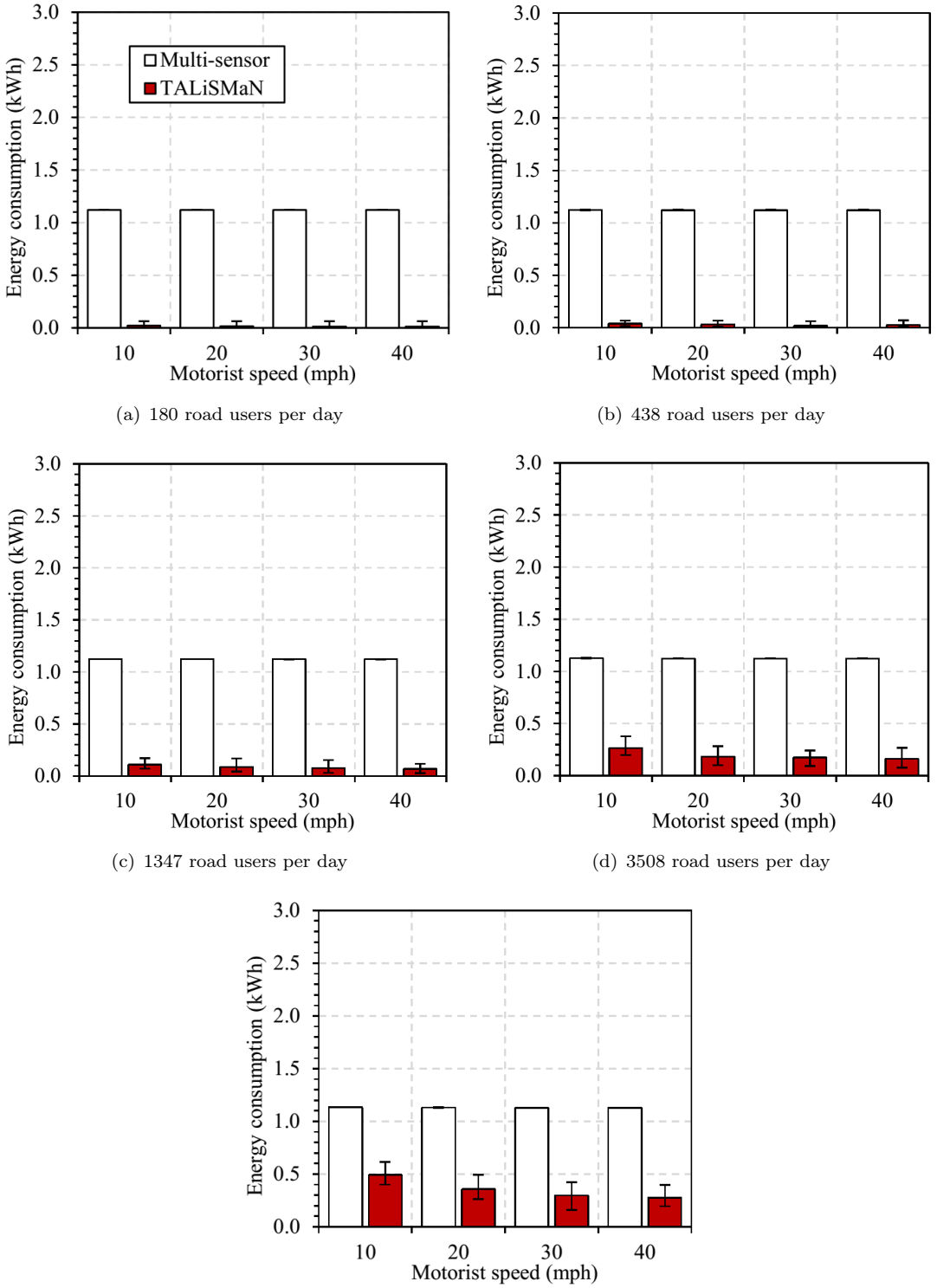

(a) 180 road users per day

(b) 438 road users per day

(c) 1347 road users per day

(d) 3508 road users per day

(e) 6554 road users per day

Figure 4.12: Energy consumed by 112 streetlights with different motorist speeds between 17:00 and 18:00 while operating Multi-sensor and TALiSMaN lighting schemes. The error bars represent the maximum and the minimum energy consumed by the schemes after 30 simulation runs.

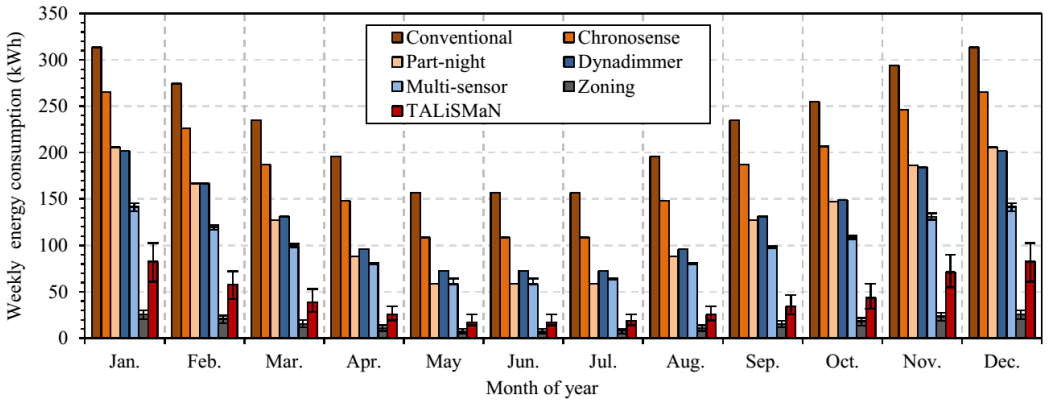

Figure 4.13: Weekly energy consumption of 112 streetlights for different months of the year. The error bars represent the maximum and the minimum energy consumption for Multi-sensor, Zoning, and TALiSMaN lighting schemes over 10 repeated simulations with $V_{comb} = 6554$ vehicles per day.

traffic volumes, operational durations, pedestrian-motorist ratios and motorist travelling speeds. Its performance has been evaluated and compared with other traffic-aware lighting schemes, i.e. Zoning and Multi-sensor.

Overall, streetlights operating TALiSMaN have a lower energy consumption than many evaluated lighting schemes, while offering comparable streetlight usefulness to Conventional (or 'always-on') lighting. TALiSMaN achieves this by adjusting the lighting levels within required lit road segments and switched off those beyond these segments. Compared to Conventional lighting scheme, TALiSMaN requires extra infrastructure, i.e. wireless sensor network, to allow streetlights to collaborate and then create the required lighting conditions. Although, TALiSMaN requires extra infrastructure to operate, the cost for this infrastructure can be absorbed within 5 years with the energy saved by operating streetlights with TALiSMaN. Furthermore, the return of this extra infrastructure is expected to be faster as TALiSMaN can offer better energy savings compared to Philips Chronosense, Dynadimmer, and Multi-sensor lighting schemes of which also require extra infrastructure to operate.

In certain circumstances, TALiSMaN may require more energy consumption compared to other traffic-aware lighting schemes. However, this occurs during the busiest hour of weekday traffic (17:00 – 18:00), especially when larger traffic volumes and pedestrian-motorist ratios are considered. As the traffic profile varies according to the time of day, for example between late evening and earlier morning when low traffic is expected, streetlights operating TALiSMaN are mostly inactive during these times. Therefore, its energy consumption is relatively lower compared to the Multi-sensor and other time-based lighting schemes. While the Zoning lighting scheme has a relatively lower energy consumption, it typically cannot offer comparable streetlight usefulness as demonstrated by the Conventional lighting scheme. Zoning can maintain near-perfect streetlight usefulness to pedestrian traffic, but motorists gain little benefit from this scheme. Thus,

disregarding Zoning, TALiSMaN provides an energy saving of 45 – 98% (depending on traffic volume) compared to the lighting schemes considered in Chapter 3. In short, although TALiSMaN is not necessarily the optimal lighting scheme, it is a relatively good solution compared to state-of-the-art.

In the next chapter, TALiSMaN is extended to energy-management for 'off-grid' streetlights; these have become popular in areas where access to the power grid is restricted.

Chapter 5

Energy-Neutral Lighting with Predictive and Adaptive Behaviour

In Chapter 4, a distributed adaptive street lighting scheme, TALiSMaN, was proposed. This scheme used sensor nodes mounted on streetlights to detect road users passing by. It switched on the streetlights to create the lighting conditions that deliver near-perfect usefulness to road users, whilst still conserving substantial energy. Based on simulation results, this scheme was able to maintain a comparable or improved streetlight usefulness to road users whilst substantially improve the energy efficiency of state-of-the-art lighting schemes. Although TALiSMaN has improved performance in terms of its energy efficiency and streetlight usefulness compared to other lighting schemes, this scheme is yet to consider the limited and variable energy budget encountered by solar-powered streetlights.

This chapter proposes TALiSMaN-Green, an enhancement of TALiSMaN, to address the shortcomings of existing solar-powered streetlights. These streetlights have limited energy storage and variable energy budget due to weather conditions. As a result, large solar panels and energy storage are required to provide a reliable source of light throughout the night. This leads to an oversized and thus overpriced system. Although these shortcomings can be solved as an optimisation problem, i.e. maximising the use of limited energy budget while offering high level of streetlight usefulness, TALiSMaN-Green lighting scheme can be considered as an acceptable solution to the problems. The novelty of TALiSMaN-Green is to use an energy demand predictor to maximise the use of limited energy budget by modulating the lighting levels requested by TALiSMaN. As a result, the proposed scheme prolongs the streetlight operational lifetime, and provides more consistent and useful street lighting to road users.

The remainder of this chapter is organised as follows: Section 5.1 demonstrates the limitation of TALiSMaN whilst operating with a limited energy budget, and Section 5.2 overviews the enhancement to TALiSMaN because of this. Section 5.3 explores the

performance of various low-complexity online predictors to estimate the energy consumption of TALiSMaN until the next sunrise. Section 5.3 investigates the estimation of the next sunrise time. In Section 5.5, the proposed TALiSMaN-Green is evaluated with a controlled experiment, and is then validated with actual traffic flow and solar readings.

5.1 Limitation of TALiSMaN

As established in Chapter 2, some had considered solar-powered streetlights to be not cost effective and visually intrusive. This is because larger solar panels and energy storage devices are needed to harvest and store the solar energy required for lighting operation throughout the night. This leads to an oversized and overpriced system. In order to size the components for solar-powered streetlights, one must consider the energy required for lighting, local weather conditions, and the efficiency of its components (solar panels, charge controllers, energy storage devices) [17]. In Chapter 4, TALiSMaN offered near-perfect streetlight usefulness (> 90 %), whilst still conserving substantial energy. This scheme used sensor nodes mounted on streetlights and switched on the lights for detected pedestrians as well as motorists. This was an advancement over the state-of-the-art lighting schemes, which naively set all streetlights in the vicinity of road users to maximum lighting level without considering the different needs of road users. Although TALiSMaN has improved performance in terms of its energy efficiency and streetlight usefulness compared to other lighting schemes, the proposed scheme is yet to consider the limited and variable energy budget encountered by solar-powered streetlights.

Whilst most lighting schemes (including TALiSMaN) have improved the energy-efficiency of 'grid-powered' streetlights, their application to 'off-grid' streetlights – powered locally by renewable energy – is restricted. This is because energy harvested from solar [27] or wind [29] fundamentally varies due to weather conditions, whereas grid-powered streetlights have a reliable electricity supply to sustain their daily operation. Furthermore, off-grid streetlights also store energy in batteries that have a restricted capacity, which limits the amount of energy that can be harvested from these sources.

A multi-sensor system [42] can prolong the operational lifetime of off-grid streetlights by reducing their power consumption by 40%. Although Chapter 4 showed TALiSMaN requires $2 - 55$ % (depending on traffic volume) of the energy required by Multi-sensor, it is unable to budget energy to ensure the streetlights can continue to operate throughout the entire night. This means streetlights may, for example, operate normally until the middle of the night, but run out of energy and be completely inoperable after that. Figure 5.1 illustrates this scenario where TALiSMaN is operating with 50% of energy required for a 16-hour lighting operation. For the first four hours, TALiSMaN is able to maintain near-perfect useful lighting (> 90% according to the streetlight usefulness

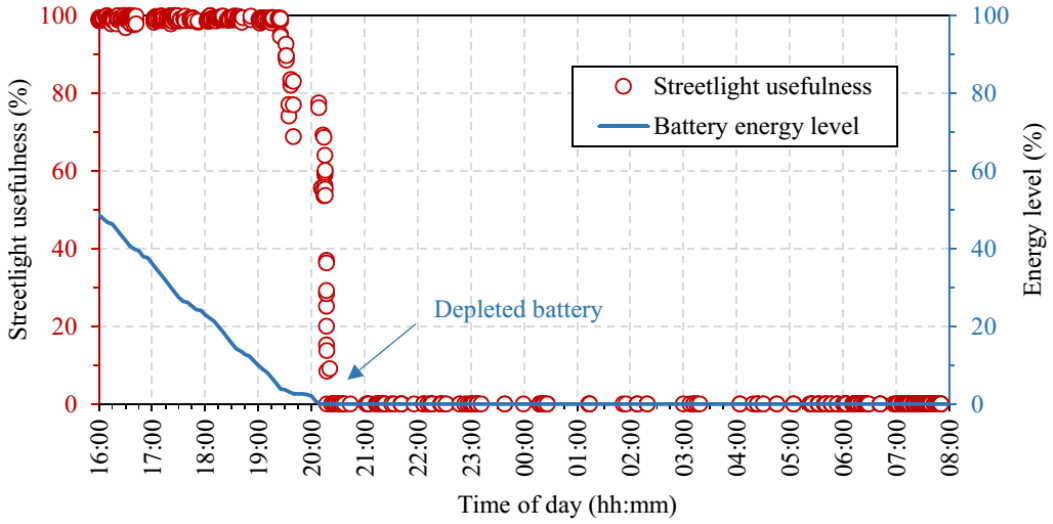

Figure 5.1: The performance of TALiSMaN whilst operating with 50% of the energy required for a 16-hour lighting operation. Streetlight usefulness drops to 0% when energy storage is depleted after four hours of operation.

model proposed in Section 3.1) to road users. However, this drops to zero after the energy storage is completely depleted at around 20:00.

5.2 Overview of TALiSMaN-Green

To address the limitation of TALiSMaN operating 'off-grid' streetlights, TALiSMaN-Green is proposed. The aim of this scheme is to deliver consistent usefulness of street lighting across a whole night, even if the stored energy is less than what would be required by TALiSMaN. The idea of the scheme is loosely based on adaptive adjustment of the operation cycle of the energy-harvesting sensor nodes [199–201].

Figure 5.2 overviews the components of TALiSMaN-Green. The operation of TALiSMaN-Green is classified into Control and Learning/Prediction modules. The Control module includes a TALiSMaN block, which monitors the presence of pedestrians and motorists, and requests a certain lighting level φ. A lighting modulation block, which reduces the requested lighting level if energy stored is predicted to be insufficient to operate TALiSMaN, is also included in the module. The Learning/Prediction module comprises a Sunrise Time Estimation block, which estimates the time when the streetlights will be switched off completely, and an Energy Demand Predictor which estimates TALiSMaN's overall energy demand until sunrise, E'_{demand}. To enable TALiSMaN-Green to learn and then estimate the energy that is likely to be required by TALiSMaN until sunrise, it uses historical data on energy potentially used by TALiSMaN. These data are provided by the Energy Use Logger, which collates data on the energy required by TALiSMaN

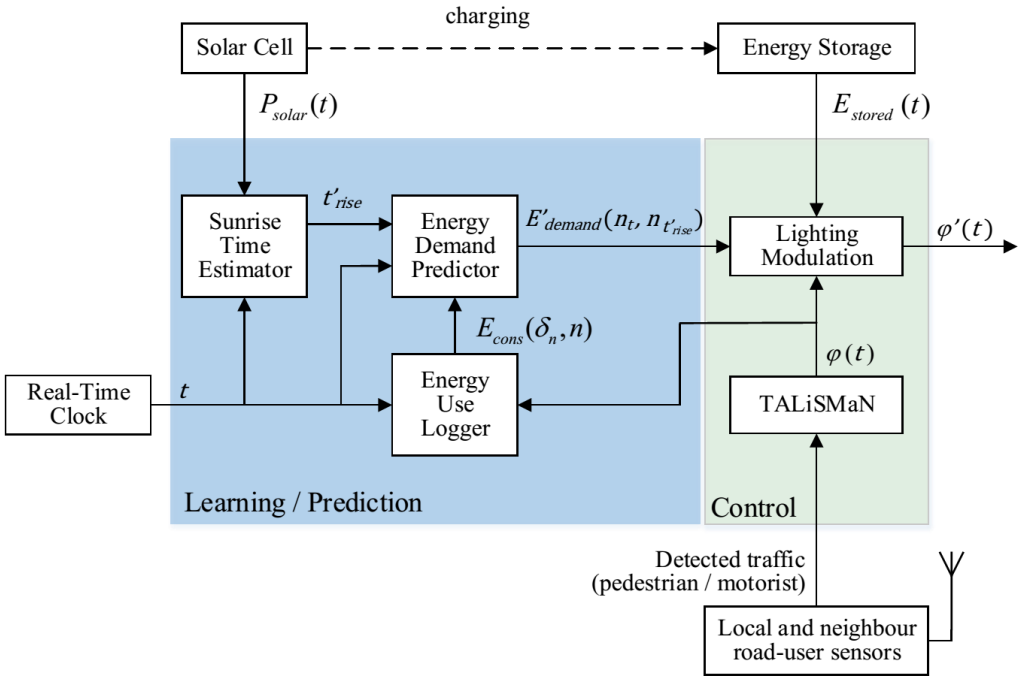

Figure 5.2: System overview of TALiSMaN-Green.

over a time interval according to its requested φ values. This block is situated in the Learning/Prediction module.

As TALiSMaN-Green is an enhancement of TALiSMaN, the solar-powered streetlights are also controlled and networked with wireless sensor nodes. These sensors are equipped with a road-user sensor to detect the presence of road users from a distance, and their real-time clock is synchronised. The solar cell block represents the actual solar panel of the streetlights and their function is to harvest solar energy. For TALiSMaN-Green, the harvested solar power acts as an input for the next sunrise time prediction. The harvested solar power is used to charge the energy storage devices and the stored energy is used to power the lamps after dark.

To predict E'_{demand}, the day is divided into N equal sized prediction timeslots. At each timeslot the energy required by TALiSMaN for creating the lighting conditions (Figure 4.2 and 4.3), E_{cons}, is logged, and then is used to estimate the energy required in future timeslots, E'_{cons}. E'_{demand} is the summation of all the E'_{cons} until sunrise and is given by:

$$E'_{demand}(n_t, n_{t'_{rise}}) = \sum_{i=n_t}^{n_{t'_{rise}}} E'_{cons}(\delta_i, i) \tag{5.1}$$

where n_t is the prediction timeslot where time t is enclosed; $n_{t'_{rise}}$ represents the prediction timeslot where next estimated sunrise time, t'_{rise}, is enclosed; δ_n represents the day

where prediction timeslot n is enclosed; and $E^{'}_{cons}$ is the predicted energy required by TALiSMaN at a specific prediction timeslot and day.

With the knowledge of $E^{'}_{demand}$, along with information on the amount of energy stored, E_{stored} this allows the requested φ values of the streetlight to be modulated, if necessary to conserve energy. TALiSMaN-Green reduces the requested φ when the amount of energy stored is predicted to be insufficient to sustain the operation of the system with the φ values requested by TALiSMaN. TALiSMaN-Green utilises a conditioning factor, α_{cond}, to modulate/reduce the requested φ value based on the ratio of E_{stored} to $E^{'}_{demand}$. The modulation of requested φ and a_{cond} are given by Eq. 5.2 and 5.3 respectively.

$$\varphi^{'}(t) = \begin{cases} \alpha_{cond}(n_t)\ \varphi(t), & E_{stored}(n) < E^{'}_{demand}(n_t, n_{t^{'}_{rise}}) \\ \varphi(t), & E_{stored}(n) \geq E^{'}_{demand}(n_t, n_{t^{'}_{rise}}) \end{cases} \tag{5.2}$$

$$\alpha_{cond}(n_t) = \frac{E_{stored}(n)}{E^{'}_{demand}(n_t, n_{t^{'}_{rise}})} \tag{5.3}$$

where $\varphi^{'}$ is the modulated lighting level; E_{stored} is the energy estimated to be stored in the energy storage device, typically the battery, at time t (Wh); $E^{'}_{demand}$ is the estimated energy demand to operate TALiSMaN from timeslot n_t until sunrise (Wh); and α_{cond} is the conditioning factor to requested φ.

In short, these additional functions require:

(a) Prediction of $E^{'}_{demand}$ until sunrise if the lighting levels requested by TALiSMaN are to be delivered.

(b) Prediction of the next sunrise time, $t^{'}_{rise}$, when streetlights are expected to be switched off.

(c) Estimation of E_{stored} in the energy storage device (e.g. battery).

(d) Knowledge of the current time, t.

This chapter focuses on items (a) and (b) as listed above, whereas for item (c), a simple energy storage model for E_{stored}, given by Eq. 5.12 and 5.13, is assumed. Streetlights operating TALiSMaN-Green are incorporated with wireless sensor nodes to form a multi-hop WSN. Thus, it is assumed that t is synchronised within the network and is available to TALiSMaN-Green.

5.3 Low-Complexity Online Predictors

There are a variety of time series modelling and prediction algorithms that can be used for estimating the energy consumption of TALiSMaN. For example, several variants of Auto-Regressive Integrated Moving Average model (ARIMA) were proposed to predict the changes in sensory data, and subsequently suppress unnecessary data propagation in WSNs [210, 211]. Although the studies showed that ARIMA gives a high prediction accuracy, the main disadvantage is that it possesses high overheads during its initial model building. To build an ARIMA model, a considerable amount of historical data is required to train the model. Furthermore, the ARIMA model requires re-computation once it is outdated.

Two primary factors affect the energy consumption dynamic of TALiSMaN are: traffic profile and traffic volume. As a result of unitary school and office hours, the traffic profile of local areas is vary repeatable on different weekdays and different weekends [187], which is illustrated by Figure 3.2. Traffic volume, however, can vary depending on the function and demography of the local area [190]. For example, locations near to business or school premises can experience higher traffic volumes which can change over time (Figure 4.8 showns the effect of traffic volumes to the energy consumption of TALiSMaN). Street lighting is a ubiquitous utility that can be found in almost all streets. Thus, using the ARIMA model may not be an efficient way for streetlight energy demand prediction. This is because it could involve numerous ARIMA models to be trained for different areas, and re-computation of the models is necessary over time.

Thus, considering the potential divergence traffic profile and traffic volume at different places, the energy demand predictor for TALiSMaN-Green should capable of online learning and then predict $E^{'}_{demand}$ according to local traffic conditions. Additionally, the predictor should consider the potential changes to traffic profile and volume over time. As WSN systems are resource-constrained, the energy demand predictor for TALiSMaN-Green also should be of relatively low demand for computing resources, such as processing power and memory storage. Therefore, this chapter focuses on investigating low-complexity online predictors only.

In the following subsections, the considered low-complexity online predictors are detailed.

5.3.1 Naïve

This predictor utilises the data at timeslot n which was previously logged at $(\varphi - 1)$ day to estimate the $E^{'}_{cons}$. The mathematical representation of this predictor is given by Eq. 5.4. This predictor has a remarkable performance in many economic and financially related estimations [202], and has been the baseline in several WSN studies related to sensory data prediction [203, 204]. In fact, studies show that Naïve is a robust predictor

in estimating temperature changes for a WSN-based building monitoring application [204].

$$E'_{cons}(\delta_n, n) = E_{cons}(\delta_n - 1, n), \quad \delta_n \geq 2 \tag{5.4}$$

where δ_n represents the day where prediction timeslot n is enclosed; and E_{cons} is the energy potentially to be consumed by a streetlight at a specific timeslot while operating at φ values requested by TALiSMaN. Note that E_{cons} can be numerically computed using Eq. 3.11, with an additional parameter δ_n indicating the day when the data at timeslot n is logged.

5.3.2 Simple Moving Average

Simple moving average (SMA) works by averaging previous D days of data. For WSN application, SMA is used to reduce the noise [205] and recover the lost sensory data [206]. However, some researchers have argued that SMA is not suitable for two dimensional sensory data that involves both spatial and temporal components [207]. Since the energy consumption of TALiSMaN involves one dimensional time series data, SMA is also considered in this investigation. SMA estimates the E'_{cons} needed at timeslot n by averaging the energy required by TALiSMaN at timeslot n from previous D days of data. Eq. 5.5 gives the mathematical representation of SMA. Based on the Eq. 5.5, Naïve can be considered as a special case of the SMA predictor when the D value is limited to one day.

$$E'_{cons}(\delta_n, n) = D^{-1} \sum_{i=\delta_n - D}^{\delta_n - 1} E_{cons}(i, n), \quad (\delta_n - 1) \geq D \geq 1 \tag{5.5}$$

where D represents the number of previous days of data.

5.3.3 Fixed Weighted Moving Average

Fixed weighted moving average (FWMA) [204], or simply referred to as weighted moving average in some literature [203,207], estimates future values as a weighted sum of previous D data. As the name implies, FWMA utilises fixed weightings, α_{fix}, to each D data, and the sum of these weightings approximates to one. However, it is not clear how the weightings were derived in literature, or how they were optimised for a given D value. In a study, $\alpha_{fix} = \{0.5, 0.25, 0.125, 0.125\}$ was used to evaluate the performance of FWMA in estimating the temperature temporal changes in a building [204]. For a similar application, however, $\alpha_{fix} = \{0.5, 0.25, 0.125, 0.0625, 0.0625\}$ was reported in

another study [208]. In this thesis, FWMA for estimating $E_{cons}^{'}$ is given by:

$$\begin{aligned} E_{cons}^{'}(\delta_n, n) =& E_{cons}(\delta_n - 1, n) + D^{-1} \sum_{i=1}^{D} \alpha_{fix}(i)[E_{cons}(\delta_n - i - 1, n) - \\ & E_{cons}(\delta_n - i - 2, n)], \quad (\delta_n - 3) \geq D \end{aligned} \tag{5.6}$$

5.3.4 Exponentially Weighted Moving Average

One of the alternative energy sources to power WSNs involves harvesting ambient energy. This configuration is essential, especially for WSNs that require an extended operational lifetime (up to decades) or embeds in structures where battery replacement is impractical [209]. Due to the dynamic of ambient conditions, the amount of harvested energy fluctuates over time, and thus an adaptive adjustment to the operation cycle of a sensor node is needed. One of the ways to permit this is by estimating harvestable energy with an exponentially weighted moving average (EWMA) [199–201]. This predictor is renowned for delivering reasonable prediction accuracy whilst imposing relatively low demand for computing power and memory. As opposed to FWMA where previous data is always assigned with fixed weightings, EWMA applies weighting which decreases exponentially. In this thesis, EWMA for estimating $E_{cons}^{'}$ is given by:

$$\begin{aligned} E_{cons}^{'}(\delta_n, n) =& \alpha_{exp}\ E_{cons}(\delta_n - 1, n - 1) + \\ & (1 - \alpha_{exp})\ \mu_D(\delta_n - 1, n), \quad (\delta_n - 2) \geq D \geq 1 \end{aligned} \tag{5.7}$$

$$\mu_D(\delta_n, n) = D^{-1} \sum_{i=\delta_n - 1}^{\delta_n - D} E_{cons}(i, n) \tag{5.8}$$

where α_{exp} is the weighting limited to $0 \leq \alpha_{exp} \leq 1$.

5.3.5 Evaluating Low-Complexity Online Predictors in Estimating the Energy Demand of TALiSMaN

There are several factors that can influence the accuracy of considered predictors in estimating the energy demand of TALiSMaN. These factors include the resolution of the prediction timeslot, N; the weighting factor, α; and number of previous D days of data required. Thus, this section investigates the values of these factors that give the most accurate energy demand prediction for TALiSMaN. Subsequently, the most efficient predictor is considered for TALiSMaN-Green implementation.

To determine the values for α and D that give minimum prediction error, $N = \{288, 144, 96, 72, 48, 24\}$ are used. As the Naïve predictor utilises data logged on the previous

day to estimate the energy demand of TALiSMaN, its D value is limited to one day. For SMA and EWMA predictors, the D value is limited to between 2 and 20 days. The weighting for EWMA is limited to $0 \leq \alpha_{exp} \leq 1$ with steps of 0.1. Whereas, for FWMA, D is limited to six days, and a weighting vector with the following values is evaluated [203]:

- 'Even' weights, $\alpha_{fix} = \{0.2, 0.2, 0.2, 0.2, 0.2\}$
- 'Heavy left' weights, $\alpha_{fix} = \{0.5, 0.25, 0.125, 0.0625, 0.0625\}$
- 'Heavy right' weights, $\alpha_{fix} = \{0.0625, 0.0625, 0.125, 0.25, 0.5\}$

For a given N, the objective is to find the value of α and D that yields the most accurate prediction for a given traffic volume and streetlight topology. The investigation is performed with the dynamics of linear streetlight topology in a residential area. As shown in Figure 5.3, this topology consists of 17 streetlights distributed across the road along a distance of 560 m. As opposed to the topology considered in Chapter 3 and 4, this scaled-down topology aims to reduce the duration of required simulation time (Section 4.3.2.2 B details on the required simulation times). Streetlights are operational between 16:00 to 08:00 the next day. The energy consumption data of these streetlights is generated by StreetlightSim according to the UK's daily traffic profiles shown in Figure 3.2 (a) with V_{comb} of 180, 438, 1347, 3508, and 6554 road users per day as previously used in Chapter 3 and 4, over a period of 20 weeks.

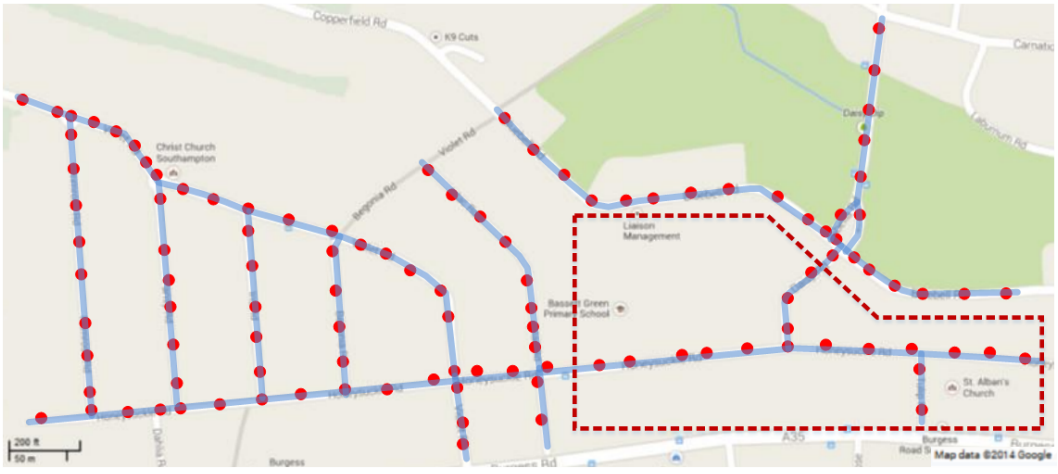

Figure 5.3: The streetlight topology (grouped with dashed lines) considered for the evaluation of energy demand predictors. The dots represent the location of the streetlights and shaded lines represent the road network (the base map was adapted from Google Maps).

The accuracy of the predictors to estimate E'_{demand} is evaluated with mean absolute error (MAE) [210] and is given by:

$$MAE = m^{-1} \sum_{i=1}^{m} |e_i| \tag{5.9}$$

where e_i is the difference between pairwise matched estimated and observed values. Here, the estimated value is the expected energy consumption of a streetlight whilst operating TALiSMaN, whereas the observed value is the actual energy used by the scheme, E_{demand}.

As shown in Figure 3.2 (a), the road traffic profiles exhibit observable trends throughout the days of week. To investigate the effect of these trends on the predictors whilst estimating E'_{demand}, three data aggregation strategies are considered in this investigation. These are:

- *Previous-D-Days* (PDD): utilises the energy potentially consumed by a streetlight on previous D days to estimate E'_{demand} at timeslot n.
- *Weekday-Weekend* (WDE): aggregates the energy potentially consumed by a streetlight according to either weekday or weekend. Therefore, this strategy requires $2D$ days of data to be available for prediction. To estimate E'_{demand} with WDE strategy, for example on a Saturday when $D = 3$ is considered, the energy potentially consumed for the street lighting on the previous two Sundays and one Saturday is required.
- *Day-of-Week* (DoW): aggregates the energy potentially consumed by a streetlight according to the day of the week. When this strategy is used, for example, to estimate E'_{demand} on a Saturday when $D = 3$ is considered, the energy potentially consumed by a streetlight on three previous Saturdays is required. Since this strategy is of higher granularity compared to PDD and WDE, this strategy requires $7D$ days of historical data to be available for prediction.

With Shapiro-Wilk normality test, some of the simulation data appear to be not normally distributed (Appendix C details the normality test to some of the simulation data generated). Thus, instead of using t-test, Mann-Whitney U-test is used in this section to evaluate the statistical significant of N, D, α and data aggregation strategy to improve the energy demand prediction of Naïve, SMA, FWMA and EWMA.

5.3.5.1 Resolution of N Value

To determine the resolution of the N value that results in the most accurate prediction for the energy demand of TALiSMaN, $N = \{24, 48, 72, 96, 144, 288\}$ is considered. From the U-test results, as shown in Table 5.1, the increasing resolution of N value has statistically significant improvement ($p < 0.05$) on prediction accuracy of FWMA and EWMA, except Naïve and SMA predictors. These results are consistent with IQRs of MAE values for various predictors at different resolutions of N value as shown in Figure 5.4. The MAE distributions shown in the figure comprise all the considered D values, traffic volumes, and data aggregation strategies. Based on the observations, the accuracy

of the predictors is improved with higher resolutions of the N value. Although there is a slight decline in the maximum MAE, the overall improvement on prediction accuracy of Naïve and SMA predictors is trivial whilst higher resolutions of N are evaluated. This can be observed where the 1st quartile, median and 3rd quartile of the MAE values are almost consistent for all the resolutions evaluated. Compared to Naïve and SMA, there is noticeable improvement in FWMA and EWMA estimating the energy demand of TALiSMaN when the resolution of N increases from 24 to 48. The IQRs of the MAE values for FWMA reduce from 6 to 3 Wh, whereas this is from 3 Wh to 2 Wh for EWMA. Additionally, the IQRs of FWMA and EWMA shift toward lower MAE values as the resolution of N value increases. However, the improvement slowly reaches a plateau where the IQRs for FWMA and EWMA remain almost consistent after $N = 48$. When evaluated with $N = 288$, the IQR of the MAE values is 3Wh and 2 Wh for FWMA and EWMA respectively.

Table 5.1: Significance (2-tailed) p-value of U-test on different resolution pairs of N value to different energy demand predictors.

	Predictor			
Tested pair	*Naïve*	*SMA*	*FWMA*	*EWMA*
24 vs. 48	0.97	<0.05	<0.05	<0.05
48 vs. 72	0.36	0.16	<0.05	<0.05
72 vs. 96	0.80	0.36	<0.05	<0.05
96 vs. 144	0.85	0.14	<0.05	<0.05
144 vs. 288	0.87	0.38	<0.05	<0.05

In short, all the predictors show the most accurate prediction when $N = 288$ is evaluated. This trend suggests that the predictors can capture more accurate energy use if the historical data is logged within a shorter time interval.

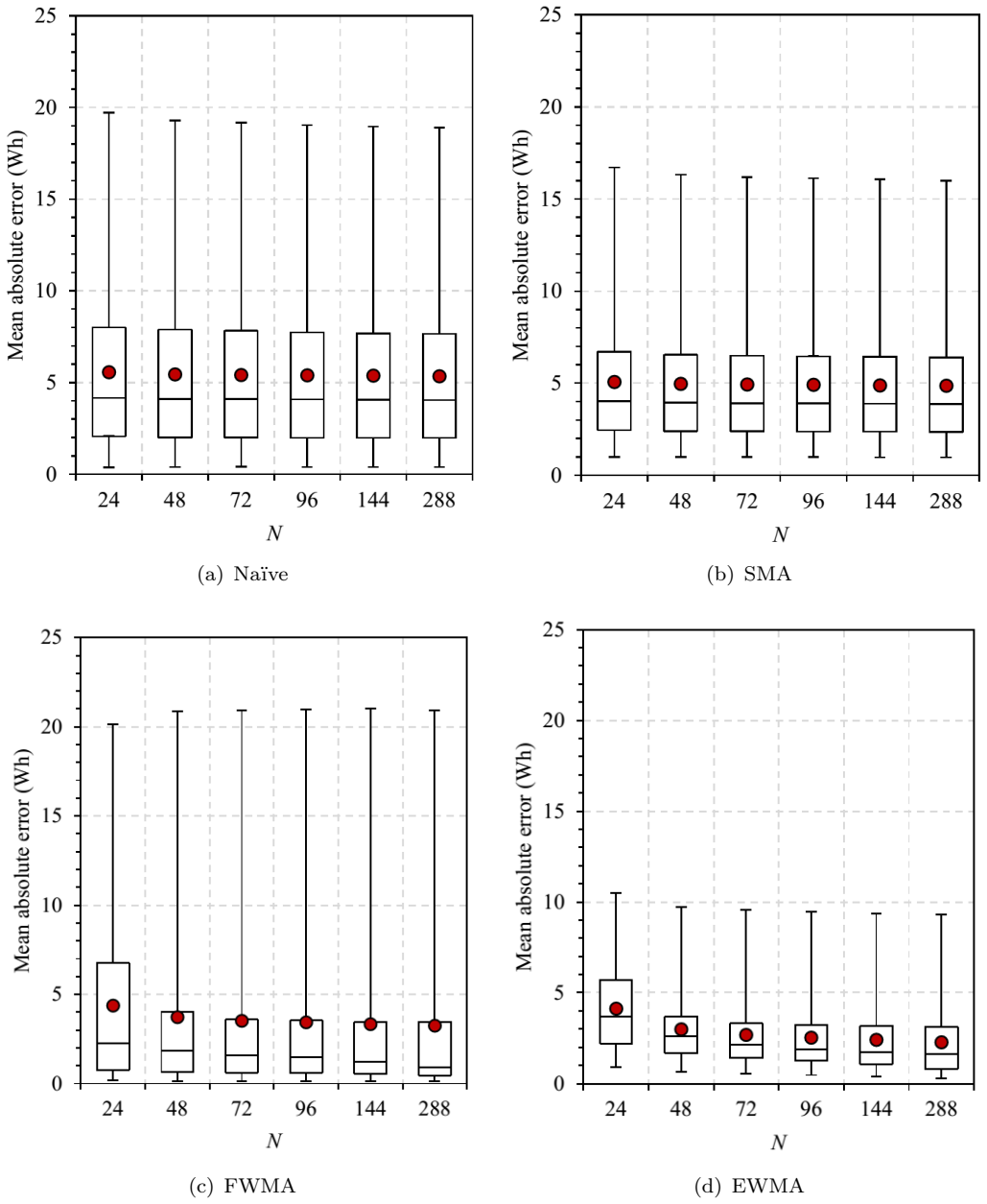

(a) Naïve (b) SMA

(c) FWMA (d) EWMA

Figure 5.4: The IQRs of the MAE values for various predictors at different N values. The dots represent the mean of MAE values, and the error bars represent the minimum and the maximum MAE values.

5.3.5.2 D Value

From Section 5.3.5.1, all the considered predictors showed improved performance prediction accuracy whilst higher resolutions of N value were evaluated. As $N = \{24, 48, 72, 96, 144, 288\}$ were considered in that section, $N = 288$ is used here to determine the number of previous D days of data that yield the most accurate energy demand prediction. The D value for Naïve and FWMA predictors is limited to one and six days respectively, thus these predictors are excluded from this investigation.

To determine the best performing D values for SMA and EWMA predictors, the D values ranging from 2 to 20 days are evaluated. Figure 5.5 shows the D values for these predictors that yield the minimum 3rd quartiles of the MAE values at $N = 288$ when historical data is aggregated with different strategies. For these predictors, the D values appear to be diverse depending on the data aggregation strategies and the traffic volumes evaluated. This trend suggests that to gain the most accurate prediction for SMA and EWMA, different D values are needed to be recomputed for roads with different traffic volumes. Also, the D values for both SMA and EWMA are relatively higher than those required by Naïve and FWMA predictors which are limited to one and six days, respectively. Thus, both SMA and EWMA will not be at their best performance to predict the energy demand of TALiSMaN before the required D days of data is collected.

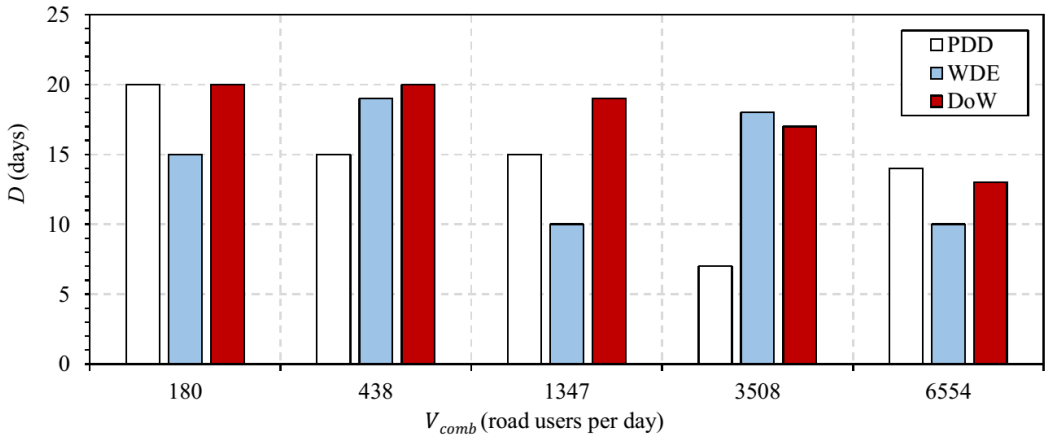

(a) Naïve

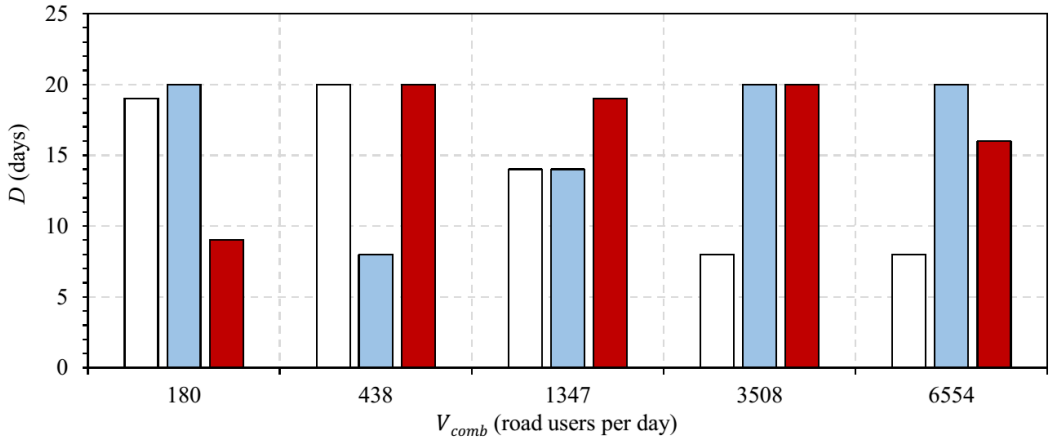

(b) SMA

Figure 5.5: The D values for (a) SMA and (b) EWMA at different traffic volumes and data aggregation strategies that yield the minimum MAE values (3rd quartiles) with $N = 288$.

5.3.5.3 Data Aggregation Strategy

To reflect the UK's daily traffic patterns shown in Figure 3.2 (a), three data aggregation strategies, namely PDD, WDE and DoW, are considered in this investigation. To determine the strategy for Naïve, SMA, FWMA and EWMA predictors that yield the most accurate energy demand prediction, $N = 288$ and the required D values for the respective predictors at different traffic volumes, as presented in Section 5.3.5.2, are adopted in this section.

From the U-test results, as shown in Table 5.2, all the predictors have shown statistically significant improvement on energy demand prediction, especially when higher traffic volumes are considered, if a suitable data aggregation strategy is used. Figure 5.6 shows the IQRs of the MAE values of the predictors whilst using these data aggregation strategies to estimate the energy demand of TALiSMaN. Based on observations, the majority of the MAE values become denser and shift to lower values with DoW, followed by WDE and PDD strategies for all the predictors except FWMA. This trend, however, is expected as StreetlightSim uses daily traffic profiles shown in Figure 3.2 (a) to generate the required historical data for this investigation. Additionally, there are distinct trends between weekdays and weekend traffic. Hence, the results are obtained; however, DoW shows slight improvement over WDE for all the considered traffic volumes. This is mainly due to the small differences between weekday and weekend traffic profiles during streetlight operational hours (16:00 – 08:00 the next day) as shown in Figure 3.2 (a). These results suggest that Naïve, SMA and EWMA have the most accurate prediction with DoW. For FWMA, the data aggregation strategies have a contrasting effect/trend compared to other predictors. This predictor shows better prediction accuracy with PDD, followed by the WDE and DoW strategies.

Table 5.2: Significance (2-tailed) p-value of U-test on different data aggregation strategy pairs to different energy demand predictors and traffic volumes.

		Traffic volume (road users per day)				
Predictor	**Tested pair**	*180*	*438*	*1347*	*3508*	*6554*
Naive	PDD vs. WDE	0.30	0.25	<0.05	<0.05	<0.05
	PDD vs. DoW	<0.05	<0.05	<0.05	<0.05	<0.05
	DoW vs. WDE	0.10	0.25	<0.05	<0.05	<0.05
SMA	PDD vs. WDE	<0.05	0.14	0.62	<0.05	<0.05
	PDD vs. DoW	0.69	0.60	<0.05	<0.05	<0.05
	DoW vs. WDE	0.16	0.42	<0.05	<0.05	<0.05
FWMA	PDD vs. WDE	<0.05	<0.05	<0.05	<0.05	<0.05
	PDD vs. DoW	<0.05	<0.05	<0.05	<0.05	<0.05
	DoW vs. WDE	<0.05	<0.05	<0.05	<0.05	<0.05
EWMA	PDD vs. WDE	<0.05	<0.05	0.68	<0.05	<0.05
	PDD vs. DoW	0.75	0.31	<0.05	<0.05	<0.05
	DoW vs. WDE	<0.05	0.21	<0.05	<0.05	<0.05

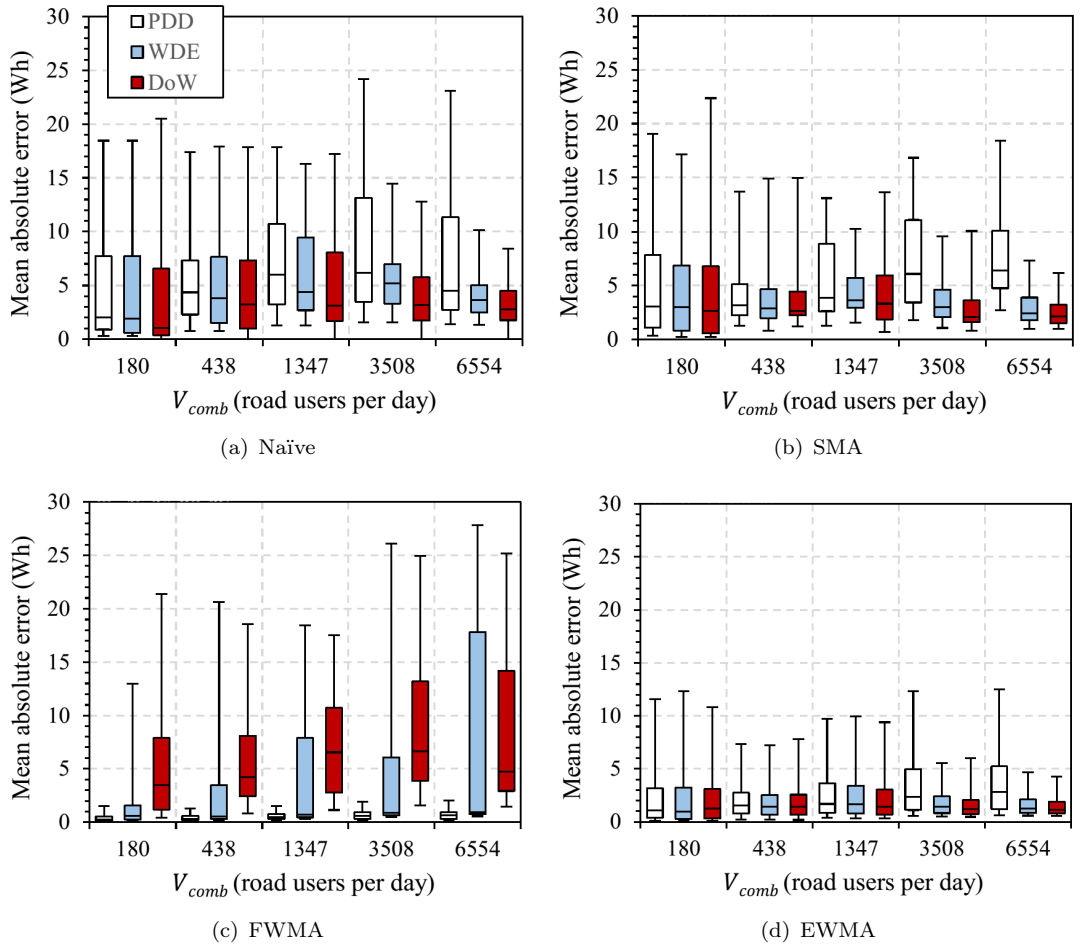

(a) Naïve (b) SMA

(c) FWMA (d) EWMA

Figure 5.6: The IQRs of the MAE values for various predictors using different data aggregation strategies at different traffic volumes. The error bars represent the maximum and the minimum MAE values.

5.3.5.4 Weighting Factor

Amongst the considered predictors, only FWMA and EWMA use weighting factors to estimate the energy demand of TALiSMaN. To determine the weighting factors that yield the most accurate energy demand prediction, the required values of N, D and data aggregation strategies for respective predictors, as presented in Section 5.3.5.1 – 5.3.5.4, are used in this section. For FWMA, three different weighting factors are considered: 'Heavy left', 'Even' and 'Heavy right'.

Figure 5.7 shows the IQRs of the MAE values for FWMA whilst estimating the energy demand of TALiSMaN with these weighting factors at $N = 288$, $D = 6$ and whilst the historical data is aggregated using PDD strategy. For FWMA, this data aggregation strategy yields the most accurate energy demand prediction. For all the considered traffic volumes, the 'Even' weighting factor yields the lowest 1st and 3rd quartiles of the MAE values, whereas the 'Heavy right' results in the highest 1st and 3rd quartiles amongst all the weighting factors considered. Based on the U-test results, as shown in

Table 5.3, the weighting factor 'Even' has statistically significant improvement on energy demand prediction to FWMA ($p < 0.05$), as compared to 'Left' and 'Right' in all the traffic volumes considered. These trends suggest that at $N = 288$, $D = 6$, and when the historical data is aggregated with the PDD strategy, FWMA has the most accurate energy demand prediction with an 'Even' weighting factor.

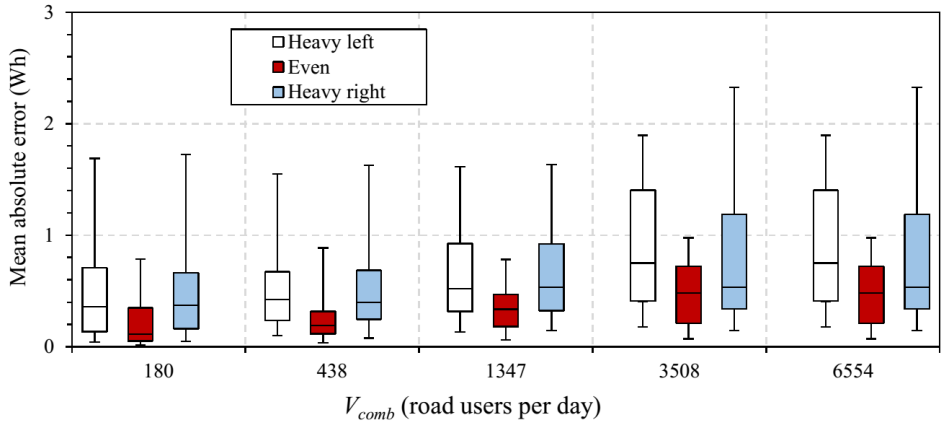

Figure 5.7: The IQRs of the MAE for FWMA with different weighting factors at $N = 288$ and PDD data aggregation strategy. The error bars represent the maximum and the minimum MAE values for each weighting factor.

Table 5.3: Significance (2-tailed) p-value of U-test on weighting factor 'Left', 'Even' and 'Right' to FWMA energy demand predictor at different traffic volumes.

	Traffic volume (road users per day)				
Tested pair	*180*	*438*	*1347*	*3508*	*6554*
Left vs. Even	<0.05	<0.05	<0.05	<0.05	<0.05
Left vs. Right	0.81	0.63	0.98	<0.05	<0.05
Right vs. Even	<0.05	<0.05	<0.05	<0.05	<0.05

For EWMA, weighting factors with range $0.0 \leq \alpha_{exp} \leq 1.0$ with steps of 0.1 are considered. To illustrate the performance of EWMA with these weighting factors, Figure 5.8 shows the IQRs of the MAE values when this predictor is evaluated with different traffic volumes. The resultant MAE values are based on $N = 288$ whilst the historical data is aggregated using the DoW strategy. As presented in Section 5.3.5.3, for EWMA, this strategy yields the most accurate energy demand prediction. Also, the D values used here are according to respective traffic volumes as presented in Section 5.3.5.2. As shown in Figure 5.8, the IQRs of the MAE values become denser and shift to lower MAE values when lower α_{exp} values are evaluated. This trend is consistent with the U-test results shown in Table 5.4, indicating that EWMA has statistically significant improvement ($p < 0.05$) on energy demand prediction with lower α_{exp} values. These trends suggest that the second term of the EWMA predictor as shown in Eq. 5.7 is not relevant for estimating the energy demand of TALiSMaN.

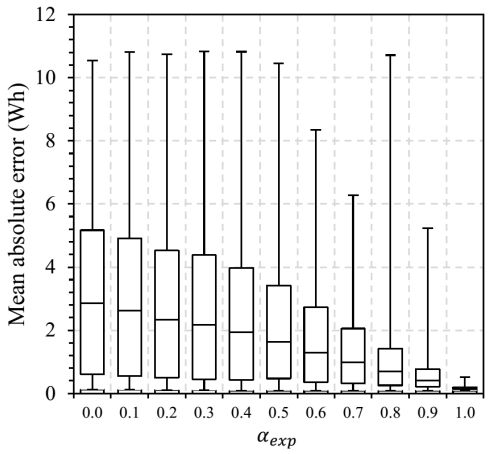

(a) $V_{comb} = 180$ road users per day

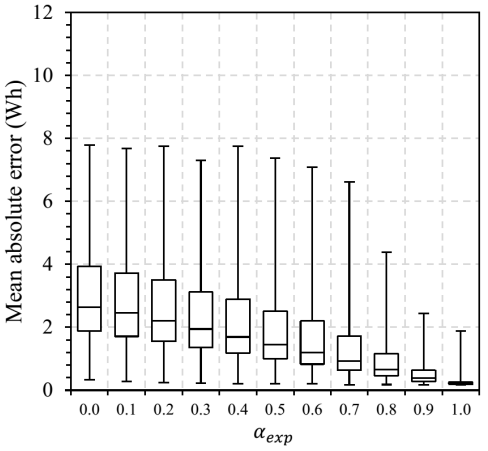

(b) $V_{comb} = 438$ road users per day

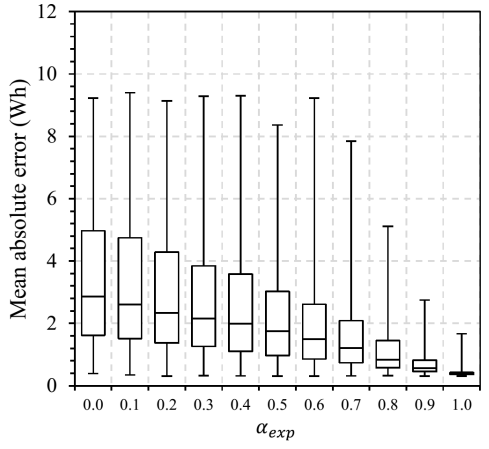

(c) $V_{comb} = 1347$ road users per day

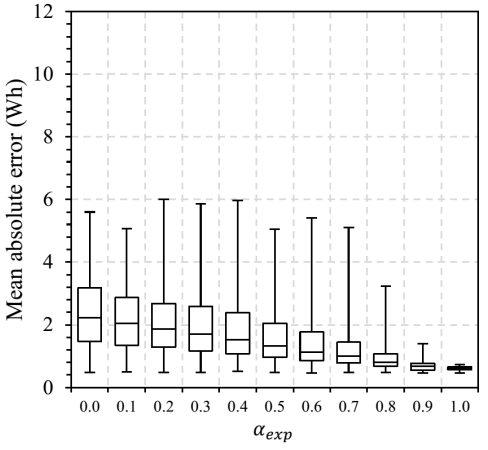

(d) $V_{comb} = 3508$ road users per day

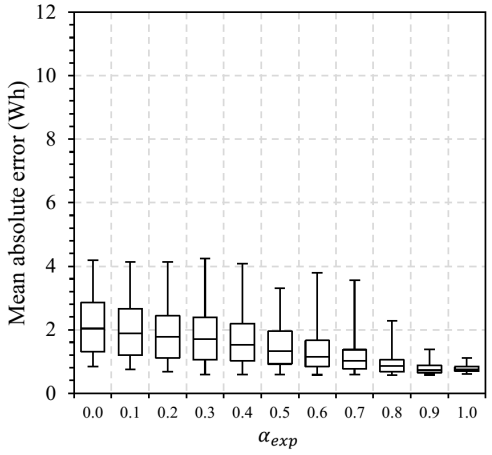

(e) $V_{comb} = 6554$ road users per day

Figure 5.8: The IQRs of the MAE values for EWMA with different weighting factors at $N = 288$, and whilst the data is aggregated with DoW strategy. The error bars represent the maximum and the minimum MAE values for each weighting factor.

Table 5.4: Significance (2-tailed) p-value of U-test on weighting factor ranging from 0.0 to 1.0 to EWMA energy demand predictors at different traffic volumes.

	Traffic volume (road users per day)				
Tested pair	*180*	*438*	*1347*	*3508*	*6554*
0.0 vs. 0.1	0.15	0.10	0.14	0.21	0.11
0.0 vs. 0.2	<0.05	<0.05	<0.05	<0.05	<0.05
0.0 vs. 0.3	<0.05	<0.05	<0.05	<0.05	<0.05
0.0 vs. 0.4	<0.05	<0.05	<0.05	<0.05	<0.05
0.0 vs. 0.5	<0.05	<0.05	<0.05	<0.05	<0.05
0.0 vs. 0.6	<0.05	<0.05	<0.05	<0.05	<0.05
0.0 vs. 0.7	<0.05	<0.05	<0.05	<0.05	<0.05
0.0 vs. 0.8	<0.05	<0.05	<0.05	<0.05	<0.05
0.0 vs. 0.9	<0.05	<0.05	<0.05	<0.05	<0.05
0.0 vs. 1.0	<0.05	<0.05	<0.05	<0.05	<0.05

To conclude, Table 5.5 summarises the required N, D, data aggregation strategy and weighting factor for Naïve, SMA, FWMA and EWMA predictors that yield the most accurate energy demand prediction. These values are resulted from streetlights operating the TALiSMaN scheme after considering the different traffic volumes that are distributed according to the UK's traffic patterns.

5.3.6 Prediction Overhead

One of the challenges in a wireless sensor nodes based application is that sensor nodes are very limited in terms of computing resources, such as processing power and memory storage [211]. The processing power of a typical sensor node can be limited to eight million instructions per second (MIPS) with restricted memory storage configurations, such as 32, 64, 128, 256 KB [196]. Thus, when integrating an energy demand predictor in TALiSMaN-Green, it needs to consider the available computing resources of the targeted platform.

As established in Section 5.3, traffic profile and traffic volume vary depending on the function and demography of the local area. Additionally, streetlight is a ubiquitous utility which can be found at most of the streets. Therefore, TALiSMaN-Green considers energy demand predictor that capable of online learning and then predict E'_{demand} according to local traffic conditions. Figure 5.9 summarises the daily amount of mathematical operations required by each predictor to search for the N, D, weighting factor and data aggregation strategy that results in minimum MAE value. As shown in the figure, Naïve is very simple with virtually zero cost to compute with an eight MIPS sensor node [196]. Considering a sensor node with eight MIPS processing capability [196], all the considered predictors require less than one second to search the required values, assuming one mathematical operation is accomplished by one instruction. Furthermore, the search can be performed during daytime, i.e. when sensing and transmitting of

Table 5.5: The N, D, data aggregation strategy and weighting factor that yield the most accurate energy demand prediction for Naïve, SMA, FWMA, and EWMA predictors and their respective MAE values at different traffic volumes.

Predictor	**Traffic volume** †	N	D‡	α^*	*AggregationStrategy***	*MAE*
Naïve	180					6.55
	438					7.32
	1347	288	1	n/a	DoW	8.06
	3580					5.76
	6554					4.49
SMA	180		20			6.79
	438		20			4.47
	1347	288	19	n/a	DoW	5.95
	3580		17			3.62
	6554		13			3.23
FWMA	180					0.54
	438					0.57
	1347	288	6	'Even'	FDD	0.74
	3580					0.95
	6554					0.94
EWMA	180		9			0.20
	438		20			0.26
	1347	288	19	0	DoW	0.42
	3580		20			0.66
	6554		16			0.83

†14% of the traffic volume (road users per day) is pedestrian and remainder is motorist.
‡D values for Naïve and FWMA is limited to one and six days respectively, whereas SMA and EWMA are evaluated with $2 \leq D \leq 20$.
*Weighting factor is not applicable (n/a) for Naïve and SMA predictors.
**Evaluated data aggregation strategies include Previous-D-Day (PDD), Weekday-Weekend (WDE) and Day-of-Week (DoW).

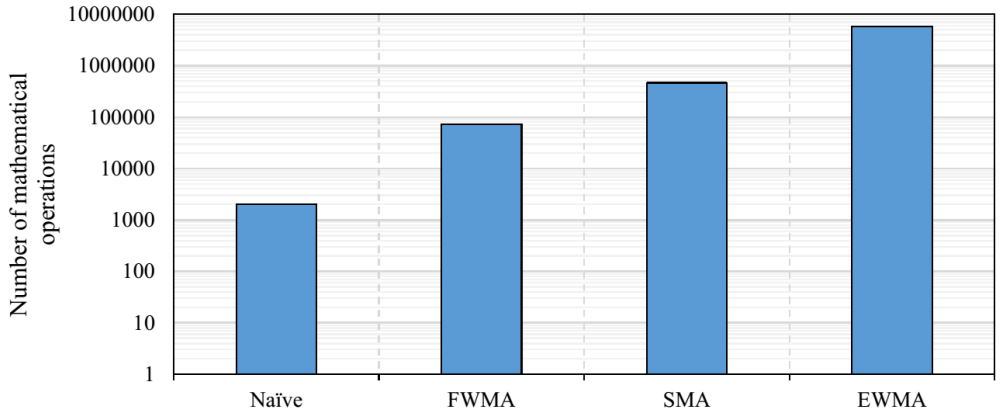

Figure 5.9: Amount of mathematical operations required for different predictors to search for the N, D, weighting factor and data aggregation strategy that result in minimum prediction error. The search is performed online and on daily basis as local traffic profile [187] and traffic volume [190] can change over time.

detected road user is not required, to minimise the potential processing latency that could be introduced to sensor. Therefore, the processing overhead for all considered predictors is negligible.

Due to the amount of historical data needed for energy demand prediction, most of the considered predictors require a considerable amount of memory storage. In Section 5.3.5, various parameters which influence the accuracy of the predictors were considered. Whilst weighting factor is purely a parameter that tunes the accuracy of the FWMA and EWMA, the N and D values, and data aggregation strategy have implications on the storage needed on the embedded device. Assuming that each E_{cons} value is represented as a single-precision floating-point format that occupies 4 bytes of memory [212], Figure 5.10 shows the maximum storage needed by each predictor against some memory configurations of a typical wireless sensor node [196]. Both SMA and EWMA require nearly 160 KB of memory to hold the data for estimating the energy demand of TALiSMaN, if $D = 20$ is required. This figure suggests that sensor nodes with at least 256 KB of memory [196] are needed if these predictors are adopted. To accommodate limited memory storage, this memory requirement can be reduced to about 46 KB with WDE data aggregation strategy, if certain prediction error is acceptable (Section 5.3.5.3). For Naïve and FWMA, the D value is limited to one and six days respectively, and thus the required memory storage is affected by the resolution of N value and the data aggregation strategy used. Naïve and FWMA showed improved prediction accuracy at $N = 288$, and when data is aggregated with DoW and PDD respectively. At these configurations, both Naïve and FWMA require about 8 KB of memory or 5% of the maximum memory required by EWMA.

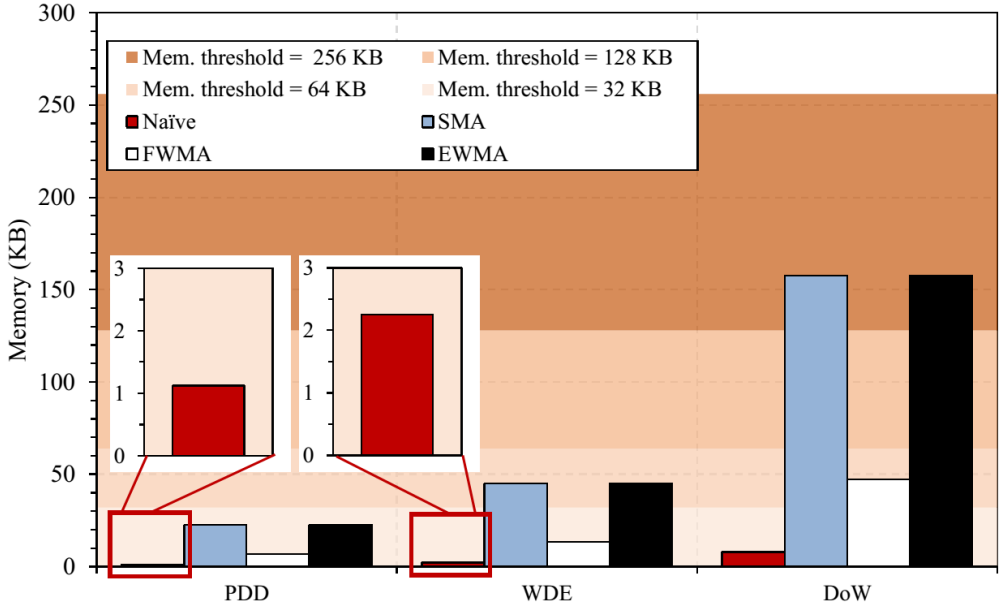

Figure 5.10: The memory footprint for various predictors at $N = 288$ against available memory configurations of a typical sensor node whilst historical data is aggregated with different strategies.

5.3.7 Predictor Selection

The purpose of predictor selection is to determine the most suitable predictor for TALiSMaN-Green. Normally, the selection of a predictor is determined by its prediction error – the differences between observed and estimated values [204]. However, a predictor selection solely based on prediction accuracy is inapplicable in the context of TALiSMaN-Green. This is because the overheads for estimating E'_{demand} also needed to be taken into account due to the limited computing resources in wireless sensor nodes [211]. Note that it is possible that the predictor with the best prediction accuracy may not be possible to be implemented into a sensor node because of the computational complexity of the algorithms involved [213]. Therefore, in selecting the predictor for TALiSMaN-Green, it needs to consider the trade-off between prediction accuracy and required computing resources.

Taking the above observations into account, the criteria for selecting the most suitable predictor for TALiSMaN-Green is based on a metric modelled by Eq. 5.10. This model uses an adjustable coefficient, α_{sel} to determine the relative weighting between a predictor's prediction accuracy and the computing resources required. The value of α_{sel} is between 0 and 1, inclusively. A larger α_{sel} value favours the prediction accuracy of a predictor, whereas a smaller value of this favours the required computing resources. The predictor that minimises the metric I_{sel} is adopted for TALiSMaN-Green.

$$I_{sel} = \alpha_{sel} R_{MAE} + (1 - \alpha_{sel}) R_{resources} \tag{5.10}$$

where R_{MAE} is the ratio of MAE to average daily energy demand of TALiSMaN at specific traffic volume; and $R_{resources}$ is the ratio of computing resources required by a predictor to available computing resources of a wireless sensor node.

As discussed in Section 5.3.6, the processing overhead is negligible for all the considered predictors. Therefore, in this thesis, the required computing resources for I_{sel} consider the maximum memory storage needed by the predictors to search for the required N, D, weighting factor, and data aggregation strategy that yield the most accurate energy demand prediction. Figure 5.11 shows the mean I_{sel} resulting from the MAE values produced by the predictors with the N, D, weighting factor, and data aggregation strategy for all the traffic volumes summarised in Table 5.5. As shown in the figure, both the FWMA and EWMA predictors exhibit the relatively lower mean I_{sel} compared to other predictors considered. EWMA predictor exhibits lower mean I_{sel} values compared to other predictors when $\alpha_{sel} > 0.65$ are considered. However, with these α_{sel} values, the selection of the most suitable predictor for TALiSMaN-Green favours the prediction accuracy rather than required computing resources needed by the predictor. In this thesis, both prediction accuracy and required computing resources are equally important, thus $\alpha_{sel} = 0.5$ is used. As shown in Figure 5.11, FWMA predictor exhibits the

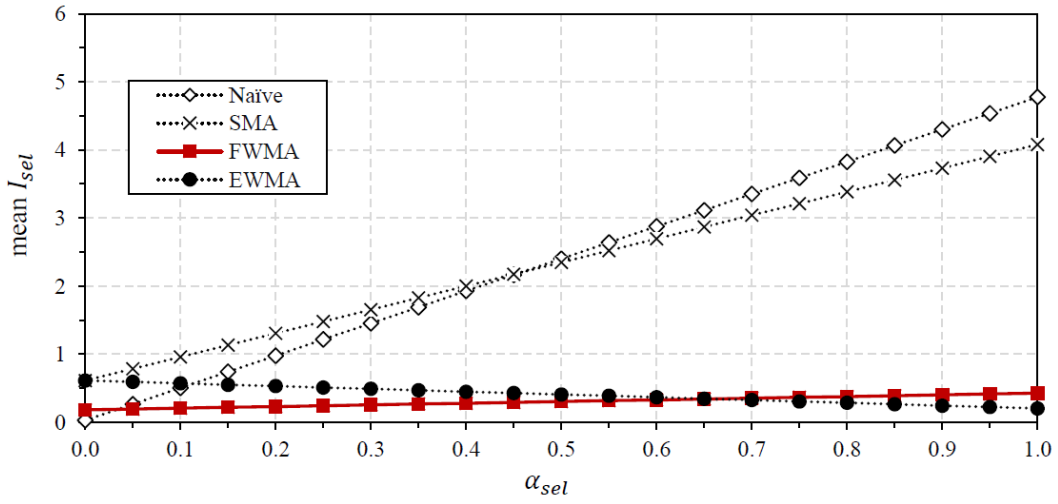

Figure 5.11: I_{sel} of various predictors at different α_{sel} values.

lowest mean I_{sel} value with this α_{sel} value, compared to other considered predictors. Owing to this, FWMA predictor is adopted in TALiSMaN-Green. The performance of TALiSMaN-Green with the FWMA energy demand predictor is presented in Section 5.5.

5.4 Sunrise Time Estimator

In Section 5.2, $E^{'}_{demand}$ is considered as a summation of several $E^{'}_{cons}$ terms. This represents the estimated streetlight operating time until sunrise for a particular day. The required number of terms is determined by the predicted next sunrise time, i.e. the time at which street lighting is no longer needed. Generally, the conventional streetlights are expected to be switched off within the civil twilight time zone. For the purpose of this thesis, 'sunrise' is considered to be the time of day when solar power readings first exceed the threshold value of 0.03 W/m^2 (approximately 7.5 lux [214], a typical light level where streetlights will switch off/on [215]).

The next sunrise time, $t^{'}_{rise}$, can be estimated using SMA predictor over D terms of previous sunrise time values, t_{rise}, as given by Eq. 5.11. The Naïve predictor is a special case of SMA when $D = 1$ is used. This also means that the last sunrise time is used for estimating $t^{'}_{rise}$. Note that Eq. 5.11 is identical to the SMA predictor used in estimating $E^{'}_{cons}$, except for the type of data used.

$$t^{'}_{rise}(\delta + 1) = D^{-1} \sum_{i=\delta-D}^{\delta-1} t_{rise}(i), \quad (\delta - 1) \geq D \tag{5.11}$$

where δ is the current day; and D is the number of previous t_{rise} values.

The prediction accuracy of both predictors to estimate is measured with MAE as given by Eq. 5.9, where e_i is the pairwise difference between $t^{'}_{rise}$ and t_{rise}. The performance

of the Naïve and SMA predictors to estimate t'_{rise} is evaluated with actual solar power readings over a year [216]. Figure 5.12 shows the scatter plot of the estimated t'_{rise} compared to t_{rise} with these predictors at various D values. Although a long-term trend of t'_{rise} can be observed with larger D values, for example $D = 20$ as shown in Figure 5.12, TALiSMaN-Green requires an estimation of next t'_{rise}. In addition, the estimated t'_{rise} values show an increased error with larger D values, as shown in Figure 5.13. Based on observations, SMA gives a reasonable estimation of t'_{rise} values as it exhibits a minimum mean prediction error of 4.5 minutes at $D = 2$. This error is insignificant compared to the overall operational duration for street lighting. Although t'_{rise} can be estimated using the last t_{rise}, this method results in almost 50% greater error compared to SMA with $D = 2$.

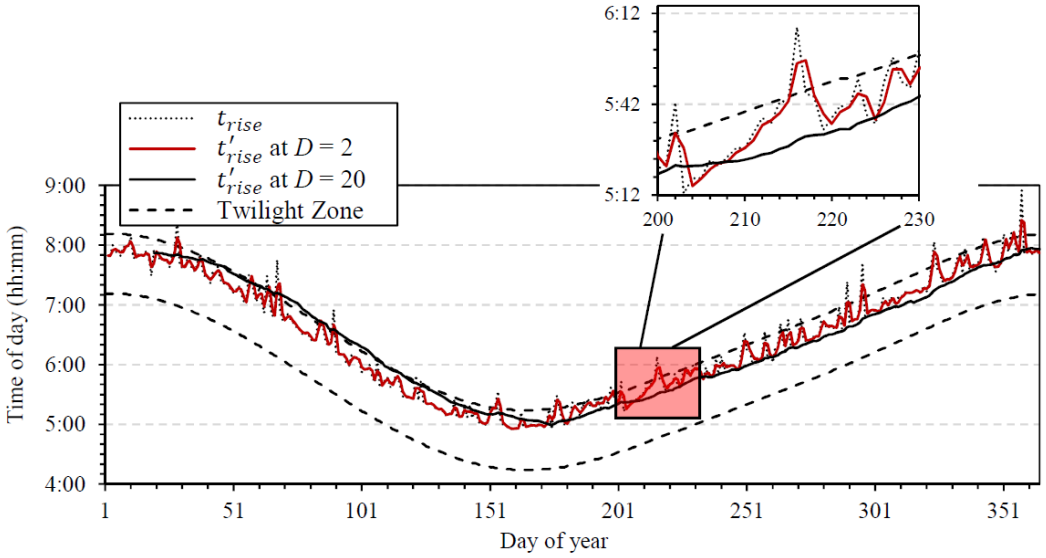

Figure 5.12: The estimated sunrise times with different D values according to solar power readings over a year taken from Humboldt State University [216]. The actual sunrise time, t_{rise}, is considered to be the time of day when solar power readings first exceed the threshold value of 0.03 W/m^2(approximately 7.5 lux [214]).

5.5 Evaluating the Performance of TALiSMaN-Green

In this section, the performance of TALiSMaN-Green is evaluated in two case studies. In order to have a performance overview of TALiSMaN-Green, Section 5.5.1 evaluates TALiSMaN-Green with controlled values, whereas Section 5.5.2 investigates TALiSMaN-Green with real traffic profiles and solar radiation readings. As established in Section 5.3.7, the FWMA predictor with PDD data aggregation strategy resulted in the minimum I_{sel} value, compared to other considered predictors. Also, as shown in Table 5.5, FWMA exhibited the most accurate energy demand prediction at $N = 288$, when an 'Even'

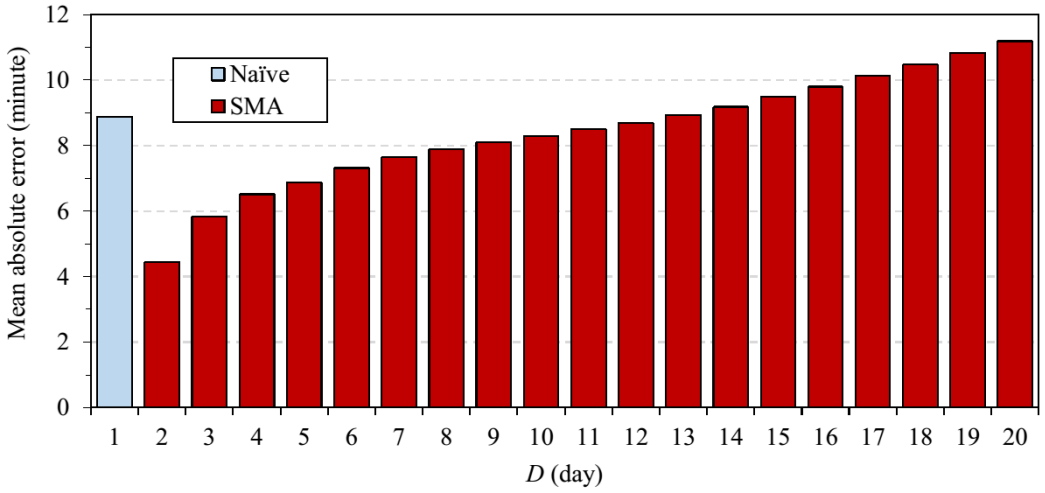

Figure 5.13: The mean MAE of Naïve and SMA predictors at different D values in estimating the next sunrise time.

weighting factor was used. Thus, to evaluate the performance of TALiSMaN-Green, FWMA with these settings is implemented in StreetlightSim.

5.5.1 Case Study A: Controlled Experiments

To gain a performance overview of TALiSMaN-Green on solar-powered streetlights, in this case study, the E_{stored} of each streetlight is abstracted to a static level. These levels are 10%, 30%, 50%, 70% and 90% of the energy actually required by TALiSMaN for a period of lighting operation. As the effectiveness of the Sunrise Time Estimator has been evaluated in Section 5.4, here streetlights are assumed to operate from 16:00 until 08:00 the next day (sunrise time), which represents one of the longest streetlight operational hours during the winter months in the UK. Thus, in this case study, the energy-harvesting system (solar cell size and battery capacity) of solar-powered streetlights is built to harvest and store energy required for a 16-hour TALiSMaN lighting operation with a 25 W LED lamp. This study is performed with the same linear streetlight topology and traffic profiles as previously used in Section 5.3.5, over a period of 12 weeks, and traffic volume is limited to 3508 road users per day (14% of them being pedestrian traffic).

5.5.1.1 Modulation of Lighting Level

When E_{stored} is predicted to be insufficient to sustain the operation of TALiSMaN until sunrise, TALiSMaN-Green use α_{cond} to reduce the φ value requested by TALiSMaN. For TALiSMaN-Green, the modulation of the requested φ is modelled by Eq. 5.2 and 5.3. Figure 5.14 shows the IQRs and the mean values of the α_{cond} whilst streetlights are operating TALiSMaN-Green, at different E_{stored} values. Overall, the mean values of

the α_{cond} are about the same as the E_{stored} values evaluated. This trend is expected as the α_{cond} adopted in TALiSMaN-Green is based on the ratio of E_{stored} to E'_{demand}. This trend also suggests that FWMA is able to predict energy demand accurately for most of the time. On close observation, as shown in Figure 5.15, the α_{cond} is relatively consistent at the beginning of the simulations, but begins to fluctuate as it approaches 08:00.

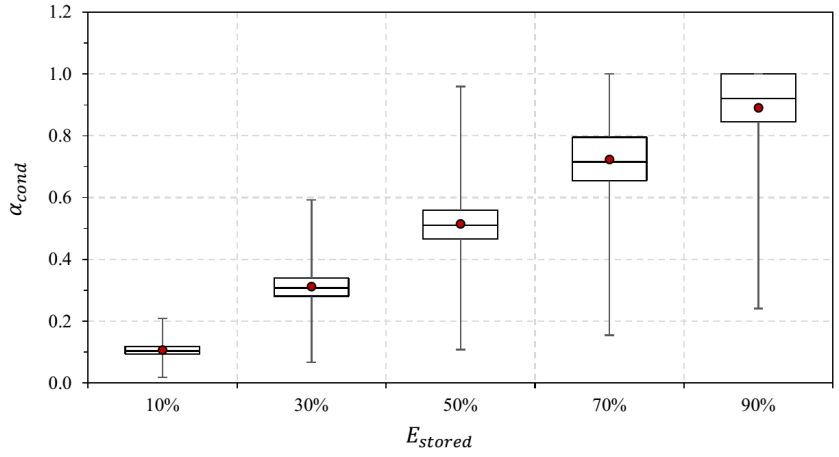

Figure 5.14: The IQRs and mean values (dot) of the α_{cond} whilst TALiSMaN-Green is evaluated with different available energy levels required by TALiSMaN for a complete night. The error bars represent the maximum and the minimum values of the α_{cond} values.

5.5.1.2 Operational Lifetime of Streetlights

The operational lifetime of a solar-powered streetlight is determined by when its energy storage is completely depleted. To evaluate the operational lifetime of streetlights, the energy consumed by a streetlight is modelled by Eq. 3.11. Figure 5.16 shows the number of depleted solar-powered streetlights whilst operating TALiSMaN and TALiSMaN-Green. As shown, the majority of the streetlights operating TALiSMaN fail well before sunrise. In Figure 5.16 (a), even with 50% of the energy needed to operate TALiSMaN, nearly 80% of the streetlights operating TALiSMaN become non-operational before 20:00, 12 hours before sunrise. With TALiSMaN-Green, this is extended to almost 07:50 the next day as shown in Figure 5.16 (b). It is worth noting that, with all the considered E_{stored} values, almost all the streetlights operating TALiSMaN-Green are still operational until 07:30 the next day, which is 30 minutes before sunrise. Although the number of depleted streetlights starts to increase after that time, it is within the twilight zone where ambient lighting begins to increase. In fact, more streetlights are still operational and offering streetlight usefulness compared to those operating TALiSMaN. Overall, with TALiSMaN-Green, the operational lifetime of solar-powered streetlights is able to cover nearly 97% of the designated operational duration (16 hours). The advantage of TALiSMaN-Green is more significant with lower E_{stored} values. For example, at 10% of the energy needed

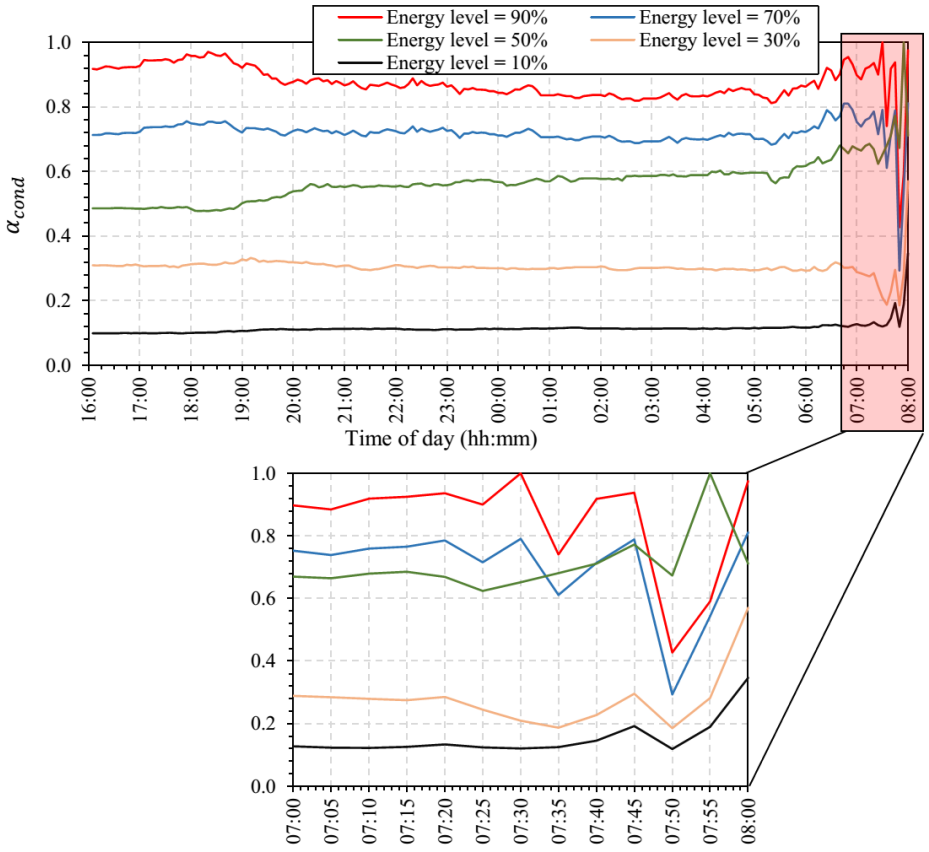

Figure 5.15: The α_{cond} values of a streetlight at different prediction timeslots between 16:00 and 08:00 the next day.

to operate TALiSMaN for a complete night, TALiSMaN-Green can prolong streetlight operational lifetime until sunrise, compared to less than two hours with TALiSMaN.

5.5.1.3 Usefulness of Street Lighting

The usefulness of street lighting to road users, whilst streetlights operate TALiSMaN and TALiSMaN-Green, is measured with the streetlight usefulness model proposed in Section 3.1. The impact of modulating the lighting conditions requested by TALiSMaN on the resultant streetlight usefulness is shown in Figure 5.17. The usefulness of street lighting experienced by road users is dependent on the α_{cond} discussed in Section 5.5.1.1. The aim of TALiSMaN-Green is to deliver consistent usefulness across the whole night. Based on the simulation results, whilst TALiSMaN provides either near-perfect or zero streetlight usefulness, TALiSMaN-Green achieves considerably more consistent usefulness throughout the night. Again, this indicates that the FWMA delivers satisfactory prediction accuracy for $E^{'}_{demand}$ value. It is worth noting that the peak usefulness of TALiSMaN-Green is typically less than the peak usefulness delivered by TALiSMaN. This is because TALiSMaN creates the lighting conditions that satisfy the needs of road users for street lighting, whereas TALiSMaN-Green trades-off streetlight usefulness for

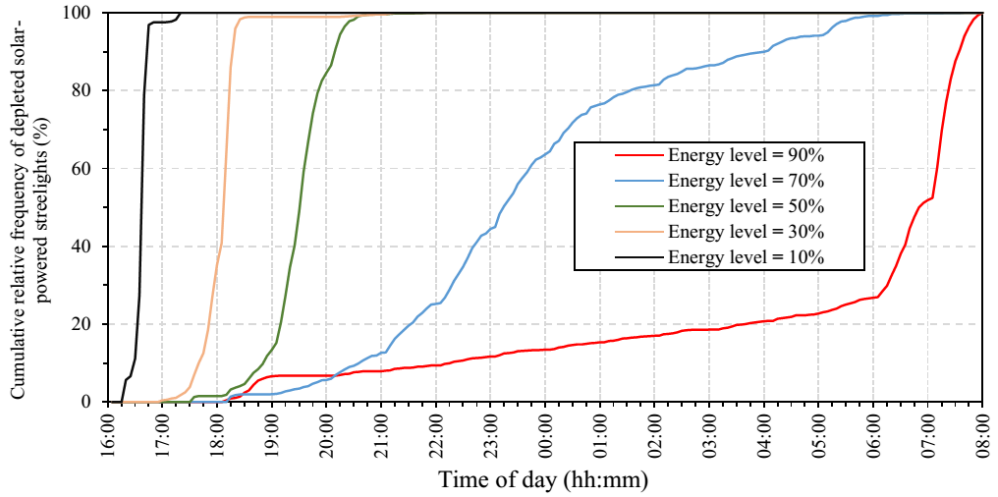

(a) TALiSMaN

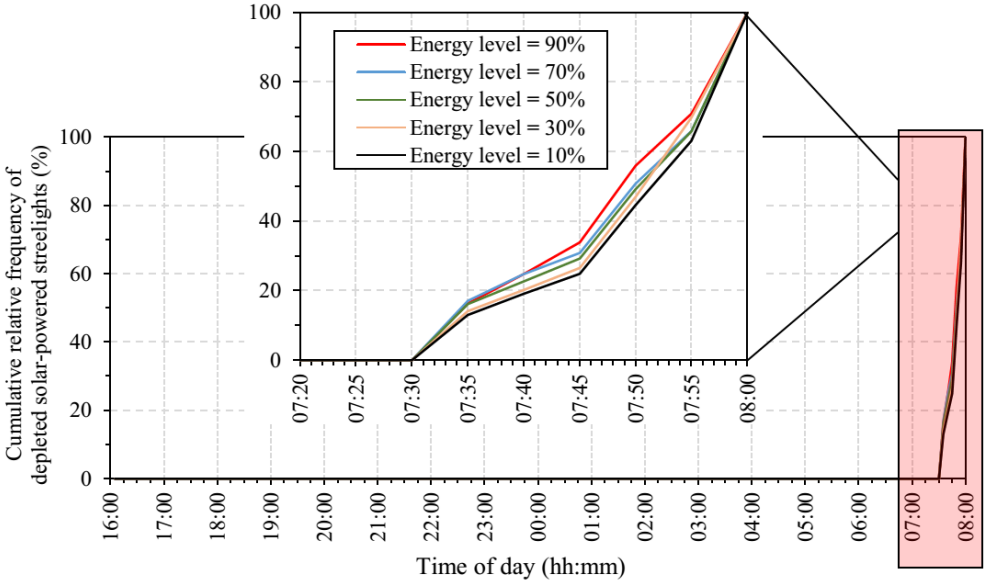

(b) TALiSMaN-Green

Figure 5.16: Simulation results showing the number of depleted solar-powered streetlights whilst operating (a) TALiSMaN and (b) TALiSMaN-Green at different energy levels required to operate TALiSMaN for a complete night.

an extended operational lifetime. With TALiSMaN-Green, streetlight usefulness shows an upper bound limiter which is consistent with E_{stored} values evaluated. This trend, however, is expected as the proposed streetlight usefulness model is influenced by lighting levels of the streetlights, which are determined by E_{stored} and E'_{demand} values. When the E_{stored} value is estimated to be insufficient for lighting across a complete night, TALiSMaN-Green modulates the lighting levels based on the ratio of E_{stored} to E'_{demand}. Thus, the results are obtained.

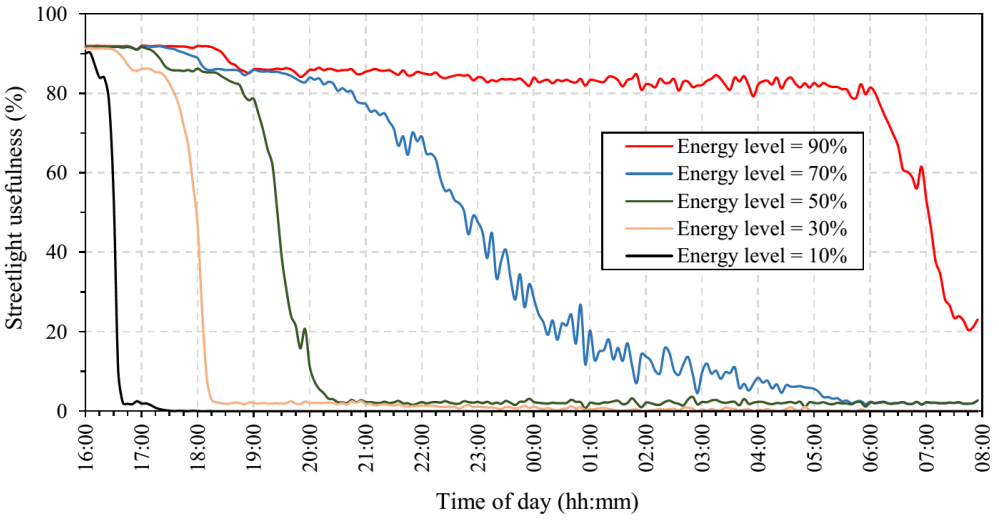

(a) TALiSMaN

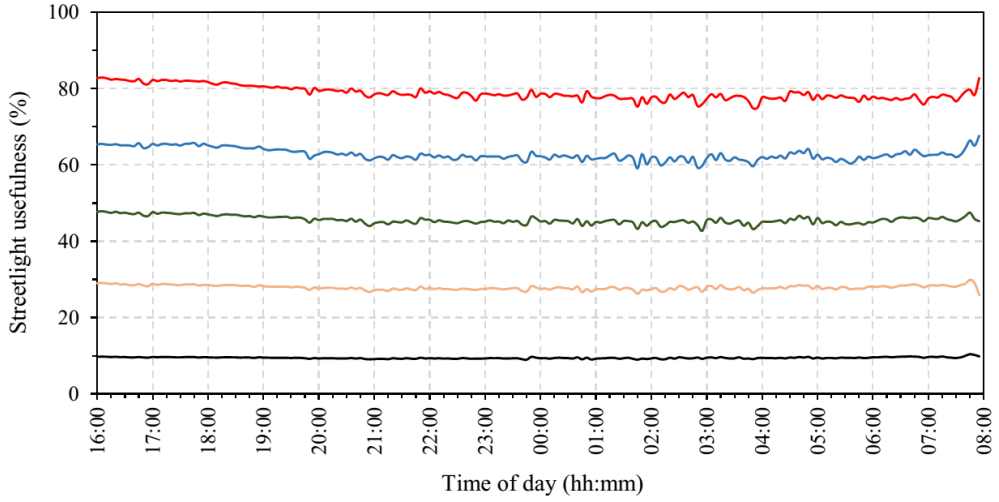

(b) TALiSMaN-Green

Figure 5.17: Simulation results showing the mean streetlight usefulness experienced by simulated road users using (a) TALiSMaN and (b) TALiSMaN-Green with different energy levels required to operate TALiSMaN for a complete night.

5.5.2 Case Study B: Real Traffic Flow and Solar Radiation Readings

To further evaluate the performance of TALiSMaN-Green on solar-powered streetlights, in this case study, actual traffic flow, observed by a vehicle-counting application [217], and solar radiation readings from Humboldt State University [216] are used. For the clarity of the simulation, the streetlights are assumed to be operated from 16:00 until 08:00 the next day, as adopted in Case Study A.

The traffic flow at Salisbury Road which is next to the Zepler Building of the University of Southampton was observed, with a webcam located at Level 4 of the building. Figure 5.18 shows the road section of Salisbury Road where the traffic flow was observed. This road is an access road to staff parking and residential areas to the south of the University.

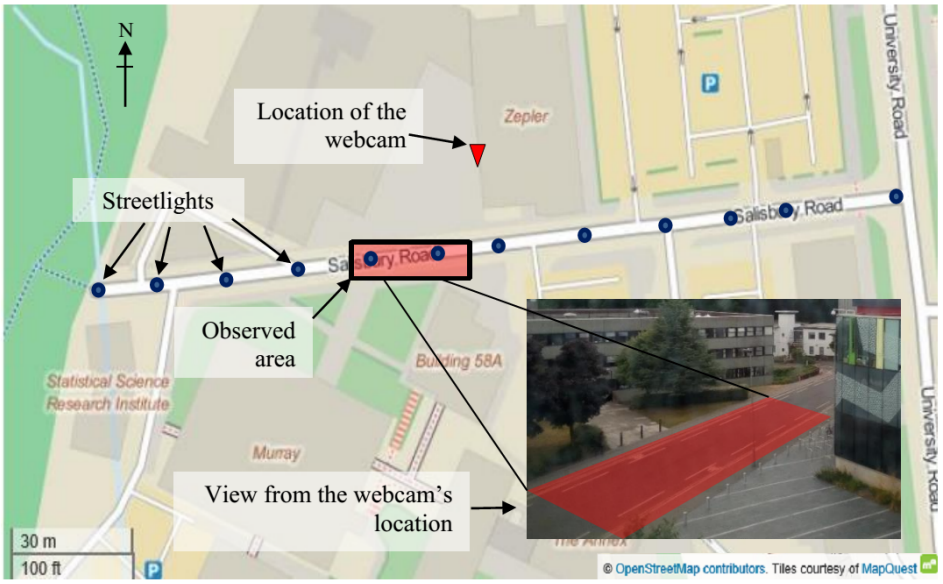

Figure 5.18: Location of real traffic flow.

There are 12 streetlights which are 13 to 20 m apart, along 200 m of road. The traffic was observed and counted from 10-02-2015 to 07-05-2015; however, due to human and technical errors encountered during these dates, such as power failures and unidentified application errors, not all the traffic was 24-hour logged. Because of this, this case study uses the traffic flow logged between 16-02-2015 and 29-03-2015 (6 weeks). Based on traffic counts during these dates, the average traffic volume is 1560 vehicles per day. Although only vehicular traffic is observed, for consistency, 14% of the traffic during the simulations is assumed to be pedestrian. Figure 5.19 shows normalised traffic profiles to their respective mean daily traffic volume during these dates.

Due to the shorter days and reduced sunlight intensity, winter is the most challenging time of year for solar-powered streetlights. To evaluate the performance of TALiSMaN-Green during these months, solar radiation readings from 21-12-2009 to 31-1-2010 (6 weeks, the same length as the real traffic flows), recorded by Solar Radiation Monitoring Station, Humboldt State University [216] are used. This dataset was used as it was high resolution (one minute interval) and open, and from a similar latitude and environment to Southampton (51° vs. 41°, coastal location).

The energy model of the solar-powered streetlight is given by Eq. 5.12 and 5.13. These models assume that energy stored in an energy storage device is a summation of residual energy from the previous lighting operation and harvested solar energy, $E_{harvest}$, and is reduced by the energy consumed during lighting operation, E_{cons}, as previously presented in Eq. 3.11. The energy harvesting system (the battery capacity and solar cell size) is built to harvest and store sufficient energy required by TALiSMaN for a one-night lighting operation. With the streetlight topology shown in Figure 5.18 and the observed traffic flow, the maximum daily energy consumed by the streetlights while operating

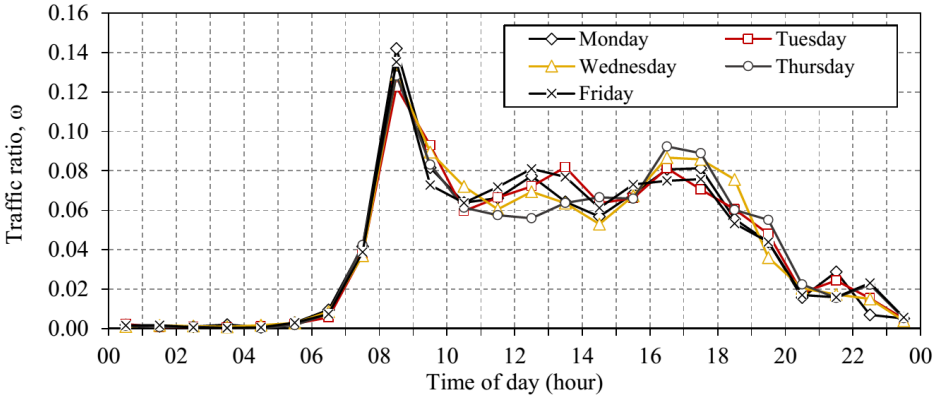

(a) TALiSMaN

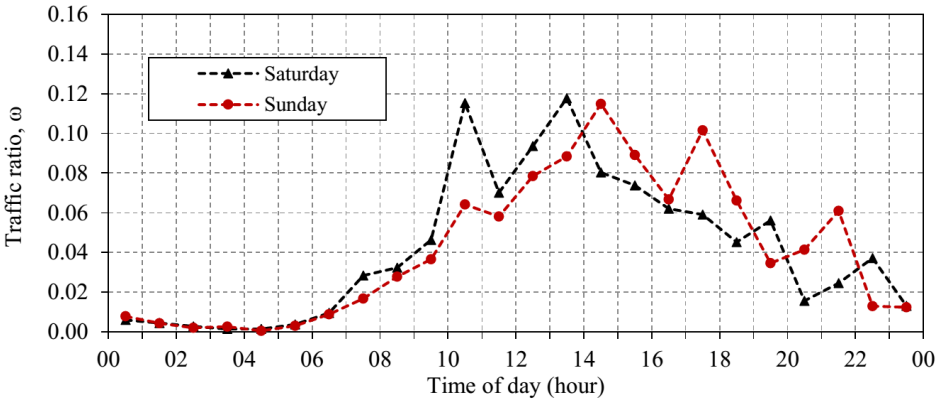

(b) TALiSMaN-Green

Figure 5.19: Normalised traffic profiles during (a) weekdays and (b) weekends observed at Salisbury Road, Southampton, UK between 16-02-2015 and 22-03-2015.

TALiSMaN is about 35 Wh. Thus, in this case study, the battery capacity of the solar-powered streetlights is limited to $E_{cap} = 35$ Wh. This energy can be harvested using a 10 W solar panel with four hours of sunlight. To vary the amount of energy harvested between streetlights, a random noise factor, α_{solar}, ranging between 0 and 1, inclusively, is also applied in these models.

$$E_{stored}(n) = \min\{E_{cap}, E_{stored}(n-1) + E_{harvest(n)} - E_{cons}(n)\} \tag{5.12}$$

$$E_{harvest}(n) = \alpha_{solar} P_{efficiency} P_{size} \int_{t=(n-1)T}^{nT} P_{solar} dt \tag{5.13}$$

where $E_{stored}(n)$ is the energy stored after n discrete timestep (Wh); E_{cap} is the capacity of the energy storage devices (Wh); $E_{harvest}(n)$ is the harvested solar energy between $(n-1)T$ and nT (Wh) based on the actual measurement value, P_{solar} (W/m^2); T is the duration of single timestep n; $P_{efficiency}$ is the solar conversion efficiency and is at 10% [218]; and P_{size} is the size ratio of the solar cell.

Figure 5.20 shows the distribution of energy stored in the streetlights according to these models before operating TALiSMaN and TALiSMaN-Green. As shown, nearly 60% of the streetlights are able to charge their energy storage up to 90 – 100%. This suggests that if the streetlights continue to operate with TALiSMaN 40% of them are unable to provide lighting until sunrise.

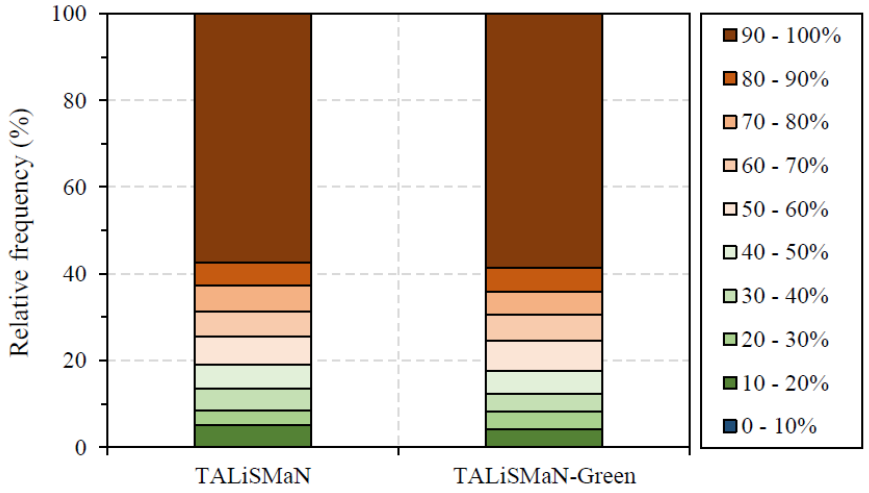

Figure 5.20: Distribution of E_{stored} of the solar-powered streetlights before a 16-hour lighting operation.

5.5.2.1 Modulation of Lighting Level

Figure 5.21 shows the IQRs and mean values of the α_{cond} values, whilst TALiSMaN-Green is evaluated with real traffic flow and solar radiation readings, over a period of six weeks. Based on the simulation results, the median and mean values of the α_{cond} are around 0.8. These results are consistent with the energy level distribution shown in Figure 5.20, where more than 60% of the streetlights were able to gain at least 80% of the energy required for a complete night. Based on these figures, the potential streetlight usefulness is expected to be limited to around 80%. This is based on the results presented in Section 5.5.1.3 which suggests that streetlight usefulness has an upper bound limiter consistent with E_{stored} values evaluated. Note that the IQRs demonstrated by TALiSMaN-Green share some similarities with the E_{stored} value of 90% as evaluated in Case Study A, where the 3rd quartile of the α_{cond} values is the maximum value. Figure 5.22 shows the α_{cond} values of an arbitrary streetlight on different times and days. As shown in the figure, day 5 has the highest α_{cond} value, followed by day 4, 7 and 6. This shows that the streetlight manages to harvest the most of the required energy on day 5, but on other days the streetlight only manages to harvest less than 50% of the energy required by TALiSMaN. The α_{cond} values remain rather consistent between 23:00 and 07:00 the next day, compared to the rest of the operational hours. This is because traffic is relatively low during these hours, and therefore little energy is consumed. As a result, the α_{cond} value exhibits relatively small changes, compared to other operational hours considered.

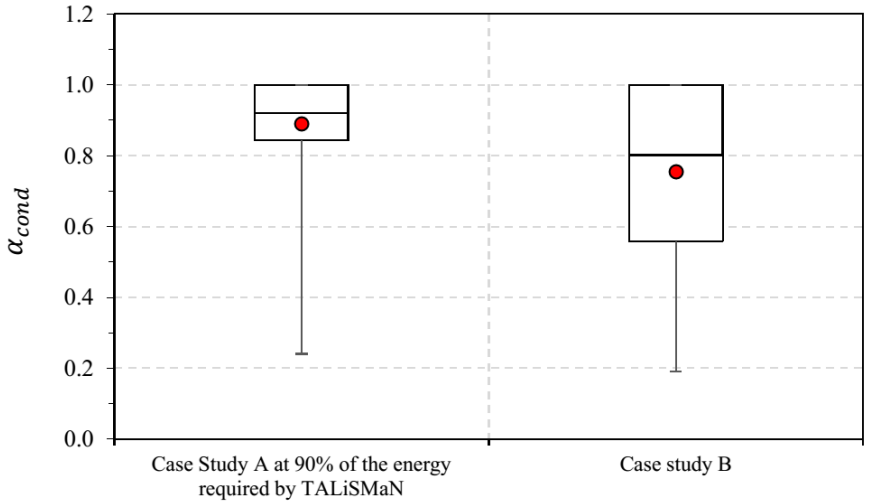

Figure 5.21: The IQRs and mean values (dot) of the α_{cond} whilst TALiSMaN-Green is evaluated with (a) E_{stored} value of 90% in Case Study A, and (b) real traffic flow and solar radiation readings.

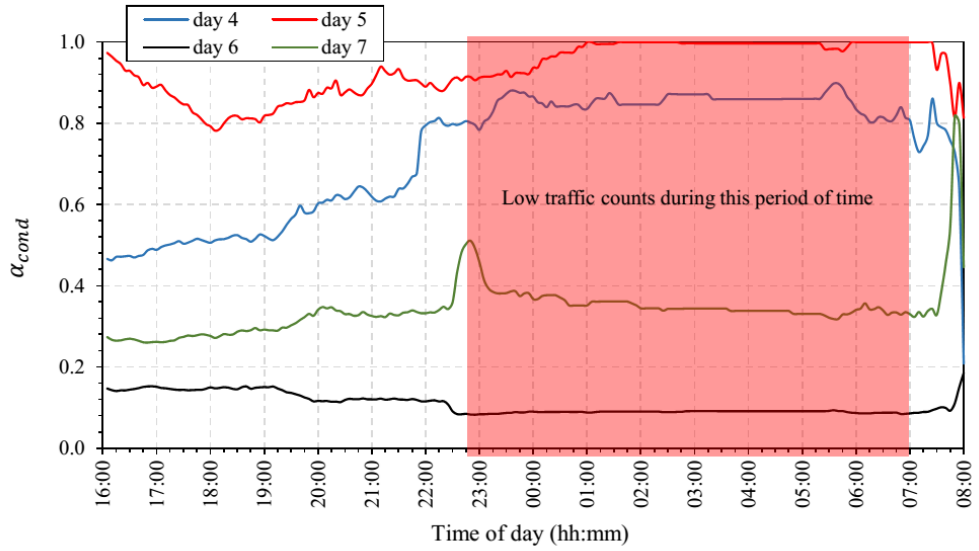

Figure 5.22: The α_{cond} values of a streetlight during different operational times and days.

5.5.2.2 Operational Lifetime of Streetlights

Figure 5.23 shows the number of depleted solar-powered streetlights whilst operating TALiSMaN and TALiSMaN-Green. Whilst streetlights are operating TALiSMaN, more than 50% of them become non-operational after 22:00. However, due to relatively low traffic count (five road users per hour on average) for the next eight hours (23:00 and 7:00 the next day), as shown in Figure 5.19, the number of non-operational streetlights remains almost consistent around 60% during these hours. With TALiSMaN-Green, almost all

the streetlights are able to provide light until 07:50 the next day, or 10 minutes before sunrise. For both TALiSMaN and TALiSMaN-Green, the number of non-operational streetlights increases to 100% exponentially, 5 minutes before sunrise. This trend is consistent with the traffic counts at Salisbury Road shown in Figure 5.19, which has a significant increment between 07:00 and 08:00.

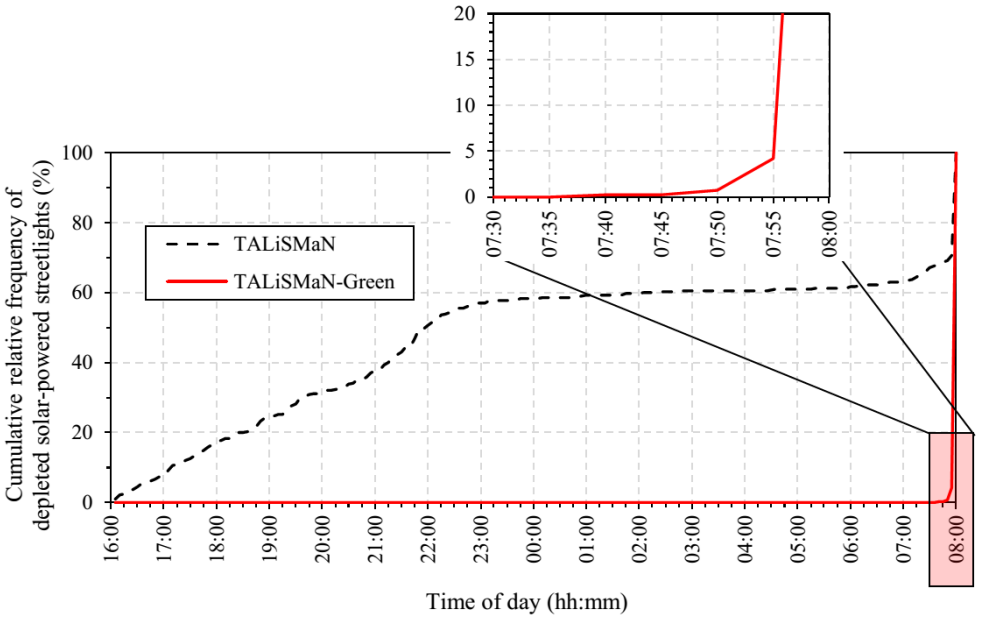

Figure 5.23: Simulation results showing the number of depleted solar-powered streetlights during operational hours from 16:00 to 08:00 the next morning whilst operating TALiSMaN and TALiSMaN-Green.

5.5.2.3 Usefulness of Street Lighting

Figure 5.24 shows the streetlight usefulness experienced by simulated road users according to the traffic flow observed at Salisbury Road (Figure 5.19). With TALiSMaN, streetlight usefulness experienced by road users decreases over time, and begins to go below 50% after 22:00. During the morning rush hour (07:00 – 08:00), usefulness is below 30%. Compared to TALiSMaN-Green, streetlight usefulness is more consistent where the majority of the road users are still able to experience streetlight usefulness between 60 and 80% (mean = 73% with standard deviation of 9%), at most of the time. Also, use a linear regression, TALiSMaN and TALiSMaN-Green show a R^2 value of 59% and 5% respectively. These figures suggest that TALiSMaN-Green is capable of maintaining relatively more consistent streetlight usefulness across the night as compared to TALiSMaN. Streetlight usefulness widely fluctuates, for both TALiSMaN and TALiSMaN-Green, between midnight and early morning (6:00 the next day). This is because the traffic count

during these hours is relatively low, thus providing an inadequate sample during simulations, compared to the rest of the times. This is also exhibited by observed traffic profiles shown in Figure 5.19. It is expected, with sufficient samples, that TALiSMaN-Green is able to maintain streetlight usefulness between 70 and 80%, across the whole night. This is based on the fact that the IQRs of the α_{cond} of the streetlights operating TALiSMaN-Green are mostly at between 0.6 and 1 as shown in Figure 5.21.

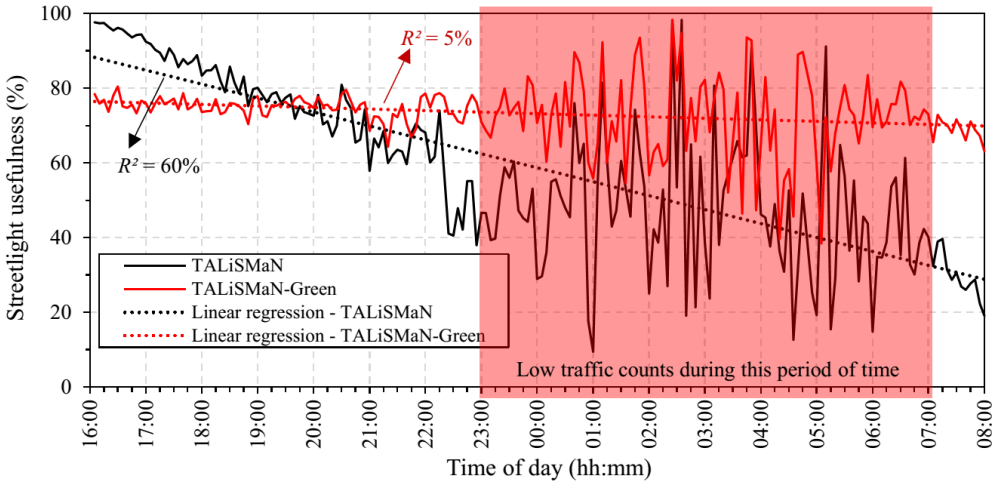

Figure 5.24: Simulation results showing mean streetlight usefulness experienced by simulated road users using TALiSMaN and TALiSMaN-Green. TALiSMaN shows a huge decline (Linear regression, $R^2 = 59\%$) in streetlight usefulness when approaching sunrise time, whereas TALiSMaN-Green remains relatively more consistent (Linear regression, $R^2 = 5\%$) throughout the entire night.

5.6 Summary

This chapter proposed TALiSMaN-Green, an adaptive lighting scheme for solar-powered streetlights. It incorporates TALiSMaN, a lighting scheme that conserves energy whilst maintaining near-perfect usefulness of grid-powered streetlights by detecting road users, and dynamically setting lighting levels in their vicinity. TALiSMaN performs relatively poorly for off-grid streetlights which come with limited energy storage, as it can allow energy reserves to become depleted before sunrise. Also, energy harvested from solar power varies due to the season and weather conditions. TALiSMaN-Green overcomes these limitations by using an energy demand predictor which forecasts the energy required by the streetlight over a complete night. TALiSMaN-Green trades-off lighting conditions required by TALiSMaN to deliver more consistent streetlight usefulness to road users, across the whole night. It also prolongs the operational lifetime of these streetlights until sunrise.

To identify a suitable energy demand predictor for TALiSMaN-Green, four low-complexity online predictors, namely Naïve, simple, fixed, and exponentially weighted moving average, were evaluated in terms of their accuracy in predicting energy potentially consumed by the solar-powered streetlight whilst operating TALiSMaN, and the computational resources required by these predictors. These predictors were evaluated with different prediction timeslots, amount of historical data required, data aggregation strategies, weighting factors, and traffic volumes. With a predictor selection metric, FWMA is found to be the most suitable predictor for TALiSMaN-Green amongst the considered predictors. This predictor has most accurate energy demand prediction with an 'Even' weighting factor, 5-minute prediction timeslot, 6-day historical data, whilst the data is aggregated with PDD strategy.

The proposed scheme together with FWMA energy demand predictor has been validated through two case studies. In Case Study A, the energy level of the streetlights is abstracted to five different levels. Based on the simulation results, the α_{cond} and streetlight usefulness experienced by simulated road users were directly proportional to these energy levels. In an extremely constrained environment, where only 10% of the energy required to run TALiSMaN was available, TALiSMaN-Green extended the operational lifetime of the streetlight from 1.5 to 16 hours, and maintained average streetlight usefulness at 10%. This compares with TALiSMaN, where simulated road users experienced zero usefulness after 1.5 hours of lighting operation.

The performance of TALiSMaN-Green is further validated in Case Study B, where real traffic flow and solar radiation readings were used. The simulation results showed that about 40% of the streetlights were not fully charged (energy level below 90%). This has demonstrated the need for TALiSMaN-Green in solar-powered streetlights. For TALiSMaN-Green, almost all the streetlights were still operational 10 minutes before sunrise. This was an increase of 9 hours (56% of the 16-hour operation) compared to TALiSMaN, where nearly 60% of the streetlights were non-operational at 23:00. In terms of streetlight usefulness, the simulated road users experienced a more consistent usefulness (mean = 73% with standard deviation of 9%) with TALiSMaN-Green, whereas the usefulness had a tendency to decline in time with TALiSMaN, and it dropped to below 30% during the morning rush hour (07:00 – 08:00).

To summarise, although TALiSMaN-Green is not necessarily the optimal solution to the shortcomings of existing solar-powered streetlights, simulation results indicating that it can prolong the operational lifetime of the streetlights while maintaining more consistent streetlight usefulness throughout the entire night.

Chapter 6

Conclusions and Future Work

6.1 Conclusions

Street lighting is a ubiquitous utility which can be found in most urban areas. It illuminates walkways and roads after dark. As presented in Chapter 1, street lighting can enhance the safety and security of road users, and thus encourages more socioeconomic activities after dark. Due to the vast deployment of street lighting and rising energy costs, sustaining lighting operation is a heavy burden, both financially and environmentally. In Chapter 2, various energy efficiency initiatives for street lighting have been considered. These initiatives include retrofitting more energy efficient lamps, reducing the lighting levels of streetlights or dimming, and using renewable energy to power streetlights. Amongst these initiatives, dimming was widely adopted in lighting control schemes to conserve energy in grid-powered streetlights. The requirements for street lighting from the perspectives of a pedestrian and a motorist were considered in Chapter 2. Although existing lighting schemes have improved the energy efficiency of Conventional or 'always-on' street lighting, their impact on road users' requirements for lighting is often omitted.

In order to investigate the impact of a street lighting scheme from the perspectives of a pedestrian and a motorist, an evaluation metric, known as the streetlight usefulness model, was proposed in Chapter 3. This model was based on the literature about the lighting needs for different visual tasks and perception of safety according to these road users. With StreetlightSim, a streetlight simulation environment developed as part of this research, the performance of existing lighting schemes has been evaluated in terms of energy efficiency and streetlight usefulness. Five existing lighting schemes, namely Conventional, Part-night, Philips Chronosense and Dynadimmer, Multi-sensor and Zoning, were evaluated. These schemes were evaluated with 112 streetlights from a residential area in Southampton, over a 16-hour simulated lighting operation (16:00 – 08:00 the next day). Simulation results showed that the Conventional or 'always-on' lighting scheme

consumed the most energy. However, it offered a near-perfect streetlight usefulness (> 90%) to both simulated pedestrian and motorist traffic. Part-night, Philips Chronosense and Dynadimmer adjusted lighting levels according to a predefined schedule. Although these schemes showed improved energy efficiency between 15 – 37% compared to Conventional, their usefulness was reduced to below 90%, and as low as zero during some streetlight operational hours. Amongst all the evaluated lighting schemes, the Zoning lighting scheme required the least energy (1 – 8% of the energy consumed by Conventional) to operate. This was because its energy is spared for pedestrian traffic only, which constitutes a mere 14% of the total simulated traffic. Although, pedestrian traffic received similar streetlight usefulness as demonstrated by the Conventional lighting scheme, motorists gained little benefit from Zoning. The Multi-sensor lighting scheme increases the lighting level from 40% to 100% when a motorist or a pedestrian is in close proximity. It reduces energy consumption by 55 – 60% compared to Multi-sensor lighting scheme. Due to a lack of information sharing, neighbouring streetlights were unable to cooperate to create the lighting conditions required by road users. As a result of this, its usefulness was limited to between 65 – 77% on average. In short, although existing lighting schemes can improve the energy use of street lighting, they have failed to address the lighting needs from the perspective of road users, as demonstrated by the Conventional method. To summarise, this chapter addresses research questions (a) and (b) listed Section 1.2.

In Chapter 4, Traffic-Aware Lighting Scheme Management Network (TALiSMaN) was proposed to address the limitations exhibited by existing lighting schemes. This scheme considers the streetlight usefulness proposed in Chapter 3 to seek a balance between reducing the energy use for street lighting whilst preserving its usefulness according to different road users' needs. The basis of this scheme is that streetlights are governed in such a way to create lighting conditions that meet lighting needs for various visual tasks and safety perception of different road users. This scheme is a distributed lighting control that operates over a short-range wireless mesh network, without relying on a centralised control. With the same simulation scenarios and parameters used in Chapter 3, TALiSMaN demonstrated a comparable streetlight usefulness (> 90%) as offered by the Conventional lighting scheme. Importantly, TALiSMaN consumed 2 – 55% of the energy needed to operate the Multi-sensor lighting scheme, the energy of which increases with increasing traffic volume. By comparison to the Zoning lighting scheme, TALiSMaN requires three times more energy. However, this is justifiable as TALiSMaN satisfies the lighting needs of both pedestrian and motorist traffic. To summarise, TALiSMaN addresses research question (c) listed in Section 1.2.

Chapter 5 proposed TALiSMaN-Green to address the limitations of solar-powered streetlights. This scheme is TALiSMaN enhanced with an energy demand predictor. By combining knowledge of the current level of energy stored and predicting sunrise time, TALiSMaN-Green prolonged the operational lifetime of solar-powered streetlights, and

maintained a more consistent level of streetlight usefulness across the entire night. When the remaining energy stored is predicted to be insufficient to sustain the operation of the street lighting, the lighting levels required by TALiSMaN are modulated to a lower level to conserve energy. As a result, this prolonged the operational lifetime of the solar-powered streetlights. To determine the most suitable energy demand predictor for TALiSMaN-Green, four low-complexity online predictors were evaluated by considering the required computational resources and their accuracy in predicting the energy demand required by TALiSMaN. Analysis showed that the fixed weighted moving average outperforms other considered predictors using an 'Even' weighting factor, 5-minute prediction timeslot, whilst the 6-day historical data is aggregated with PDD strategy.

The performance of TALiSMaN-Green was evaluated with two case studies. For both case studies, the energy harvesting system (solar cell size and battery capacity) of solar-powered streetlights was sized to harvest and store sufficient energy required by TALiSMaN for a 16-hour lighting operation per night with a 25 W LED lamp. For Case Study A, the performance of TALiSMaN-Green is analysed where the energy level of the solar-powered streetlights was abstracted to a level. Based on a 16-hour simulated lighting operation, TALiSMaN-Green enabled the limited energy budget of the solar-powered streetlights to distribute fairly over a complete night, even in a highly constrained scenario. As lighting levels requested by TALiSMaN were modulated based on the ratio of the remaining energy in energy storage to the predicted energy demand to operate TALiSMaN, the streetlight usefulness of TALiSMaN-Green is directly proportional to the available energy level evaluated. For example, with 30% of the energy stored which is required to run TALiSMaN, TALiSMaN-Green maintained streetlight usefulness at about 30%. Whilst the streetlights were designated for a 16-hour simulated lighting operation, with the same energy level, the streetlight usefulness of TALiSMaN declined to zero after two hours of operation. In contrast, TALiSMaN-Green can extend the operational lifetime of almost all the streetlights until 30 minutes before sunrise.

For Case Study B, actual traffic flows were used to evaluate the performance of TALiSMaN-Green. To resemble the operation of solar-powered streetlights in the winter season, actual solar readings during winter months were used during simulations. Using six weeks of traffic flow along with solar readings during winter months, the simulation results showed that about 60% of the streetlights are able to charge their energy storage at between 90 – 100%. For a 16-hour simulated lighting operation, about 60% of the solar-powered streetlights became non-operational after seven hours whilst operating TALiSMaN. However, with TALiSMaN-Green, almost all the streetlights were still operational 10 minutes before sunrise. In terms of streetlight usefulness, TALiSMaN-Green was able to maintain it at 60 – 80% (mean = 73% with standard deviation of 9%). For TALiSMaN, streetlight usefulness declined during operational hours, and below 30% before sunrise. In short, TALiSMaN-Green addresses research question (d) listed in Section 1.2.

In summary, this thesis has evaluated the energy efficiency and usefulness of existing street lighting schemes. Although these schemes have improved the energy efficiency of street lighting, they were unable to maintain a comparable streetlight usefulness as demonstrated by the Conventional lighting scheme. TALiSMaN addressed this problem by maximising the usefulness of the streetlights with a reasonable energy consumption. The obtained results showed that TALiSMaN can offer comparable or improved streetlight usefulness of the existing schemes with 1 – 2% energy consumption of the Conventional lighting scheme. Although TALiSMaN outperformed existing lighting schemes, its application to solar-powered streetlights was limited. This led to TALiSMaN-Green, an energy-neutral lighting scheme with predictive and adaptive behaviour. The results were promising as TALiSMaN-Green can prolong the operational lifetime of solar-powered streetlights 10 minutes before sunrise whilst maintaining streetlight usefulness at 60 – 80% throughout the entire night. Although both TALiSMaN and TALiSMaN-Green are not necessarily the optimal solution, simulation results suggest that both of schemes are relative good compared to the state-of-the-art. Compared to Conventional lighting scheme, TALiSMaN schemes require extra infrastructure, i.e. WSN to operate. However, this extra investment can be absorbed by energy saved and offset by smaller solar-powered streetlight system required to operate TALiSMaN schemes. The undertaken research has also contributed to international conference and journal publications as listed in Section 1.3. Also, the author also been invited to participate in a panel discussion at the OMNeT++ Community Summit 2015.

6.2 Future Work

The research that has been undertaken in this thesis has successfully answered the research questions in Section 1.2. However, there are still additional investigations that could be carried out as this is a comprehensive application area. This section lists some of the extension works from this research.

- To relay and to enable information exchange between streetlights, TALiSMaN and TALiSMaN-Green require a reliable and real-time routing protocol to govern information flow. This is because information about the detected road user is time sensitive, and will have limited use if it is delayed. Due to the fact that the travelling direction of traffic is not available to TALiSMaN schemes, the information is shared amongst all neighbouring streetlights within a 150 m radius. In this thesis, both TALiSMaN schemes adopted a refined packet flooding protocol for this. Although the simulation results suggested that the refined protocol is adequate to support the operation of the TALiSMaN schemes, it suffers a packet loss rate of between 23 and 29%. Due to the packet loss, streetlights can remain active even though no traffic is in proximity. Consequently, this increases energy

consumption for the street lighting. To ensure the information is received by all neighbouring streetlights, the TALiSMaN schemes continue to broadcast the last operational status of the streetlights for an additional 15 seconds. However, this approach can create unnecessary network congestion, and increase channel competition. To further improve the performance of the TALiSMaN schemes, a low-power acknowledgement-based protocol could be used.

- TALiSMaN schemes utilise traffic sensors to detect the presence of pedestrian and motorist traffic. During the simulations, this traffic was detected from a distance of 13 m. However, the performance of various sensors to detect the presence of the traffic can vary [101], and thus this needs further investigation. Currently, there are several sensors that could be used for detecting traffic, for example, passive infrared, audio, vibration, inductive loop, magnetic, and radar, and each has its own limitation. To improve road user detection and to extend the detection range, a multi-sensor array could be considered. This, however, requires further research.

- One of the side effects of operating TALiSMaN schemes is that streetlights are regularly dimmed. Dimming the streetlights with high frequency can cause streetlights to flash and could bring discomfort to nearby residents; however, to what extent still needs further investigation.

In this thesis, the performance of TALiSMaN schemes has been evaluated via simulation. Thus, some aspects of WSN have been abstracted. For example, issues regarding security, time synchronization, and resilience to errors (sensing and radio transmission) are yet to be fully investigated in this thesis. Owing to this, TALiSMaN requires further evaluation, and a field test could be conducted to validate the actual potential of the schemes in real environment. This, however, requires hardware design and implementation to support the operation of TALiSMaN schemes.

Appendix A

Selected Publications

S. P. Lau, G. V. Merrett, A. S. Weddell, and N. M. White, "A Traffic-Aware Street Lighting Scheme for Smart Cities using Autonomous Networked Sensors", Computers & Electrical Engineering, Special Issue on Green Engineering Towards Sustainable Smart Cities, 2015.

S. P. Lau, G. V. Merrett, A. S. Weddell, and N. M. White, "StreetlightSim: A simulation environment to evaluate networked and adaptive street lighting", in Proceedings of IEEE Asia Pacific Conference on Wireless and Mobile, Bali, 2014, pp. 66 – 71

S. P. Lau, A. S. Weddell, G. V. Merrett and N. M. White, "Energy-neutral solar-powered street lighting with predictive and adaptive behaviour", in Proceedings of 2nd International Workshop on Energy Neutral Sensing Systems, Memphis, 2014, pp. 13 – 18.

Appendix B

Performance of IEEE 802.15.4 in TALiSMaN

This section presents the performance of refined packet flooding, which was presented in Section 4.3.1, in supporting TALiSMaN over IEEE 802.15.4 network. The performance of the protocol is evaluated in terms of its packet loss ratio and packet delivery latency. Since flooding is not designed to provide guarantee of packet delivery, a high packet loss is expected by the refined packet flooding protocol. Figure B.1 shows the protocol suffers 23 – 29% packet loss ratio whilst TALiSMaN operates at different traffic volumes. Although the protocol suffers from increasing packet loss as traffic volume increases, it is still sufficient to support TALiSMaN operation. This is because all the simulated road users are able to experience near-perfect ($> 90\%$) streetlight usefulness as shown in Figure 4.7.

In Section 4.3.1, the operation states of TALiSMaN have a validity of 2 s was considered. This is based on the average distance of 30 m between streetlights and speed limit of 30 mph ($\sim$13 m/s) for residential roads in the UK. Figure B.2 shows the end-to-end delay of the protocol whilst TALiSMaN is evaluated with different traffic volumes. The simulation results show that packet delivery latency increases between 1 and 3 ms or requires 3 to 15% more time when traffic volume of 180 road users per day is evaluated. However, these results are expected as the communication channel becomes congested with packets resulted from increasing number of road users. Based on the simulation results, this protocol is able to have packet delivered below 30 ms which is below the validity period of 2 s required by TALiSMaN.

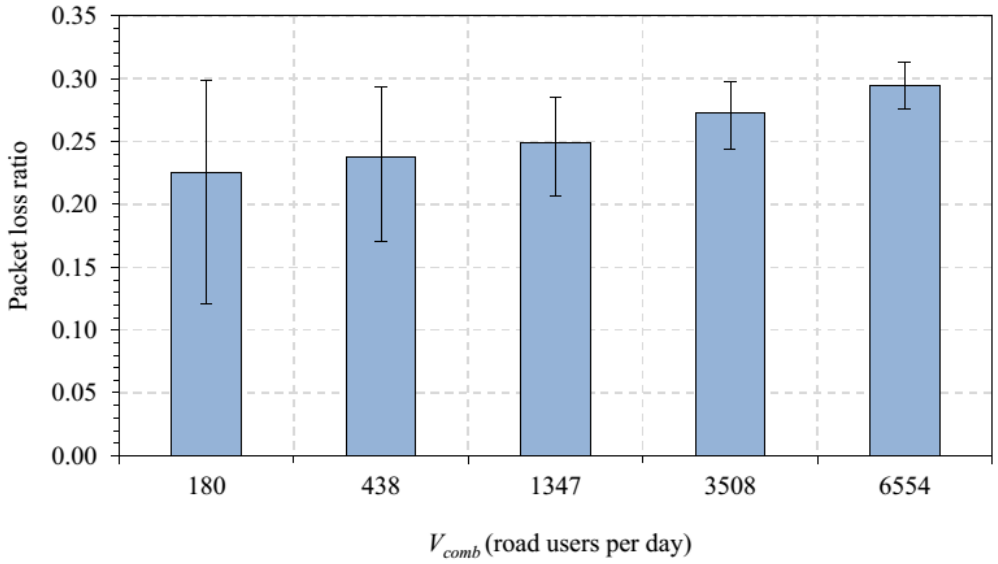

Figure B.1: Packet loss ratio (mean) of the refined packet flooding whilst TALiSMaN is evaluated with different traffic volumes. The error bars represent the maximum and the minimum packet delivery ratios.

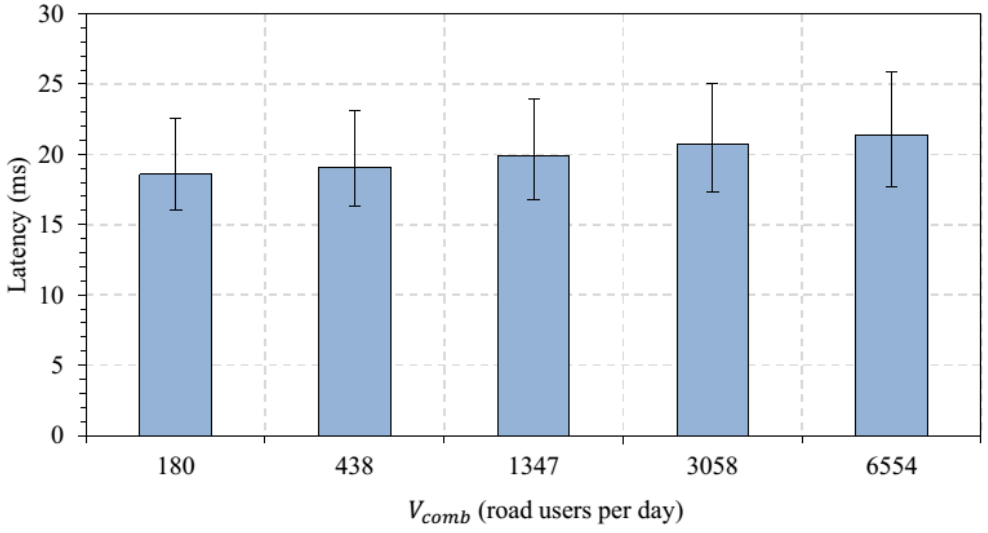

Figure B.2: End-to-end delay (mean) of the refined packet flooding whilst TALiSMaN is evaluated with different traffic volumes. The error bars represent the maximum and the minimum packet delivery latency.

Appendix C

Shapiro-Wilk Normality Test

This section presents the Shapiro-Wilk (S-W) normality test on the simulation data generated in Chapter 4 and 5. The objective of this test is to assess the distribution of the simulation data, thus appropriate statistical tests can be used in this thesis. If the p-value of the S-W test is < 0.05, then the null hypothesis of the test is rejected that the data is from a normality-distributed population.

Table C.1 and C.2 show the statistical results of the S-W test on some of the simulation data used in Chapter 4 and 5, respectively. As shown in Table C.1, some simulation data appear to be normality-distributed. However, as shown in Table C.2, the significance (2-tailed) p-value of the S-W test is < 0.05 for mean absolute error generated in Chapter 5. Owing to this, these data are not from a normality-distributed population.

Table C.1: Statistical result of S-W normality test for energy consumed by the traffic-aware lighting schemes at different pedestrian-motorist ratios during streetlight operational hour 17:00 – 18:00.

Lighting scheme	**Ratio**	**Traffic volume (road users per day)**									
		180		*438*		*1347*		3508		*6554*	
		W	p	W	p	W	p	W	p	W	p
Multi-sensor	0%	0.96	0.23	0.86	<0.05	0.88	<0.05	0.61	<0.05	0.64	<0.05
	14%	0.89	<0.05	0.97	0.64	0.99	0.98	0.88	<0.05	0.87	<0.05
	30%	0.95	0.19	0.98	0.75	0.98	0.90	0.98	0.73	0.57	<0.05
	50%	0.86	<0.05	0.95	0.15	0.95	0.18	0.97	0.51	0.98	0.57
	70%	0.96	0.29	0.98	0.58	0.97	0.44	0.98	0.90	0.99	0.97
Zoning	14%	0.87	<0.05	0.98	0.78	0.96	0.28	0.96	0.32	0.98	0.82
	30%	0.96	0.40	0.94	0.12	0.92	<0.05	0.97	0.42	0.96	0.38
	50%	0.95	0.12	0.98	0.88	0.97	0.49	0.95	0.13	0.94	0.10
	70%	0.98	0.74	0.97	0.50	0.98	0.59	0.96	0.30	0.98	0.86
TALiSMaN	0%	0.89	<0.05	0.96	0.26	0.92	<0.05	0.98	0.87	0.56	<0.05
	14%	0.94	0.10	0.97	0.35	0.94	<0.05	0.96	0.32	0.97	0.43
	30%	0.97	0.58	0.97	0.54	0.98	0.76	0.99	0.95	0.98	0.87
	50%	0.98	0.68	0.70	<0.05	0.54	<0.05	0.91	<0.05	0.96	0.36
	70%	0.97	0.51	0.75	<0.05	0.52	<0.05	0.99	0.97	0.90	<0.05

Table C.2: Statistical result of S-W normality test for mean absolute error given by FWMA and EWMA energy demand predictors at different weighting factors, α, and traffic volumes.

Predictor	α	**Traffic volume (road users per day)**									
		180		*438*		*1347*		*3508*		*6554*	
		W	p	W	p	W	p	W	p	W	p
FWMA	Left	0.87	<0.05	0.91	<0.05	0.93	<0.05	0.91	<0.05	0.92	<0.05
	Even	0.83	<0.05	0.87	<0.05	0.96	<0.05	0.93	<0.05	0.89	<0.05
	Right	0.98	<0.05	0.91	<0.05	0.91	<0.05	0.86	<0.05	0.82	<0.05
EWMA	0.0	0.59	<0.05	0.72	<0.05	0.65	<0.05	0.71	<0.05	0.90	<0.05
	0.1	0.59	<0.05	0.72	<0.05	0.65	<0.05	0.71	<0.05	0.90	<0.05
	0.2	0.59	<0.05	0.72	<0.05	0.65	<0.05	0.71	<0.05	0.91	<0.05
	0.3	0.59	<0.05	0.72	<0.05	0.66	<0.05	0.71	<0.05	0.91	<0.05
	0.4	0.59	<0.05	0.72	<0.05	0.66	<0.05	0.72	<0.05	0.91	<0.05
	0.5	0.59	<0.05	0.72	<0.05	0.66	<0.05	0.72	<0.05	0.91	<0.05
	0.6	0.59	<0.05	0.73	<0.05	0.67	<0.05	0.73	<0.05	0.92	<0.05
	0.7	0.59	<0.05	0.73	<0.05	0.67	<0.05	0.74	<0.05	0.92	<0.05
	0.8	0.59	<0.05	0.73	<0.05	0.69	<0.05	0.77	<0.05	0.88	<0.05
	0.9	0.61	<0.05	0.70	<0.05	0.66	<0.05	0.87	<0.05	0.89	<0.05
	1.0	0.80	<0.05	0.31	<0.05	0.37	<0.05	0.97	<0.05	0.94	<0.05

References

[1] K. Pease, "A review of street lighting evaluations: Crime reduction effects," *Surveillance of Public Space: CCTV, Street Lighting and Crime Prevention*, vol. 10, pp. 47–76, 1999.

[2] B. Welsh and D. Farrington, "Effects of improved street lighting on crime: a systematic review," *Campbell Systematic Reviews*, vol. 4, no. 13, 2008.

[3] S. Atkins, S. Husain, A. Storey, and Unit Crime Prevention, *The influence of street lighting on crime and fear of crime.* London: Home Office London, 1991.

[4] M. Ramsay, R. Newton, and Unit Crime Prevention, *The effect of better street lighting on crime and fear: A review.* London: Home Office London, 1991.

[5] P. O. Wanvik, "Effects of road lighting: An analysis based on Dutch accident statistics 1987–2006," *Accident Analysis & Prevention*, vol. 41, no. 1, pp. 123–128, 2009.

[6] P. Waide, S. Tanishima *et al.*, *Light's Labour's Lost: Policies for Energy-efficient Lighting.* Paris: OECD Publishing, 2006.

[7] International Energy Agency, "Key world energy statistics," 2014.

[8] Department for Environment, Food and Rural Affairs, "Greenhouse Gas Conversion Factor Repository," 2014. [Online]. Avaiable: http://www.ukconversionfactorscarbonsmart.co.uk/Filter.aspx?year=13. [Accessed 20 Jun. 2015].

[9] L. Northeast Group, *Global LED and Smart Street Lighting: Market Forecast (2014–2025).* Washington: Northeast Group, LLC, 2014.

[10] N. C. Council, "Street lighting energy saving - nottinghamshire county council," 2012. [Online]. Available: http://www3.nottinghamshire.gov.uk/travelling/roads/road-design-and-maintenance/street-lighting/energy-saving-project/. [Accessed 19 Mar. 2012].

[11] K. Hyodhyad and P. Srikaew, "Result of road lighting energy saving project implementation through the use of public private partnership scheme," in *Energy and Sustainable Development: Issues and Strategies (ESD), 2010 Proceedings of the International Conference on.* IEEE, 2010, pp. 1–4.

[12] U.S. Department of Energy, "Solid-state lighting gateway demonstration results," 2014. [Online]. Available: https://www1.eere.energy.gov/buildings/ssl/gatewaydemos_results.html. [Accessed 01 Apr. 2014].

[13] F. Li, D. Chen, X. Song, and Y. Chen, "LEDs: A Promising Energy-Saving Light Source for Road Lighting," in *Power and Energy Engineering Conference, 2009. APPEEC 2009. Asia-Pacific*, March 2009, pp. 1–3.

[14] L. Caroe and D. Derbyshire, "New dark age on our streets: Up to 75% of councils are dimming the lights to save money," 10 Nov. 2010. [Online]. Avaiable: http://www.dailymail.co.uk/news/article-1328243/Up-75-cent-councils-dimming-street-lights-save-money.html. [Accessed 12 Mar. 2015].

[15] Warwickshire County Council, "Part night lighting," [Online]. Available: http://www.warwickshire.gov.uk/partnightlighting. [Accessed 11 Nov. 2013].

[16] N. Zotos, C. Stergiopoulos, K. Anastasopoulos, G. Bogdos, E. Pallis, and C. Skianis, "Case study of a dimmable outdoor lighting system with intelligent management and remote control," in *Telecommunications and Multimedia (TEMU), 2012 International Conference on.* IEEE, 2012, pp. 43–48.

[17] F. Leccese, "Remote-control system of high efficiency and intelligent street lighting using a ZigBee network of devices and sensors," *Power Delivery, IEEE Transactions on*, vol. 28, no. 1, pp. 21–28, 2013.

[18] S. Escolar, J. Carretero, M.-C. Marinescu, and S. Chessa, "Estimating Energy Savings in Smart Street Lighting by Using an Adaptive Control System," *International Journal of Distributed Sensor Networks*, vol. 2014, 2014.

[19] E. Nefedov, M. Maksimainen, S. Sierla, C.-W. Yang, P. Flikkema, I. Kosonen, and T. Luttinen, "Energy efficient traffic-based street lighting automation," in *Industrial Electronics (ISIE), 2014 IEEE 23rd International Symposium on.* IEEE, 2014, pp. 1718–1723.

[20] S.-I. Hong, H.-S. Ryu, D.-H. Yoon, C.-G. In, J.-C. Park, and C.-H. Lin, "A development of LED-IT-sensor integration streetlight management system on Ad-hoc," in *TENCON 2011–2011 IEEE Region 10 Conference.* IEEE, 2011, pp. 1331–1335.

[21] R. Müllner and A. Riener, "An energy efficient pedestrian aware Smart Street Lighting system," *International Journal of Pervasive Computing and Communications*, vol. 7, no. 2, pp. 147–161, 2011.

[22] M. H. Moghadam and N. Mozayani, "A street lighting control system based on holonic structures and traffic system," in *Computer Research and Development (ICCRD), 2011 3rd International Conference on*, vol. 1. IEEE, 2011, pp. 92–96.

[23] P. Elejoste, I. Angulo, A. Perallos, A. Chertudi, I. J. G. Zuazola, A. Moreno, L. Azpilicueta, J. J. Astrain, F. Falcone, and J. Villadangos, "An easy to deploy street light control system based on wireless communication and LED technology," *Sensors*, vol. 13, no. 5, pp. 6492–6523, 2013.

[24] S. Pizzuti, M. Annunziato, and F. Moretti, "Smart street lighting management," *Energy Efficiency*, vol. 6, no. 3, pp. 607–616, 2013.

[25] M. Wu, H. Huang, B. Huang, C. Tang, and C. Cheng, "Economic feasibility of solar-powered led roadway lighting," *Renewable energy*, vol. 34, no. 8, pp. 1934–1938, 2009.

[26] S. Hiranvarodom, "A comparative analysis of photovoltaic street lighting systems installed in Thailand," in *Photovoltaic Energy Conversion, 2003. Proceedings of 3rd World Conference on*, vol. 3. IEEE, 2003, pp. 2478–2481.

[27] M. A. Costa, G. H. Costa, A. S. dos Santos, L. Schuch, and J. R. Pinheiro, "A high efficiency autonomous street lighting system based on solar energy and LEDs," in *Power Electronics Conference, 2009. COBEP'09. Brazilian.* IEEE, 2009, pp. 265–273.

[28] M. Costa, L. Schuch, L. Michels, C. Rech, J. Pinheiro, and G. Costa, "Autonomous street lighting system based on solar energy and LEDs," in *Industrial Technology (ICIT), 2010 IEEE International Conference on.* IEEE, 2010, pp. 1143–1148.

[29] S. Georges and F. Slaoui, "Case study of hybrid wind-solar power systems for street lighting," in *Systems Engineering (ICSEng), 2011 21st International Conference on.* IEEE, 2011, pp. 82–85.

[30] M. Becherif, M. Ayad, and D. Hissel, "Modelling and control study of two hybrid structures for street lighting," in *Industrial Electronics (ISIE), 2011 IEEE International Symposium on.* IEEE, 2011, pp. 2215–2221.

[31] University of Malaya, "Outdoor lighting using wind-solar hybrid renewable energy sources," 25 May 2014 [Online]. Available: http://www.sciencedaily.com/releases/2014/05/140525204734.htm. [Accessed 25 Feb. 2015].

[32] J. Lagorse, D. Paire, and A. Miraoui, "Sizing optimization of a stand-alone street lighting system powered by a hybrid system using fuel cell, PV and battery," *Renewable Energy*, vol. 34, no. 3, pp. 683–691, 2009.

[33] British Standards Institution, *BS 5489-1:2003 Code of practice for the design of road lighting.* London: BSI, 2003.

[34] ——, *BS EN 13201-2:2003 Road Lighting: Performance Requirements.* London: BSI, 2003.

[35] P. Raynham, "An examination of the fundamentals of road lighting for pedestrians and drivers," *Lighting Research and Technology*, vol. 36, no. 4, pp. 307–313, 2004.

[36] N. Davoudian and P. Raynham, "What do pedestrians look at at night?" *Lighting Research and Technology*, vol. 44, no. 4, pp. 438–448, 2012.

[37] S. Fotios and T. Goodman, "Proposed UK guidance for lighting in residential roads," *Lighting Research and Technology*, vol. 44, no. 1, pp. 69–83, 2012.

[38] A. Haans and Y. A. de Kort, "Light distribution in dynamic street lighting: Two experimental studies on its effects on perceived safety, prospect, concealment, and escape," *Journal of Environmental Psychology*, vol. 32, no. 4, pp. 342–352, 2012.

[39] Ascom, "Notes on GPRS Performance Issue," 2009 [Online]. Available: http://www.cn.ascom.com/cn/notes-gprs-performance.pdf. [Accessed 8 Sept. 2013].

[40] E. A. Oliver, "Exploiting the short message service as a control channel in challenged network environments," in *Proceedings of the third ACM workshop on Challenged networks.* ACM, 2008, pp. 57–64.

[41] G. Intelligence, "The mobile economy 2015," 2015. [Online]. Avaiable: http://www.gsmamobileeconomy.com/GSMA_Global_Mobile_Economy_Report_2015.pdf. [Accessed 12 Mar. 2015].

[42] J. H. Sun, J. F. Su, G. S. Zhang, Y. Li, and C. Zhao, "An energy-saving control method based on multi-sensor system for solar street lamp," in *Digital Manufacturing and Automation (ICDMA), 2010 International Conference on*, vol. 1. IEEE, 2010, pp. 192–194.

[43] V. Singhvi, A. Krause, C. Guestrin, J. H. Garrett Jr, and H. S. Matthews, "Intelligent light control using sensor networks," in *Proceedings of the 3rd international conference on Embedded networked sensor systems.* ACM, 2005, pp. 218–229.

[44] M. S. Pan, L. W. Yeh, Y. A. Chen, Y. H. Lin, and Y. C. Tseng, "A WSN-based intelligent light control system considering user activities and profiles," *Sensors Journal, IEEE*, vol. 8, no. 10, pp. 1710–1721, 2008.

[45] Y. Lin, W. Cheng, C. Wu, and Y. Sun, "An intelligent lighting control system based on ergonomic research," in *2011 International Conference on Consumer Electronics, Communications and Networks (CECNet)*, 2011, pp. 4744–4747.

[46] P. O. Wanvik, "Effects of road lighting on motorways," *Traffic injury prevention*, vol. 10, no. 3, pp. 279–289, 2009.

[47] Commission Internationale de I'Eclairage, *CIE 115-1995: Recommendation for the Lighting of Road for Motor and Pedestrian Traffic.* Vienna: CIE Publication, 1995.

[48] ——, *CIE 115-2010: Lighting of Roads for Motor and Pedestrian Traffic.* Vienna: CIE Publication, 2010.

[49] British Standards Institution, *BS 5489-1:2013. Code of Practice for the Design of Road Lighting - Part 1: Lighting of Roads and Public Amenity Areas.* London: BSI, 2013.

[50] European Committee for Standardization, *CEN / TR 13201-1 Road lighting - Part 1: Selection of lighting classes.* Brussels: CEN, 2013.

[51] IES, *ANSI / IES Recommended Practice for Roadway Lighting.* NY: IES, 2014.

[52] Standards New Zealand, *Lighting for roads and public spaces: Vehicular traffic (Cat.V) lighting - Performance and design requirements.* Wellington: Standards New Zealand, 2005.

[53] The Illuminating Engineering Institute of Japan, *JIS Z 91110: Recommended Level of Illumination.* Tokyo: The Illuminating Engineering Institute of Japan, 2010.

[54] Commission Internationale de I'Eclairage, "Techincal report 100-1992: Fundamentals of the visual task of night driving," CIE, Vienna, Tech. Rep., 1992.

[55] M. S. Horswill and F. P. McKenna, *A cognitive approach to situation awareness: theory and application.* Aldershot: Ashgate Publishing, 2004, ch. Drivers' hazard perception ability: situation awareness on the road, pp. 155–175.

[56] D. A. Schreuder, "Visibility aspects of the driving task: Foresight in driving. a theoretical note," SWOV Institute for Road Safety Research, Leidschendam, Tech. Rep., 1991.

[57] J. M. Wood, R. A. Tyrrell, and T. P. Carberry, "Limitations in drivers' ability to recognize pedestrians at night," *Human Factors: The Journal of the Human Factors and Ergonomics Society*, vol. 47, no. 3, pp. 644–653, 2005.

[58] A. Bacelar, "The contribution of vehicle lights in urban and peripheral urban environments," *Lighting Research and Technology*, vol. 36, no. 1, pp. 69–76, 2004.

[59] R. Bhagavathula, R. B. Gibbons, and C. J. Edwards, "Relationship between roadway illuminance level and nighttime rural intersection safety," in *Transportation Research Board 94th Annual Meeting*, no. 15–1874, 2015, pp. 8–15.

[60] L. Staplin, "Nighttime hazard detection on freeways under alternative reduced lighting conditions," in *Proceedings of the Human Factors and Ergonomics Society Annual Meeting*, vol. 29, no. 7. SAGE Publications, 1985, pp. 725–729.

[61] Ö. Güler and S. Onaygil, "The effect of luminance uniformity on visibility level in road lighting," *Lighting Research and Technology*, vol. 35, no. 3, pp. 199–213, 2003.

[62] A. Mayeur, R. Brémond, and J. C. Bastien, "Effects of the viewing context on target detection. implications for road lighting design," *Applied ergonomics*, vol. 41, no. 3, pp. 461–468, 2010.

[63] R. Brémond, V. Bodard, E. Dumont, and A. Nouailles-Mayeur, "Target visibility level and detection distance on a driving simulator," *Lighting Research and Technology*, vol. 45, no. 1, pp. 76–89, 2013.

[64] V. Viliūnas, H. Vaitkevičius, R. Stanikūnas, P. Vitta, R. Bliumas, A. Auškalnytė, A. Tuzikas, A. Petrulis, L. Dabašinskas, and A. Žukauskas, "Subjective evaluation of luminance distribution for intelligent outdoor lighting," *Lighting Research and Technology*, vol. 46, no. 4, pp. 421–433, 2014.

[65] W. P. Berg, H. M. Alessio, E. M. Mills, and C. Tong, "Circumstances and consequences of falls in independent community-dwelling older adults," *Age and ageing*, vol. 26, no. 4, pp. 261–268, 1997.

[66] S. Fotios and C. Cheal, "Obstacle detection: A pilot study investigating the effects of lamp type, illuminance and age," *Lighting Research and Technology*, vol. 41, no. 4, pp. 321–342, 2009.

[67] ——, "Using obstacle detection to identify appropriate illuminances for lighting in residential roads," *Lighting Research and Technology*, vol. 45, pp. 362–376, 2013.

[68] Philips Lighting Academy, "Basics of light and lighting," 2008 [Online]. Available: http://www.lighting.philips.com/pwc_li/cn_zh/connect/tools_literature/assets/downloads/basics_of_light.pdf. [Accessed 02 Apr. 2013].

[69] A. E. Patla and J. N. Vickers, "How far ahead do we look when required to step on specific locations in the travel path during locomotion?" *Experimental brain research*, vol. 148, no. 1, pp. 133–138, 2003.

[70] D. B. Elliott, A. Vale, D. Whitaker, and J. G. Buckley, "Does my step look big in this? a visual illusion leads to safer stepping behaviour," *PLoS One*, vol. 4, no. 2, pp. –, 2009.

[71] J. M. Hausdorff, D. A. Rios, and H. K. Edelberg, "Gait variability and fall risk in community-living older adults: a 1-year prospective study," *Archives of physical medicine and rehabilitation*, vol. 82, no. 8, pp. 1050–1056, 2001.

[72] T. Fujiyama, C. Childs, D. Boampong, and N. Tyler, "Investigation of lighting levels for pedestrians: some questions about lighting levels of current lighting standards," in *Proceedings of the 2005 International Conference on Walking in the 21st Century*, 2005, pp. –.

[73] E. T. Hall, "The hidden dimension ." 1966.

[74] P. Raynham and T. Saksvikronning, "White light and facial recognition," *The Lighting Journal*, vol. 68, no. 1, pp. 29–33, 2003.

[75] Department of Energy & Climate Change, *Prices of fuels purchased by non-domestric consumers in the UK*. London: DECC Press Office, 2014.

[76] Grah Lighting, "Street lighting technology comparison," [Online]. Available: http://www.grahlighting.eu/en/street-lighting-technology-comparison. [Accessed 20 Dec. 2013].

[77] C. Knight, "Field surveys of the effect of lamp spectrum on the perception of safety and comfort at night," *Lighting Research and Technology*, vol. 42, no. 3, pp. 313–329, 2010.

[78] N. Mpisketzis, G. Polymeropoulos, M. Kostic, and F. Topalis, "Efficiency of road lighting installations from the point of view of mesopic vision," in *Proceedings of the 3rd Mediterranean Conference on Power Generation, Transmission and Distribution, Med Power 2002*, 2002, pp. –.

[79] Hampshire County Council, "Street Lighting Private Finance Initiative: 2010-2035," 06 Sept. 2013. [Online]. Available: http://www3.hants.gov.uk/roads/street-lighting/pfi-summary.htm. [Accessed 29 Jul. 2015].

[80] Surrey County Council, "Street lighting replacement programme," 20 Nov. 2014. [Online]. Available: http://new.surreycc.gov.uk/roads-and-transport/road-maintenance-and-cleaning/street-lights-traffic-signals-and-signs/street-lights/street-lighting-replacement-programme. [Accessed 08 Jul. 2015].

[81] M. Schiler, *Simplified design of building lighting*. John Wiley & Sons, 1997, vol. 28.

[82] W. T. Grondzik, A. G. Kwok, B. Stein, and J. S. Reynolds, *Mechanical and electrical equipment for buildings*. John wiley & sons, 2011.

[83] Kingfisher Lighting Ltd., "Antares - Product Specifications," [Online]. Available: http://www.kingfisherlighting.com/download/clientfiles/files/Antares.zip. [Accessed 19 Dec. 2013].

[84] ——, "Citta - Product Specifications," [Online]. Available: http://www.kingfisherlighting.com/download/clientfiles/files/Citta.zip. [Accessed 19 Dec. 2013].

[85] CREE, "XSP1 LED Street Light-Horizontal Tenon-Type II Data & Spec Sheets," 2012. [Online]. Available: http://www.cree.com/~/media/Files/Cree/Lighting/Streetlights/XSP%20Series%20Streetlight/XSP1Type2. [Accessed 18 Dec. 2013].

[86] ——, "XSP2 LED Street Light-Horizontal Tenon-Type II Data & Spec Sheets," 2012. [Online]. Available: http://www.cree.com/~/media/Files/Cree/Lighting/Streetlights/XSP%20Series%20Streetlight/XSP2Type2. [Accessed 18 Dec. 2013].

[87] DMX Technologies, "DMX High Power LED Streetlight Manual," [Online]. Available: www.dmxledlights.com/docs/Solar_LED_Streetlights_Manual.pdf. [Accessed 09 Aug. 2013].

[88] Y. Narukawa, M. Ichikawa, D. Sanga, M. Sano, and T. Mukai, "White light emitting diodes with super-high luminous efficacy," *Journal of physics D: Applied physics*, vol. 43, no. 35, pp. –, 2010.

[89] J. R. Tuenge, "Assessment of led technology in ornamental post-top luminaires (host site: Sacramento, ca)," Pacific Northwest National Laboratory (PNNL), Richland, WA (US), Tech. Rep., 2011.

[90] Pacific Northwest National Laboratory, "Demonstration assessment of light emitting diode (led) street lighting," Tech. Rep.

[91] Energy Solutions, "Led street lighting," Tech. Rep., Dec. 2008.

[92] Pacific Northwest National Laboratory, "Demonstration assessment of light-emiting diode (LED) roadway lighting on resdential and commercial streets," U.S. Department of Energy, Tech. Rep., Jun. 2010.

[93] J. D. Bullough, N. P. Skinner, and J. A. Brons, "Analysis of energy efficient highway lighting retrofits," Tech. Rep., 2015.

[94] M. Kostic and L. Djokic, "Recommendations for energy efficient and visually acceptable street lighting," *Energy*, vol. 34, no. 10, pp. 1565–1572, 2009.

[95] Matheson, Andrew, "Reducing Energy Consumption - Street Lighting," 2008. [Online]. Available: http://www.highland.gov.uk/NR/rdonlyres/4530DD7E-366C-4B9A-9B3F-9D2E5BE62C92/0/Item8TEC8708.pdf. [Accessed 3 Jun. 2012].

[96] A. Siddiqui, A. W. Ahmad, H. K. Yang, C. Lee *et al.*, "ZigBee based energy efficient outdoor lighting control system," in *Advanced Communication Technology (ICACT), 2012 14th International Conference on.* IEEE, 2012, pp. 916–919.

[97] Somerset County Council, "Somerset County Council: Reduction of street lighting in Somerset," 2011. [Online]. Available: http://www.somerset.gov.uk/irj/public/council/initiatives/initiative?rid=/guid/30afb148-555c-2e10-10be-ae0d39444537. [Accessed 19 Mar. 2012].

[98] Koninklijke Philips Electronics N. V., "Different ways: The Dynadimmer and the Chronosense," 2010[Online]. Available: http://www.lighting.philips.co.

uk/subsites/oem/product_pages/dynadimmer_overview.wpd. [Accessed 21 May 2012].

[99] I. Mclaren and D. Curry, "Facts and myths surrounding streetlight photocells."

[100] R. Lockwood and T. Selwyn, "A review of local authority road lighting initiatives aimed at reducing costs, carbon emissions and light pollution." 2011.

[101] Y. Wu, C. Shi, and W. Yang, "Study of acquisition streetlights background signal by multi-sensor array," in *Control Automation and Systems (ICCAS), 2010 International Conference on*. IEEE, 2010, pp. 1000–1003.

[102] E. Juntunen, E. Tetri, O. Tapaninen, S. Yrjänä, V. Kondratyev, A. Sitomaniemi, H. Siirtola, E. Sarjanoja, J. Aikio, and V. Heikkinen, "A smart led luminaire for energy savings in pedestrian road lighting," *Lighting Research and Technology*, vol. 47, no. 1, pp. 103–115, 2015.

[103] Delft University of Technology, "Intelligent street lighting at TU Delft saves up to 80% on energy," 11 Jul. 2011. [Online]. Available: http://home.tudelft.nl/en/current/latest-news/article/detail/intelligente-straatverlichting-tu-delft-kan-tot-80-energie-besparen/. [Accessed 21 May 2012].

[104] C. Liu, Q. Wang, and F. Zhang, "Design and development of city street-lighting energy-saving system," in *Circuits, Communications and System (PACCS), 2010 Second Pacific-Asia Conference on*, vol. 1. IEEE, 2010, pp. 178–182.

[105] S. A. E. Mohamed *et al.*, "Smart street lighting control and monitoring system for electrical power saving by using VANET," *Int'l J. of Communications, Network and System Sciences*, vol. 6, no. 08, pp. 351–360, 2013.

[106] Ofcom, "Communications Market Report 2012," 2012. [Online]. Available: http://stakeholders.ofcom.org.uk/binaries/research/cmr/cmr12/CMR_UK_2012.pdf. [Accessed 12 Sept. 2013].

[107] Z. Zhuang, K.-H. Kim, and J. P. Singh, "Improving energy efficiency of location sensing on smartphones," in *Proceedings of the 8th international conference on Mobile systems, applications, and services*. ACM, 2010, pp. 315–330.

[108] A. Carroll and G. Heiser, "An analysis of power consumption in a smartphone," in *USENIX annual technical conference*, vol. 14, 2010, pp. –.

[109] C. Volosencu, D. I. Curiac, O. Banias, C. Ferent, D. Pescaru, and A. Doboli, "Hierarchical approach for intelligent lighting control in future urban environments," in *Automation, Quality and Testing, Robotics, 2008. AQTR 2008. IEEE International Conference on*, vol. 1. IEEE, 2008, pp. 158–163.

[110] J. Zhang, G. Qiao, G. Song, H. Sun, and J. Ge, "Group decision making based autonomous control system for street lighting," *Measurement*, vol. 46, no. 1, pp. 108–116, 2013.

[111] G. Liu, "Sustainable feasibility of solar photovoltaic powered street lighting systems," *International Journal of Electrical Power & Energy Systems*, vol. 56, pp. 168–174, 2014.

[112] R. Panguloori, P. Mishra, and S. Kumar, "Power distribution architectures to improve system efficiency of centralized medium scale pv street lighting system," *Solar Energy*, vol. 97, pp. 405–413, 2013.

[113] S. Nunoo, J. C. Attachie, and C. K. Abraham, "Using solar power as an alternative source of electrical energy for street lighting in ghana," in *Innovative Technologies for an Efficient and Reliable Electricity Supply (CITRES), 2010 IEEE Conference on*. IEEE, 2010, pp. 467–471.

[114] Mayflower, "Mayflower Complete Lighting Control - How it works," 2015. [Online]. Available: http://www.mayflowercontrol.com/Content.aspx?key=how-it-works. [Accessed 04 Aug. 2015]].

[115] G. Maizonave, F. S. dos Reis, J. Lima, A. Bombardieri, F. Chiapetta, G. Ceccon, R. Souza, R. Dos Reis *et al.*, "Integrated system for intelligent street lighting," in *Industrial Electronics, 2006 IEEE International Symposium on*, vol. 2. IEEE, 2006, pp. 721–726.

[116] J. Lee, K. Nam, S. Jeong, S. Choi, H. Ryoo, and D. Kim, "Development of ZigBee based street light control system," in *Power Systems Conference and Exposition, 2006. PSCE'06. 2006 IEEE PES*. IEEE, 2006, pp. 2236–2240.

[117] Y. G. Zhang, L. N. Zhao, L. N. Wang, and S. Y. Zhang, "A web-based management system for urban road lighting," in *Web Information Systems and Mining (WISM), 2010 International Conference on*, vol. 2. IEEE, 2010, pp. 279–282.

[118] SSE Enterprise Lighting, "Lighting - Report a fault," 2015. [Online]. Available: http://lightsoninhampshire.co.uk/public/ReportAccessible.aspx.. [Accessed 21 Jul. 2015].

[119] H. Chung, N. Ho, S. Y. R. Hui, and W. Mai, "Case study of a highly-reliable dimmable road lighting system with intelligent remote control," in *Power Electronics and Applications, 2005 European Conference on*. IEEE, 2005, pp. 1–10.

[120] Y. Yao, D. Zhang, C. Wang, and Y. Sun, "Design of remote street lamp monitoring and communicating node controller based on spread spectrum carrier," in *Industrial Electronics, 2006 IEEE International Symposium on*, vol. 3. IEEE, 2006, pp. 1642–1645.

[121] C. Jing, D. Shu, and D. Gu, "Design of streetlight monitoring and control system based on wireless sensor networks," in *Industrial Electronics and Applications, 2007. ICIEA 2007. 2nd IEEE Conference on.* IEEE, 2007, pp. 57–62.

[122] R. Caponetto, G. Dongola, L. Fortuna, N. Riscica, and D. Zufacchi, "Power consumption reduction in a remote controlled street lighting system," in *Power Electronics, Electrical Drives, Automation and Motion, 2008. SPEEDAM 2008. International Symposium on.* IEEE, 2008, pp. 428–433.

[123] S. Cho and V. Dhingra, "Street lighting control based on lonworks power line communication," in *Power Line Communications and Its Applications, 2008. ISPLC 2008. IEEE International Symposium on.* IEEE, 2008, pp. 396–398.

[124] Y. Chen and Z. Liu, "Distributed intelligent city street lamp monitoring and control system based on wireless communication chip nrf401," in *Networks Security, Wireless Communications and Trusted Computing, 2009. NSWCTC'09. International Conference on*, vol. 2. IEEE, 2009, pp. 278–281.

[125] L. Li, X. Chu, Y. Wu, and Q. Wu, "The development of road lighting intelligent control system based on wireless network control," in *Electronic Computer Technology, 2009 International Conference on.* IEEE, 2009, pp. 353–357.

[126] L. Jianyi, J. Xiulong, and M. Qianjie, "Wireless monitoring system of street lamps based on ZigBee," in *Wireless Communications, Networking and Mobile Computing, 2009. WiCom'09. 5th International Conference on.* IEEE, 2009, pp. 1–3.

[127] G. W. Denardin, C. H. Barriquello, R. Pinto, M. F. Silva, A. Campos, R. N. do Prado *et al.*, "An intelligent system for street lighting control and measurement," in *Industry Applications Society Annual Meeting, 2009. IAS 2009. IEEE.* IEEE, 2009, pp. 1–5.

[128] W. Yue, S. Changhong, Z. Xianghong, and Y. Wei, "Design of new intelligent street light control system," in *Control and Automation (ICCA), 2010 8th IEEE International Conference on.* IEEE, 2010, pp. 1423–1427.

[129] M. Mendalka, M. Gadaj, L. Kulas, and K. Nyka, "Wsn for intelligent street lighting system," in *Information Technology (ICIT), 2010 2nd International Conference on.* IEEE, 2010, pp. 99–100.

[130] S. Viraktamath and G. V. Attimarad, "Power saving mechanism for street lights using wireless communication," in *Signal Processing, Communication, Computing and Networking Technologies (ICSCCN), 2011 International Conference on.* IEEE, 2011, pp. 282–285.

[131] C.-l. Fan and Y. Guo, "The application of a ZigBee based wireless sensor network in the LED street lamp control system," in *Image Analysis and Signal Processing (IASP), 2011 International Conference on.* IEEE, 2011, pp. 501–504.

[132] Q. Li-jun, S. Zi-zheng, and J. Feng, "Intelligent streetlight energy-saving system based on lonworks power line communication technology," in *Electric Utility Deregulation and Restructuring and Power Technologies (DRPT), 2011 4th International Conference on*. IEEE, 2011, pp. 663–667.

[133] C. Atıcı, T. Ozcelebi, and J. J. Lukkien, "Exploring user-centered intelligent road lighting design: a road map and future research directions," *Consumer Electronics, IEEE Transactions on*, vol. 57, no. 2, pp. 788–793, 2011.

[134] G. W. Denardin, C. H. Barriquello, A. Campos, R. Pinto, M. A. Dalla Costa, R. N. do Prado *et al.*, "Control network for modern street lighting systems," in *Industrial Electronics (ISIE), 2011 IEEE International Symposium on*. IEEE, 2011, pp. 1282–1289.

[135] L. Lian and L. Li, "Wireless dimming system for LED street lamp based on ZigBee and GPRS," in *System Science, Engineering Design and Manufacturing Informatization (ICSEM), 2012 3rd International Conference on*, vol. 2. IEEE, 2012, pp. 100–102.

[136] F. Domingo-Perez, A. Gil-de Castro, J. Flores-Arias, F. Bellido-Outeirino, and A. Moreno-Munoz, "Lighting control system based on DALI and wireless sensor networks," in *Innovative Smart Grid Technologies (ISGT), 2012 IEEE PES*. IEEE, 2012, pp. 1–6.

[137] A. Lavric, V. Popa, and I. Finis, "The design of a street lighting monitoring and control system," in *Electrical and Power Engineering (EPE), 2012 International Conference and Exposition on*. IEEE, 2012, pp. 314–317.

[138] S. Siregar and D. Soegiarto, "Solar panel and battery street light monitoring system using GSM wireless communication system," in *Information and Communication Technology (ICoICT), 2014 2nd International Conference on*. IEEE, 2014, pp. 272–275.

[139] J. Liu, C. Feng, X. Suo, and A. Yun, "Street lamp control system based on power carrier wave," in *Intelligent Information Technology Application Workshops, 2008. IITAW'08. International Symposium on*. IEEE, 2008, pp. 184–188.

[140] IEEE Std., *802.15.4-2003 IEEE Standard for Information Technology Part 15.4: Wireless Medium Access Control (MAC) and Physical Layer (PHY) Specification for Low-Rate Wireless Personal Area Network (LR-WPANs)*. NY, USA: IEEE, 2003.

[141] M. Sun, K. Sun, and Y. Zou, "Analysis and improvement for 802.15. 4 multi-hop network," in *Communications and Mobile Computing, 2009. CMC'09. WRI International Conference on*, vol. 2. IEEE, 2009, pp. 52–56.

[142] ZigBee Alliance, Inc., *ZigBee Specification*, 2008.

[143] J. N. Al-Karaki and A. E. Kamal, "Routing techniques in wireless sensor networks: a survey," *Wireless communications, IEEE*, vol. 11, no. 6, pp. 6–28, 2004.

[144] P. Baronti, P. Pillai, V. W. Chook, S. Chessa, A. Gotta, and Y. F. Hu, "Wireless sensor networks: A survey on the state of the art and the 802.15. 4 and ZigBee standards," *Computer communications*, vol. 30, no. 7, pp. 1655–1695, 2007.

[145] C. Perkins and E. Royer, "Ad-hoc on-demand distance vector routing," in *Mobile Computing Systems and Applications, 1999. Proceedings. WMCSA '99. Second IEEE Workshop on*, Feb 1999, pp. 90–100.

[146] W. R. Heinzelman, J. Kulik, and H. Balakrishnan, "Adaptive protocols for information dissemination in wireless sensor networks," in *Proceedings of the 5th annual ACM/IEEE international conference on Mobile computing and networking.* ACM, 1999, pp. 174–185.

[147] Y.-C. Tseng, S.-Y. Ni, Y.-S. Chen, and J.-P. Sheu, "The broadcast storm problem in a mobile ad hoc network," *Wireless networks*, vol. 8, no. 2-3, pp. 153–167, 2002.

[148] Z. J. Haas, J. Y. Halpern, and L. Li, "Gossip-based ad hoc routing," *IEEE/ACM Transactions on Networking (ToN)*, vol. 14, no. 3, pp. 479–491, 2006.

[149] Y. Zhang and L. Cheng, "Flossiping: a new routing protocol for wireless sensor networks," in *Networking, Sensing and Control, 2004 IEEE International Conference on*, vol. 2. IEEE, 2004, pp. 1218–1223.

[150] J. Gao, Y. Xu, and X. Li, "Directed flooding with self-pruning in wireless sensor networks," in *Integration Technology, 2007. ICIT'07. IEEE International Conference on.* IEEE, 2007, pp. 619–622.

[151] Z. Tang and Q. Hu, "A cross-layer flooding strategy for wireless sensor networks," in *Industrial and Information Systems (IIS), 2010 2nd International Conference on*, vol. 2. IEEE, 2010, pp. 377–380.

[152] W. Yen, C.-W. Chen, and C.-h. Yang, "Single gossiping with directional flooding routing protocol in wireless sensor networks," in *Industrial Electronics and Applications, 2008. ICIEA 2008. 3rd IEEE Conference on.* IEEE, 2008, pp. 1604–1609.

[153] J. Lu and K. Whitehouse, "Flash flooding: Exploiting the capture effect for rapid flooding in wireless sensor networks," in *INFOCOM 2009, IEEE*, April 2009, pp. 2491–2499.

[154] J. Chunguo, W. Yan, S. Wenyi, and S. Xin, "Design of street light pole controller based on WSN," in *Electronic Measurement & Instruments (ICEMI), 2011 10th International Conference on*, vol. 3. IEEE, 2011, pp. 147–150.

[155] R. P. Pantoni and D. Brandão, "A geocast routing algorithm intended for street lighting system based on wireless sensor networks," in *Industry Applications (INDUSCON), 2010 9th IEEE/IAS International Conference on.* IEEE, 2010, pp. 1–6.

[156] R. Pantoni and D. Brandão, "A confirmation-based geocast routing algorithm for street lighting systems," *Computers & Electrical Engineering*, vol. 37, no. 6, pp. 1147–1159, 2011.

[157] A. Maria, "Introduction to modeling and simulation," in *Proceedings of the 29th conference on Winter simulation.* IEEE Computer Society, 1997, pp. 7–13.

[158] Information Science Institute, University of Southern California, "The Network Simulator - ns-2," 2015. [Online]. Available: http://www.isi.edu/nsnam/ns/. [Accessed 13 Jun. 2012].

[159] G. Riley, "Large-scale network simulations with GTNetS," in *Simulation Conference, 2003. Proceedings of the 2003 Winter*, vol. 1, 2003, pp. 676–684.

[160] E. Weingärtner, H. Vom Lehn, and K. Wehrle, "A performance comparison of recent network simulators," in *Communications, 2009. ICC'09. IEEE International Conference on.* IEEE, 2009, pp. 1–5.

[161] N. Kamoltham, K. N. Nakorn, and K. Rojviboonchai, "From ns-2 to ns-3-implementation and evaluation," in *Computing, Communications and Applications Conference (ComComAp), 2012.* IEEE, 2012, pp. 35–40.

[162] A. Varga and R. Hornig, "An overview of the OMNeT++ simulation environment," in *Proceedings of the 1st international conference on Simulation tools and techniques for communications, networks and systems & workshops.* ICST (Institute for Computer Sciences, Social-Informatics and Telecommunications Engineering), 2008, pp. –.

[163] A. Sobeih, W. P. Chen, J. C. Hou, L. C. Kung, N. Li, H. Lim, H. Y. Tyan, and H. Zhang, "J-sim: A simulation environment for wireless sensor networks," in *Proceedings of the 38th annual Symposium on Simulation.* IEEE Computer Society, 2005, pp. 175–187.

[164] R. Barr, Z. J. Haas, and R. Van Renesse, "Jist: Embedding simulation time into a virtual machine," in *EuroSim congress on modelling and simulation*, 2004.

[165] S. Adams and L. Yu, "An evaluation of traffic simulation models for supporting ITS development," *Center for Transportation Training and Research, Texas Southern University, Tech. Rep*, 2000.

[166] M. Behrisch, L. Bieker, J. Erdmann, and D. Krajzewicz, "Sumo–Simulation of Urban MObility," in *The Third International Conference on Advances in System Simulation (SIMUL 2011), Barcelona, Spain*, 2011.

[167] M. Piorkowski, M. Raya, A. L. Lugo, P. Papadimitratos, M. Grossglauser, and J.-P. Hubaux, "TraNS: realistic joint traffic and network simulator for VANETs," *ACM SIGMOBILE Mobile Computing and Communications Review*, vol. 12, no. 1, pp. 31–33, 2008.

[168] D. R. Choffnes and F. E. Bustamante, "An integrated mobility and traffic model for vehicular wireless networks," in *Proceedings of the 2nd ACM international workshop on Vehicular ad hoc networks.* ACM, 2005, pp. 69–78.

[169] C. Sommer, Z. Yao, R. German, and F. Dressler, "Simulating the influence of IVC on road traffic using bidirectionally coupled simulators," in *INFOCOM Workshops 2008, IEEE.* IEEE, 2008, pp. 1–6.

[170] F. K. Karnadi, Z. H. Mo, and K. C. Lan, "Rapid generation of realistic mobility models for VANET," in *Wireless Communications and Networking Conference, 2007. WCNC 2007. IEEE.* IEEE, 2007, pp. 2506–2511.

[171] S. Eichler, B. Ostermaier, C. Schroth, and T. Kosch, "Simulation of car-to-car messaging: Analyzing the impact on road traffic," in *null.* IEEE, 2005, pp. 507–510.

[172] C. Schroth, F. Dötzer, T. Kosch, B. Ostermaier, and M. Strassberger, "Simulating the traffic effects of vehicle-to-vehicle messaging systems," in *Proceedings of the 5th International Conference on ITS Telecommunications.* Citeseer, 2005, pp. –.

[173] M. Fellendorf and P. Vortisch, "Microscopic traffic flow simulator VISSIM," in *Fundamentals of Traffic Simulation.* Springer, 2010, pp. 63–93.

[174] C. Lochert, A. Barthels, A. Cervantes, M. Mauve, and M. Caliskan, "Multiple simulator interlinking environment for IVC," in *Proceedings of the 2nd ACM international workshop on Vehicular ad hoc networks.* ACM, 2005, pp. 87–88.

[175] C. Lochert, B. Scheuermann, M. Caliskan, and M. Mauve, "The feasibility of information dissemination in vehicular ad-hoc networks," in *Wireless on Demand Network Systems and Services, 2007. WONS'07. Fourth Annual Conference on.* IEEE, 2007, pp. 92–99.

[176] Y. Yang and R. Bagrodia, "Evaluation of vanet-based advanced intelligent transportation systems," in *Proceedings of the sixth ACM international workshop on VehiculAr InterNETworking.* ACM, 2009, pp. 3–12.

[177] T. Yang, Y. Wang, H. Xiong, L. Yu, Y. Deng, J. Hu, and Z. Chen, "A simulative platform that evaluates the energy save rate of the street lamp system based on JiST/STRAW," in *Instrumentation, Measurement, Computer, Communication and Control, 2011 First International Conference on.* IEEE, 2011, pp. 458–461.

[178] Y. Tao, L. Kong, Y. Wang, H. Jian-Bin, and C. Zhong, "PKU-STRAW-L: a simulative platform evaluate the power-saving rate of the intelligent street lamp system," in *Ubiquitous Intelligence & Computing and 9th International Conference on Autonomic & Trusted Computing (UIC/ATC), 2012 9th International Conference on*. IEEE, 2012, pp. 525–532.

[179] M. Popa and A. Marcu, "A solution for street lighting in smart cities," *Carpathian Journal of Electronic and Computer Engineering*, vol. 5, no. 91, pp. 91–96, 2012.

[180] G. Paravati, F. Lamberti, A. Sanna, E. H. Ramirez, and C. Demartini, "An immersive visualization framework for monitoring, simulating and controlling smart street lighting networks," in *Proceedings of the 5th International ICST Conference on Simulation Tools and Techniques*. ICST (Institute for Computer Sciences, Social-Informatics and Telecommunications Engineering), 2012, pp. 17–26.

[181] SCALABLE Network Technologies, Inc., "QualNet," [Online]. Available: http://web.scalable-networks.com/content/qualnet. [Accessed 17 Dec. 2013].

[182] OPNET Technologies, Inc., "Application and Network Performance with OPNET: Monitoring, Troubleshooting, Auditing, and Prediction," [Online]. Available: http://www.opnet.com/. [Accessed 13 Jun. 2012].

[183] M. Saleem, G. A. Di Caro, and M. Farooq, "Swarm intelligence based routing protocol for wireless sensor networks: Survey and future directions," *Information Sciences*, vol. 181, no. 20, pp. 4597–4624, 2011.

[184] D. A. Schreuder, *Road lighting for safety*. Thomas Telford, 1998.

[185] A. Mayeur, R. Bremond, and J. C. Bastien, "The effect of the driving activity on target detection as a function of the visibility level: Implications for road lighting," *Transportation research part F: traffic psychology and behaviour*, vol. 13, no. 2, pp. 115–128, 2010.

[186] OMNeT++ Network Simulation Framework, "Simulation Models," [Online]. Available: http://www.omnetpp.org/models. [Accessed 10 Apr. 2014].

[187] United Kingdom. Department for Transport, *Traffic dataset: Traffic distribution by time of day on all roads in Great Britain*, London, 2011.

[188] S. P. Lau, "StreetlightSim," University of Southampton, 07 Feb. 2014. [Online]. Available: http://www.streetlightsim.ecs.soton.ac.uk.

[189] D. Paulin, "Full cutoff lighting: the benefits," *Lighting Design and Application*, pp. 54–56, 2001.

[190] United Kingdom. Department for Transport, *Traffic dataset: Street-level traffic figures for all regions and local authorities (Minor roads)*, London, 2011.

[191] W. Daamen and S. P. Hoogendoorn, "Free speed distributions for pedestrian traffic," in *Trb-annual meeting, Washington*, 2006.

[192] "MiXiM (mixed simulator)," 2012 [Online]. Available: http://mixim.sourceforge.net/index.html. [Accessed 20 Mar. 2012].

[193] A. Köpke, M. Swigulski, K. Wessel, D. Willkomm, P. Haneveld, T. E. Parker, O. W. Visser, H. S. Lichte, and S. Valentin, "Simulating wireless and mobile networks in omnet++ the mixim vision," in *Proceedings of the 1st international conference on Simulation tools and techniques for communications, networks and systems & workshops*. ICST (Institute for Computer Sciences, Social-Informatics and Telecommunications Engineering), 2008, pp. –.

[194] M. Johnson, M. Healy, P. van de Ven, M. Hayes, J. Nelson, T. Newe, and E. Lewis, "A comparative review of wireless sensor network mote technologies," in *Sensors, 2009 IEEE*, Oct 2009, pp. 1439–1442.

[195] E. Upton, "Raspberry pi zero: The $5 computer."

[196] Texas Instruments, "Data sheet: A True System-on-Chip Solution for 2.4 GHz IEEE 802.15.4 and ZigBee Application," feb. 2011. [Online]. Available: http://www.ti.com/lit/ds/swrs081b/swrs081b.pdf. [Accessed 06 Feb. 2015].

[197] European Commission, "Database-Eurostat: Transport-Large Urban Zone," 12 Oct. 2015 [Online]. Available: http://appsso.eurostat.ec.europa.eu/nui/submitViewTableAction.do. [Accessed 23 Oct. 2015].

[198] UK Hydrographic Office, "Her Majesty's Nautical Almanac Office," 2014. [Online]. Available: http://astro.ukho.gov.uk/surfbin/first_beta.cgi. [Accessed 23 Jul. 2014].

[199] M. I. Ali, B. M. Al-Hashimi, J. Recas, and D. Atienza, "Evaluation and design exploration of solar harvested-energy prediction algorithm," in *Design, Automation & Test in Europe Conference & Exhibition (DATE), 2010*. IEEE, 2010, pp. 142–147.

[200] A. Cammarano, C. Petrioli, and D. Spenza, "Pro-energy: A novel energy prediction model for solar and wind energy-harvesting wireless sensor networks," in *Mobile Adhoc and Sensor Systems (MASS), 2012 IEEE 9th International Conference on*. IEEE, 2012, pp. 75–83.

[201] M. Gorlatova, A. Wallwater, and G. Zussman, "Networking low-power energy harvesting devices: Measurements and algorithms," *Mobile Computing, IEEE Transactions on*, vol. 12, no. 9, pp. 1853–1865, 2013.

[202] R. J. Hyndman and G. Athanasopoulos, *Forecasting: principles and practice*. OTexts, 2014.

[203] J. D. Deng and Y. Zhang, "Light-weight online predictive data aggregation for wireless sensor networks," in *Proceedings of Workshop on Machine Learning for Sensory Data Analysis*. ACM, 2013, p. 35.

[204] F. A. Aderohunmu, G. Paci, D. Brunelli, J. D. Deng, L. Benini, and M. Purvis, "An application-specific forecasting algorithm for extending wsn lifetime," in *Distributed Computing in Sensor Systems (DCOSS), 2013 IEEE International Conference on*. IEEE, 2013, pp. 374–381.

[205] S. R. Jeffery, G. Alonso, M. J. Franklin, W. Hong, and J. Widom, "Declarative support for sensor data cleaning," in *Pervasive Computing*. Springer, 2006, pp. 83–100.

[206] J. M. Hellerstein, W. Hong, S. Madden, and K. Stanek, "Beyond average: Toward sophisticated sensing with queries," in *Information Processing in Sensor Networks*. Springer, 2003, pp. 63–79.

[207] Y. Zhuang, L. Chen, X. S. Wang, and J. Lian, "A weighted moving average-based approach for cleaning sensor data," in *Distributed Computing Systems, 2007. ICDCS'07. 27th International Conference on*. IEEE, 2007, pp. 38–38.

[208] C. Yang, R. Cardell-Oliver, and C. McDonald, "Combining temporal and spatial data suppression for accuracy and efficiency," in *Intelligent Sensors, Sensor Networks and Information Processing (ISSNIP), 2011 Seventh International Conference on*. IEEE, 2011, pp. 347–352.

[209] R. Vullers, R. Schaijk, H. Visser, J. Penders, and C. Hoof, "Energy harvesting for autonomous wireless sensor networks," *IEEE Solid-State Circuits Magazine*, vol. 2, no. 2, pp. 29–38, 2010.

[210] C. J. Willmott and K. Matsuura, "Advantages of the mean absolute error (mae) over the root mean square error (rmse) in assessing average model performance," *Climate research*, vol. 30, no. 1, p. 79, 2005.

[211] M. Tubaishat and S. Madria, "Sensor networks: an overview," *Potentials, IEEE*, vol. 22, no. 2, pp. 20–23, 2003.

[212] D. Goldberg, "What every computer scientist should know about floating-point arithmetic," *ACM Computing Surveys (CSUR)*, vol. 23, no. 1, pp. 5–48, 1991.

[213] C. Liu, K. Wu, and M. Tsao, "Energy efficient information collection with the ARIMA model in wireless sensor networks," in *Global Telecommunications Conference, 2005. GLOBECOM'05. IEEE*, vol. 5. IEEE, 2005, pp. 2470–2474.

[214] R. W. Thimijan and R. D. Heins, "Photometric, radiometric, and quantum light units of measure: a review of procedures for interconversion," *HortScience*, vol. 18, no. 6, pp. 818–822, 1983.

[215] D. GASPAROVSKY, "Measurement of daylight illuminance levels in transient periods for public lighting control," *Przegląd Elektrotechniczny*, vol. 89, no. 6, pp. 320–323, 2013.

[216] S. Wilcox and A. Andreas, "Solar radiation monitoring station (sorms): Humboldt state university, arcata, california (data)," National Renewable Energy Laboratory (NREL), Golden, CO (United States), Tech. Rep., 2007.

[217] A. Sobral, "Vehicle Detection, Tracking and Counting," 28 May 2012. [Online]. Available: https://www.behance.net/gallery/Vehicle-Detection-Tracking-and-Counting/4057777. [Accessed 09 Dec. 2014].

[218] P. Corke, P. Valencia, P. Sikka, T. Wark, and L. Overs, "Long-duration solar-powered wireless sensor networks," in *Proceedings of the 4th workshop on Embedded networked sensors*. ACM, 2007, pp. 33–37.